

Evaluation of Sugar Biosynthetic Enzymes and Studies on Jadomycin Biosynthesis

by

Stephanie M. Forget

Submitted in partial fulfilment of the requirements
for the degree of Doctor of Philosophy

at

Dalhousie University
Halifax, Nova Scotia
November 2017

© Copyright by Stephanie M. Forget, 2017

TABLE OF CONTENTS

List of Tables	x
List of Figures	xi
Abstract	xviii
List of Abbreviations and Symbols Used	xix
Acknowledgments	xxvii
CHAPTER 1: INTRODUCTION.....	1
1.1. Inhibition of Bacterial Cell Wall Biosynthesis	5
1.2. Chemical Probes for Glycan Biochemical Pathway Elucidation	10
1.3. Glycosylated Bacterial Secondary Metabolites.....	12
1.3.1. Natural Product Glycodiversification	15
1.4. Aims of the Thesis	19
CHAPTER 2: STUDIES ON CARBOHYDRATE-RECOGNIZING ENZYMES	23
2.1. Introduction to Rhamnose Sugar Biosynthesis	23
2.1.1. Thymidyltransferase: RmlA/Cps2L	24
2.1.2. Rhamnose Biosynthetic Tailoring Enzymes: RmlB, RmlC, RmlD	25
2.1.3. Rhamnosyltransferases Involved in LPS Cell Wall Biosynthesis.....	26
2.2. Kinetic Evaluation of Glucose 1-phosphate Analogues with a Thymidyltransferase (Cps2L).....	28
2.2.1. Analytical substrate evaluation with Cps2L.....	30
2.2.2. Kinetic Evaluation using IPP-PNP-XO Coupled Spectrophotometric Assay	34

2.2.3. Determination of K_d values using waterLOGSY NMR Binding Experiments.....	39
2.2.4. Chemoenzymatic Synthesis of Sugar Nucleotides (2.8,2.9, 2.11, 2.15)	43
2.2.5. Conclusions.....	44
2.3. Mechanistic Evaluation of a Nucleoside Tetraphosphate (p_4dT) with a Thymidyltransferase	45
2.3.1. Evaluation of p_4dT as a Cps2L Substrate	47
2.3.2. Conclusions.....	52
2.4. Evaluation of Rhamnose Biosynthetic Enzymes (RmlBCD) for Chemoenzymatic Applications	53
2.4.1. Analytical Assays to Probe Substrate Tolerance of RmlBCD.....	53
2.4.2. Chemoenzymatic Synthesis of dTDP-1C-Rha	62
2.4.3. Conclusion and Future Work	64
2.5. Characterization of a Promiscuous Glycosyltransferase (Sv0189) from <i>S. venezuelae</i> ISP5230.....	65
2.5.1. Identification of Sv0189 as a Glycosyltransferase for Glycodiversification	65
2.5.2. Cloning and Expression of Sv0189.....	71
2.5.3. Establishing Glycosyltransferase Activity with Sv0189	73
2.5.4. Sv0189 Initial Acceptor Screening Assay.....	77
2.5.5. Development of a Secondary Acceptor Screen for Sv0189	84
2.5.6. Conclusions.....	87
CHAPTER 3: DIVERSIFICATION OF THE JADOMYCIN FAMILY NATURAL PRODUCTS	88
3.1. Introduction to Jadomycin Family Natural Products	88

3.1.1. E-ring Variability in Jadomycin Family Natural Products	90
3.1.2 Modification of the Jadomycin Sugar Moiety.....	91
3.1.3. Biological Activities of Jadomycin Family Natural Products	95
3.2. Furan and Lactam Jadomycin Biosynthetic Congeners Isolated from <i>Streptomyces venezuelae</i> ISP5230 Cultured with <i>N</i>ϵ-trifluoroacetyl-L-Lysine	96
3.2.1. Previous Studies on Jadomycin Lysine (JdK).....	98
3.2.2. Jadomycin Productions with TFAL	99
3.2.3. Discussion of the Biosynthetic Origins of 3.2-3.4	108
3.2.4. Antimicrobial and Cancer Cell Line Bioassays	109
3.2.5. Conclusions.....	112
3.3. Biosynthetic 4,6-dehydratase Gene Deletion: Isolation of a Glucosylated Jadomycin Natural Product Provides Insight into the Substrate Specificity of Glycosyltransferase JdS	113
3.3.1. Isolation of Glucosylated Jadomycin 3.9 from <i>S. venezuelae</i> Δ <i>jadT</i>	113
3.3.2. Identification of the Glycosyltransferase	116
3.3.3. Evaluation of <i>S. venezuelae</i> Δ <i>sv0189</i> Δ <i>jadT</i> and <i>S. venezuelae</i> Δ <i>jadS</i> Δ <i>jadT</i>	118
3.3.4. Conclusions.....	121
3.4. Introduction of a Non-Native L-digitoxyltransferase into <i>S. venezuelae</i>.....	122
3.4.1. Homologous Recombination Using pKC1139 (Method 1)	130
3.4.2. Integrative Insertion Using pSET152 (Method 2).....	132
3.4.3. Heterologous Expression Using pSE34 (Method 3).....	133
3.4.4. Analysis of <i>kijC3</i> , <i>kiC4</i> , <i>kijC4</i> Δ <i>kijC3</i> complemented <i>S. venezuelae</i> (Method 1)	134

3.4.5. Conclusions and Future Work.....	151
CHAPTER 4: EXPERIMENTAL	152
4.1. General Methods	152
4.1.1. NMR Methods.....	152
4.1.2. HRMS and LCMS Running Conditions.....	153
4.1.3. UV Spectroscopy Methods	154
4.1.4. Analytical HPLC Method.....	154
4.1.5. Normal Phase Chromatography.....	154
4.1.6. Ion Pair Reversed-Phase Chromatography.....	155
4.1.7. Preparatory HPLC Method.....	155
4.1.8. SDS-PAGE Gel Running Conditions.....	155
4.1.9. Bioinformatics Methods.....	156
4.1.10. General Bacterial Maintenance	157
4.1.11. Methods for Primer and DNA Handling.....	157
4.1.12. Genomic DNA Extraction Protocols.....	158
4.1.13. PCR and Colony PCR methods.....	158
4.1.14. Restriction Digestion Protocols	160
4.1.15. Ligation Protocols	160
4.1.16. Agarose Gel Running Conditions and Visualization	161
4.1.17. Transformation of NEB® 5-alpha and NEB® 10-beta Competent <i>E. coli</i>	162
4.1.18. Miniprep Plasmid Isolation from <i>E. coli</i>	162

4.1.19. Protocol for Competent <i>E. coli</i>	163
4.1.20. <i>E. coli</i> Transformation Protocol	164
4.1.21. <i>E. coli</i> - <i>Streptomyces</i> Conjugation Protocol.....	164
4.1.22. List of Plasmids and Strains	166
4.1.23. Media Recipes.....	169
4. 2. Experimental Chapter 2.2	171
4.2.1. Disodium Uridine 5'-(2-amino-2-deoxy- α -D-glucopyranosyl bisphosphate) (2.8).....	172
4.2.2. Disodium Deoxythymidine 5'-(3-amino-3-deoxy- α -D-glucopyranosyl bisphosphate) (2.9).....	173
4.2.3. Tributylammonium deoxythymidine 5'-(3-azido-3-deoxy- α -D- glucopyranosyl bisphosphate) (2.11).....	175
4.2.4. Tributylammonium deoxyuridine C-(1-deoxy- α -D-glucopyranosyl bisphosphate)methane (2.15)	176
4.2.5. IPP-PNP-XO Coupled Kinetic Assays	177
4.2.6. K_d Determination Using waterLOGSY NMR Spectroscopy	178
4.3. Experimental Chapter 2.3	179
4.3.1. p_4dT HPLC Assays and Specific Activity with Cps2L.....	179
4.3.2. ^{31}P NMR Experiments with p_4dT	180
4.4. Experimental Chapter 2.4	180
4.4.1. Expression and Purification of Recombinant Enzymes	181
4.4.2. General Conditions for Analytical Cps2L, RmlB-D Assays.....	182
4.4.3. Tributylammonium 5'-deoxythymidine-C-(1-deoxy- β -L-rhamnopyranosyl bisphosphate) methane (dTDP-1C-Rha).....	183

4.5. Experimental for Chapter 2.5	185
4.5.1. AntiSMASH Analysis	185
4.5.2. Assembly of pET28a::sv0189	185
4.5.3. Preparation of pET28a::NHis ₆ sv0189	186
4.5.4. Transformation of <i>E. coli</i> BL21(DE3) pLysS.....	187
4.5.5. Expression and Purification of Sv0189	187
4.5.6. Determination of Kinetic Parameters	189
4.5.7. First Round of Acceptor Screening.....	190
4.5.8. Secondary Acceptor Screening	193
4.6. Experimental for Chapter 3.2	194
4.6.1. <i>S. venezuelae</i> Cultures with TFAL	194
4.6.2. ¹³ C-Supplemented Cultures with TFAL Productions	195
4.6.3. Isolation of Natural Products from TFAL Production	195
4.6.4. Jadomycin TFAL (3.1)	197
4.6.5. Jadomycin TFAL Lactam (3.2).....	197
4.6.6. Jadomycin Furan Aldehyde (3.3).....	197
4.6.7. Jadomycin Furan Alcohol (3.4)	197
4.6.8. Microbroth Antimicrobial Assay	205
4.6.9. Cell Toxicity Assay	206
4.6.10. NCI-60 Cancer Cell Line Screening	207
4.7. Experimental for Chapter 3.3	207

4.7.1. Culture Conditions for Small Scale Jadomycin Productions	207
4.7.2. Work-up for Small Scale Jadomycin Productions.....	208
4.7.3. Scale-Up Jadomycin Production with <i>S. venezuelae</i> Δ <i>jadT</i>	208
4.7.4. Extraction of Natural Products from Bacterial Cultures.....	209
4.7.5. Purification of Glucosylated Jadomycin DS (3.9)	209
4.7.6. Preparation of conjugation vector pKC1139 Δ <i>sv0189</i>	212
4.7.7. Preparation of conjugation vector pKC1139 Δ <i>jadS</i> Δ <i>jadT</i>	213
4.7.8. Generation of <i>S. venezuelae</i> Δ <i>jadS</i> Δ <i>jadT</i> , <i>S. venezuelae</i> Δ <i>jadT</i> Δ <i>sv0189</i> , and <i>S. venezuelae</i> Δ <i>sv0189</i> strains	213
4.8. Experimental for Chapter 3.4	214
4.8.1. Assembly of pKC1139:: <i>jadUV</i>	214
4.8.2. Assembly of pKC1139:: <i>kijC3</i>	215
4.8.3. Assembly of pKC1139:: <i>kijC4</i>	215
4.8.4. Assembly of pKC1139:: <i>kijC4kijC3</i>	216
4.8.5. Assembly of pKC1139:: <i>kijC4(XhoI)</i>	217
4.8.6. Assembly of pKC1139 Δ <i>jadV</i>	217
4.8.7. Assembly of pSE34:: <i>kijC4</i>	218
4.8.8. Protoplast Formation Protocol	219
4.8.9. <i>S. venezuelae</i> ISP5230 Protoplast Transformation with pSE34:: <i>kijC4</i>	219
4.8.10. Small-Scale Jadomycin Production with Complemented Mutants (Method 1)	220
4.8.11. Scaled-Up Production with <i>S. venezuelae</i> :: <i>kijC4</i>	220

4.8.12. Scaled-Up Production with <i>S. venezuelae</i> $\Delta jadV$	222
4.8.13. NaBD ₄ reaction with Product from up <i>S. venezuelae</i> $\Delta jadV$	223
CHAPTER 5: CONCLUSIONS AND FUTURE DIRECTIONS	224
REFERENCES	232
APPENDIX A: SUPPLEMENTARY MATERIALS FOR CHAPTER 2.2.	248
APPENDIX B: SUPPLEMENTARY MATERIALS FOR CHAPTER 2.3.	264
APPENDIX C: SUPPLEMENTARY MATERIALS FOR CHAPTER 2.4	271
APPENDIX D: SUPPLEMENTARY MATERIALS FOR CHAPTER 2.5	274
APPENDIX E: SUPPLEMENTARY MATERIALS FOR CHAPTER 3.2	278
APPENDIX F: SUPPLEMENTARY MATERIALS FOR CHAPTER 3.3.....	303
APPENDIX G: SUPPLEMENTARY MATERIALS FOR CHAPTER 3.4	314

List of Tables

Table 1. Evaluation of Glc 1-P analogues as Cps2L substrates.....	32
Table 2. Kinetic parameters for Cps2L substrates.	36
Table 3. Inhibition constants 2.4 and 2.6 with Cps2L.....	37
Table 4. Substrate scope assay ^a with RmlB, RmlC and RmlD.	55
Table 5. GT1 family glycosyltransferases in the <i>S. venezuelae</i> ISP5230 (ATCC 10712) genome.	66
Table 6. Sv0189 kinetics with UDP and 2-chloro-4-nitro-phenol- β -D- glucopyranoside (pH 8.0).	74
Table 7. HPLC data from initial Sv0189 acceptor screen after 24 h.	83
Table 8. Antimicrobial assay results for 3.1 and 3.2 against Gram-positive MRSA, <i>S. warneri</i> and VRE.....	111
Table 9. Antimicrobial assay results for 3.1 and 3.2 against Gram-negative <i>P. aeruginosa</i> and <i>P. vulgaris</i> , and yeast strain <i>C. albicans</i>	111
Table 10. Cell toxicity assays for 3.1 and 3.2	112
Table 11. Methods for heterologous gene complementation in <i>Streptomyces</i>	128
Table 12. Strains and plasmids in this thesis.	167
Table 13. NMR characterization data for 3.1	197
Table 14. NMR characterization data for 3.2	200
Table 15. NMR characterization data for 3.3	202
Table 16. NMR characterization data for 3.4	204
Table 17. NMR characterization data for 3.9	211

List of Figures

Figure 1. Carbohydrate derived drugs in clinical use.	2
Figure 2. Carbohydrate monomers in eukaryotic glycans.....	4
Figure 3. (A) A generalized biosynthetic pathway for bacterial deoxysugars; (B) examples of the diversity of deoxysugars derived from NDP-4-keto-6-deoxy- α -D-glucose.....	5
Figure 4. (A) Targets for inhibition in peptidoglycan biosynthesis; (B) Bacterial cell wall biosynthesis inhibitors.	7
Figure 5. (A) Glycolipids associated with bacteria by classification type; (B) Examples of carbohydrates that are associated with the glycoproteins of pathogenic strains.....	9
Figure 6. Examples of bioorthogonal and precursor directed approaches for glycan biosynthetic studies. (A) Staudinger ligation; (B) oxime ligation; (C) precursors and sugar nucleotides, the latter generated <i>in situ</i> , employed as glycosyltransferase inhibitors; (D) the oxo-carbenium intermediate of inverting glycosyltransferases..	11
Figure 7. Glycosylated drugs and the bacteria from which they were originally isolated.	14
Figure 8. Doxorubicin and sugar modified analogues.	15
Figure 9. Method of “neoglycorandomization” used to generate digitoxin library.	16
Figure 10. Glycodiversification of streptolydigin analogues by combinatorial biosynthesis.	17
Figure 11. Glycosyltransferase activity of GFT-D(M4) with 4-methylumbelliferone and sucrose.	18
Figure 12. (A) The physiological reaction catalysed by Cps2L; (B) The mechanistic transition state in the Cps2L reaction mechanism; (C) Examples of sugar phosphates and phosphonates that have been identified as Cps2L substrates.	25

Figure 13. Enzymatic synthesis of dTDP-Rha by <i>P. aeruginosa</i> .	26
Figure 14. LPS core structures of <i>P. aeruginosa</i> strain PAO1. Rha unit installed by rhamnosyltransferases MigA and WapR.	28
Figure 15. Glc 1-P analogues 2.1-2.6 evaluated as Cps2L substrates and/or inhibitors.	30
Figure 16. Coupled spectrophotometric enzyme assay to measure Cps2L activity using PNP and XO to detect released phosphate.	34
Figure 17. Kinetic inhibition assays in the presence of constant dTTP (1 mM) and variable 2.4, 2.5 and 2.6 .	38
Figure 18. A simplified representation of magnetization transfer in waterLOGSY NMR.	40
Figure 19. WaterLOGSY NMR spectra with 2.6 and Cps2L.	41
Figure 20. Determination of K_d for 2.6 binding to Cps2L in the presence of dTTP.	43
Figure 21. Ordered Bi-Bi reaction mechanism of Cps2L.	47
Figure 22. Catalysis by Cps2L (i) physiological reaction and (ii-iv) plausible reaction pathways and products for the reaction between Glc 1-P and p ₄ dT catalysed by Cps2L.	48
Figure 23. Thymidyltransferase-catalysed production of dTDP-Glc from p ₄ dT and Glc 1-P.	49
Figure 24. Thymidyltransferase catalysed production of triphosphate (P ₃) from p ₄ dT.	51
Figure 25. Analytical scale RmlB-D assay.	54
Figure 26. Precursor scan of m/z 321 (LCMS, negative mode) for the reaction of dTTP and (A) Glc 1-P or (B) 2.18 with Cps2L, RmlB, RmlC and RmlD.	59
Figure 27. Proposed enzyme mechanisms of (A) RmlB, (B) RmlC, and (C) RmlD.	62

Figure 28. (A) Chemo-enzymatic synthesis of dTDP-1C-Rha; (B) $^{31}\text{P}\{^1\text{H}\}$ NMR spectrum (200 MHz, D_2O) and (C) HPLC trace of purified dTDP-1C-Rha.	64
Figure 29. Glucosylation of oleandomycin by OleD.	67
Figure 30. Characterized natural products produced by <i>S. venezuelae</i> ISP5230 and corresponding gene clusters.	69
Figure 31. Pairwise protein alignment of Sv0189 and OleD.	70
Figure 32. TAE-agarose (1%) DNA gels showing restriction digests in screening for pET28a::NHis ₆ Sv0189.	71
Figure 33. SDS-PAGE showing fractions from Sv0189 protein expression.	73
Figure 34. Sv0189 activity in various buffers and pH values.	75
Figure 35. Glycosyltransferase activity detection assay with 4-methylumbelliferone (A11).	76
Figure 36. General scheme for Sv0189 primary screening assay.	77
Figure 37. Bar graph ranking acceptors from series A.	79
Figure 38. Bar graph ranking acceptors from series B.	81
Figure 39. Bar graph ranking acceptors from series C.	82
Figure 40. Appearance of wells for select acceptors, positive control (A11), and negative control (DMSO), in the absence (-) and presence (+) of Sv0189.	84
Figure 41. Secondary acceptor screening assay for Sv0189.	85
Figure 42. HPLC traces from secondary screen of Series A (select examples).	86
Figure 43. HPLC traces from secondary screen of Series B (select examples).	86
Figure 44. HPLC traces from secondary screen of Series C (select examples).	87

Figure 45. (A) Generic jadomycin structure with labelled ABCDE rings; (B) structure of JdB ; (C) Proposed spontaneous mechanism for E-ring formation.	89
Figure 46. Structures of oxazolidine-ring containing jadomyicins JdS , JdDS , JdT , and JdDT	90
Figure 47. Scope of jadomycin analogues derived from precursor-directed amino acid incorporation.	91
Figure 48. Genes related to L-digitoxyl biosynthesis in <i>S. venezuelae</i> (inset) and scheme depicting the reactions catalysed by pathway enzymes.	92
Figure 49. Jadomyicins with modified sugar moieties.	93
Figure 50. Jadomyicins 3.1-3.4 isolated from a culture with TFAL.	97
Figure 51. The jadomycin derived from L-ornithine, JdOct , and structures for the jadomycin derived from L-lysine, JdKα , and JdKϵ	98
Figure 52. TLC plates from indicated purification steps for 3.1-3.4 and NMR tubes showing colour of isolated products in solution.	100
Figure 53. Irradiation of the 3a proton at 5.67 ppm of the major 3.1 diastereomer and at 5.72 ppm in the minor compound.	101
Figure 54. $^{19}\text{F}\{^1\text{H}\}$ NMR spectra (470 MHz) in methanol- <i>d</i> ₄ (A) jadomycin TFAL 3.1 , a mixture of 3a <i>S</i> /3a <i>R</i> diastereomers; (B) jadomycin lactam 3.2	102
Figure 55. 1- ^{13}C glucose metabolism by <i>S. venezuelae</i> and incorporation in jadomyicins.	103
Figure 56. ^{13}C incorporation in 3.2	104
Figure 57. Key HMBC correlations showing amide connectivity in ^{13}C -labelled 3.2 . (700 MHz, methanol- <i>d</i> ₄)	105
Figure 58. Key HMBC correlation demonstrating the presence of an aldehyde functional group in 3.3 . (700 MHz, chloroform- <i>d</i> ₃)	106

Figure 59. (A) Expansion of an edited-HSQC spectrum of the yellow precipitate containing compounds 3.3 and 3.4 (B) expansion of a COSY NMR spectrum of the yellow precipitate 3.4 . (700 MHz, chloroform- <i>d</i> ₃)	107
Figure 60. Proposed mechanistic origin of jadomycins 3.1-3.4 based on common biosynthetic intermediate 3.6 . It is plausible that 3.7 is the common biosynthetic intermediate for 3.1-3.4	109
Figure 61. Structure of glucosylated jadomycin DS (3.9) and HMBC expansion showing attachment of the glucose moiety at C12 of the angucycline ring.....	115
Figure 62. LC-MS ² fragmentation of 3.9	116
Figure 63. TAE-agarose gel showing PCR amplification products with appropriate flanking primers for <i>S. venezuelae</i> wild-type, Δ <i>jadT</i> , Δ <i>sv0189</i> , Δ <i>jadT</i> Δ <i>sv0189</i> and Δ <i>jadS</i> Δ <i>jadT</i>	118
Figure 64. HPLC traces of the methanol extract from the phenyl column for <i>S. venezuelae</i> wild-type, Δ <i>jadT</i> , Δ <i>sv0189</i> , Δ <i>jadT</i> Δ <i>sv0189</i> and Δ <i>jadS</i> Δ <i>jadT</i>	120
Figure 65. Left: Jadomycin cultures after 48 h. Centre: TLC showing extracts alongside standards for jadomycin DS (JdDS) and glucosylated jadomycin DS (3.9); Right: TLC for wild-type JdDS , and jadomycin aglycone from the Δ <i>jadS</i> Δ <i>jadT</i> strain	121
Figure 66. Examples of glycodiversification by combinatorial biosynthesis.....	123
Figure 67. Structures of natural products decorated with α -L-digitoxose.....	125
Figure 68. Sequence identity alignments between biosynthetic glycosyltransferases in jadomycin (Sv5997), lobophorin, and kijanimicin gene clusters, and Sv0189 (<i>S. venezuelae</i> GT1 family glycosyltransferase).....	126
Figure 69. (A) Proposed glycosylation by KijC4 (pink) and KijC3 (blue); (B) Anticipated structure of a modified jadomycin.....	126
Figure 70. L-digitoxose biosynthetic gene cluster from the wild-type strain with structural genes shaded in blue and regulatory genes in green.	132
Figure 71. <i>S. venezuelae</i> :: <i>kijC3</i> cultured with D-serine.....	137

Figure 72. <i>S. venezuelae::kijC3-2</i> , <i>S. venezuelae::kijC3-4</i> , and wild-type cultures with TFAL.	139
Figure 73. <i>S. venezuelae::kijC3-2</i> , <i>S. venezuelae::kijC3-4</i> , and wild-type cultures with ABA.	141
Figure 74. LCMS precursor 306 (positive) scan of the methanol extract from an <i>S. venezuelae::kijC3-2</i> culture with ABA and proposed structures corresponding to the observed <i>m/z</i> signals.	142
Figure 75. <i>S. venezuelae::kijC4-1</i> , <i>S. venezuelae::kijC4-2</i> , <i>S. venezuelae::kijC4kijC3</i> , wild-type <i>S. venezuelae::kijC4</i> (XhoI), <i>S. venezuelae ΔjadV-1</i> , <i>S. venezuelae ΔjadV-2</i> , and wild-type cultures with D-serine.	145
Figure 76. <i>S. venezuelae::kijC4-2</i> cultured with L-Ile and L-Phe.	146
Figure 77. LCMS precursor scans with parent ion <i>m/z</i> 306 (positive) of (A) JdDS from wild-type strain; (B) methanol extract from <i>ΔjadV</i> strain, (C) reaction mixture of extract from <i>ΔjadV</i> strain with NaBD ₄	147
Figure 78. N-terminal protein sequence alignments of old and new JadV protein sequences against other 4-ketoreductases.	148
Figure 79. Possible sugar nucleotides produced as a result of <i>jadV</i> deletion.	149
Figure 80. Expansion of ¹ H NMR spectra of JdDS from the wild-type strain, of the purified material from <i>S. venezuelae ΔjadV</i> and of the purified material from the <i>S. venezuelae::kijC4</i> strain. L-digitoxose and 2,6-dideoxy-D-erythro-4-hexulose are shown in the panel.	150
Figure 81. Standard curve used to convert absorbance units (AU) to concentration (μM).	190
Figure 82. Series A chemical structures for Sv0189 acceptor screening.	191
Figure 83. Series B chemical structures for Sv0189 acceptor screening.	192
Figure 84. Series C chemical structures for Sv0189 acceptor screening.	193
Figure 85. Summary of hexose 1-phosphate and NTP substrates evaluated with Cps2L.	225

Figure 86. Summary of substrate scope study with RmlB, RmlC and RmlD.	227
Figure 87. Conceptual example of aglycone exchange using JadS, the glycosyltransferase from jadomycin biosynthesis, and Sv0189.	228
Figure 88. (A) Recently described jadomycin lactam congeners; (B) jadomycin ring scaffolds.	229
Figure 89. Proposed general scheme for precursor-directed approach to jadomycin glycodiversification.	230

Abstract

Carbohydrates are ubiquitous in biological systems, possessing diversity in terms of both structure and function. Studies pertaining to bacterial enzymes that recognize and process carbohydrates in cell wall biosynthesis and secondary metabolism are presented in this thesis.

L-rhamnose (Rha) is a carbohydrate monomer that serves as a building block in the cell wall-associated glycans of pathogenic bacteria. Gene products involved in Rha biosynthesis (RmlA-D) are essential for virulence and represent attractive targets for antibacterial development. These enzymes were evaluated with a series of substrate analogues to probe their substrate specificity. The RmlA/Cps2L enzyme was highly tolerant to substrate changes, whereas the RmlB-D enzymes were stringent in terms of their ability to turn over unnatural substrates. All enzymes in the Rml pathway turned over the phosphonate analogue of Glc 1-P enabling the chemo-enzymatic preparation of the phosphonate analogue of dTDP-Rha.

A number of bacterial secondary metabolites are glycosylated, including the jadomycins, a family of angucycline antibiotics produced by *Streptomyces venezuelae* ISP5230. Using precursor-directed biosynthesis, two jadomycin derivatives incorporating *N* ϵ -trifluoroacetyl-L-lysine (TFAL) were isolated, a jadomycin with the usual oxazolone ring and a 3a oxidized analogue. In the same production, two shunt products containing a furan B-ring were isolated, representing a new scaffold for angucyclines. A jadomycin decorated with D-glucose, in place of L-digitoxose, was isolated from a strain bearing a deletion of the biosynthetic 4,6-dehydratase gene. The glycosyltransferase JadS was identified as the catalyst responsible for appending the glucose moiety, demonstrating flexibility towards sugar donors. Studies towards the complementation of *S. venezuelae* with an iterative L-digitoxyltransferase from the kijanimicin gene cluster are described. Finally, the *S. venezuelae* GT1 family glycosyltransferase Sv0189 was characterized as a UDP-glycosyltransferase with a broad acceptor scope.

Overall, this work has characterized the substrate scope of several bacterial carbohydrate-recognizing enzymes that will serve as a basis for inhibitor design or for use in chemo-enzymatic applications.

List of Abbreviations and Symbols Used

A	absorbance
Au	unit of absorbance
ABA	4-amino butanoic acid
Ac	acyl
Amp	ampicillin
Apr	apramycin
APS	ammonium persulfate
bp	base pair
Dnase	deoxyribonuclease
Bn	benzyl
br	broad
Cam	chloramphenicol
CAZy	carbohydrate active enzyme
CIP	calf intestinal pyrophosphatase
COSY	correlation spectroscopy
Cps2L	thymidyltransferase from <i>Streptococcus pneumoniae</i>
CV	column volume(s)

δ	chemical shift
d	doublet
DATDH	2,4-diacetamido-2,4,6-trideoxy- α -D-hexose
DMSO	dimethylsulfoxide
DNA	deoxyribonucleic acid
dNTP	deoxy nucleoside 5'-triphosphate
dTDP	deoxythymidine 5'-diphosphate
dTDP-1C-Glc	deoxythymidine 5'-diphosphono α -D-glucopyranoside
dTMP	deoxythymidine 5'-monophosphate
dTTP	deoxythymidine 5'-triphosphate
ϵ	extinction coefficient
EC	enzyme classification
EDTA	ethylenediaminetetraacetic acid
EPI	enhanced product ion
ESI	electrospray ionization
EU	enzyme unit
EWG	electron withdrawing group
FucNAc	<i>N</i> -acetyl-L-fucosamine

Gal	D-galactose
Gal 1-P	α - D-galactose 1-phosphate
Glc	D-glucose
Glc 1-P	α - D-glucose 1-phosphate
GlcN	D-glucosamine
GlcNAc	<i>N</i> -acetyl-D-glucosamine
h	hour
His ₆	hexa-histidine tag
HMBC	heteronuclear multiple bond correlation
HPLC	high performance liquid chromatography
HRMS	high resolution mass spectrometry
IC ₅₀	half maximal inhibitory concentration
IPP	inorganic pyrophosphatase from <i>Escherichia coli</i>
IPTG	isopropyl β -D-1-thiogalactopyranoside
JadS	L-digitoxyltransferase from <i>Streptomyces venezuelae</i>
JadT	NDP-4,6-dehydratase from <i>Streptomyces venezuelae</i>
Jd	jadomycin
Kan	kanamycin

kb	kilobase
k_{cat}	enzyme turnover number
K_{d}	dissociation constant
K_{m}	Michaelis constant
K_{i}	inhibition constant
LB	lysogeny broth
LC	liquid chromatography
LPS	lipopolysaccharide
LRMS	low resolution mass spectrometry
m	multiplet
m/z	mass to charge ratio
Man	D-mannose
MESG	2-amino-6-mercapto-7-methylpurine ribonucleoside
MHz	megahertz
MIC	minimum inhibitory concentratin
MigA	rhamnosyltransferase from <i>Pseudomonas aeruginosa</i>
min	minute
MOPS	3-morpholinopropane-1-sulfonic acid

Nal	nalidixic acid
MRSA	methicillin-resistant <i>Staphylococcus aureus</i>
MurNAc	<i>N</i> -acetylmuramic acid
MS	mass spectrometry
MS ²	tandem mass spectrometry
MSM	minimal salt media
MWCO	molecular weight cut-off
MYM	malt yeast maltose
NAD	nicotinamide adenine dinucleotide
NADH	reduced nicotinamide adenine dinucleotide
NDP	nucleoside diphosphate
NMR	nuclear magnetic resonance
NCBI	National Center for Biotechnology Information
nOe	nuclear Overhauser effect
NTP	nucleoside triphosphate
OD	optical density
OleD	glycosyltransferase from <i>Streptomyces antibioticus</i>
OS	oligosaccharide

P ₃	triphosphate
p ₄ dT	deoxythymidine 5'-tetrphosphate
PAGE	polyacrylamide gel electrophoresis
PBS	phosphate buffered saline
PCR	polymerase chain reaction
pH	potential of hydrogen
P _i	inorganic phosphate
PKS-II	polyketide synthetase type II
PP _i	diphosphate
PNP	purine nucleoside phosphorylase from human
ppm	parts per million
q	quartet
qPCR	quantitative PCR
R _f	retention factor
Rha	L-rhamnose
Rha-1C-P	β- L-rhamnose 1-phosphonate
RmlA	thymidyltransferase from <i>Pseudomonas aeruginosa</i>
RmlB	dTDP-Glc 4,6-dehydratase from <i>Pseudomonas aeruginosa</i>

RmlC	dTDP-Glc 3,5-epimerase from <i>Pseudomonas aeruginosa</i>
RmlD	dTDP-Glc 4-ketoreductase from <i>Pseudomonas aeruginosa</i>
RNA	ribonucleic acid
rpm	rotation per minute
R _T	retention time
s	singlet (NMR assignments) or second (time unit)
SAR	structure activity relationship
SDS	sodium dodecyl sulfate
S _N 2	bimolecular reaction
SOC	super optimal broth with catabolite suppression
Sv0189	glycosyltransferase from <i>Streptomyces venezuelae</i>
t	triplet
TOF	time-of-flight
TAE	tris-acetate-EDTA buffer
TBA	tributylammonium
TEMED	<i>N,N,N',N'</i> -tetramethylethane-1,2-diamine
TFAL	<i>Nε</i> -trifluoroacetyl- L-lysine

TLC	thin layer chromatography
Tris	2-amino-2-(hydroxymethyl)propane-1,3-diol
Tsr	thiostrepton
UDP	uridine diphosphate
und	undecaprenyl
UTP	uridine triphosphate
UV	ultraviolet
v/v	volume per volume (%)
v/w	volume per weight (%)
VRE	vancomycin-resistant enterococci
WapR	rhamnosyltransferase from <i>Pseudomonas aeruginosa</i>
waterLOGSY	water-ligand observed <i>via</i> gradient spectroscopy
XO	xanthine oxidase from bovine milk
Xyl	D-xylose

Acknowledgments

Foremost, I am gratefully indebted to my supervisor, David Jakeman, for his mentorship and guidance over the years and for providing me with countless opportunities to improve and hone my skills and knowledge.

The work presented in this thesis demanded a great deal of collaborative effort and would not have been accomplished without the contributions of various individuals. I'd like to thank my colleagues, past and present, for making the lab a supportive and pleasant work environment. There are some colleagues to whom I am particularly indebted: Dr. Andrew Robertson for always sharing his enthusiasm (and expertise!) on all aspects surrounding natural products; Dr. Deborah Smithen for providing me with many interesting molecules to assay (Section 2.2-2.3); and Dr. Jian-She Zhu for insightful discussions and for synthesizing the compounds evaluated in Section 2.4. Many thanks are owed to the undergraduates who contributed to these studies. Alison Jee is recognized for her tremendous eye for detail and persistence in developing kinetic experiments (Section 2.2). I'd also like to acknowledge Alison for providing the enzymes used in biochemical assays (Section 2.2-2.3). Jungwook Na is thanked for assistance with jadomycin isolation in Section 3.3. Farren Clarke assisted with the molecular biology described in Section 2.5. Additional thanks are extended to current group members Madison Carroll and Brandon Groves, and to former group member Andrew Robertson for proof reading portions of this thesis.

Dr. David Overy and Dr. Russ Kerr (University of Prince Edward Island) are thanked for running antimicrobial assays. Brad Hatli (UPEI) is thanked for

providing guidance and protocols for the genetic manipulation of *Streptomyces* (Section 3.3-3.4), and is thanked along with Dr. Russ Kerr for sending the pSET152 and pSE34 vectors. Our collaborators from Dr. David Palmer's research group (University of Saskatchewan) are thanked for synthesis of the compounds assayed in Section 2.2. Ray Syvitski and Nadine Merklely from NRC Halifax helped with the implementation of waterLOGSY experiments. I would like to extend thanks to Xiao Feng for running high-resolution mass spectrometry samples and to Mike Lumsdem (Dalhousie University), Ian Burtan (NRC Halifax), and Camilo Martinez-Farina (NRC Halifax) for support with NMR experiments. I'd like to thank my committee members, Dr. Bruce Grindley, Dr. Stephen Bearne, and Dr. Alison Thompson for their input and support. I am grateful for the financial assistance provided by the Beatrice Hunter Research Foundation CRTP program, funded by the Canadian Cancer Society (Nova Scotia Division) and The Killam Trusts. Finally, I'd like to thank my friends and family for bearing with me on this journey.

Chapter 1: Introduction

As our understanding of biological systems expands evermore into the realm of genetics, the need to study systems at a biochemical and atomic level has not dissipated, rather the contrary.¹ On a continuing basis, small molecules are required to study pathways, to treat diseases, for use as biomarkers, as diagnostic tools, and in countless industrial applications. The study of carbohydrates in biological systems, termed glycobiology, imposes unique challenges and relies heavily on a chemistry toolkit; unlike DNA, automated methods for sequencing glycans (polysaccharides) are not available, and unlike proteins, building block (monomer) sequences cannot be read from a genetic template. “Glycoconjugate” is a term that applies to a biological compound containing a sugar moiety; these include glycosylated proteins, nucleic acids, lipids, and secondary metabolites. Carbohydrates are ubiquitous in cells; glycans and glycoconjugates serve vital functions in cellular systems, for energy storage, structural integrity, signaling, recognition, virulence, and protection.² The roles of glycans in immune recognition and pathway signaling have attracted interest from the scientific community as targets for therapeutic development. For example, the study of interactions between cell-surface glycans and recognition enzymes (lectins) are being studied as an avenue for cancer treatment.² Understanding the metabolism of carbohydrates by human and microbial digestive tract enzymes could result in improved therapies for the management of diabetes. Carbohydrates themselves may possess bioactive

properties, and a number of carbohydrate-based drugs are available on the market, including heparin, an anticoagulant; oseltamivir and zanamivir, anti-influenza neuraminidase inhibitors; and miglitol, acarbose, and voglibose, α -glucosidase inhibitors used to treat diabetes (Figure 1).²

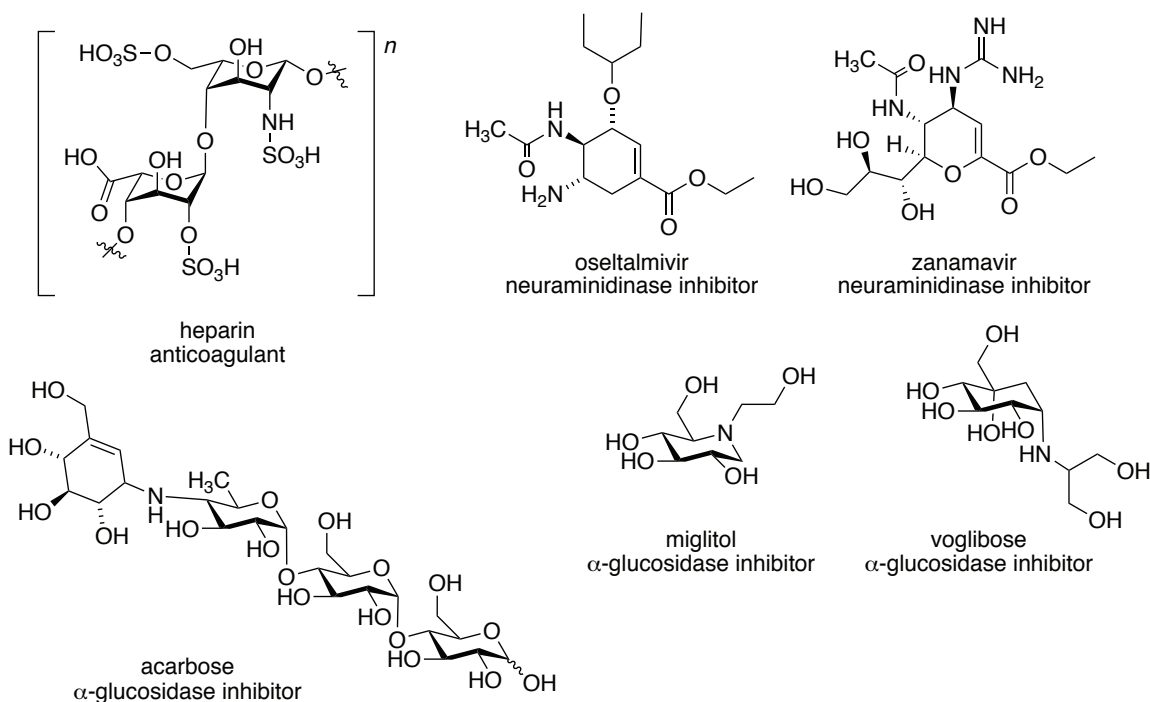


Figure 1. Carbohydrate derived drugs in clinical use.

An array of enzymes are involved in the biosynthesis of glycoconjugates; these include the glycosyltransferases that control the transfer of sugars to a respective acceptor molecule, be it a protein, lipid, small molecule, or oligosaccharide, the large number of enzymes that manipulate the hexose ring, including epimerases, dehydratases, reductases, methyltransferases, etc., and the enzymes that produce the activated sugar donors that serve as glycosyltransferase substrates, such as nucleotidyltransferases. The study of these enzymes not only sheds light on the biological systems in which they function, but also serve as a

basis for exploiting these systems for various applications. Use of biosynthetic enzymes in chemo-enzymatic synthesis provides access to molecules that may be challenging to prepare synthetically and can be used to obtain unnatural analogues.^{3,}

4

There are significant differences in the ways in which organisms utilize carbohydrates, depending upon their prevalence, chemical structures of carbohydrate monomers, patterns of monomer assembly in polysaccharides, and functions within the living system. The carbohydrates that play a role in eukaryotic biology are dominated by ten carbohydrate monomers, with structural variation arising from assembly into oligo- and polysaccharides (Figure 2).⁵ In contrast, 344 structurally unique monomers have been found in prokaryotes, where unusual, complex carbohydrates are predominantly associated with glycans found on the bacterial cell wall or with secondary metabolites.⁶ This has implications for the development of antibiotics, as it is now well recognized that antibiotic resistance poses a widely distributed and significant threat to human health, a problem that requires new interventions.^{7, 8}

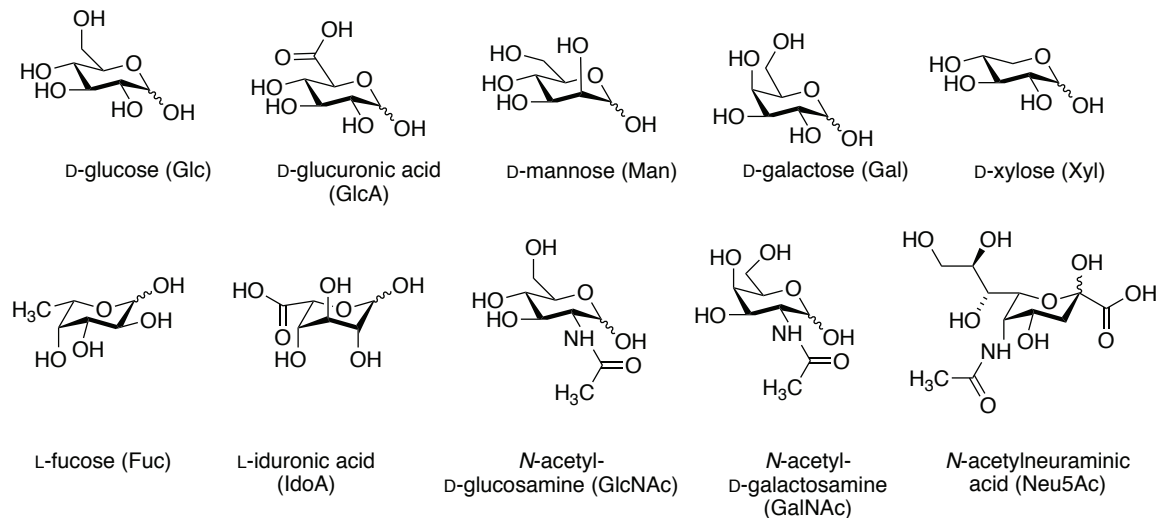


Figure 2. Carbohydrate monomers in eukaryotic glycans.

Glucose is biosynthetically converted to NDP-4-keto-6-deoxy- α -D-glucose, a key intermediate that is common to many bacterial deoxysugar pathways.⁹ The diversity observed in the final monosaccharides arises from additional tailoring enzymes, usually lacking eukaryotic homologues; bacterial sugars can possess various modifications including keto, nitro, amine, and deoxy groups (Figure 3).¹⁰⁻¹² Bacterial secondary metabolites are produced by bacteria in response to environmental stress, and are widely believed to serve as a defense mechanism as they often possess antibacterial and antifungal properties that ward off competing species. Other possible roles include quorum sensing, nutrient response, and communication. Unlike primary metabolites, these molecules are not required to support essential cell functions. Befitting their role in defense, bacterial secondary metabolites possess bioactive properties that render them amenable to development as human therapeutic agents.

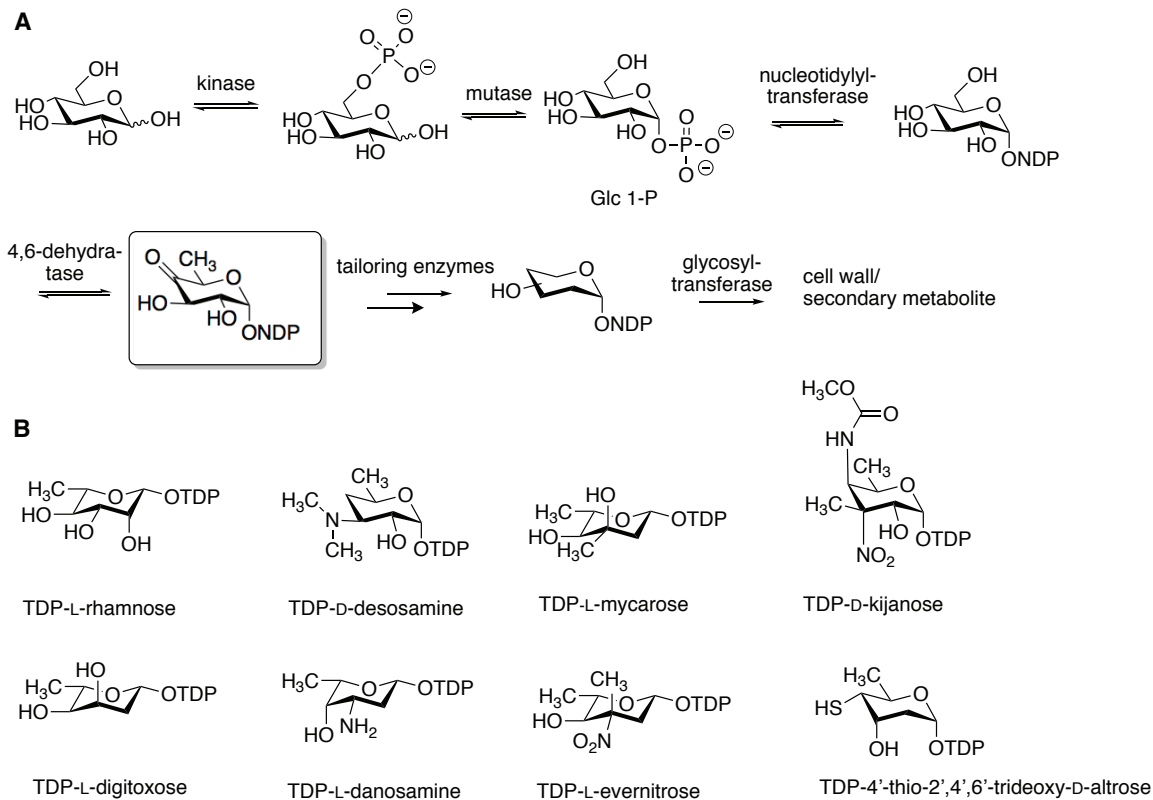


Figure 3. (A) A generalized biosynthetic pathway for bacterial deoxysugars; (B) examples of the diversity of deoxysugars derived from NDP-4-keto-6-deoxy- α -D-glucose.

1.1. Inhibition of Bacterial Cell Wall Biosynthesis

The bacterial cell wall is key to structural integrity and serves as a protective agent from external stress and osmotic pressure, and is also implicated in pathogenic virulence.¹³ The cell wall as a structure is present in all bacteria, including Gram-positive (i.e. *Streptococcus pneumoniae*), Gram-negative (i.e. *Pseudomonas aeruginosa*) and mycobacterial strains (i.e. *Mycobacterium tuberculosis*), although the chemical composition of the cell membranes and associated glycans are highly

variable between types.¹⁴ Many antibiotics act by inhibiting or interrupting cell wall biosynthesis, thus several of these pathways are established drug targets.¹⁵

Key to bacterial virulence and protection is the peptidoglycan layer, a polymer that consists of alternating monomers of *N*-acetylglucosamine (GlcNAc) and *N*-acetylmuramic acid (MurNAc), which are cross-linked by pentapeptide bonds, and that constitute an essential component of bacterial cell walls (Figure 4A). β -Lactams, such as penicillin, function by inhibiting the cross-linking of peptidoglycan units, resulting in weakening and lysis of the cell wall causing bacterial death.¹⁵

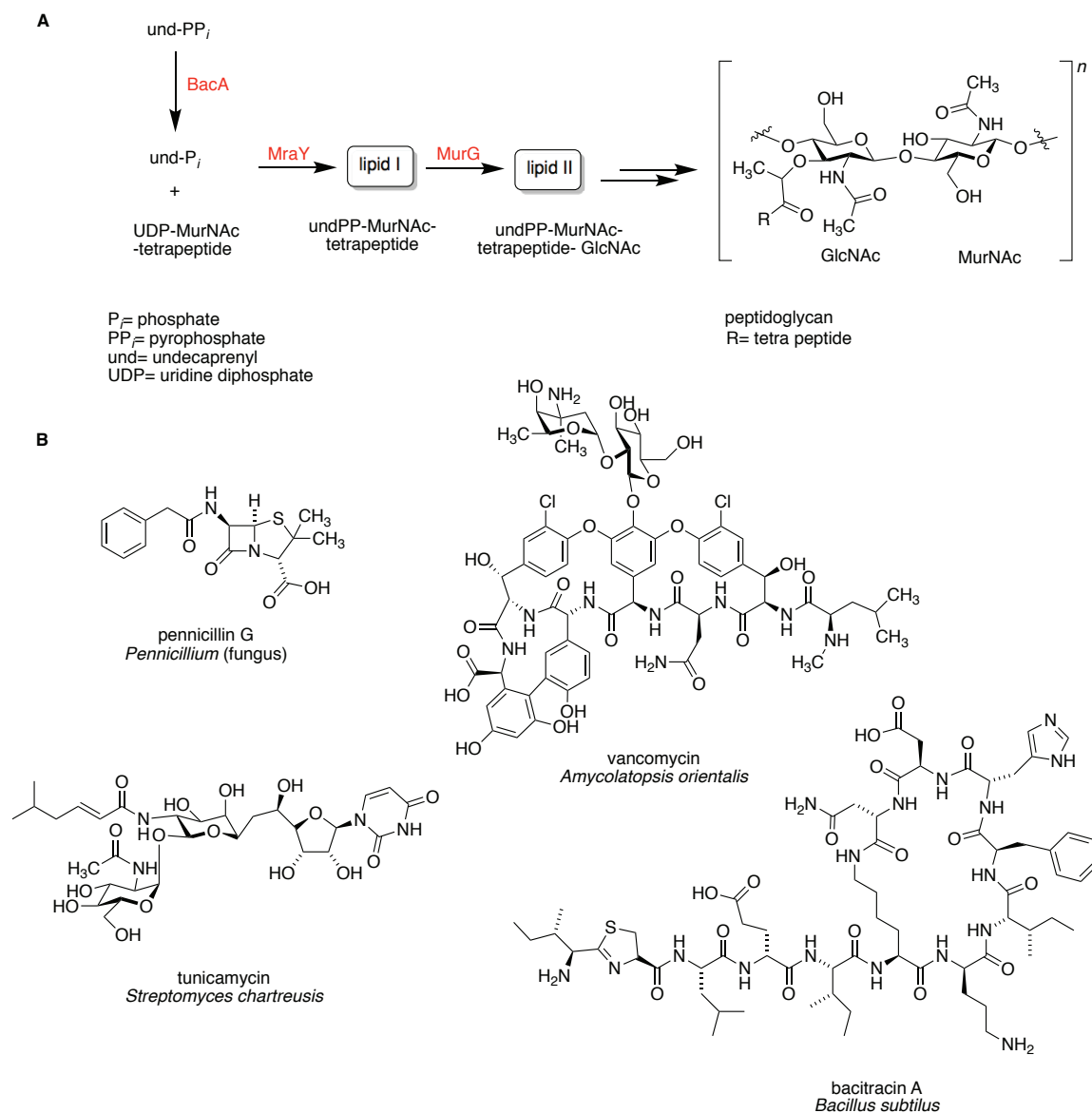


Figure 4. (A) Targets for inhibition in peptidoglycan biosynthesis; (B) Bacterial cell wall biosynthesis inhibitors.

A number of antibiotics have been developed to target various aspects of peptidoglycan biosynthesis, including precursors to peptidoglycan that are lipid-anchored by an undecaprenyl tether and enzymes associated with these biosynthetic intermediates (Figure 4B).¹⁶ Lipid II is the monomeric precursor to peptidoglycan serving as a common, conserved intermediate in bacterial cell wall assembly across

various species, and is a particularly good target for Gram-positive bacteria, which possess an exposed thick peptidoglycan layer at the cell surface. The glycopeptide antibiotic vancomycin, and its closely related structural analogues, bind to lipid II, to prevent the biosynthetic assembly of peptidoglycan.¹⁷ Vancomycin-resistant bacteria possess modified peptidoglycan tetrapeptide structural components that inhibit binding of this class of antibiotic.¹⁶ Lipid II is the mechanistic target of a number of antibiotics, including various glycopeptides, lantibiotics, defensins and teixobactin.¹⁶ Bacitracin, a peptide antibiotic, interferes with peptidoglycan assembly by a different mechanism, by interfering with BacA-mediated dephosphorylation of the isoprenyl carrier that transports peptidoglycan components on the cell surface.¹⁸ Tunicamycin and related analogues represent another class of molecules, fatty acyl nucleosides, that inhibit MraY in the biosynthesis of Lipid I, a precursor to Lipid II.^{19, 20} Tunicamycin also interferes with *N*-glycosylation of proteins, an important post-translational modification in mammalian cells, resulting in significant toxicity that has precluded its implementation into clinical use. This property has served as a tool for studying related biochemical processes in cell lines.^{21, 22}

Broad-spectrum antibiotics are those that target pathways common to most strains of bacteria including peptidoglycan assembly and represent the preferred strategy of the pharmaceutical industry. Emerging health threats such hospital-acquired *Clostridium difficile* infections are associated with over-use of these broad-spectrum antibiotics, and provide a strong case in favor of narrow spectrum antibiotics that target pathogenic bacteria selectively.²³ Glycans that are unique to

specific strain types serve as candidate targets for narrow spectrum-antibiotics. Lipopolysaccharides (LPS) are unique to Gram-negative bacteria and possess variability amongst strains. Teichoic acids are characteristically found on the cell surface of Gram-positive strains, and trehalose-linked lipids are associated with mycobacteria (Figure 5).¹⁴ The presence of rare sugars in the glycans of pathogenic bacteria also present opportunities for tailored approaches, such as *N*-acetyl-L-fucosamine (FucNAc) from *P. aeruginosa* and 2,4-di-acetamido-2,4,6-trideoxyhexose (DATDH) from *Neisseria meningitides*, which are found linked to surface-associated glycoproteins.¹⁴

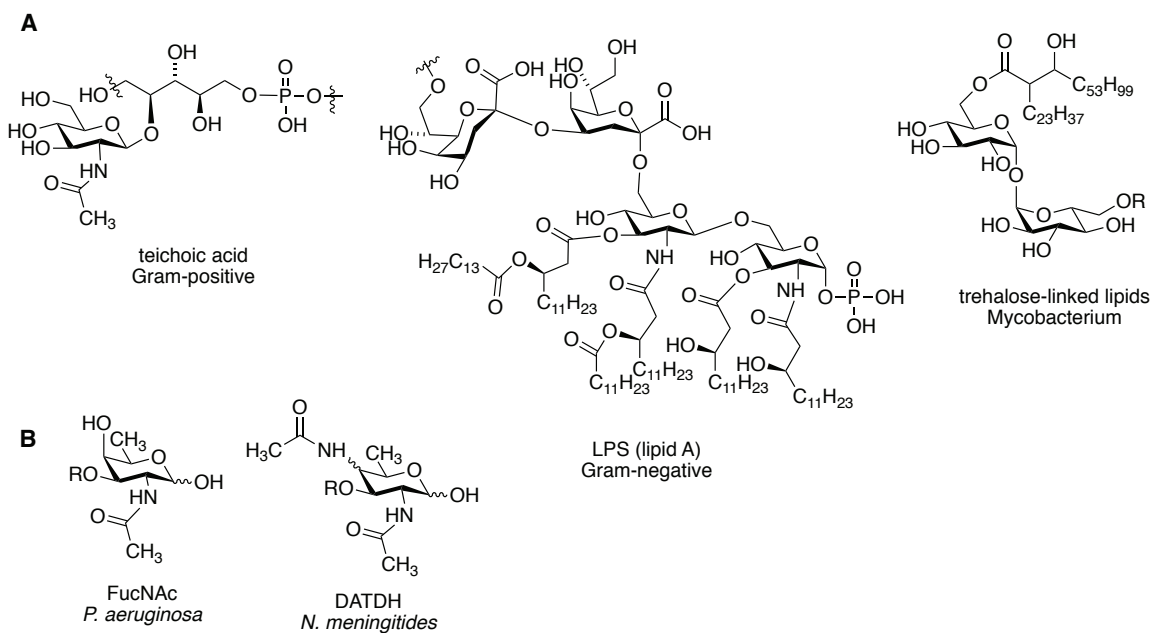


Figure 5. (A) Glycolipids associated with bacteria by classification type; (B) Examples of carbohydrates that are associated with the glycoproteins of pathogenic strains.¹⁴

1.2. Chemical Probes for Glycan Biochemical Pathway Elucidation

The term bioorthogonal encompasses use of chemical probes that undergo reactions within a biological system without otherwise disrupting biochemical processes. The primary focus in the field is in the development of tools to study biochemical pathways. Typically, this is accomplished by introducing a small functionalized molecule (ie. aldehyde, alkyne, azide), that is metabolized in the same manner as an analogous physiological substrate, followed by reaction *in vivo*, usually *via* a click reaction, with a chemical partner that enables visualization of the resultant conjugate. The Bertozzi group, attributed to pioneering bioorthogonal approaches and to coining the term, developed the Staudinger ligation in the early 2000s (Figure 6A).²⁴ Since then, a handful of reactions have been developed by the Bertozzi group and others, and have been well documented in various reviews.²⁵⁻²⁹ It is worth emphasizing the stringent requirements for these reactions that are essentially click chemistry reactions with additional constraints that arise from *in vivo* applications. In short, chemical probes must be reactive at room temperature in aqueous environments near neutral pH, have high target specificity, and produce stable, detectable conjugates all the while being sufficiently fast to react before clearance from the biological system.²⁵ These approaches have been of particular significance for the study of glycans, that are not readily amenable to genetic approaches like proteins are, by providing tools to study the roles of cell surface glycans associated with eukaryotic cells in development and disease.^{28, 30} The Paulson research group has employed a similar strategy to observe sialic acids on the surface of living cells by modification of sialic acids using mild oxidation conditions to introduce an

aldehyde functionality followed by aniline-catalyzed ligation with an aminoxy biotin-tag, enabling visualization (Figure 6 B).³¹

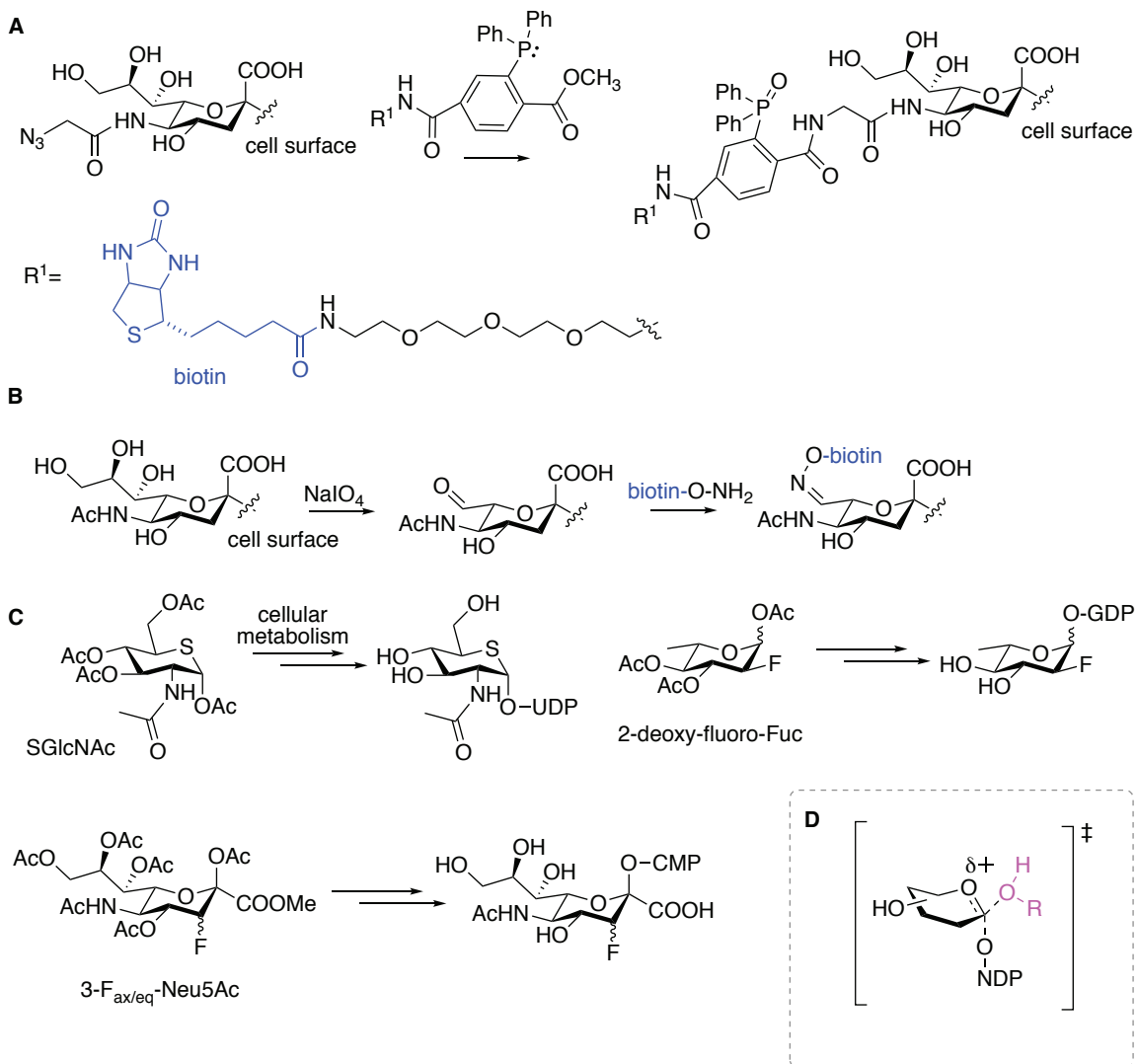


Figure 6. Examples of bioorthogonal and precursor directed approaches for glycan biosynthetic studies. (A) Staudinger ligation; (B) oxime ligation; (C) precursors and sugar nucleotides, the latter generated *in situ*, employed as glycosyltransferase inhibitors; (D) the oxo-carbenium intermediate of inverting glycosyltransferases. NDP= nucleotide diphosphono glucose, where N can be U= uridine, C= cytidine, G= guanidine.

Analogues of physiological substrates may also be used to disrupt or inhibit biochemical pathways. In work by the Vocadlo group, feeding cells a 5-thio-sugar analogue of *N*-acetyl glucosamine enabled the sugar to be metabolized yielding the corresponding sugar nucleotide (Figure 6C). The resulting *in situ* generated sugar nucleotide served as an inhibitor of uridine diphospho-*N*-acetylglucosamine: polypeptide β -*N*-acetylglucosaminyltransferase (OGT), an enzyme involved in glycosylation of various intracellular proteins.³² A similar approach was adapted to the study of sialyl- and fucosyltransferases by the Paulson research group using fluorinated sugar analogues.³³ Both of these studies employ sugar analogues that function as inhibitors by destabilizing the oxo-carbenium intermediate that serves as the key transition state of glycosyltransferases (Figure 6D).³⁴

1.3. Glycosylated Bacterial Secondary Metabolites

Most of the antibiotics described in Section 1.1 were isolated from bacteria or fungi. Humans have long recognized the therapeutic potential of the natural products that surround us, with plants serving as a pillar of traditional medicines.³⁵ The 20th century brought about revolutionary scientific advances that gave human society the tools to mine and exploit these resources, with implications on human health and longevity that are fundamental to modern medicine.³⁶ The importance of natural products is reflected in the number of drugs containing natural product scaffolds; nearly 50% of all of the drugs developed since 1981 are either natural products, semi-synthetic natural product derivatives, or contain a natural-product derived pharmacophore.³⁷ Re-discovery of known compounds and increasing reliance on synthetic libraries for screening purposes resulted in a reduced emphasis on natural

products bioprospecting approaches by pharmaceutical enterprises from the 1980s onward.^{38, 39} However, recent advances in whole genome sequencing, leading to decreased cost and increased availability, have inspired a resurgence of the field.⁴⁰ The genomes of sequenced bacteria often possess multiple gene clusters encoding putative undiscovered natural products, expanding the prospects for discovery of new metabolites and opportunities for combinatorial biosynthesis.^{41, 42}

The appendage of a sugar moiety has been shown to have significant effect on a compound's physiochemical properties, defining its solubility, pharmacology, target-recognition, target-specificity, and toxicity.^{43, 44} Undoubtedly, these properties affect the bioactivity of glycosylated small molecules; many antibiotics, including vancomycin and erythromycin, and many cancer therapeutics such as the calicheamicins, are glycosylated natural products isolated from bacteria (Figure 7).⁴⁵ There are no predictive models to ascertain the role of any specific carbohydrate. Each glycoside, therefore, has to be evaluated on its own terms, offering opportunities to tailor molecular properties through glycosylation. Glycosylated natural products account for 20% of the arsenal of isolated bacterial natural products, and, as previously stated, over 340 distinct carbohydrates are represented within these compounds.⁶ The roles of each of these glycosides are highly varied within an ecological and pharmacological context. Intriguingly, in a 2014 analysis of sequenced bacterial genomes, a significant proportion (40%) of predicted secondary metabolite gene clusters encoded saccharides, compared to only 13% of all characterized gene clusters.⁴¹

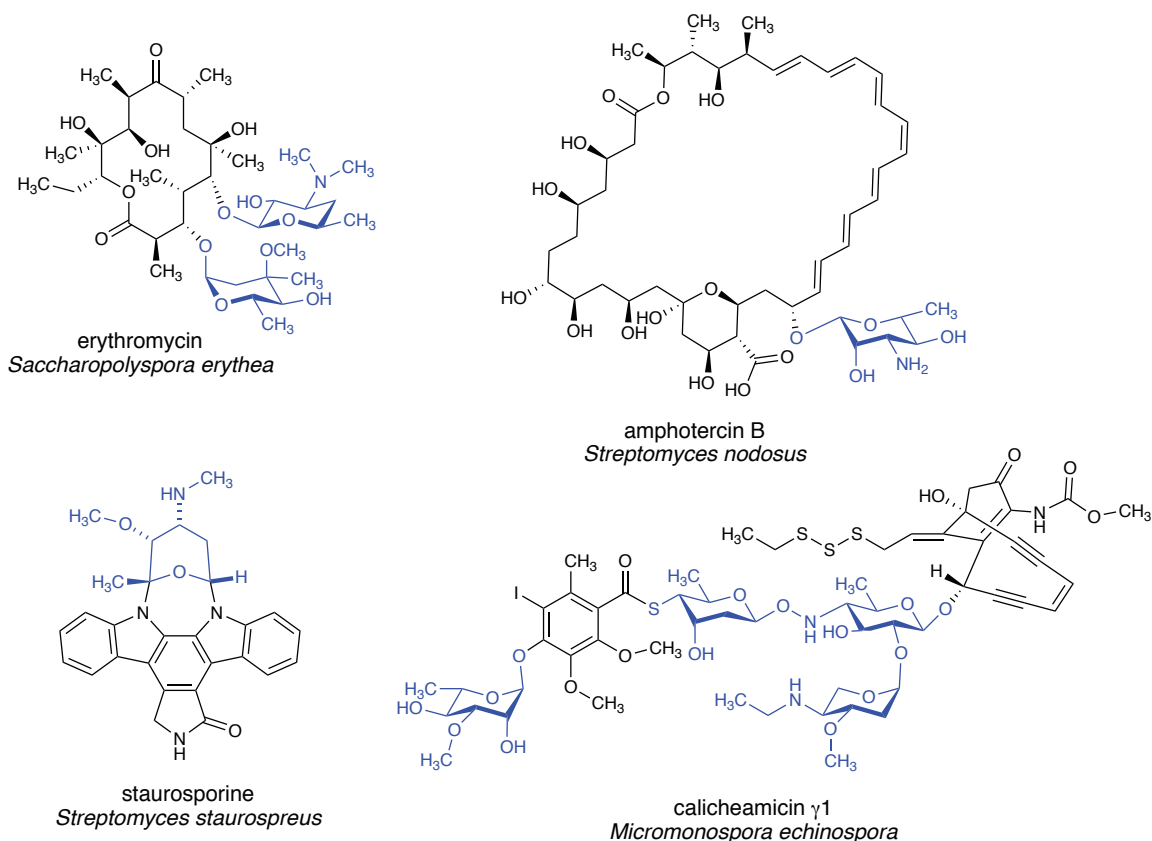


Figure 7. Glycosylated drugs and the bacteria from which they were originally isolated.

Doxorubicin is an anthracycline produced by *Streptomyces pecceticus* used clinically as a chemotherapeutic drug, and cleaves DNA to induce cell toxicity.⁴⁶ Evaluation of structure-activity relationships (SAR) in doxorubicin analogues showcases an early example where the sugar was found to be essential for bioactivity. L-Daunosamine, the natural sugar appended to doxorubicin, was found to enable a strong binding interaction between DNA and doxorubicin. Inversion of the hydroxyl group at the C-4' position of the L-daunorubicin resulted in a small enhancement in activity (*in vitro*), whereas inversion about the C-1' anomeric center resulted in a significant decrease in activity (Figure 8).⁴⁶ A disaccharide analogue of

doxorubicin, sabarubicin, has been shown to possess improved DNA-cleavage capabilities in comparison to the parent compound, and has been carried to phase II clinical trials for solid tumour treatment in Europe.^{47, 48}

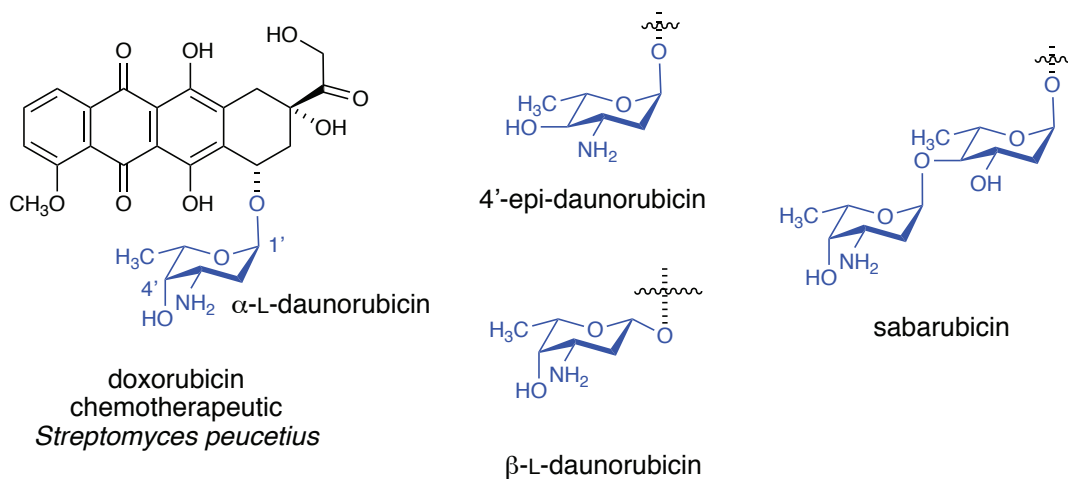


Figure 8. Doxorubicin and sugar modified analogues.

1.3.1. Natural Product Glycodiversification

The diverse array of naturally occurring sugars in prokaryotes, and numerous examples of sugar modification impacting bioactivity, have led to mounting interest in glycodiversification efforts, also referred to as glycorandomization. The methods to diversify carbohydrate structures appended to natural products encompass chemical, genetic (*in vivo*) and enzymatic (*in vitro*) approaches.²³ Glycodiversification of natural products stems from the potential to tune bioactivity. Modification of the glycosyl component of complex natural products presents multiple challenges, not the least of which is the access to the requisite functionally protected aglycone and appropriate sugars for chemical couplings. Access to a supply of the aglycone may be limited to whether it is from a natural source or the

product of a multi-step synthesis. Likewise, access to different sugar coupling partners also requires a tailored synthetic scheme for individual sugars. To meet these challenges, a number of complementary glycodiversification strategies have been explored. Thorson and coworkers have engineered glycosyltransferases to generate vancomycin analogues with variable sugar moieties using an *in vitro* experimental approach.⁴⁹ Semi-synthetic approaches have also been described: click chemistry has been employed by Lin and Walsh to prepare a tyrocidine library.⁵⁰ In another semi-synthetic approach by Thorson and coworkers, aglycones of digitoxin were functionalized with methoxyamine and reacted with free sugars to form neoglycosides, generating a library of 78 digitoxin analogues (Figure 9).⁵¹

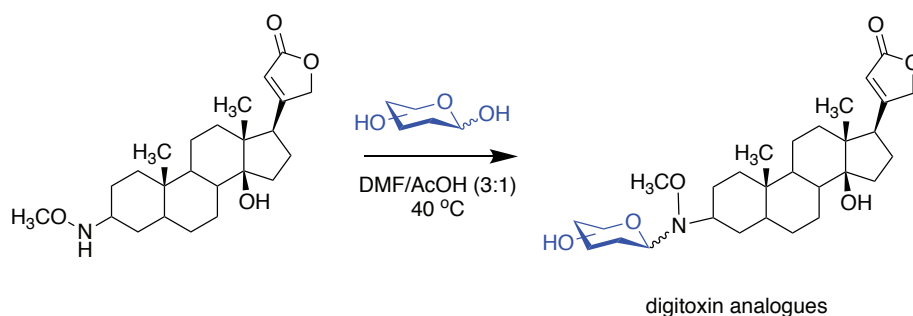


Figure 9. Method of “neoglycorandomization” used to generate digitoxin library.

Combinatorial biosynthetic approaches, which implement genetic engineering techniques such as gene deletion and complementation to modify biosynthesis *in vivo*, have also been described.⁴³ A significant number of glycosyltransferases involved in bacterial secondary metabolite biosynthesis have been shown to be flexible with respect to sugar donor specificity, a feature that is cornerstone to the success of combinatorial approaches, including, UrdGT2 (urdamycin biosynthesis),⁵² DesI (pikromycin),⁵³ StagG (staurosporine),⁵⁴ EmlGT

(elloramycin),⁵⁵ CalGI, CalG4 (calicheamicin),⁵⁶ GftD, GfTE (vancomycin),⁵⁶ RebG (rebecamycin),⁵⁷ YjiC (flavanoids),⁵⁸ and JadS^{59, 60} (jadomycin, section 3.3).^{47,48} As a representative example, diversified sugar analogues of streptolydigin, a potent inhibitor of bacterial RNA polymerase, were generated by removing the genes responsible for L-rhodinose biosynthesis, and incorporating genes encoding the biosynthesis of other deoxyhexoses, including L-amicitose, L-amictose, D-amictose, L-digitoxose, and D-olivose (Figure 10).⁶¹ Further discussion on combinatorial methods can be found in Section 3.4.

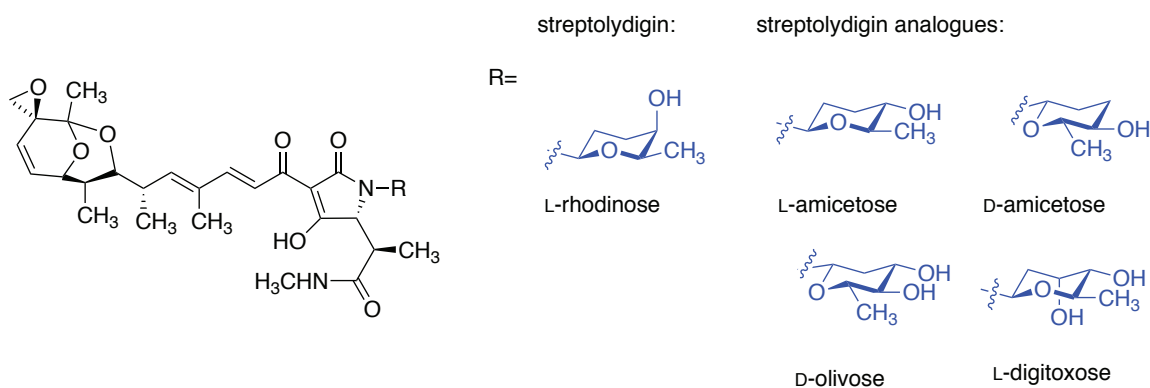


Figure 10. Glycodiversification of streptolydigin analogues by combinatorial biosynthesis.

Efforts to develop *in vitro* glycosyltransferase assays have been arising in response to the growing list of glycosyltransferases shown to possess relaxed substrate specificity. A number of recent reports have described recombinant plant glycosyltransferases, evaluated *in vitro*, to possess broad acceptor tolerances.⁶²⁻⁶⁶ MiCGT, a C-glycosyltransferase able to transfer Glc and Xyl to a number of phenolic compounds, and UGT73AE1, found to generate *N*- and *S*-glucosylated products, were both isolated from Chinese medicinal plants.^{67, 68} While there are

relatively fewer studies using bacterial glycosyltransferases, some promiscuous glycosyltransferases have been evaluated *in vitro*, including the macrolide glycosyltransferases, MGT from *Streptomyces lividans*, BcGT-1 and BcGT-3 from *Bacillus cereus*,^{69, 70} XcGT-2 from *Xanthomonas campestris*,⁷¹ and flavonoid glycosyltransferase YjiC from *Bacillus licheniformis*.⁵⁸ A benchmark of glycodiversification is exemplified by work in the Thorson research group with OleD, a macrolide glycosyltransferase isolated from *Streptomyces antibioticus*, that has been evolved to expand its substrate scope through iterations of directed evolution, improving its tolerance towards acceptors and donors; this topic is discussed in greater detail in Section 2.5.1.⁷²⁻⁷⁴ Recently, protein engineering using saturation mutagenesis of a glucansucrase GFT-D, that utilizes sucrose as a donor, a cheaper and more readily accessible alternative to the nucleotide diphosphosugar (NDP-sugar) donors used by the previously mentioned glycosyltransferases, was demonstrated to increase its glycosyltransferase activity towards flavonoids (Figure 11).⁷⁵

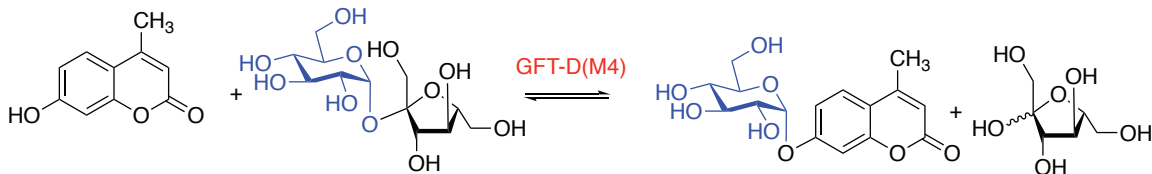


Figure 11. Glycosyltransferase activity of GFT-D(M4) with 4-methylumbelliferone and sucrose.

1.4. Aims of the Thesis

This thesis will examine topics surrounding the study of bacterial carbohydrates and the enzymes involved in their biosynthesis in various contexts. In Chapter 2, a number of studies on various bacterial enzymes involved in sugar processing were studied. The enzymes studied are found in bacterial biosynthetic pathways that are targets for antibiotic development, therefore, understanding the kinetic and substrate scope of these enzymes provides data necessary to develop effective inhibitors.

Chapter 2 aims:

- A primary aim was to provide a thorough substrate scope and kinetic characterization of the thymidyltransferase Cps2L from *Streptococcus pneumoniae*. This was accomplished by assaying unnatural glucose 1-phosphate substrate analogues. A continuous UV-based coupled assay to monitor Cps2L reactivity was developed to facilitate these aims. NMR binding experiments were explored for their utility to study ligand binding with Cps2L and to determine dissociation constants (K_d). In conjunction with the primary aims, compounds that were not identified as substrates were screened as inhibitors. A related project goal was to probe the utility of Cps2L as a catalyst for the chemoenzymatic preparation of unnatural sugar nucleotides.
- The aim of the second study was to determine whether substrates with additional anionic charge compared to the physiological substrate may function as Cps2L transition state mimics. To this end, we evaluated a nucleoside tetraphosphate (p₄dT) as a Cps2L substrate. Accommodation

of p₄dT by Cps2L suggested that additional steric bulk and negative charge was tolerated. Having identified p₄dT as a substrate, the secondary aim was to describe the catalytic mechanism and to identify the products using NMR spectroscopy.

- In the third study enzymes involved in rhamnose biosynthesis (RmlB, RmlC and RmlD) from *Pseudomonas aeruginosa* have been evaluated for their substrate scope. This has not previously been explored in detail and had shed light on the ability of these enzymes to process unnatural analogues. The hypothesis was that analogues of the substrate possessing substitutions of amino and/or fluoro substituents about the hexose ring could serve as rhamnosyltransferase inhibitors if processed by the rhamnose biosynthetic enzymes to generate rhamnose nucleotide analogues. The aim was to isolate and characterize new sugar nucleotides and evaluate them as inhibitors of Cps2L and rhamnosyltransferases.
- The primary goal in the fourth study was to characterize a recombinant GT1 family glycosyltransferase Sv0189 from *Streptomyces venezuelae*. Analysis by sequence homology suggested that Sv0189 would possess relaxed specificity towards glycosyl acceptors and may therefore serve as a glycosylating tool for chemoenzymatic applications as a method for late stage functionalization of complex molecules. This is an unusual property for bacterial glycosyltransferases, of which most characterized types are associated with particular biosynthetic pathways and products, and thus warranted further exploration. The initial aim was to determine

glycosyltransferase activity and establish the physiological glycosyl donor. After establishing glycosyltransferase activity, the secondary aim was to develop an assay that would enable acceptor screening of a large library.

In Chapter 3, new analogues of a family of glycosylated bacterial secondary metabolites, the jadomycins, were prepared with an emphasis on modifying the sugar moiety. The jadomycins possess antibacterial and cytotoxic properties and our interest lies in exploring the structure activity relationships impacting these properties.

Chapter 3 aims:

- With the aim of further exploring the potential for jadomycin derivitization by precursor directed biosynthesis using non-proteinogenic amino acids, the producing organism, *Streptomyces venezuelae*, was cultured with *N*-trifluoroacetal-L-lysine (TFAL). TFAL was selected to provide access to a jadomycin incorporating lysine, which was previously reported to be insufficiently stable for isolation and characterization. TFAL was also selected for incorporation of fluorine into the final natural product, ¹⁹F being an element that is relatively abundant in pharmaceutical compounds but that is essentially absent from natural systems. Specific aims were to characterize new natural products and to evaluate their bioactivity in antimicrobial and cancer cell line panels.
- Two studies were carried out to access glycovariants of the jadomycins. Such studies are important for structure-activity relationship analysis of

the jadomycin sugar component that has been relatively unexplored in contrast to E-ring variation. The first of these studies involved analysis of the jadomycins produced by an *S. venezuelae* mutant with a deletion of the 4,6-dehydratase dideoxy biosynthetic gene (*jadT*). The second study involved heterologous complementation with glycosyltransferases (*kijC3* and *kijC4*) from the kijanimicin biosynthetic gene cluster of *Actinomadura kijaniata*.

Chapter 2: Studies on Carbohydrate-Recognizing Enzymes

2.1. Introduction to Rhamnose Sugar Biosynthesis

Streptococcus pneumoniae is a highly infectious, Gram-positive bacterium responsible for many invasive pneumococcal diseases, including pneumonia, meningitis and sepsis. A prevalent pathogenic organism, *S. pneumoniae* has shown widespread clinical resistance to penicillin and chloramphenicol, as well as to synergistic treatments involving β -lactams and aminoglycosides.^{76, 77} In some virulent strains, L-rhamnose (Rha) has been identified as essential for viability and virulence and is found as part of cell-wall anchored polysaccharides and capsular polysaccharides.^{9, 78} A key step in bacterial cell wall biosynthesis involves sugar nucleotide pyrophosphorylases (EC 2.7.7.-), the enzymes that catalyse the condensation of sugar 1-phosphates and nucleotide triphosphates (NTP), producing the activated sugar donors (nucleoside diphosphate, NDP-sugar) that serve as glycosyltransferase substrates.¹¹ Prior to incorporation into bacterial cell walls, various intermediate enzymes may further modify the hexose ring of the nucleotides. For instance, conversion of deoxythymidine diphosphate α -D-glucose (dTDP-Glc) to dTDP- β -L-rhamnose (dTDP-Rha) is mediated by three processing enzymes: dTDP-glucose-4,6-dehydratase, (RmlB, EC 4.2.1.46), dTDP-4-keto-6-deoxyglucose-3,5-epimerase, (RmlC, EC 5.1.3.13), and dTDP-4-dehydrorhamnose reductase (RmlD, EC 1.1.1.133).⁷⁹ Glycosyltransferases (EC 2.4.1.-) transfer sugars from donor to acceptor molecules in the assembly of glycoconjugates. Of the molecules that function as glycosyl donors, high-energy sugar nucleotides (NDP-sugars) are the most common.¹¹ A detailed understanding of these enzymes,

including kinetic and mechanistic information, is important for the rational design of targeted compounds.

2.1.1. Thymidyltransferase: RmlA/Cps2L

Cps2L (EC 2.7.7.24) is a bacterial thymidyltransferase (nucleotidyltransferase) cloned from *S. pneumoniae* that catalyses the first step in the biosynthesis of Rha (Figure 12A),⁸⁰ an essential constituent of the cell wall in many bacterial species.⁸¹ Thymidyltransferases are responsible for generating activated sugars in the form NDP-sugars, which serve as substrates for glycosyltransferases and represent potential broad-spectrum antibacterial targets given homology across various species.^{82, 83} The reaction proceeds *via* an S_N2 mechanism, where the oxygen of α -D-glucose 1-phosphate (Glc 1-P) attacks the α -phosphate of deoxythymidine triphosphate (dTTP), resulting in the displacement of diphosphate (PP_i) and formation of dTDP-Glc (Figure 12B).⁸⁴ Nucleotidyltransferases have also been studied for application in the chemo-enzymatic preparation of sugar nucleotide analogues for enzymatic glycodiversification studies,^{49, 85, 86} and used to prepare phosphonate⁸⁷ and carbacyclic⁸⁸ sugar nucleotide analogues that have been put forward as putative glycosyltransferase inhibitors (Figure 12C). This thesis will present studies that have further elaborated the substrate scope of Cps2L, contributing to a more complete description of its tolerance towards various Glc 1-P analogues (compounds **2.1-2.6** in Section 2.2) and a tetraphosphate nucleoside analogue (p₄dT in Section 2.3).

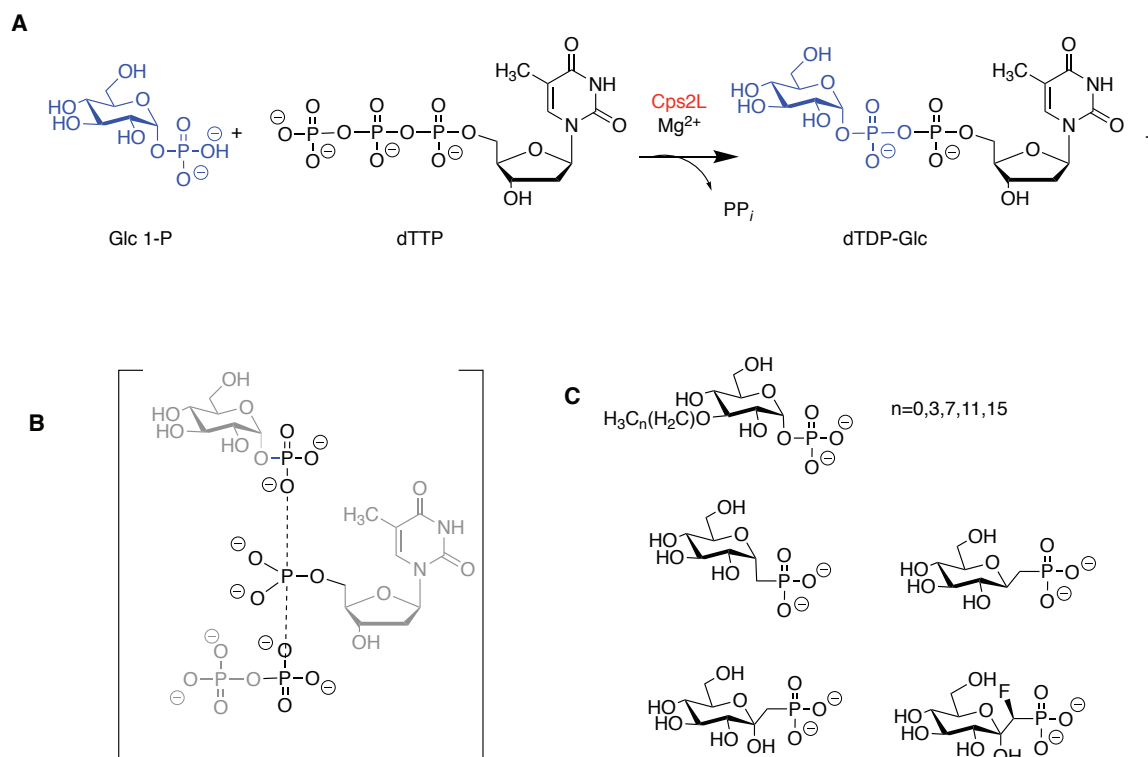


Figure 12. (A) The physiological reaction catalysed by Cps2L; (B) The mechanistic transition state in the Cps2L reaction mechanism; (C) Examples of sugar phosphates and phosphonates that have been identified as Cps2L substrates.^{3, 87, 89}

2.1.2. Rhamnose Biosynthetic Tailoring Enzymes: RmlB, RmlC, RmlD

Rha biosynthetic genes *rmlABCD* have been identified as essential for Gram-positive strains.^{13, 78, 90, 91} In previous studies, the enzymes involved in Rha biosynthesis in *Pseudomonas aeruginosa* have been identified and their enzymatic activity established *in vitro*.^{79, 84, 92-98} Four enzymes are involved in the conversion of α -D-glucose 1-phosphate (Glc 1-P) to dTDP-Rha: RmlA, a thymidyltransferase, RmlB, a 4,6-dehydratase, RmlC, a 3,5-epimerase, and RmlD, a 4-keto reductase (Figure 13). A more detailed look into the mechanisms of these enzymes is presented in Section 2.4. Chemo-enzymatic syntheses of the end

product, dTDP-Rha, have been reported previously using recombinant enzymes.⁹⁹⁻

101

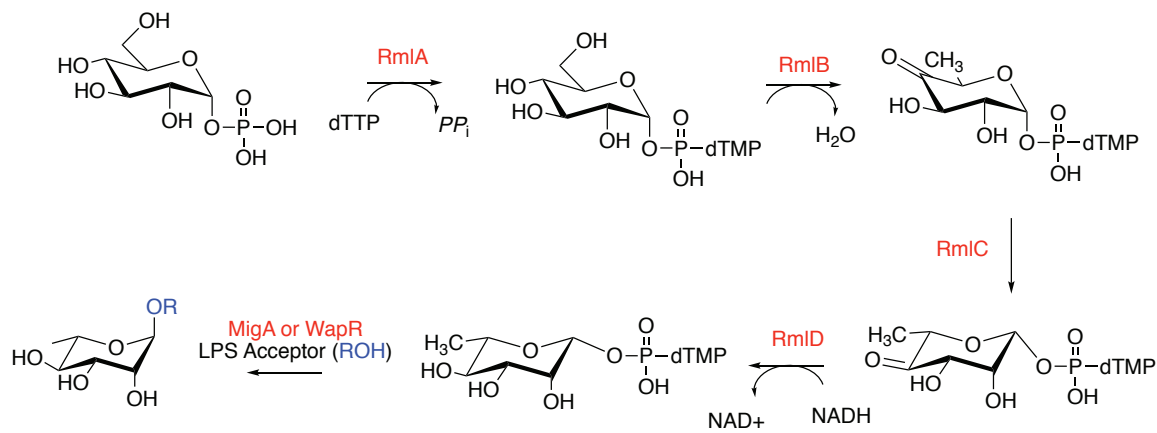


Figure 13. Enzymatic synthesis of dTDP-Rha by *P. aeruginosa*.

Recombinant RmlB, RmlC and RmlD have been evaluated to establish whether these enzymes are able to process modified sugars (Glc 1-P analogues), and used in the chemoenzymatic synthesis of a novel phosphonate analogue, deoxythymidine diphosphono β -L-rhamnose (dTDP-1C-Rha). These are discussed in Section 2.4.

2.1.3. Rhamnosyltransferases Involved in LPS Cell Wall Biosynthesis

LPS and rhamnolipids are found on the outer cellular membrane of *Pseudomonas aeruginosa*, a Gram-negative bacterium listed by the World Health Organization as being amongst the greatest pathogenic threats to human health.⁸ LPS plays a role in structural integrity and is also a virulence factor. LPS is composed of three distinct components: lipid A, core oligosaccharide (OS), and O antigen. Previous studies have implicated two rhamnosyltransferases, MigA and WapR, GT2 family glycosyltransferases (carbohydrate active enzymes (CAZy) database), in the

biosynthesis of the outer core OS component of LPS, and have proposed that these may serve as suitable targets for targeted antibiotics.¹⁰² The product of each enzyme generates a distinct glycoform; gene knockout studies have identified WapR as an α -1,3-rhamnosyltransferase that generates the capped glycoform and MigA as an α -1,6-rhamnosyltransferase that generates the uncapped glycoform which lacks the *O* antigen component (Figure 14).¹⁰² The study of bacterial cell-wall affiliated glycosyltransferases *in vitro* is challenging, in part because the enzymes that are produced by standard recombinant methods in *E. coli* are often poorly soluble, but also because it may be challenging to obtain sufficient quantities of the required donor and acceptor molecules to study them. Thus, sufficient supplies of sugar donor, prepared utilizing the RmlB-D enzymes described in Section 2.4, are required to study MigA, WapR and similar enzymes. A new glycosyltransferase, Sv0189, is characterized and evaluated in the context of developing a catalyst for glycodiversification of natural product scaffolds is discussed Section 2.5.

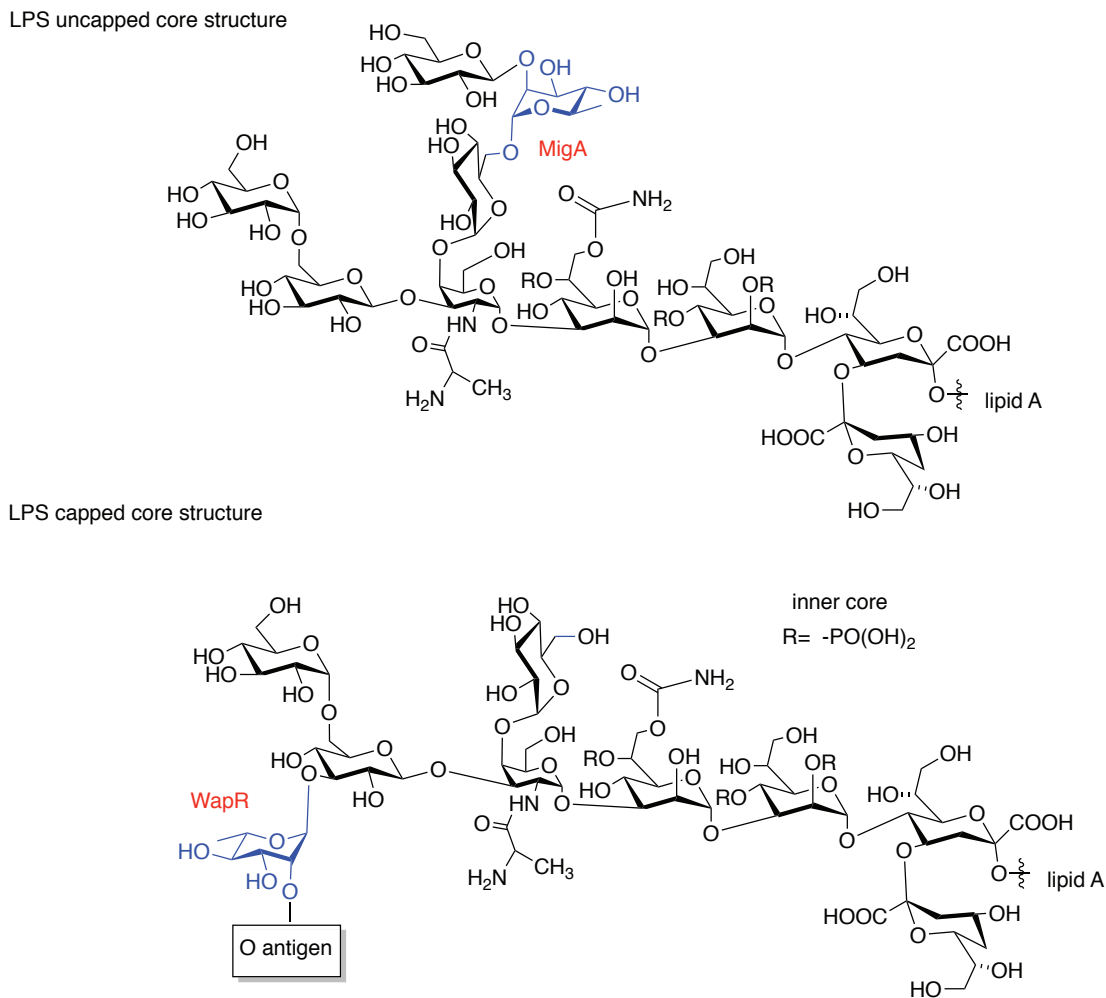


Figure 14. LPS core structures of *P. aeruginosa* strain PAO1. Rha (blue) installed by rhamnosyltransferases MigA and WapR.¹⁰²

2.2. Kinetic Evaluation of Glucose 1-phosphate Analogues with a Thymidyltransferase (Cps2L)

Excerpts from this section are taken from: S. M. Forget, A. Jee, D. A. Smithen, R. Jadghdane, S. Anjum, S. A. Beaton, D.R.J. Palmer, R.T. Syvitski, D.L. Jakeman. (2015) *Org. Biomol. Chem.* 13, 866-875. Compounds **2.1-2.4** were synthesized by R. Jagdane, S. Anjum and D.R. Palmer (University of Saskatchewan). Compounds **2.5**

and **2.6** were synthesized by S. A. Beaton and D.A. Smithen. A. Jee is thanked for her assistance in performing kinetic assays and for purification of Cps2L.

The present study details the enzymatic evaluation glucose of Glc 1-P analogues (**2.1-2.6**, Figure 15) selected to further probe the substrate tolerance of thymidyltransferase Cps2L. Kinetic evaluation of individual substrates and inhibitors has provided an effective means to probe the Cps2L active site and to identify structure-activity relationships. We have previously employed a 7-methyl-6-thioguanosine (MESG)-based coupled spectrophotometric kinetic assay,¹⁰³ for the quantitation of inorganic phosphate (P_i) in solution to measure Cps2L kinetics. However the assay proved challenging in our hands owing to the thermal instability of MESG towards base-catalysed decomposition. Indeed, MESG decomposes at ambient temperature, with a half-life of 4 h at pH 8, which led to difficulties when acquiring kinetic data.¹⁰⁴ A handful of literature methods employ a coupled assay using xanthine oxidase (XO) and purine nucleoside phosphorylase (PNP) to quantify phosphate: These assays have been employed for kinetic evaluation of UDP-*N*-acetylglucosamine enolpyruvyl transferase (MurA)¹⁰⁵ and DNA polymerases.¹⁰⁶ For enzymes releasing diphosphate (PP_i), such as nucleotidyltransferases, reactions are typically coupled to inorganic pyrophosphatase (IPP) to produce two molecules of phosphate, although alternative methods to detect PP_i have been described.¹⁰⁷

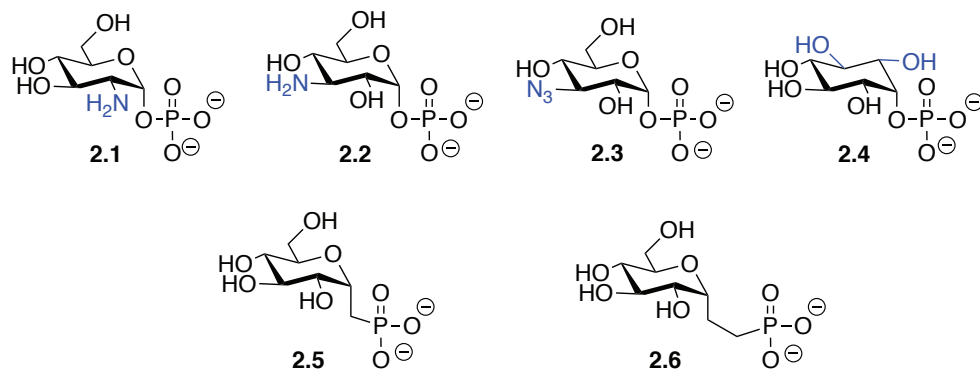


Figure 15. Glc 1-P analogues **2.1-2.6** evaluated as Cps2L substrates and/or inhibitors.

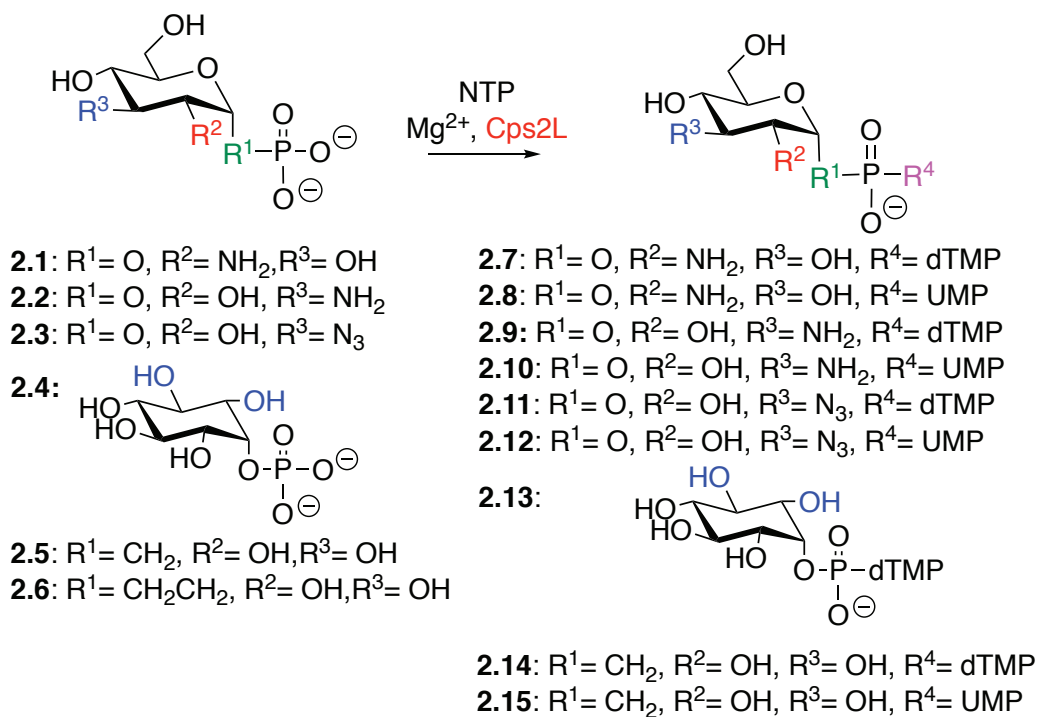
A phosphate-detecting assay based on IPP (EC 3.6.1.1), PNP (EC 2.4.2.1), and XO (EC 1.17.3.2) for the kinetic evaluation of Cps2L substrates and inhibitors through measurement of released P_i has been described and implemented. Additionally, the application of water-ligand observed *via* gradient spectroscopy (waterLOGSY) NMR binding experiments for the determination of a dissociation constant (K_d) for one of the sugar phosphate analogues (**2.6**) found to be a Cps2L inhibitor has been described.

2.2.1. Analytical substrate evaluation with Cps2L

Sugar phosphates **2.1-2.6** were evaluated as substrates for Cps2L (Table 1). Previous studies have shown that Cps2L has broad substrate tolerance, and can turnover sugar phosphates containing modifications at C-2 and C-3, as well as phosphonate analogues.^{80, 87, 89} Reaction progress with recombinant Cps2L was monitored using HPLC, and enzymatic sugar nucleotide production was confirmed using LC-MS². Studies within the Jakeman group have previously reported that commercially available glucosamine (GlcN) 1-phosphate **2.1** was efficiently turned

over to produce dTDP and uridine diphosphate (UDP) sugar nucleotides, **2.15** and **2.16**.⁸⁰ Both **2.2** and **2.3** were identified as Cps2L substrates when coupled with deoxythymidine triphosphate (dTTP) or uridine triphosphate (UTP); however, UTP conversion required significantly more time and quantitative conversion was not achieved. Studies with RmlA, a Cps2L homologue with 89% overall sequence identity, have shown lower tolerance to sugar phosphates with modifications at C-3 and C-4 compared to C-2 and C-6, and that use of an alternate nucleotide triphosphate (NTP) in conjunction with an alternate sugar 1-phosphate has a cumulative negative influence on enzyme efficiency, a trend that was consistent with our data.^{23, 108-110} The relatively sluggish turnover of **2.3** may be explained by the increased linear length of the azido group, as it has previously been reported that increasing 3-*O* alkoxy chain length in a series of Glc 1-P analogues resulted in increasingly sluggish conversion rates.⁸⁹

Table 1. Evaluation of Glc 1-P analogues as Cps2L substrates.



Compound	EU Cps2L	NTP	Product	% Conversion	Time (h)
2.1^a	2	dTTP	2.7	95	0.5
2.1^a	2	UTP	2.8^b	95	24
2.2	2	dTTP	2.9^b	100	0.5
2.2	8	UTP	2.10	21	48
2.3	8	dTTP	2.11^b	100	17
2.3	8	UTP	2.12	22	4d
2.4	40	dTTP	2.13	18	8d
2.4	40	UTP	-	0	>24
2.5^a	2	dTTP	2.14	95	0.5

Compound	EU Cps2L	NTP	Product	% Conversion	Time (h)
2.5^a	2	UTP	2.15^b	65	0.5
2.6	10	dTTP	-	0	> 24

^aValues⁸⁷ obtained previously; ^bSugar nucleotides were scaled-up and isolated for full characterization.

myo-Inositol 2-phosphate **2.4** provided a pseudo-sugar scaffold to probe Cps2L substrate tolerance. Our analysis of the structure of RmlA, which has identical active site residues with Cps2L, in complex with dTDP-Glc suggested that **2.4** would be accommodated in the active site.⁸⁴ The resulting inositol-nucleotide, lacking an anomeric centre, would serve as a putative glucosyltransferase inhibitor. Carbaglucose 1-phosphate has been demonstrated to be turned over to produce the UDP-sugar by a bacterial, but not eukaryotic, nucleotidyltransferase, demonstrating potential for specific inhibition.⁸⁸ *myo*-Inositol 2-phosphate **2.4** was a substrate when coupled with dTTP; however, product formation to produce **2.13** never surpassed 24% and required high Cps2L concentrations to achieve appreciable conversions; product formation was not observed upon incubation with UTP. Signals identified as breakdown products (dTDP) and deoxythymidine monophosphate (dTMP) were observable by analysis using HPLC, alongside the peak for the product, sugar nucleotide **2.13**. Methylene phosphonate **2.5** has previously been identified as a Cps2L substrate.⁸⁷ Phosphonate **2.6**, which contains an additional methylene linker between the pseudo-anomeric center and the phosphorus, was found not to be a substrate.

2.2.2. Kinetic Evaluation using IPP-PNP-XO Coupled Spectrophotometric Assay

Glc 1-P analogues **2.1-2.6** were evaluated using a continuous spectrophotometric coupled kinetic assay that was selected as a more robust alternative to MESG-based and to discontinuous HPLC-based assays: Cps2L catalysis was coupled with IPP to produce P_i , which was in turn used as a substrate for PNP, along with inosine. XO was then used to catalyse the final reaction in the sequence, namely the oxidation of hypoxanthine to uric acid that produces a change in absorbance at λ_{290} such that initial reaction velocities can be monitored spectrophotometrically (Figure 16). We demonstrated the utility of this assay with nucleotidyltransferases by determining the kinetic parameters for the Cps2L-catalysed conversion of Glc 1-P to dTDP-Glc in the presence of saturating dTTP, from which we established K_m , k_{cat} , and k_{cat}/K_m values that were comparable to those obtained in previous studies using HPLC and MESG-coupled assays (Table 2).^{87, 111}

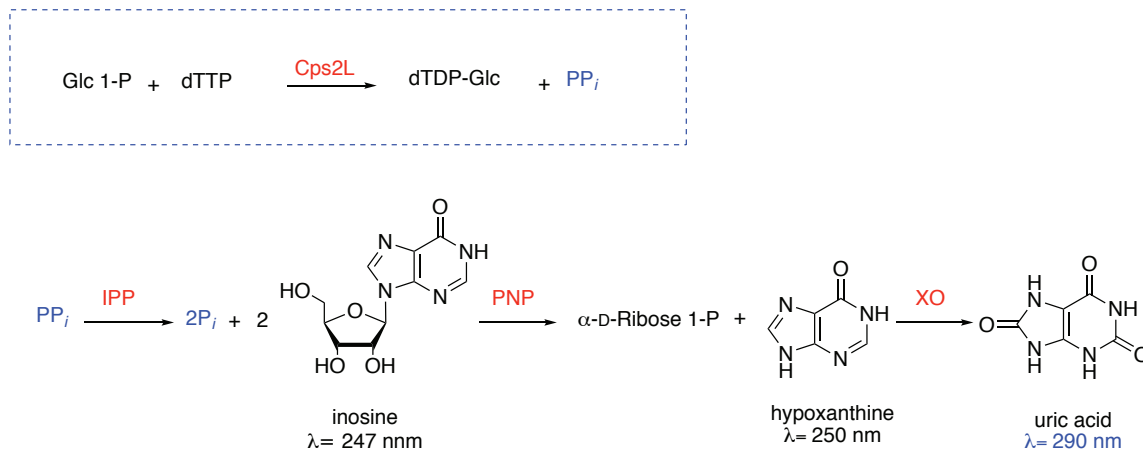


Figure 16. Coupled spectrophotometric enzyme assay to measure Cps2L activity using PNP and XO to detect released phosphate.

Sugar phosphates **2.1**, **2.2**, and **2.3**, had K_m values that were an order of magnitude larger than Glc 1-P. The observed preference for 2-amino sugar **2.1** over

3-amino sugar **2.2** is predominantly a function of the k_{cat} as the apparent binding constants differ only by a factor of one and a half. Comparison of **2.2** and **2.3** suggests that substitution of an amino group for an azido group resulted in a 100-fold reduction in k_{cat} , but had no effect on the K_{m} value. This may be rationalized by a nonproductive binding event, where **2.3** binds to Cps2L with a similar affinity and where reduced k_{cat} is a function of misalignment of the phosphate for efficient catalysis. The K_{m} value for **2.1** was unchanged in the presence of dTTP or UTP, and the change in specificity was attributed to the k_{cat} value, which decreased 100-fold with UTP. Kinetic evaluation showed that specificity was affected by both an increase in K_{m} and a reduction in k_{cat} for C-2 and C-3 modified sugars, which is different from the trend observed in a previous series of compounds, which included galactose 1-phosphate (Gal 1-P), and the phosphonate analogues of Glc 1-P and Gal 1-P, that were found to have unchanged K_{m} values in comparison to Glc 1-P.⁸⁷

Table 2. Kinetic parameters for Cps2L substrates.

Variable substrate	NTP	k_{cat} (s^{-1})	K_{m} (μM)	$k_{\text{cat}} / K_{\text{m}}$ ($\text{uM}^{-1}\text{s}^{-1}$)
Glc 1-P	dTTP	24	83 ± 10	0.28
Glc 1-P	UTP	0.016	160 ± 7	0.0096
2.1	dTTP	4.5	690 ± 29	0.0065
2.1	UTP	0.1	700 ± 160	0.00015
2.2	dTTP	0.08	1100 ± 100	0.000072
2.3	dTTP	0.0003	1100 ± 330	0.00000027
2.5	dTTP	0.55	180 ± 17	0.031
2.5	UTP	0.01	380 ± 53	0.00028

A K_{m} of 180 μM , a k_{cat} 5.5 s^{-1} , and a $k_{\text{cat}}/K_{\text{m}}$ of 0.031 $\text{M}^{-1}\text{s}^{-1}$ was found for methylphosphonate **2.5** when evaluated as a Cps2L substrate. In a previous study, it was determined that **2.5** had hundred-fold reduced efficiency with Cps2L compared to Glc 1-P, whereas the present study found the difference to be ten-fold, suggesting that **2.5** was a better substrate than previously reported.⁸⁷ *myo*-Inositol 2-phosphate **2.4** was turned over too slowly to be evaluated as a substrate with the spectrophotometric assay and was therefore probed as an inhibitor of the physiological reaction (Table 3). Product formation with **2.4** required near equimolar concentrations of enzyme and extended reaction times to achieve 20-40% conversion. Inhibition assays with **2.4** gave the best fit to a mixed inhibition model, from which K_{i} value of 8.9 mM was obtained.

Table 3. Inhibition constants **2.4** and **2.6** with Cps2L.

Inhibitor	K_i (mM) ^a	Inhibition model
2.4	8.9 ± 4.7	Mixed
2.6	1.2 ± 0.2	Competitive

^aGlc 1-P as the variable substrate.

Phosphonate analogue **2.6** was evaluated as an inhibitor, having established that it was not a Cps2L substrate. The kinetic data obtained were fitted to standard inhibition equations using non-linear regression software, providing a K_i value of 1 mM for ethylphosphonate **2.6**. The Lineweaver-Burk plot demonstrated that the mode of inhibition was best described using a competitive model with respect to Glc 1-P, the natural substrate of Cps2L (Figure 17).

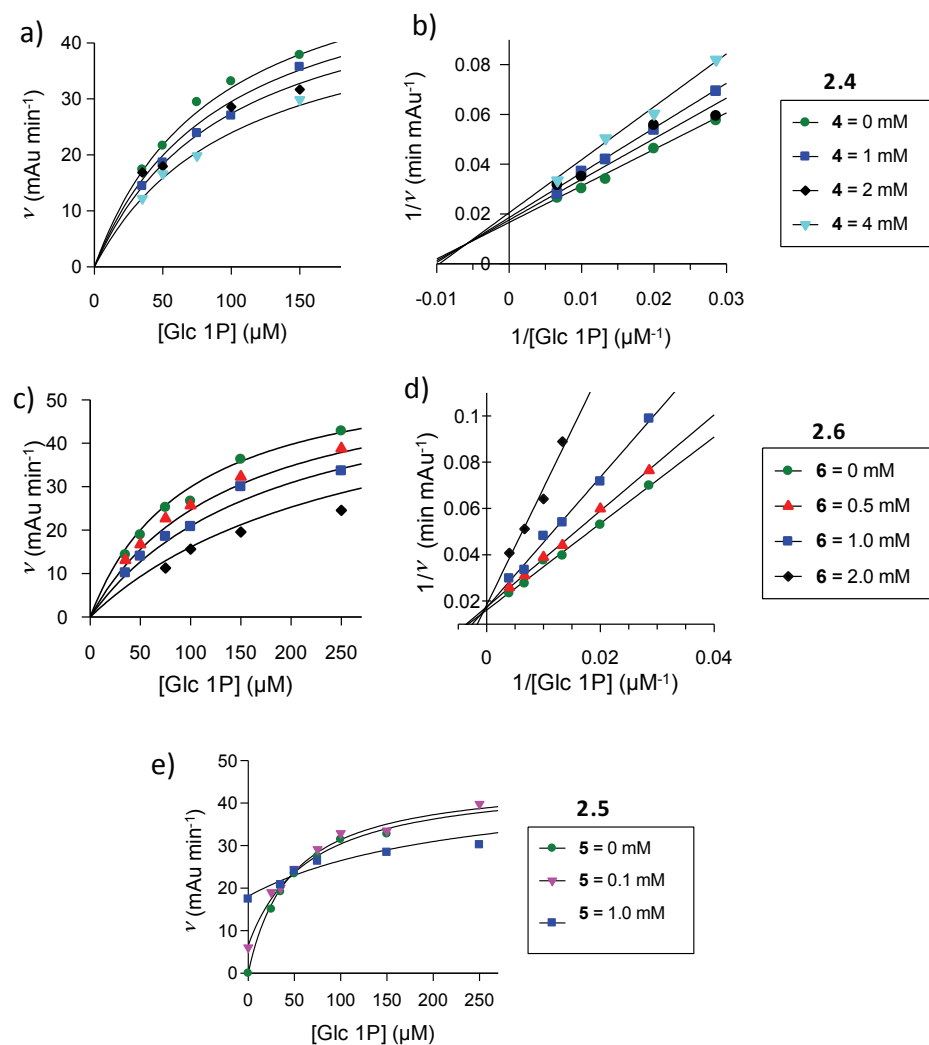


Figure 17. Kinetic inhibition assays in the presence of constant dTTP (1 mM) and variable **2.4**, **2.5** and **2.6**. Cps2L inhibition by **2.4**: a) Michaelis-Menten and b) Lineweaver-Burk plots; inhibition by **2.6**: c) Michaelis-Menten and d) Lineweaver-Burk plots used to determine K_i and mode of inhibition. e) Competitive substrate model between **2.5** and Glc 1-P.

For the purposes of comparison, methylphosphonate **2.5** was evaluated as an inhibitor of the physiological reaction; at 100 μ M **2.5** no obvious effect on reaction rates was observed, whereas at 1 mM **2.5**, some rate suppression was observed,

along with a non-zero rate at 0 μM Glc 1-P indicating that **2.5** was turning over to sugar nucleotide **2.14** within the timeframe of the kinetic assay. Production of **2.14** was confirmed by HPLC. The obtained rates were fit to a competitive substrate model from which a ten-fold difference in catalytic efficiency between **2.5** and Glc 1-P was calculated, $0.08 \text{ M}^{-1}\text{s}^{-1}$ and $0.83 \mu\text{M}^{-1}\text{s}^{-1}$, respectively, which agreed with the kinetic data obtained from the individual substrate assays, confirming that **2.5** does not inhibit Cps2L.

2.2.3. Determination of K_d values using waterLOGSY NMR Binding Experiments

As an alternative method to the kinetic coupled assay for the determination of binding, compound **2.6** was evaluated using waterLOGSY NMR. Essentially, irradiation of bulk water facilitates the transfer of magnetization from the enzyme to enzyme-bound small molecules through water molecules present in the active site.^{112, 113} This results in a differential nOe for small molecules that bind, and therefore opposite phasing is observed for molecules that interact with the enzyme in the processed NMR spectrum (Figure 18). In some cases, known substrates may not show binding. For example, substrates that require a co-substrate for binding, as in an ordered Bi-Bi mechanism, may not show binding in the absence the co-substrate.³ Both inhibitors and substrates will show binding in a waterLOGSY NMR experiment, therefore further analysis, such as enzyme kinetics, may be required to gain more information regarding the nature of the binding interaction.

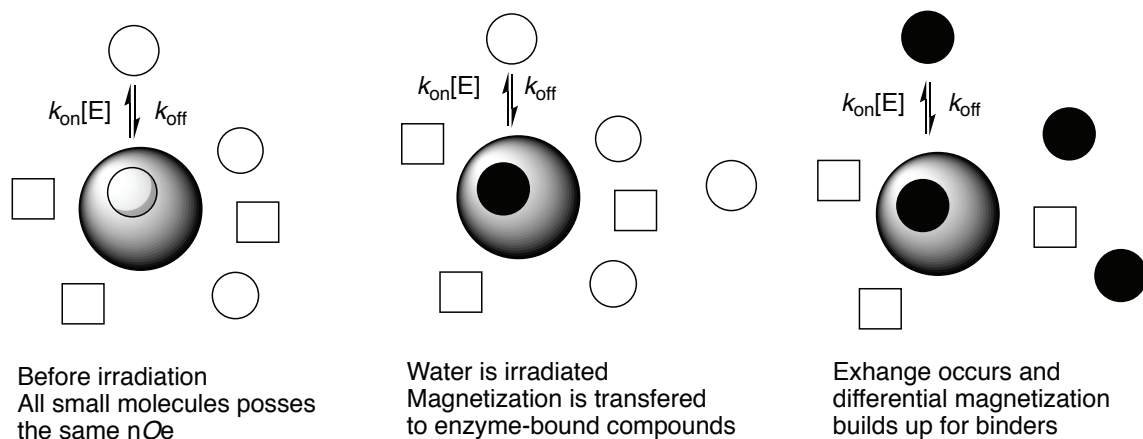


Figure 18. A simplified representation of magnetization transfer in waterLOGSY

NMR. The big circles represent an enzyme, the smaller circles represent binding molecules, and the squares represent non-binding molecules. Shading in black illustrates magnetization transfer from protein to ligand.

WaterLOGSY spectra were acquired with **2.6** in the presence and absence of Cps2L in order to confirm binding to the enzyme, which is determined by a change in phasing for binding signals in the processed spectra; **2.6** only bound to Cps2L in the presence of dTTP (Figure 19), a result that agrees with the accepted ordered Bi-Bi reaction mechanism for Cps2L.^{84, 114}

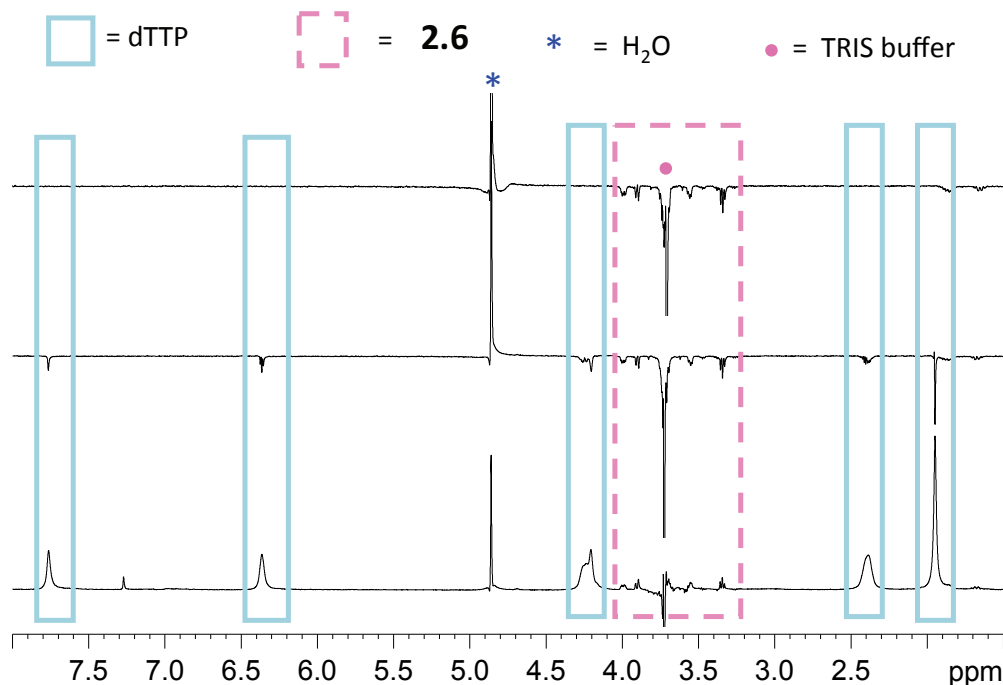


Figure 19. WaterLOGSY NMR spectra with **2.6** and Cps2L. Top: **2.6** and Cps2L, no binding; middle: **2.6** and dTTP, no binding; bottom: **2.6**, dTTP and Cps2L, binding.

Having qualitatively established binding of **2.6** to Cps2L, we sought to determine the K_d value for the enzyme-ligand complex using a waterLOGSY method described by Dalvit and co-workers.¹¹³ After establishing a lower concentration limit for **2.6** at which positive signals, indicative of binding, could still be observed, aliquots of a 100 mM aqueous solution of **2.6** (1-8 μ L) were titrated into a solution containing Cps2L and dTTP. A waterLOGSY NMR spectrum was recorded after each addition. Control experiments were also carried out without Cps2L in order to generate a correction curve for the contribution of free ligand. Two clearly defined signals were selected to perform the analysis, derived from H-4 (3.35 ppm) and H-6 (3.88 ppm) of ethylphosphonate **2.6**, and the corrected signal

intensities were plotted as a function of the concentration of **2.6** and fit to a standard dose-response curve by non-linear regression. This provided us with K_d values of 17 (± 4) and 23 (± 8) mM for H-4 and H-6, respectively (Figure 20). This dissociation constant measured from the waterLOGSY experiment was significantly larger than the K_i of 1.2 mM that was determined using the coupled spectrophotometric assay. In our experimental data, the K_d curves are shallow and therefore likely overestimate the true dissociation constant. This same observation was made by Fielding *et al.* upon evaluating binding of L-tryptophan to bovine serum albumin: they attributed overestimated K_d values to effects caused predominantly by spin diffusion, which at high ligand concentration results in the loss of polarization acting against the nOe transfer due to cross relaxation mechanisms, rather than to effects from non-specific binding.^{115, 116} Our results corroborate that waterLOGSY signal intensity is not a direct function of ligand binding and, as such, caution must be taken with experimental design and interpretation of results. A more recent study suggested that accurate K_d values may be obtained with further optimization of experimental setup; therein the authors conclude that overestimated K_d values arise from ligand re-binding events during signal acquisition as a direct function of the mixing time.¹¹⁷ Nevertheless, both the spectrophotometric kinetic assay and the waterLOGSY NMR binding experiment identified **2.6** as possessing a weak (mM) binding affinity towards Cps2L.

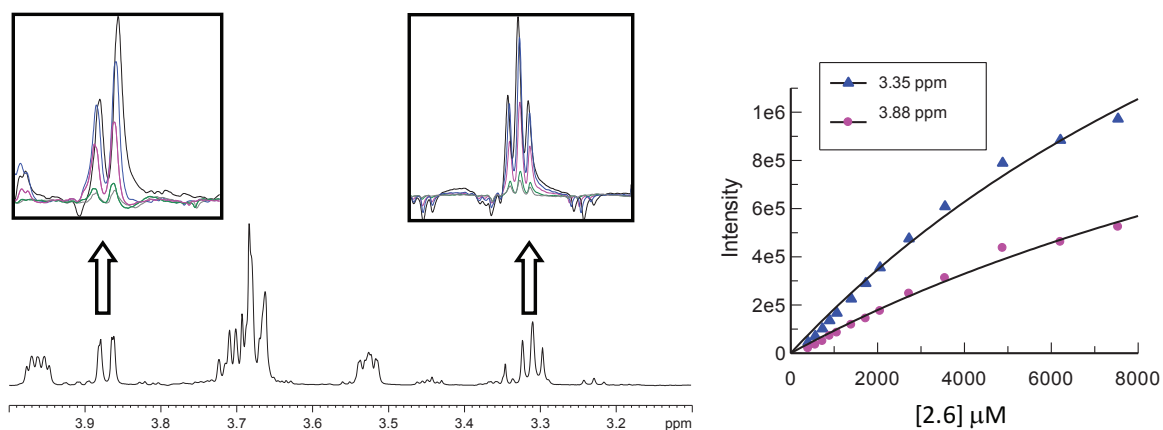


Figure 20. Determination of K_d for **2.6** binding to Cps2L in the presence of dTTP. Left: Change in signal intensity observed in waterLOGSY NMR spectra; Right: Plot of corrected signal intensity versus concentration of **2.6**: ▲ H-4; ● H-6.

2.2.4. Chemoenzymatic Synthesis of Sugar Nucleotides (**2.8**, **2.9**, **2.11**, **2.15**)

Chemoenzymatic syntheses were performed on a milligram scale in order to isolate the sugar nucleotide products from the reactions of **2.1** and UTP to yield **2.8** (26%), of **2.2** and dTTP to yield **2.9** (86%), of **2.3** and dTTP to yield **2.11** (33%) and **2.5** to **2.15** (13%). The discrepancy in the yields compared to the conversions as observed in the analytical HPLC experiments was attributed either to incomplete conversion to the sugar nucleotide on the larger scale (in the case of **2.11**) or to the use of different purification procedures. In the purification of **2.8**, **2.11**, and **2.15** a final desalting step with a single Sephadex® LH-20 column was performed instead of our previous method that was used for the purification of **2.9**,⁸⁷ which utilized a Dowex and then a Sephadex® G-10 column, decreasing the overall yield. The chemoenzymatic preparation of the inositol nucleotide product **2.13** was attempted. Unfortunately, attempts to isolate **2.13** were unsuccessful, likely due to poor initial turnover to product; on a milligram scale, a maximum of 11% conversion was

observed and purification led to the isolation of 0.86 mg of **2.13** that was not sufficiently pure for further characterization as detailed through analysis of NMR spectroscopy

2.2.5. Conclusions

Using a spectrophotometric IPP-PNP-XO coupled assay, the substrate tolerance of Cps2L was probed using six Glc 1-P analogues: a 2-amino sugar **2.1**, a 3-amino sugar **2.2**, a 3-azido sugar **2.3**, a carbocyclic inositol **2.4**, and two phosphonates **2.5** and **2.6**. The four phosphates were found to be Cps2L substrates, and the rate of conversion followed the trend **2.1**>**2.2**>**2.3**>>**2.4**. The general trend was that modification at the 2-position was better tolerated than modification at the 3-position. Inositol **2.4** was a very poor substrate, demonstrating that loss of the ring oxygen or the addition of steric bulk at this position, or a combination of these, was not tolerated within the Cps2L active site. Although isosteric phosphonate **2.5** had previously been identified as a substrate, we found that the non-isosteric compound **2.6** was not a substrate. NMR binding studies using waterLOGSY experiments were performed with compound **2.6** which identified this compound as a weak Cps2L binder, but the method may not be appropriate for quantitation given an apparent overestimation of the K_d value. Inhibition studies using the spectrophotometric assay were performed with **2.4** and **2.6**, and both were identified as mM inhibitors.

2.3. Mechanistic Evaluation of a Nucleoside Tetraphosphate (p₄dT) with a Thymidyltransferase

Excerpts from this section are taken from: S.M. Forget, D.A. Smithen, A. Jee, D.L. Jakeman. *Biochemistry* (2015) 54, 1703-1707. Synthesis of p₄dT was performed by D.A. Smithen. A. Jee performed the purification of Cps2L.

Nature utilises the phosphate group in fundamental roles in almost all biological processes. The biological roles of naturally occurring mono- and dinucleoside polyphosphates (p_nN and Np_nN; where N = nucleoside, p = phosphate, n = 2-7) are not well understood. Although these compounds have been detected within cells in nanomolar concentrations, there remains a debate about the significance of these polyphosphates as they are believed to be the shunt products of promiscuous cellular reactions.¹¹⁸ The most well-studied are the adenine nucleotides, Ap_nA, which have been linked to various intracellular processes and extracellular signaling pathways, but there have been fewer studies examining the roles of mononucleoside polyphosphates.¹¹⁸⁻¹²⁰ Adenosine 5'-tetraphosphate (p₄A) has been found in human plasma and is amongst the most potent endogenous vasoconstrictors known.¹²¹ Another study identified p₄A as a competitive inhibitor of tryptophanyl-tRNA synthetase, and analysis of a crystal structure suggested that p₄A bound in a manner that mimicked the catalytic transition state.¹²² p₄A analogues in which select bridging phosphate oxygens have been substituted for methylene linkers were found to be inhibitors of (asymmetrical) dinucleoside tetraphosphatases.¹²³ Only a few reports have examined the abundance and function of pyrimidine polyphosphates. Pyrimidine dinucleoside polyphosphates have been detected in *Saccharomyces*

cerevisiae and *Escherichia coli* and found to accumulate upon temperature shift and exposure to cadmium.¹²⁴

In this study we examined the reaction of Cps2L (EC 2.7.7.24), a thymidyltransferase cloned from *Streptococcus pneumoniae*, with a monopyrimidine polyphosphate, deoxythymidine 5'-tetrphosphate (p₄dT). The promiscuity of Cps2L and other nucleotidyltransferases with respect to the sugar donor and nucleotide have previously been documented, and was expanded on in Section 2.2 of this thesis.^{3, 110, 111} Many aspects of the Cps2L mechanism, and more generally of nucleotidyltransferase mechanisms, have previously been dissected.¹²⁵ The enzymatic reaction is widely accepted to proceed by an ordered Bi-Bi reaction mechanism, in which binding of dTTP precedes binding of the sugar phosphate (Figure 21).^{3, 84, 114} This class of enzymes possesses an allosteric site with a purported role in regulation upon binding of deoxythymidine 5'-diphospho L-rhamnose, a downstream product.⁸⁴ p₄dT contains an additional phosphate group relative to the physiological substrate, dTTP, and understanding the interactions with Cps2L may provide additional insights into the pathway of phosphate transfer in nucleotidyltransferase reactions, in particular answering whether the active site can accommodate additional ionic charge and increased steric bulk. In this chapter, possible pathways by which p₄dT may act as a Cps2L substrate are examined, and a reaction pathway is proposed based upon analysis using HPLC, LC-MS² and NMR spectroscopy.

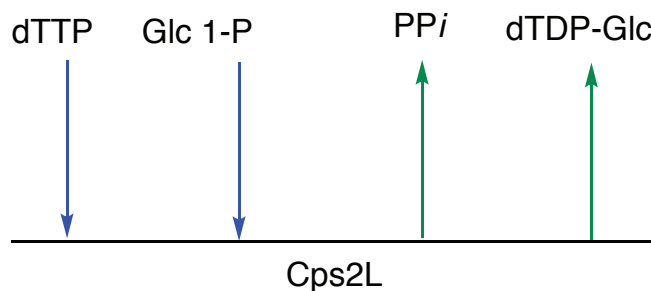


Figure 21. Ordered Bi-Bi reaction mechanism of Cps2L.

2.3.1. Evaluation of p₄dT as a Cps2L Substrate

Three pathways delineating possible outcomes for the activity of p₄dT as a Cps2L substrate are illustrated in Figure 22. In the first proposed pathway ((**ii**), Figure 22), p₄dT is hydrolyzed, potentially enzymatically, releasing monophosphate (P_i) and dTTP, which then reacts with Glc 1-P to produce deoxythymidine 5'-diphospho D-glucose (dTDP-Glc) in the same manner as the physiological reaction ((**i**), Figure 22). A second pathway ((**iii**), Scheme 1) would proceed by the reaction of p₄dT and Glc 1-P to produce dTDP-Glc, releasing triphosphate (P₃); this requires Glc 1-P to attack the α-phosphorus of p₄dT, resulting in departure of P₃, a process that closely resembles the accepted reaction mechanism.⁸⁴ Finally, the third scenario ((**iv**), Figure 22) would produce an alternate sugar nucleotide, dTTP-Glc, which would be produced from the attack of Glc 1-P at the β-phosphorus of p₄dT, releasing diphosphate (PP_i), a product released in the physiological reaction.

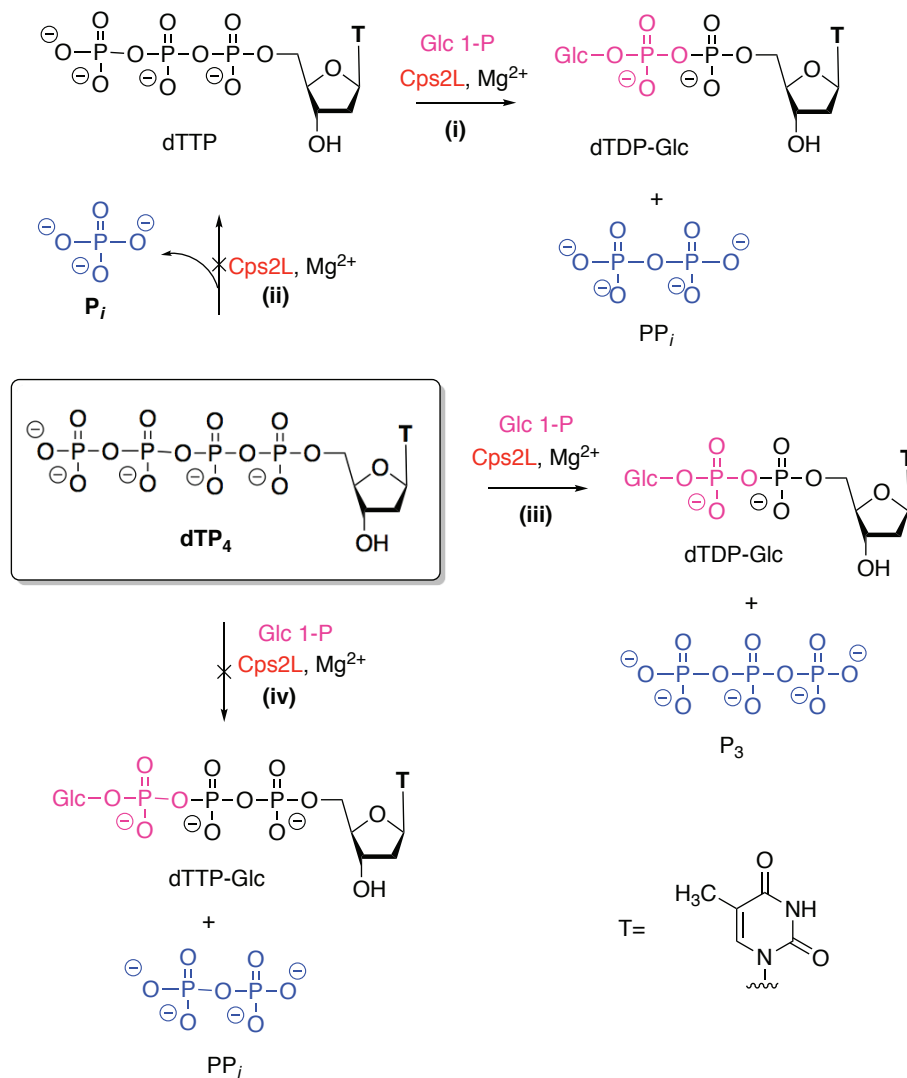


Figure 22. Catalysis by Cps2L (i) physiological reaction and (ii-iv) plausible reaction pathways and products for the reaction between Glc 1-P and p₄dT catalysed by Cps2L.

To confirm the activity of p₄dT as a Cps2L substrate, a reaction with Glc 1-P was monitored by HPLC. Whilst the reaction did not reach completion, a new signal with a retention time (R_T) of 5.6 min emerged in the HPLC trace recorded at 1 h and an accumulation of this product was observed over 5 h, whereupon integration of the traces indicated 25% conversion (Figure 23). The R_T of the observed product

matched that of a dTDP-Glc standard (R_T 5.7 min), and furthermore, LC-MS² analysis of the reaction mixture confirmed the product mass and characteristic fragmentation expected for dTDP-Glc fragment (parent ion scan $[M-H]^-$ m/z 563, fragments to dTMP $[M-H]^-$ m/z 321); these data ruled out pathway (iv), as no evidence of deoxythymidine 5'-triphospho α -D-glucose (dTTP-Glc) was observed. We measured the specific activities of dTTP and p₄dT under the same conditions; a specific activity of 0.2 μmolmin^{-1} was found for dTTP and 0.02 μmolmin^{-1} for p₄dT. Thus, turnover to product was reduced 10-fold for p₄dT in comparison to dTTP.

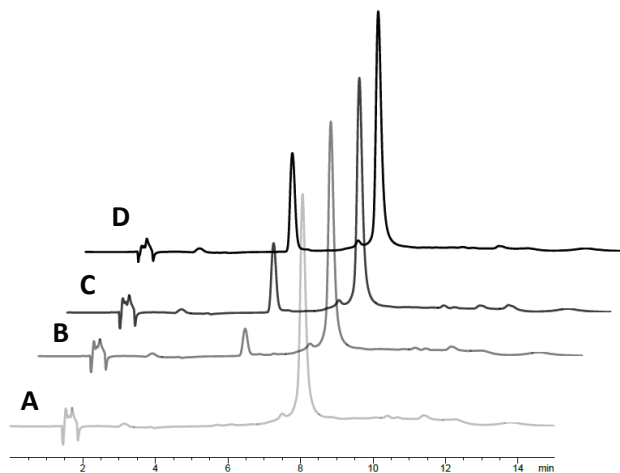


Figure 23. Thymidyltransferase-catalysed production of dTDP-Glc (R_T 5.7 min) from p₄dT (R_T 8.0 min) and Glc 1-P. (A) 1 min, dTDP-Glc (0%), (B) 1 h, dTDP-Glc (8%), (C) 3 h, dTDP-Glc (19%), and (D) 5 h, dTDP-Glc (25%). The sample comprised p₄dT (5 mM), Glc 1-P (5 mM), MgCl₂ (100 μM), D₂O (10% volume) and Cps2L (95 μM) in buffered H₂O.

To distinguish whether pathway (ii) or (iii) resulted in the production of dTDP-Glc, ³¹P NMR spectra documenting the reaction progress were recorded in

order to analyze the reaction products. The detection of P_i and PP_i in the reaction mixture would indicate that hydrolysis of p_4dT to $dTTP$ was occurring (pathway **(ii)**). Alternatively, the detection of P_3 would confirm that p_4dT was acting as substrate (pathway **(iii)**). All samples used for NMR analysis were prepared with $100 \mu\text{M Mg}^{2+}$ (an essential cofactor), which resulted in approximately a 100-fold reduction in rate compared to a reaction containing the standard 1 mM Mg^{2+} , with a measured specific activity of $0.0003 \mu\text{molmin}^{-1}$. The 10-fold reduction in magnesium concentration overcame broadening of the ^{31}P signals due to the presence of Mg^{2+} . However, signal overlap rendered the distinction of PP_i or P_3 from p_4dT signals ambiguous when analyzing the reaction mixture directly at pH 7.0. To address the issue of signal overlap in ^{31}P NMR spectra, solutions were titrated from pH 7 to pH 10 using aqueous NaOH (0.2 M). In a standard sample (Figure 24A), it is apparent that PP_i and P_3 shifts are well resolved at pH 10. Adjustment of the reaction sample (Figure 24D) to pH 10 deconvoluted the signals between δ -20 and -25, enabling the identification of the β -phosphorus P_3 signal at δ -20. Spiking the solution with P_3 resulted in an increase in intensity of the β -phosphorus signal at δ -20 and an increase in intensity of the α -phosphorus signal at δ -5.

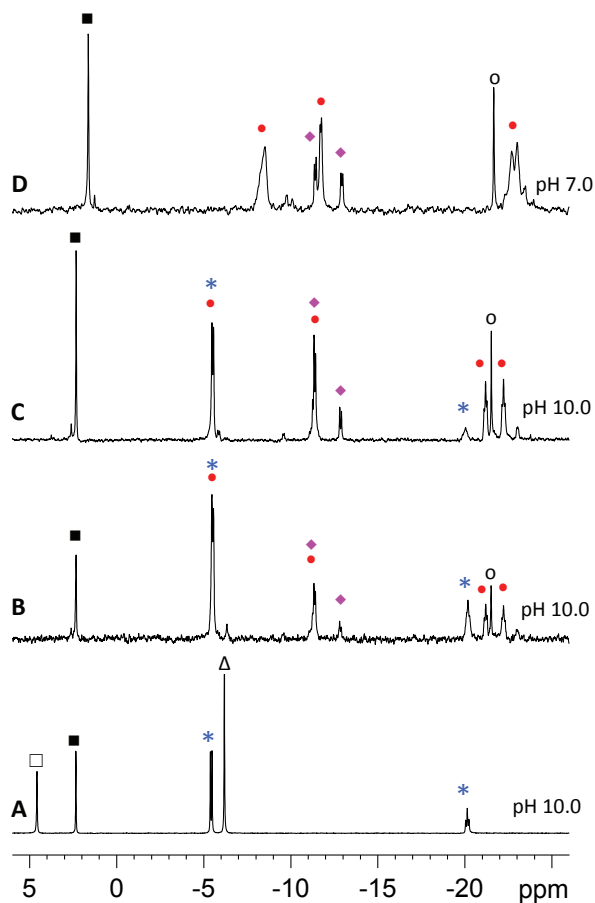


Figure 24. Thymidyltransferase catalysed production of triphosphate (P_3) from p_4dT . $^{31}P\{^1H\}$ NMR (202 MHz, 10% D_2O in H_2O) spectra; A, B and C were acquired with 256 scans, whilst spectrum C was recorded with 3200 scans. (A) a reference sample containing ~ 5 mM P_3 , PP_i , P_i , and Glc 1-P at pH 10 with 95 μM Cps2L; (B) same as (C) with the addition of 2 mM P_3 ; (C) reaction progress at 5 h recorded after adjustment to pH 10; (D) same sample as panel D in Figure 23D; reaction progress recorded at 5 h at pH 7. (\square) P_i ; (\blacksquare) Glc 1-P; (*) P_3 ; (Δ) PP_i ; (\bullet) p_4dT ; (\blacklozenge) dTDP-Glc; (o) trimetaphosphate ($Na_3P_3O_9$, internal reference). The signal at δ -6.2 in B is a small amount of PP_i that is present in the commercial P_3 .

A similar analysis of the physiological reaction, whereupon the same NMR experiments were conducted in order to observe the products from the reaction of dTTP with Glc 1-P, clearly showed the production of PP_i at δ -6. An additional HPLC experiment demonstrating the stability of p₄dT in the presence and absence of Cps2L over a time period of 24 h demonstrated a maximum breakdown to dTTP of 6%, an observation that offers further evidence against pathway (ii). The reverse reaction of a uridylyltransferase to produce nucleoside polyphosphates has been described previously;¹²⁶ uridine 5'-tetraphosphate and uridine 5'-pentaphosphate were enzymatically synthesized by the reaction of uridine 5'-diphospho glucose with P₃ or tetraphosphate using a uridylyltransferase from *S. cerevisiae*.

2.3.2. Conclusions

As far as can be established, this study represents the first evaluation of a thymidylyltransferase with a nucleoside tetraphosphate substrate. Our study has illustrated that p₄dT serves as a Cps2L substrate, with a 10-fold decrease in activity compared to the physiological substrate dTTP, and supports a pathway where nucleophilic phosphate attacks the α -phosphate of p₄dT releasing P₃. This demonstrates that Cps2L can accommodate an additional phosphate group in its active site while maintaining catalytic proficiency. We propose that as a future avenue of inhibitor design that charged species that may serve as mimics of the Cps2L transition state. This discovery may have implications in the design of nucleotidylyltransferase inhibitors and other enzymes capable of recognizing nucleoside polyphosphates.

2.4. Evaluation of Rhamnose Biosynthetic Enzymes (RmlBCD) for Chemoenzymatic Applications

Dr. Jian-She Zhu is thanked for synthesis of fluorinated Glc 1-P analogues (**2.16-2.19, 2.20**).¹²⁷

In this study substrate tolerances of enzymes RmlB, C and D have been evaluated with a series of dTDP-Glc analogues, these being generated *in situ* from the reaction of the Glc 1-P analogues with Cps2L. The analogue scope included functional substitutions of hydroxyl groups for amino groups (**2.1** and **2.2**) or for fluorine groups (**2.16-2.20**) and methylene substitution (phosphonates **2.5** and **2.18**). If processed by all three Rml enzymes, the produced sugar nucleotides, analogues of dTDP-Rham would be anticipated to act as inhibitors of rhamnosyltransferases through destabilization of the oxo-carbenium mechanistic intermediate (amino and fluoro substituted) or by preventing sugar transfer (phosphonates). A chemoenzymatic preparation of the phosphonate analogue of dTDP-Rha was accomplished, producing a novel phosphonate dTDP-1C-Rha, anticipated to act as an inhibitor against the enzymes in the rhamnose biosynthetic pathway and rhamnosyltransferases MigA and WapR, and as a feedback inhibitor of Cps2L.

2.4.1. Analytical Assays to Probe Substrate Tolerance of RmlBCD

Recombinant Cps2L, RmlB, RmlC and RmlD were expressed in *E. coli* and purified by nickel-affinity chromatography as previously described.^{80, 111} Cps2L is the name given to the RmlA enzyme from *S. pneumoniae*.⁸⁰ The thymidyltransferase (RmlA/Cps2L) possesses an allosteric binding pocket that has been implicated in

product inhibition by the final product of the pathway, dTDP-Rha.^{84, 114} In order to prohibit inhibition of the first step by downstream products, the assay was set up to allow the first step, namely the *in situ* production of NDP-sugars using Cps2L, to reach completion prior to the addition of the remaining enzymes (Figure 25). This step was monitored by HPLC and LCMS, and it was established that the reactions reached completion after 1 h at 37 °C.

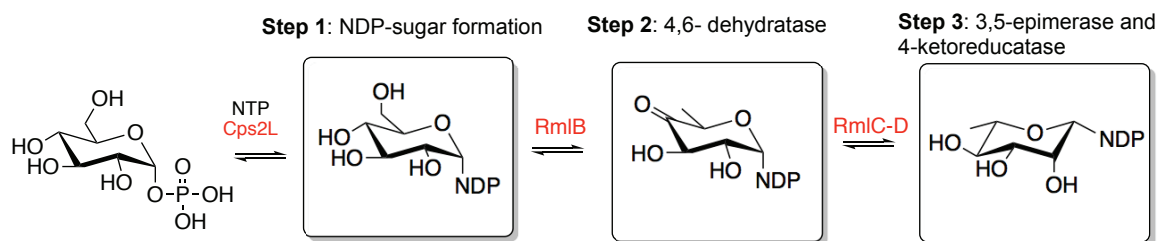
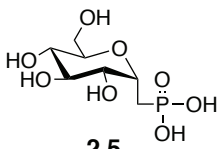
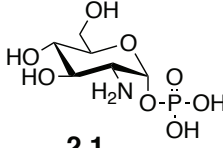
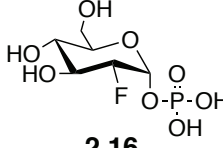
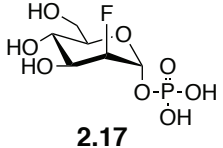


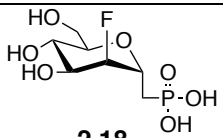
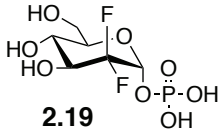
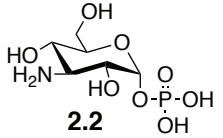
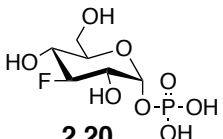
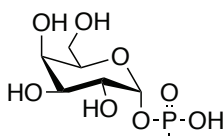
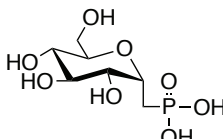
Figure 25. Analytical scale RmlB-D assay.

Reaction conditions for RmlB-D were adapted from the literature; the inclusion of nicotinamide adenine dinucleotide (NAD), formate dehydrogenase, and ammonium formate as reaction components was necessary to achieve full conversion to dTDP-Rha.¹⁰⁰ In step 2, after the initial incubation with Cps2L, RmlB was added and allowed to react for one hour at room temperature. At this point, an aliquot of the reaction was monitored by LCMS prior to addition of the last two enzymes, RmlC and RmlD. For the physiological reaction with Glc 1-P the masses corresponding to the products of Cps2L and RmlB reactions were both present by LCMS in comparable amounts (judging by signal intensity), this observation was not consistent with literature reports suggesting this reaction achieves complete conversion.^{99, 128, 129} Both RmlC and RmlD were added in step 3, followed by incubation at room temperature with monitoring of reaction aliquots at two and

sixteen hours. We had observed in trial assays that RmlC products were unstable, resulting in decomposition of the intermediate NDP-sugar, an observation consistent with literature reports.^{99, 100} The Glc 1-P analogues evaluated had previously been established as Cps2L substrates and the corresponding NDP-sugar product masses were detected by LCMS, as anticipated (Table 4).^{80, 127, 130} Consumption of dTTP, the limiting reagent, was used to determine the percent conversion by HPLC.

Table 4. Substrate scope assay^a with RmlB, RmlC and RmlD. Masses in the table correspond to the anticipated *m/z* of products [M-H]⁻ at the indicated step. Masses shaded out were not observed.

Entry	Sugar	NTP	Step 1 (Cps2L)	Step 2 (RmlB)	Step 3 (RmlC-D)
1	Glc 1-P	dTTP	563	545	547
2	 2.5	dTTP	561	543	545
3	 2.1	dTTP	562	544	546
4	 2.16	dTTP	565	547	549
5	 2.17	dTTP	565	547	549

Entry	Sugar	NTP	Step 1 (Cps2L)	Step 2 (RmlB)	Step 3 (RmlC-D)
6	 <p>2.18</p>	dTTP	563	545	547 ^{b,c}
7	 <p>2.19</p>	dTTP	583	565	567
8	 <p>2.2</p>	dTTP	562	544	546
9	 <p>2.20</p>	dTTP	565	547	549
10	 <p>Gal 1-P</p>	dTTP	563	545	547
11	Glc 1-P	UTP	565	547	549
12	 <p>2.5</p>	UTP	563	545	547 ^c

^aReaction conditions: **Step 1:** 4 mM Glc 1-P/analogue, 2 mM NTP, 9 μ M Cps2L, 8 mM Mg^{2+} , Tris·HCl 50 mM, pH 7.5; **Step 2:** following components added to indicated concentrations (concentrations from step 1 halved): 20 mM ammonium formate, 0.1 mM NAD, 0.2 EU formate dehydrogenase, 6.3 μ M RmlB; **Step 3:** following components added to indicated concentrations (concentrations from step 1 quartered); 25 μ M RmlC, 10 μ M RmlD; ^bIncomplete conversion to product; ^cAn additional product m/z 529 was observed.

The following discussion reflects an interpretation of the data based on the masses observed by LCMS and the corresponding products were not isolated, except for dTDP-1C-Rha (Section 2.4.3). UDP-glc (Table 4, Entry 11) was tolerated by all

three (RmlB-D) enzymes. In that reaction, after the addition of RmlB, a 1:1 RmlB product to Cps2L product was observed by LCMS after 2 hours, the same ratio observed with the physiological substrate. The expected final product (m/z 549) was the sole product detected after 16 h. The phosphonate analogue of Glc 1-P (**2.5**, Table 4, Entry 1 and 12) was accepted by all three enzymes, and product masses corresponding to dTDP-1C-Rha (m/z 545, [M-H]⁻) and UDP-1C-Rha (m/z 547, [M-H]⁻) were observed by LCMS, although production of UDP-1C-Rha did not reach completion over 16 h. Thus, while tolerated, the rate of turnover using both an unnatural nucleotide base (uridine) and sugar analogue was sluggish. The step 2 RmlB product was observed for amino sugars **2.1** and **2.2** (Table 4, Entry 3 and 8) but no products were observed after the addition of RmlC and RmlD in step 3. After the addition of RmlB, the 2-deoxy-2-amino sugar **2.1** possessed a 1:6 and the 3-deoxy-3-amino sugar **2.2** a 1:1 RmlB product to Cps2L product ratio by LCMS. RmlB has previously been shown to accept dTDP-Glc analogues with deoxy and azido functionalities at C-3.¹³¹ After the addition of RmlC and RmlD, these amino sugar products were subject to breakdown, as indicated by emergence of a prominent signal for dTDP (m/z 401, [M-H]⁻) according to analysis using LCMS. The generation of dTDP arises from the elimination of the phosphate at the anomeric position, which occurs slowly either enzymatically as a non-specific reaction or due to chemical decomposition of an unstable intermediate. Deoxyfluoro sugars **2.16**, **2.17**, and **2.19** did not produce the anticipated product analogues with any of the enzymes (RmlB-D), and the observation of dTDP (m/z 401, [M-H]⁻) by LCMS indicated cleavage of the phosphate at the anomeric position. The mono-

fluorinated analogues (**2.16** and **2.17**) showed breakdown after the addition of RmlB, while the Cps2L product of difluorinated analogue (**2.19**) was detected by LCMS at the same time point. However, after addition of RmlC-D, only dTDP was identified in the LCMS experiment of the assay with difluoro sugar **2.19**, indicating breakdown of the sugar nucleotide over time. The presence of electronegative fluorine atoms at the 2-position of the hexose ring may increase the susceptibility of the anomeric center to breakdown. The products from the reaction of 2-deoxy-fluoro manno-configured phosphonate **2.18** (Table 4, Entry 6) were anticipated to be resistant to anomeric breakdown due to the absence of a labile C-O-P bond. Analyses by LCMS of the reaction after step 3 using a precursor ion scan of m/z 321 ($[M-H]^-$ of dTMP) revealed a mixture of product signals (Figure 26).

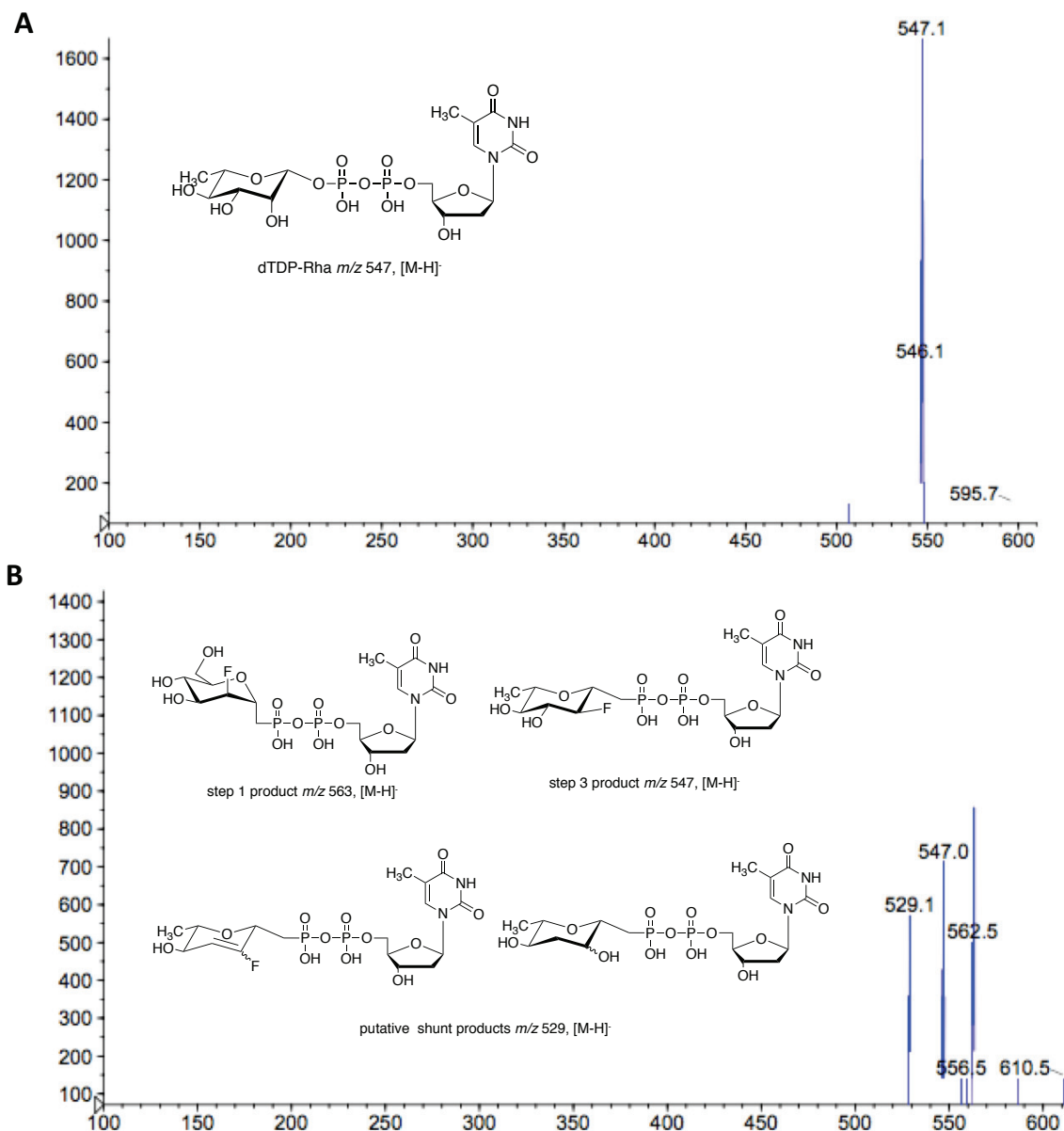


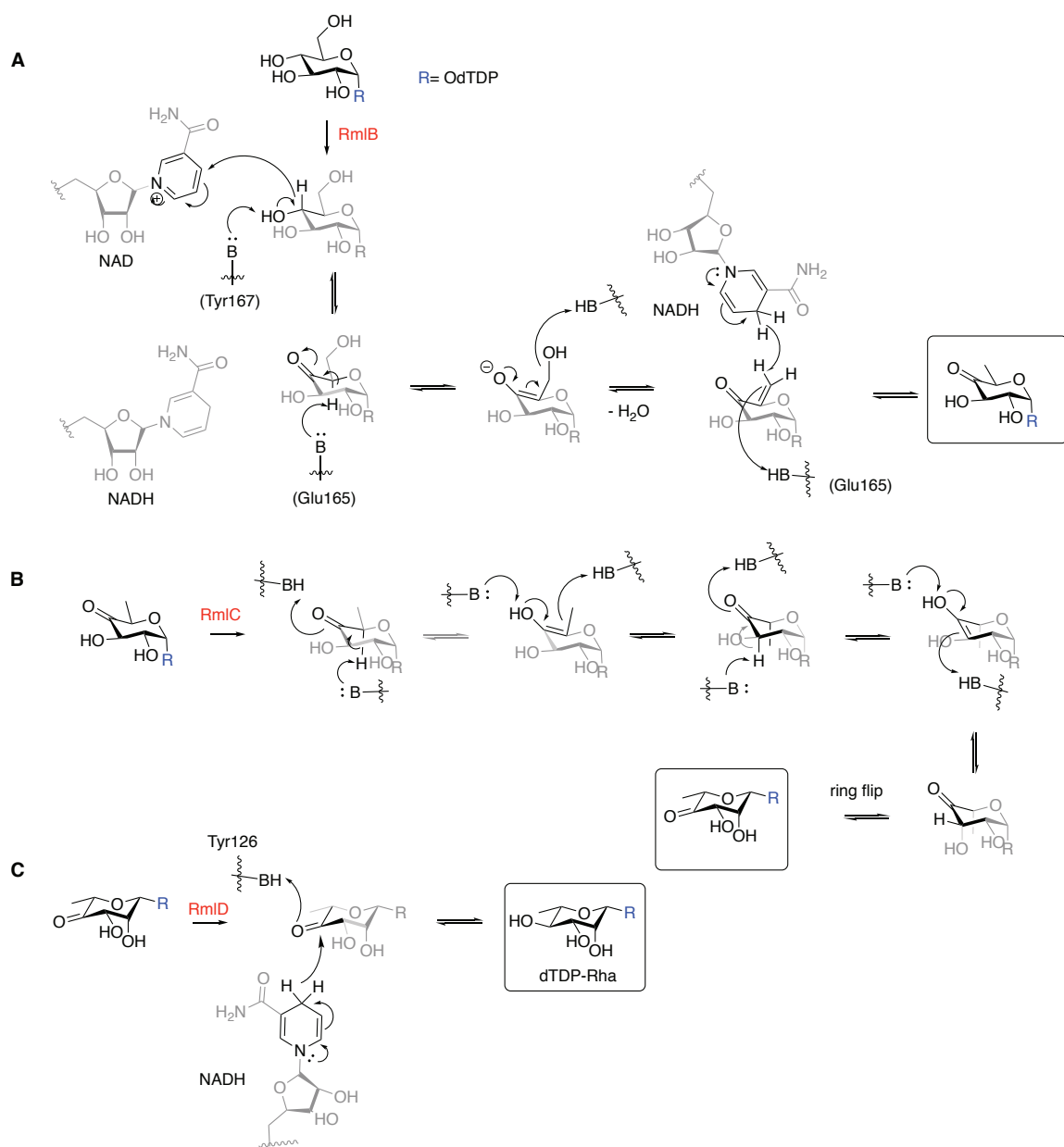
Figure 26. Precursor scan of m/z 321 (LCMS, negative mode) for the reaction of dTTP and (A) Glc 1-P or (B) **2.18** with Cps2L, RmlB, RmlC and RmlD. Proposed structures correspond to observed masses thus shown regioselectivity and stereochemistry may not be accurate.

These corresponded to the Cps2L product (m/z 563), the final product (m/z 547), and a putative shunt product (m/z 529). The origin of this shunt product was

unclear, a signal corresponding to the 6-deoxy-4-keto product (m/z 545) was not observed after addition of RmlB (Step 2), although, as discussed, a range of product to substrate ratios have been observed at this step therefore the absence of a product signal does necessarily indicate that the product is not present, for instance below a detection threshold. The putative shunt product was only observed after addition of RmlC and RmlD (Step 3, m/z 529), and the mass is consistent with a 6-deoxygenated and dehydrated product or elimination of fluoride. Characterization of the product by NMR will facilitate elucidation of this putative new product and inferences to be made about the possible mechanistic roles of RmlB, RmlC and RmlD in its formation, and may also provide mechanistic insight for observed hydrolysis with other substrates. If fluorine is indeed eliminated in the mechanism, this would be readily observed by ^{19}F NMR spectroscopy, as the corresponding singlet signal for fluoride ($\sim\delta$ -120)^{119,120} is distinct from the fluoride signal of **2.18** ($\sim\delta$ -200, Zhu, J.-S. and Jakeman, D.L. (2017), unpublished data).^{132, 133} Evaluation of Gal 1-P (Table 4, Entry 10) demonstrated that dTDP-Gal was not a substrate for RmlB, which suggests that inversion of a hydroxyl group at C-4 of the hexose ring shuts down the RmlB reaction mechanism, and may serve as an inhibitor of the reaction. The Cps2L product, dTDP-Gal, was observed after the addition of RmlC and RmlD, although some decomposition to dTDP was also present in the mixture after 16 h, as detected by LCMS.

Collectively, the mechanisms of the RmlB, RmlC, and RmlD involve direct oxidation, reduction, and elimination of water, at the C-3, C-4, C-5 and C-6 positions of the hexose ring (Figure 27).^{79, 93-96, 114, 134} In considering the reaction

mechanisms of the enzymes, we had predicted that compounds with modifications to the C-2 position (**2.1**, **2.16-2.19**) may serve as substrates, since this site is not directly involved in the mechanism, although this not supported by our results. Likewise, the presence of equatorial amino (**2.2**) and fluoro (**2.20**) groups at C-3 were not tolerated. The presence of functional groups such as amino (protonated at pH 7.0) and fluoro increase the acidity of the protons attached to the same carbon, and the presence of functional groups may also affect the mode of binding or ring conformation. The evaluation of α -D-mannose 1-phosphate (Man 1-P) in these assays will enable us to probe whether an inversion is tolerated at C-2 or whether the observed hydrolysis was caused by the presence of either amino (**2.1**) or fluoro (**2.16, 2.17, 2.19**) groups.



2.4.2. Chemoenzymatic Synthesis of dTDP-1C-Rha

The phosphonate analogues of sugar phosphates contain a carbon-phosphorus bond in place of the oxygen-phosphorus anomeric linkage, a substitution that produces an isosteric, non-hydrolyzable analogue.¹³⁵ Phosphonate analogues have thus been put forward as potential inhibitors for glycosyltransferases and as tools to study

biosynthetic pathways.^{111, 132, 136-139} To isolate the phosphonate analogue of dTDP-Rha, a reaction was initiated from dTDP-1C-Glc, the latter having been prepared following published procedures.⁸⁷ A reaction was then set up with dTDP-1C-Glc and RmlB-D. The reactions was incubated at room temperature and monitored by LCMS. The enzymatic conversion monitored by LCMS was complete within 4 h, showing dTDP-1C-Rha as the sole product (m/z 545, $[M-H]^-$). Purification was accomplished in two steps using an ion-pair reversed-phase column followed by an LH20 gel filtration column to yield 1.4 mg dTDP-1C-Rha (Figure 28) from 2.5 mg dTDP-1C-Glc (60%). The HPLC trace of the product contained a single peak with R_T 5.9 min. In the proton NMR spectrum, a single species was apparent, possessing the characteristic diastereotopic H-1'' methylene signals at 2.25 and 2.06 ppm appearing as ddd with $^1J_{H1'',P} \sim 20$ Hz. A doublet integrating to three (δ 1.30, $^2J_{H-6''CH_3,H-6''} 5.7$ Hz) was consistent with dehydration of the 6-hydroxyl group, and overall the signals were consistent with those reported for the phosphonate analogue of Rha 1-P.¹¹¹ Two doublets ($^2J_{P-\alpha,P-\beta} = 26$ Hz) in the phosphorus NMR spectrum were characteristic of sugar nucleotides, and the chemical shift 13 ppm of P- β fell within the expected range for a phosphonate.^{87, 130} High resolution mass spectrometry (HRMS) data was in agreement with the chemical formula of dTDP-1C-Rha (m/z 545.0956 detected for $[M-H]^- C_{17}H_{27}N_2O_{14}P_2$). Evaluation of dTDP-1C-Rha in an inhibition assay against Cps2L with Glc 1-P as the variable substrate identified it as a competitive inhibitor with a K_i of 468 μ M (Zhu, J.-S. and Jakeman, D.L. (2017) unpublished data) using the MESG-PNP-XO coupled assay described in Section 2.2. The strength of inhibition was not significantly improved in comparison

the reported K_i of 536 μM for β -L-rhamnose 1C-phosphonate with a competitive mode of inhibition.¹¹¹

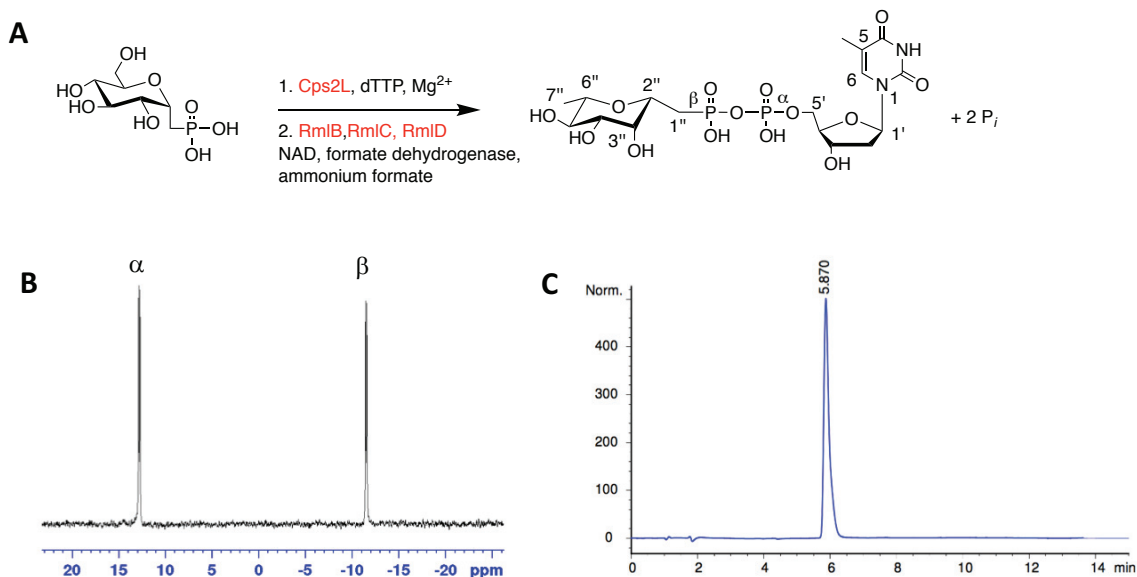


Figure 28. (A) Chemo-enzymatic synthesis of dTDP-1C-Rha; (B) $^{31}\text{P}\{^1\text{H}\}$ NMR spectrum (200 MHz, D_2O) and (C) HPLC trace of purified dTDP-1C-Rha.

2.4.3. Conclusion and Future Work

We have established that the rhamnose biosynthetic enzymes, *RmlB-D*, are able to convert the phosphonate analogues of dTDP-Glc and UDP-Glc to produce rhamnosyl-phosphonates, dTDP-1C-Rha and UDP-1C-Rha. An uncharacterized product was detected by LCMS when evaluating fluoro phosphonate **2.18**. Analogues containing amino groups (**2.1**, **2.2**) or fluorine atoms (**2.16-2.20**) at the C-2 and C-3 positions of the hexose rings were found not to be substrates for the enzymes, and were prone to hydrolysis over the time course of assay monitoring. We propose that further insight into these results could be gained from the characterization of the shunt product observed in the assay containing 2-deoxy-2-

fluoro- α -D-mannose 1-phosphonate (**2.18**) and by evaluation of Man 1-P as a putative substrate, which lacks an amino/fluoro group but the C-2 hydroxyl is inverted in comparison to Glc 1-P. dTDP-1C-Rha was identified as a weak inhibitor (K_i of 468 μ M) of Cps2L. In collaboration with Dr. Joseph Lam and Dr. Matt Kimber (University of Guelph), and Dr. Inka Brockhausen (Queens University), we began to develop rhamnosyltransferase activity assays with recombinant MigA and WapR. However, although some evidence of enzymatic turnover was observed (data not shown), reproducibility and low turnover rates associated with these assays limited our ability to evaluate dTDP-1C-Rha as an inhibitor. Understanding the interactions of RmlB-D with the various analogues will facilitate the identification of inhibitors for these processes.

2.5. Characterization of a Promiscuous Glycosyltransferase (Sv0189) from *S. venezuelae* ISP5230

In this section, we studied a GT-1 family glycosyltransferase identified within the *S. venezuelae* genome, a strain that is routinely used in the Jakeman laboratory. Progress towards characterization of the recombinant enzyme, Sv0189, as a potential glycodiversification catalyst will be discussed.

2.5.1. Identification of Sv0189 as a Glycosyltransferase for Glycodiversification

The CAZy database identified 66 glycosyltransferases in the genome of *Streptomyces venezuelae* ISP5230. Five of these belong to the GT1 family glycosyltransferases, which are predominant in small molecule biosynthesis, are listed in Table 5.¹⁴⁰

Table 5. GT1 family glycosyltransferases in the *S. venezuelae* ISP5230 (ATCC 10712) genome.

Name	Gene annotation	Protein Annotation	% Identity to OleD	Antismash cluster
Sv0537	SVEN_RS02570	WP_015031743.1	21.8	8/9: lantipeptide-terpene ^a
Sv0189	SVEN_RS00895	WP_041663413.1	74.5	3 cf_putative ^a
Sv3444	SVEN_RS17030	WP_015034645.1	20.5	42: cf_fatty acid
Sv5997	SVEN_RS29750	WP_015037178.1	23.2	66: T2pks (JadS)
Sv6866	SVEN_RS34005	WP_015038047.1	23.0	None detected

^aThese genes are found in proximity to the indicated predicted secondary gene clusters.

The gene *sv5997* encodes to the L-digitoxyltransferase JadS (Sv5997) from the jadomycin biosynthetic gene cluster, while the other four gene products remain uncharacterized.¹⁴¹ Our attention was drawn to Sv0189 (*sv0189*) for its high sequence identity to OleD (74%), a macrolide-inactivating glycosyltransferase that has been the focus of a number of studies related to glycodiversification, including directed evolution as a means to broaden its substrate scope.¹⁴²⁻¹⁴⁵ OleD inactivates oldeandomycin, produced by the native strain *Streptomyces antibioticus*, and a host of other macrolide antibiotics including, carbocin, tylosin, and erythromycin, where glucosylation serves as a mechanism of host resistance for the producing strain (Figure 29).¹⁴² While the *oleD* gene is not located within the oleandomycin biosynthetic gene cluster, another gene, *oleI*, found within the gene cluster, encodes

a glycosyltransferase OleI that was found to perform the same reaction, although OleI was found to be stringent in terms of activity towards oleandomycin.^{142, 145} The prevalence of OleD and close homologues in *Streptomyces* have led to a proposed role in a general resistance mechanism against macrolide antibiotics, either *in lieu* of, or in cooperation with other resistance mechanisms.^{142, 146, 147} Proteins similar to OleD are widespread in the genus *Streptomyces*, and a BLASTP search returned 100 homologous proteins with 82% identity or greater (accessed 08.22.17), furthering support for the proposition that these proteins may serve a more general role, perhaps as a xenobiotic resistance mechanism. A flexible glycosyltransferase from *Saccharothrix esapensis*, Ses60320, was also identified as being encoded outside of predicted secondary metabolite gene clusters.¹⁴⁸

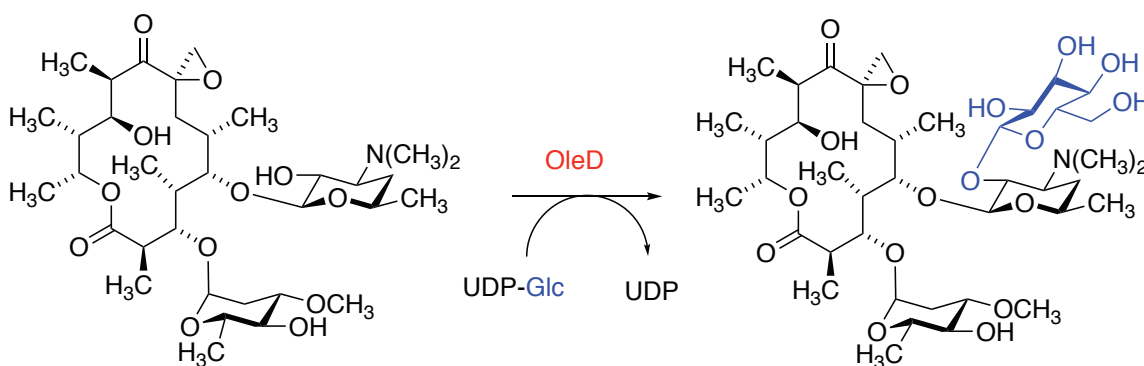


Figure 29. Glucosylation of oleandomycin by OleD.

In another study, discussed in Section 3.3 of this thesis, we hypothesized that Sv0189 may be involved in the production of a glucosylated jadomycin analogue isolated in a *jadT* deletion strain of *S. venezuelae*. However, this hypothesis was disproven as it was found that the pathway-specific glycosyltransferase JadS was the catalyst.⁵⁹ In the same study, it was found that genetic deletion of *sv0189* from

the genome produced no apparent changes in cell growth or phenotype and thus was not an essential gene. In order to determine whether *sv0189* was found within a biosynthetic gene cluster for which it was likely to possess specificity towards an associated secondary metabolite, an AntiSMASH analysis was performed (AntiSMASH V4.0.1, accessed 08.14.17) on the *S. venezuelae* genome; AntiSMASH is a free online prediction software tool that predicts secondary metabolite gene clusters from an input nucleotide sequence.¹⁴⁹ Within the *S. venezuelae* genome, 84 predicted secondary metabolite gene clusters were detected, eight of which have been linked to characterized natural products including chloramphenicol (cluster 14), the jadomycins (cluster 67), gaburedin (cluster 46), venezuelin (cluster 10), foroxymithine (cluster 80), (+)-isodauc-8-en-11-ol (cluster 9), venemycin (cluster 8a), and isopyochelin (cluster 8b, Figure 30).^{141, 150-156} *sv0189* was not found within any of the predicted gene clusters, although it was situated in close proximity, just four genes, from cluster 3, which is described as a putative gene cluster with 6% gene similarity to a number of disparate secondary metabolite clusters including those encoding hygromycin B (saccharide), herbimycin (macrolide), collismycin A (2,29-bipyridyl), yatakemycin (cyclopropapyrroloindole) and alnumycin (naphthoquinone). Considering the possibility that Sv0189 serves a role in self-resistance against a macrolide antibiotic, no putative macrolide gene clusters (polyketide synthase type 1) were identified in the *S. venezuelae* ISP5230 genome, with the exception of cluster 8 that had been found to produce isopyochelin and related analogues.¹⁵⁵ In short, Sv0189 was not found to be associated with any known secondary metabolite gene clusters, and thus

the physiological acceptor remained unknown. It is unclear whether Sv0189 physiologically serves a purpose in deactivation of a host-produced secondary metabolite or more broadly in a general xenobiotic resistance mechanism, or whether there is some other function that has not yet been determined.

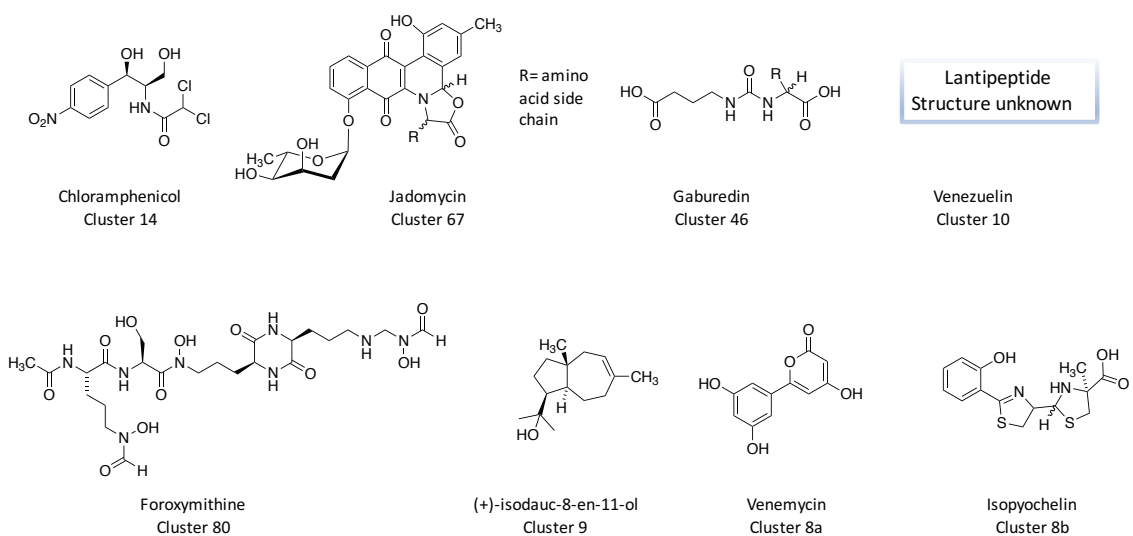


Figure 30. Characterized natural products produced by *S. venezuelae* ISP5230 and corresponding gene clusters.

UDP-Glc was honed in on as the sugar nucleotide donor, also being the preferred donor for OleD, with both protein sequences possessed binding motifs for pyrimidine nucleotides.^{74, 144, 157} A sequence alignment of wild-type OleD and Sv0189 revealed that two positions that are consistently mutated in evolved iterations of OleD are different in Sv0189 compared to wild-type OleD. The mutants ASP, TDP-16 and Loki all contain the mutations P67T and S132F, which correspond to T69 and W132 in Sv0189 (Figure 31).^{143, 158, 159} The P67 position is situated in a variable loop region that has been associated with donor binding, and the S132 position is considered highly conserved (S or T) and is associated with

2.5.2. Cloning and Expression of Sv0189

The gene *sv0189* was cloned from *S. venezuelae* ISP5230 and ligated with *E. coli* expression vector pET28a using Gibson assembly methodology. At this stage, the construct included both C-His₆ and N-His₆ terminal tags; therefore, a stop codon was introduced in front of the C-terminal His₆ sequence by site-directed mutagenesis in order to retain only the N-terminal His₆ tag. Figure 32 shows the restriction digest analysis performed to confirm the assembly of the desired *E. coli* expression vector, pET28a::NHis₆*sv0189*, where successful introduction of the desired mutation introduced a unique EcoRI restriction and removed a unique HindIII site. Plasmids in lanes 1, 2, 4, and 5 show the expected digestion pattern for the desired mutation. *E. coli* BL21(DE3) pLysS was transformed with pET28a::NHis₆*sv0189* for heterologous expression.

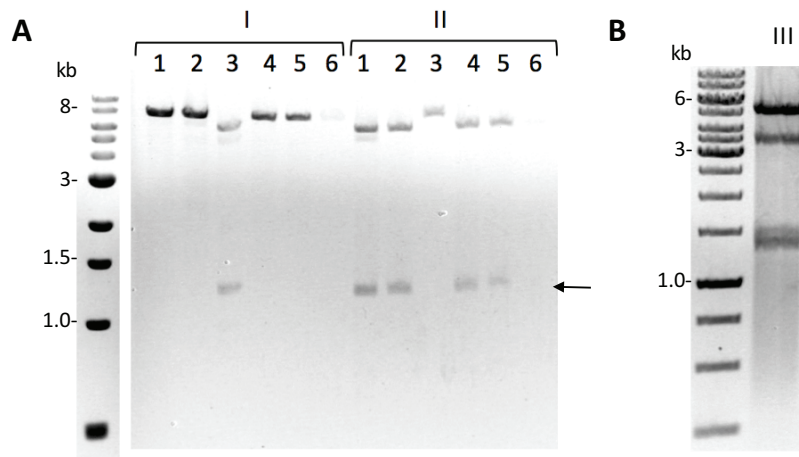


Figure 32. TAE-agarose (1%) DNA gels showing restriction digests in screening for pET28a::NHis₆*sv0189* after site directed mutagenesis (A) (I) NdeI and HindIII; (II) NdeI and EcoRI (B) isolated pET28a::NHis₆*sv0189* from *E. coli* BL21(DE3) pLysS digested with EcoRI and XbaI.

Overexpression using isopropyl β -D-thiogalactopyranoside (IPTG) induction was confirmed by sodium dodecyl sulfate polyacrylamide gel electrophoresis (SDS-PAGE, Figure 33). The protein was purified by nickel affinity chromatography. Fractions containing Sv0189 (52 kDa) were combined and buffer exchanged using a Sephadex® PD-10 pre-packed column into Tris·HCl (50 mM, pH 8.0). The protein solution was divided into aliquots and stored at -70 °C until use. The protein was found to be soluble throughout the purification process, and no precipitation was evident after a freeze-thaw cycle. In parallel, *jadS*, the glycosyltransferase from the jadomycin gene cluster identified as promiscuous with respect to donor specificity (Section 3.3) was cloned and ligated with pet28a using the same methods. Following overexpression and purification using IPTG and Ni affinity chromatography, respectively as above, JadS was identified by SDS page (data not shown). However, JadS was found to precipitate immediately after elution from the Ni column. Further optimization of the purification conditions will be required to isolate and characterize JadS *in vitro*.

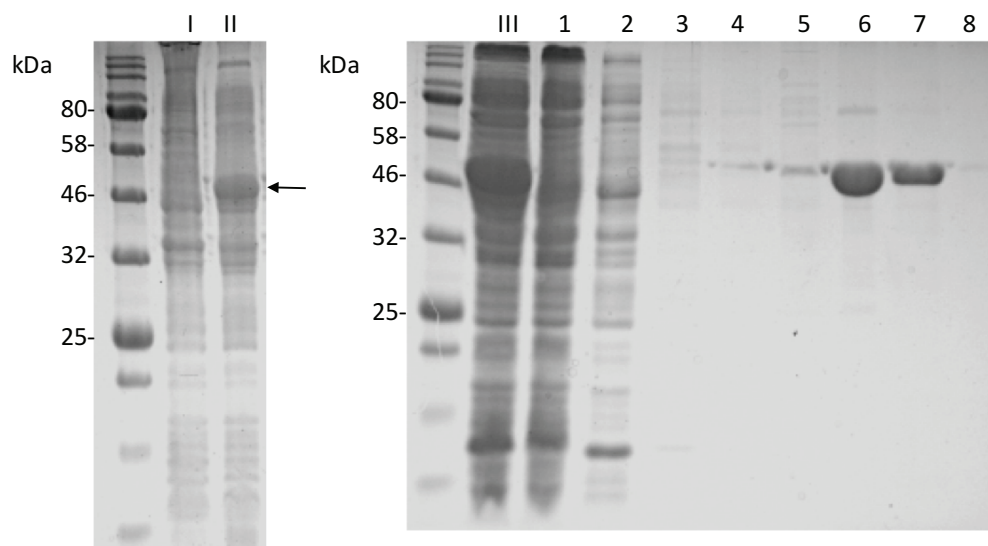


Figure 33. SDS-PAGE showing fractions from Sv0189 protein expression. (I) sample before IPTG induction; (II) sample after IPTG induction with arrow indicating induced Sv0189; (III) cell lysis solution before Ni column loading; (1-8) fractions from purification by Ni-affinity chromatography.

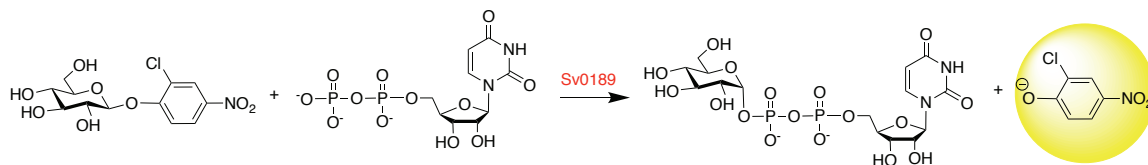
2.5.3. Establishing Glycosyltransferase Activity with Sv0189

With a stable and soluble protein in hand, we sought to establish glycosyltransferase activity with Sv0189. An initial assay was performed to monitor activity in the direction of UDP-Glc formation, by reaction of activated donor, 2-chloro-4-nitrophenol- β -D-glucopyranoside, with UDP. Transfer of glucose to UDP, releasing 2-chloro-4-nitrophenolate, was monitored at λ 410 nm and qualitatively observed through evolution of a yellow colour in the reaction well.¹⁵⁸

The assay produced a linear initial rate and evolution of yellow colour was visually observed consistent with enzymatic activity. Furthermore, the rate increased and/or decreased proportionally to the concentration of Sv0189 included

in the assay, and in the absence of Sv0189, the wells remained colourless. A Q1 neg LCMS scan of the reaction mixture showed a peak corresponding UDP-Glc at m/z 565 [M-H]⁻, providing evidence of product formation. Michaelis-Menten kinetics with respect to each UDP and 2-chloro-4-nitro-phenol- β -D-glucopyranoside were determined (Table 6). The K_m value for UDP, 0.13 mM, was comparable to that described for OleD, 0.25 mM, and was consistent with UDP-Glc as a physiological substrate.⁷⁴ While the k_{cat} and k_{cat}/K_m values were relatively low, this was attributed primarily to the low affinity (K_m 6.5 mM) of the donor, 2-chloro-4-nitro-phenol- β -D-glucopyranoside. The rates with dTDP were also evaluated, and were found to be reduced approximately 100-fold in comparison to UDP.

Table 6. Sv0189 kinetics with UDP and 2-chloro-4-nitro-phenol- β -D-glucopyranoside (pH 8.0).



	Variable substrate	
	UDP	2-chloro-4-nitro-phenol- β -D-glucopyranoside
K_m	0.13 mM	6.5 mM
k_{cat}	1.1 min ⁻¹	3.6 min ⁻¹
k_{cat}/K_m	8.2 mM ⁻¹ min ⁻¹	0.5 mM ⁻¹ min ⁻¹

The initial rate of the reaction in the direction of UDP formation was monitored in different buffers at variable pH strengths (Figure 34). The optimum pH was in the range of 7-7.5 and the reaction was most sluggish in 2-amino-2-(hydroxymethyl)propane-1,3-diol (Tris) buffer compared to phosphate-buffer saline (PBS) and 3-morpholinopropane-1-sulfonic acid (MOPS) buffer at the same pH value of 7.5. Use of a phosphate buffer, produced the fastest reaction rate, suggesting that high phosphate (50 mM) does not inhibit glycosyltransferase activity.

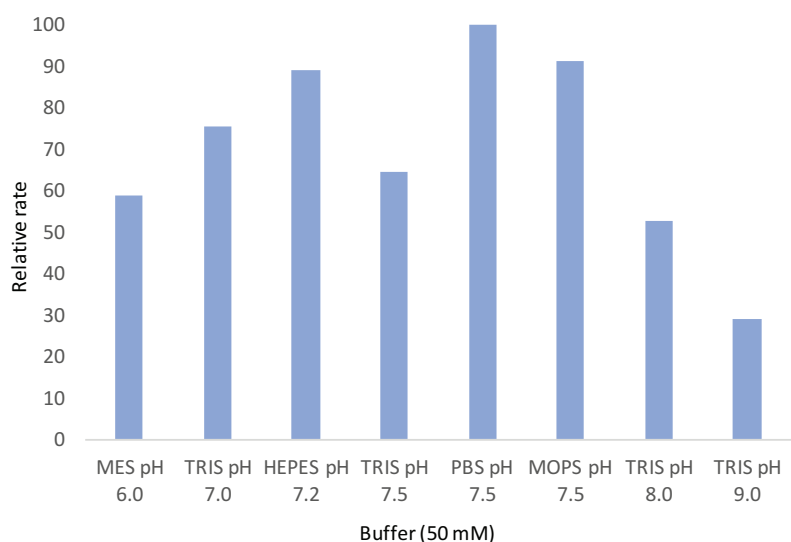


Figure 34. Sv0189 activity in various buffers and pH values.

An assay was developed to monitor the activity of Sv0189 in the forward direction, to confirm acceptor glycosylation, using a similar colorimetric assay with 4-methylumbelliferone (**A11**, 1 mM) as the acceptor (Figure 35).¹⁵⁸ The assay employed a catalytic concentration of UDP (0.01 mM) for *in situ* formation of UDP-Glc by Sv0189 (2.5 μ M); transfer of glucose to **A11** regenerates UDP, which upon

reaction with 2-chloro-4-nitro-phenol- β -D-glucopyranoside (concentration in excess, 1 mM), releases 2-chloro-4-nitro-phenol, the production of which was monitored by UV absorbance. Reaction progression and colour evolution is dependant on cycling of UDP. In the presence of **A11**, monitoring by UV (A_{410}) gave a rate greater than the control (no acceptor). An aliquot of the reaction mixture was analyzed by HPLC to confirm production of the glucosylated acceptor, β -D-glucose-4-methylumbelliferone. By HPLC, a new signal at 3.5 min was observed and was confirmed as the glucosylated acceptor by spiking the sample with commercial β -D-Glc-4-methylumbelliferone.

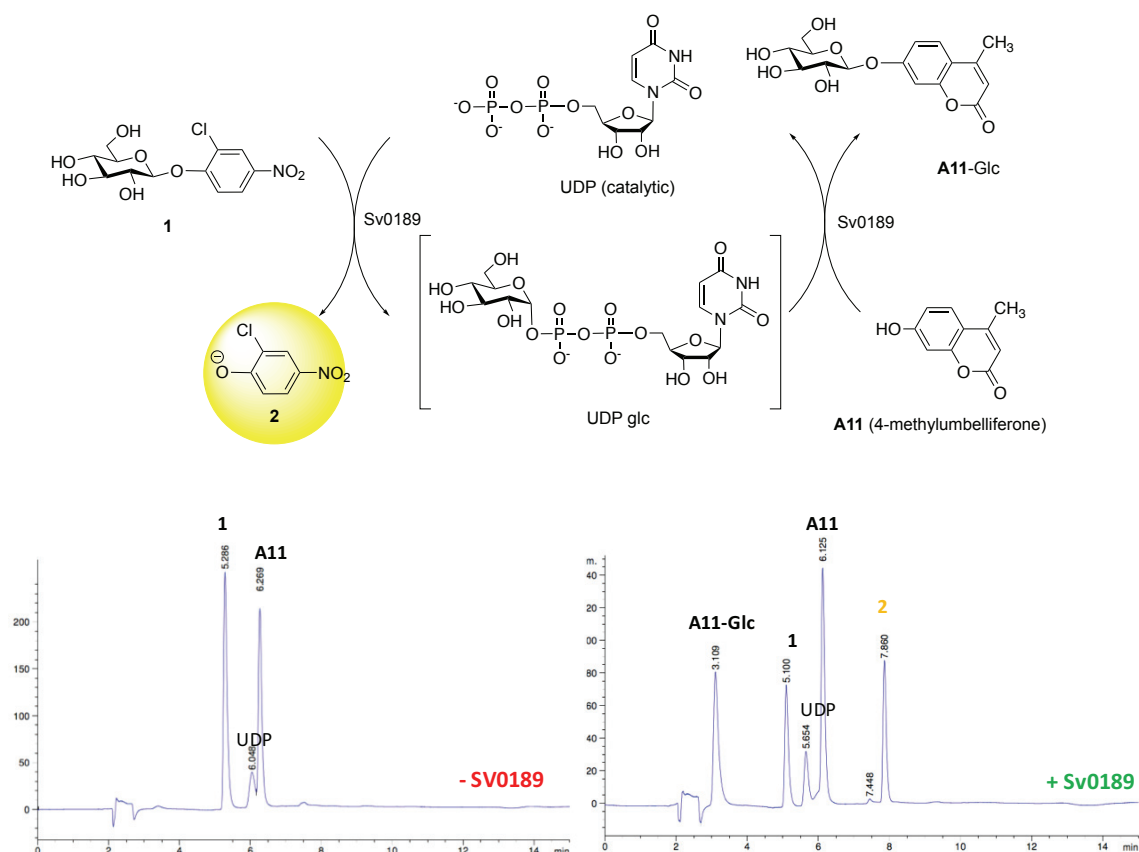


Figure 35. Glycosyltransferase activity detection assay with 4-methylumbelliferone (**A11**).

2.5.4. Sv0189 Initial Acceptor Screening Assay

Having established glycosyltransferase activity, a diverse set of 72 acceptors was screened; series A comprised 25 small molecules, series B comprised 27 natural products, and series C comprised 24 synthetic pharmaceuticals. A primary screen to monitor initial kinetic rates was developed with optimization of the assay described previously for **A11** (Figure 36). Positive hits were defined as those with greater initial rates than the positive control (**A11**, 4-methylumbelliferone), and negative hits possessed slower initial rates compared to a negative control (DMSO). The rate observed with the negative control (DMSO) provided a baseline for hydrolysis of 2-chloro-4-nitro-phenol- β -D-glucopyranoside in the presence and absence of Sv0189. The observed kinetic rates had plateaued after 1 h for the positive control (**A11**). The reaction was quenched after 3 h.

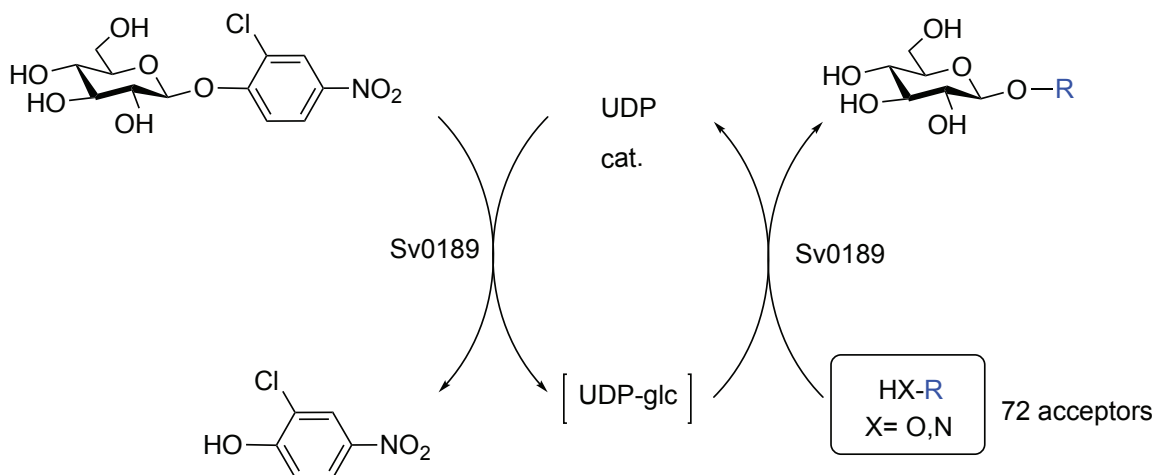


Figure 36. General scheme for Sv0189 primary screening assay.

Acceptors with rates greater than the negative and lower than the positive controls were considered putative hits but were not carried through to secondary

screening. Results from the primary screen are summarized in Figures 37-39, where compounds have been ranked based on the observed kinetic rate, and the structures of all putative acceptors are included in the experimental section. Series A hits showed a bias for compounds with two aromatic rings over compounds with a single aromatic ring. The top hits, those with the fastest initial rates, were all bis-aromatic, including a number of anthraquinones (**A5**, **A14**, **A12**, **A15**, and **A20**) and benzhydrol (**A18**), while mono-aromatic compounds such as phenol (**A1**), benzylalcohol (**A2**), aniline (**A7**), and benzylamine (**A8**) were putative hits. Phenolic, primary and secondary alcohols were found amongst the compounds with the fastest initial rates, but amines and anilines were also identified as putative hits, suggesting Sv0189 is capable of *N*-glycosylation.

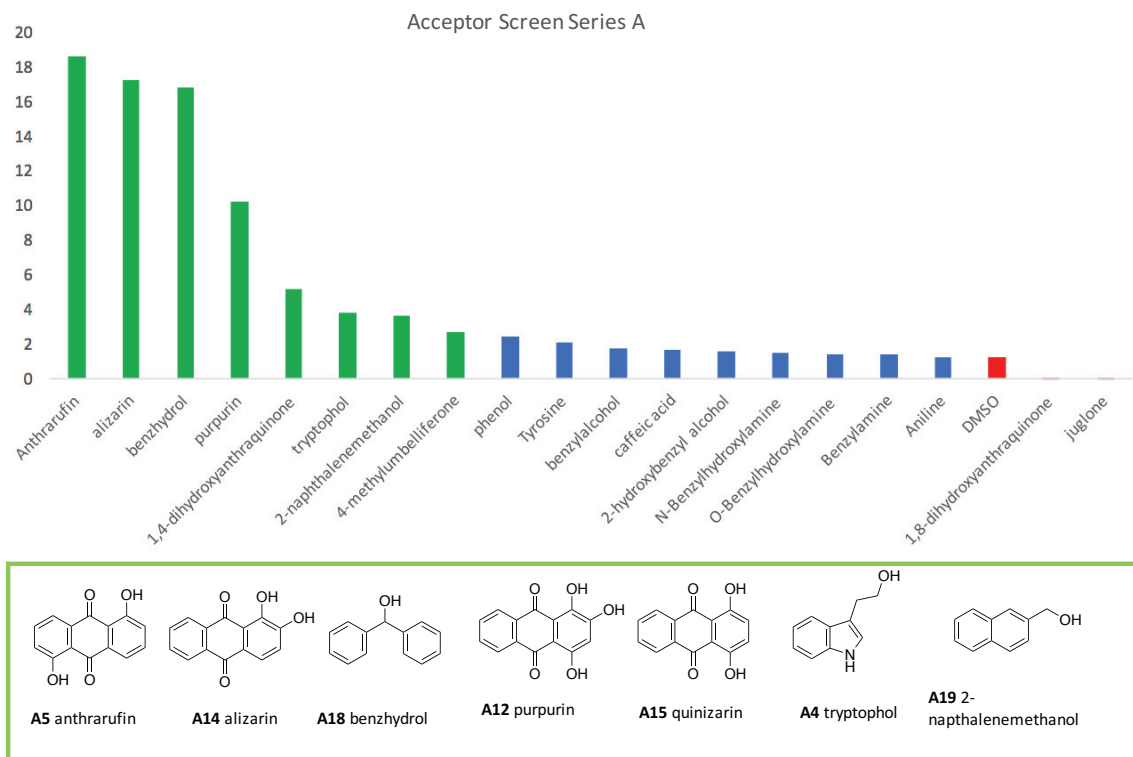


Figure 37. Bar graph ranking acceptors from series A. Green indicates positive hits, blue putative hits, and red negative hits. The structures of top hits are shown in the box.

Series B screening identified a diverse set of structures as positive hits. Resveratrol (**B26**), a bis-phenolic compound, gave the greatest initial rate, comparable to the rates observed with anthrarufin (**A5**), alizarin (**A14**) and benzyhydrol (**A18**) from series A. Other hits in this series included complex natural products such as geldanamycin (**B2**) and aureomycin (**B10**); glucosylation of these molecules has not been reported previously. Radicol (**B3**), resveratrol (**B26**), and quercetin (**B4**) have been reported as OleD substrates.⁷⁴ Some of the hits, including a polyketide polyether, nigericin (**B9**), and macrolide, oligomycin A (**B11**) were non-aromatic. Intriguingly, the two other macrolide antibiotics screened,

erythromycin (**B6**) and clarithromycin (**B7**), possessed putative inhibitory activity, as the rate was essentially flat, and lower than the negative control (DMSO). After 24 h, the wells corresponding to **B6** and **B7** were colourless, while the negative controls had turned yellow due to hydrolysis of 2-chloro-4-nitro-phenol- β -D-Glc by Sv0189 (Figure 40). Two of the natural products produced by *S. venezuelae* were screened, chloramphenicol (**21**) and jadomycin DS aglycone (**B23**), neither of which were identified as good acceptors.

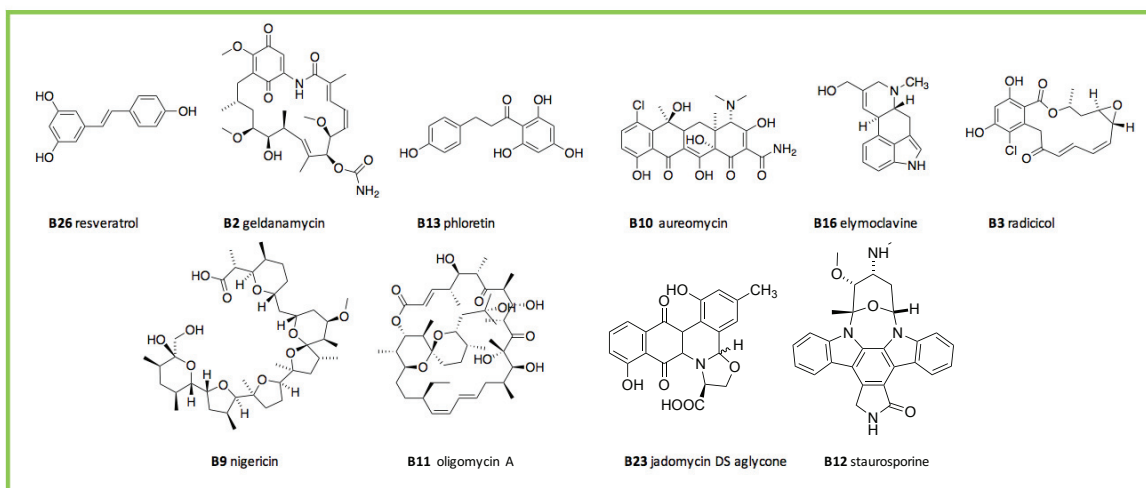
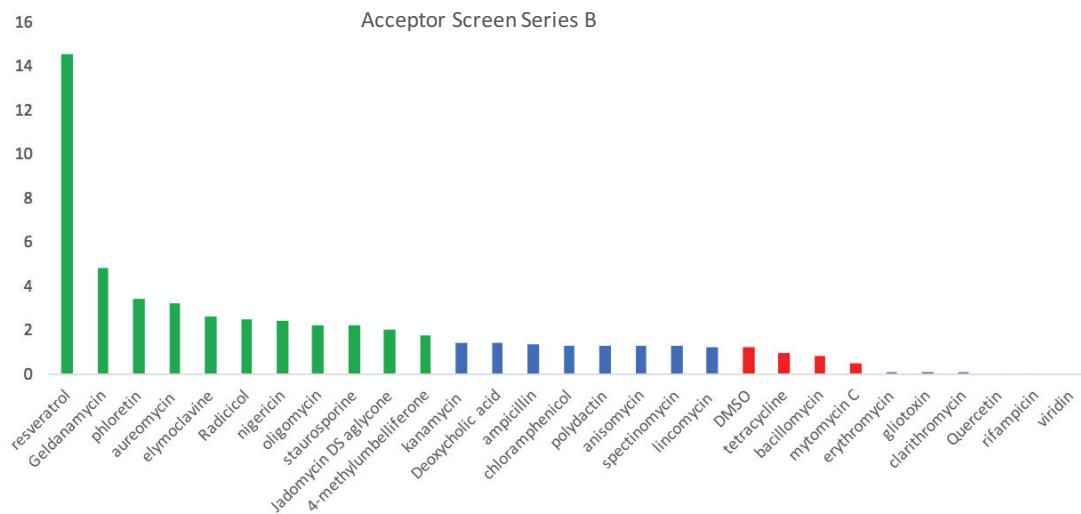


Figure 38. Bar graph ranking acceptors from series B. Green indicates positive hits, blue putative hits, and red negative hits. The structures of top hits are shown in the box.

Evaluation of Series C generated a surprising number of positive hits. The top hit, with the fastest initial rate, was fluconazole (**C7**), which was somewhat remarkable on examination of the sterically crowded tertiary hydroxyl group. Other top hits included posaconazole (**C6**), carvedilol (**C2**), and pitavastatin (**C9**) which all possessed secondary hydroxyl functionalities. Secondary amine-containing

compounds such as desmethyl mirtazapine (**C13**), rimiprilat (**C22**) and solifenacin (**C12**) were also identified as hits. The tertiary amine-containing chlorpromazine (**C24**) that was previously found to be a substrate for an evolved OleD variant was identified as a positive hit.¹⁶⁰ Sorafenib (**C16**) was also a hit: however, analysis of the structure does not reveal a likely site of glycosylation. Such results emphasize the requirement for secondary screening. Glucosylation of most of the identified hits in series C would generate novel compounds.

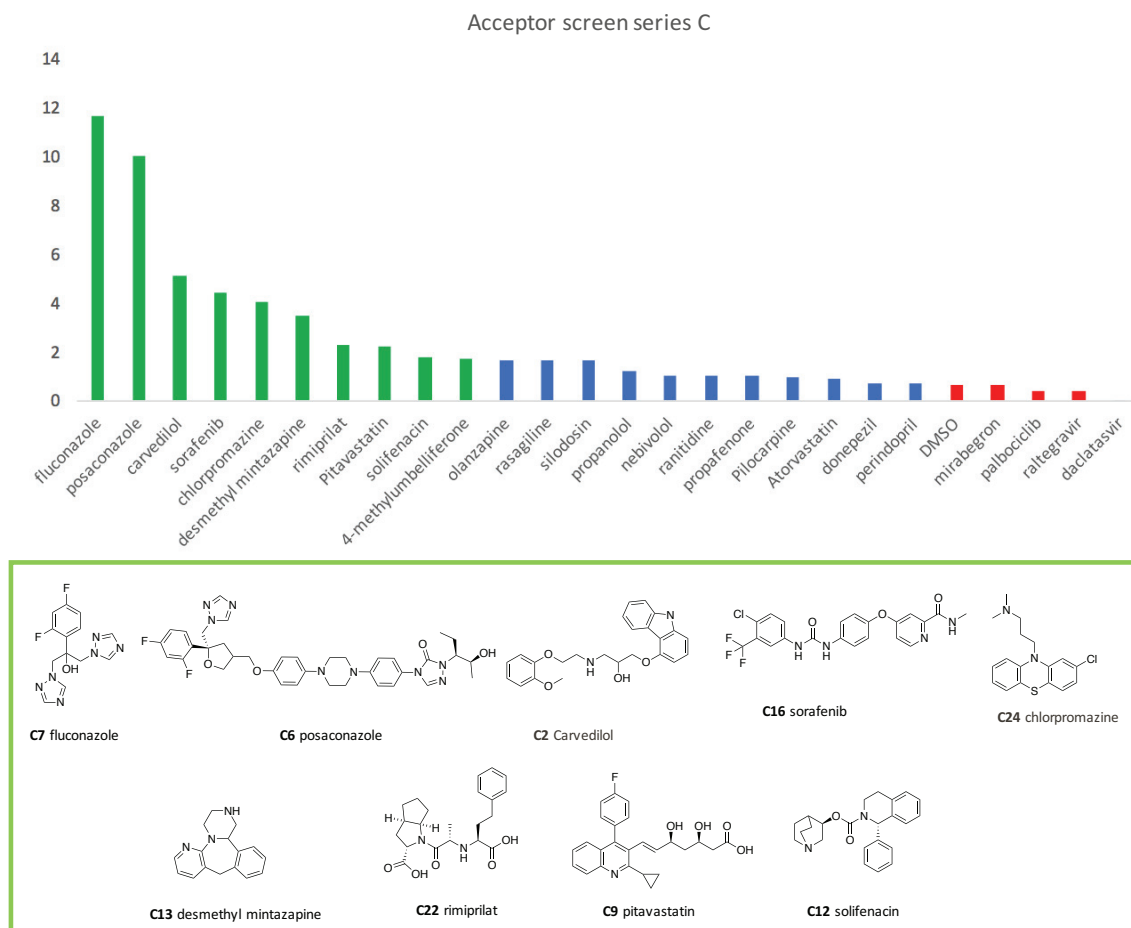


Figure 39. Bar graph ranking acceptors from series C. Green indicates positive hits, blue putative hits, and red negative hits. The structures of top hits are shown in the box.

Subsequent to ranking based on initial kinetic rates, HPLC traces for compounds identified as hits were collected from the reaction wells after 24 h. While in many cases precipitation of the acceptors, low concentrations, lack of absorbance at λ 254 nm for non-aromatic compounds, and incompatibility with the standardized HPLC method resulted in ambiguous data, new signals were observed for some acceptors (Table 7).

Table 7. HPLC data from initial Sv0189 acceptor screen after 24 h.

Compound	R _T (min)	R _T putative glucosylated product(s) (min)	% Conversion to putative product*
A4 Tryptophol	6.7	5.3	19
A11 4-methylumbelliferone	6.6	3.6	10
A12 purpurin	8.9	6.5	16
A14 alizarin	8.6	6.1	69
B2 geldanamycin	7.7	6.2	10
B3 gadicicol	9.7	7.9	20
B4 quercetin	6.7	> 6 new signals	
B10 aureomycin	5.6	4.7	46
B13 phloretin	7.3	5.0	40

* Percent conversions calculated from the area (A) under product and algycone peaks using the formula $(A_{\text{glucosylated product}}) / [(A_{\text{glucosylated product}}) + (A_{\text{algycone acceptor}})]$.

Several limitations of the assay, intended as a general survey of the acceptor scope, were noted, most significantly limiting was insolubility of some of the acceptors (i.e. anthraquinones) in 10% DMSO, leading to erratic kinetic rates that in some cases generated false positives. In many cases, the addition of Sv0189

improved acceptor solubility (Figure 40). Furthermore, when the assay with 4-methylumbelliferone (**A11**) was repeated at pH 7.0, the percent conversion was found to improve from 10% (pH 8.0) to 45%.

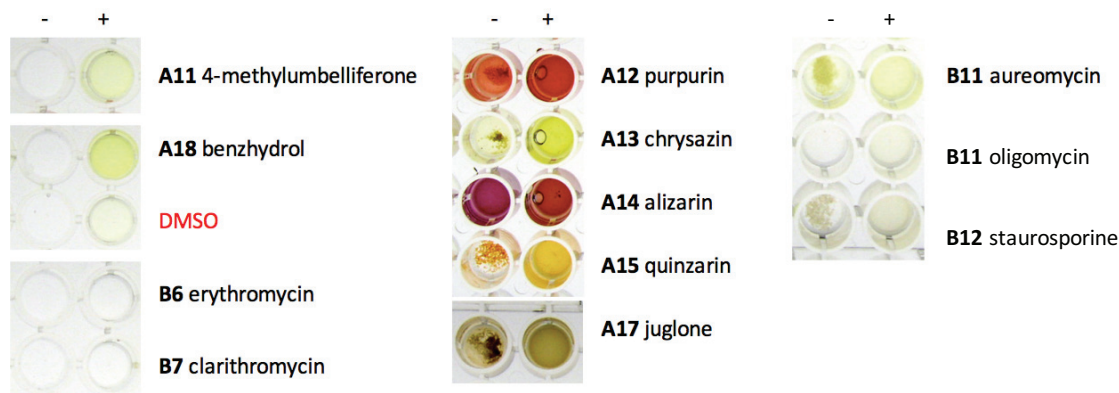


Figure 40. Appearance of wells for select acceptors, positive control (**A11**), and negative control (DMSO), in the absence (-) and presence (+) of Sv0189.

Quercetin (**B4**), which we had anticipated would be a substrate given its bis-phenolic structure, was identified as a negative hit in the primary screen (flat initial kinetic rate). However analysis of the HPLC trace revealed a number of new signals consistent with glycosylated analogues.

2.5.5. Development of a Secondary Acceptor Screen for Sv0189

As a follow-up to the initial screen, a secondary screen was developed to facilitate characterization of glucosylated products by HPLC and LCMS to further examine the top hits from each series. Acceptors selected for secondary screening were reacted with UDP-Glc and in a coupled reaction with calf intestinal alkaline phosphatase (CIP), which was included to degrade produced UDP to drive the reaction and bypass potential product inhibition (Figure 41).¹⁴²

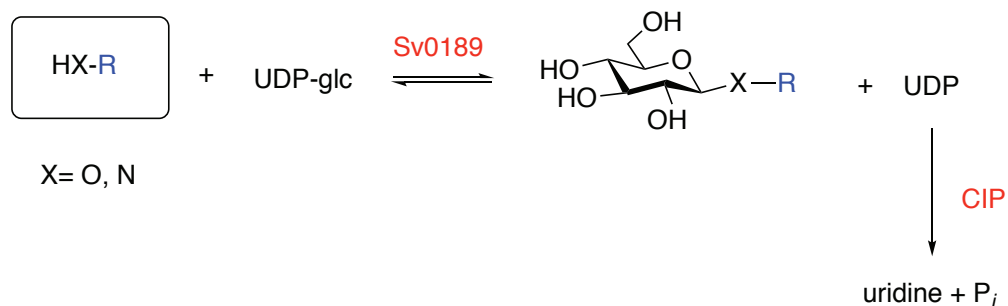


Figure 41. Secondary acceptor screening assay for Sv0189.

In the negative control with DMSO and without acceptor, analysis of the HPLC trace showed that UDP-Glc had been completely converted to uridine, indicating hydrolysis of UDP-Glc by Sv0189 over the 40 h assay period. The acceptor and donor concentrations were reduced in the secondary assay in an attempt to improve solubility. However, some acceptors precipitated during work-up. Thus, some uncertainty is associated with reported percent conversions. Figures 42-44 show a selection of the HPLC traces collected from the secondary screening assay along with calculated percent conversions. Overall, the conversions are improved compared to the primary screen: further optimization of the assay, such as adjustment to pH 7.0 rather than 8.0, and a change in buffer from Tris to MOPS, would likely further improve percent conversions. This experiment will be performed in due course.

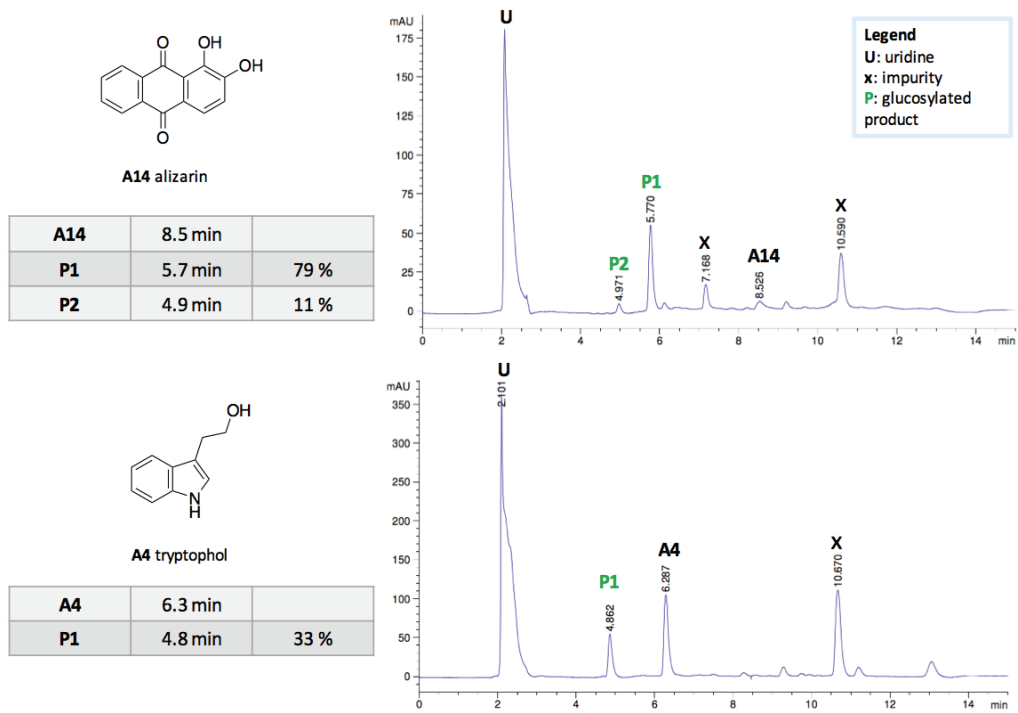


Figure 42. HPLC traces from secondary screen of Series A (selected examples).

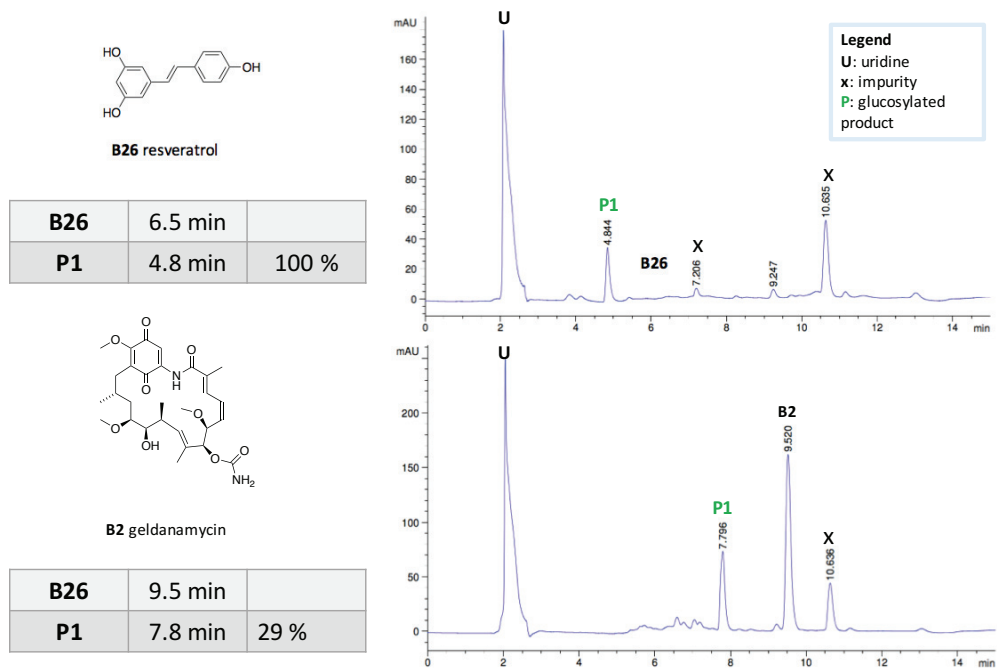


Figure 43. HPLC traces from secondary screen of Series B (selected examples).

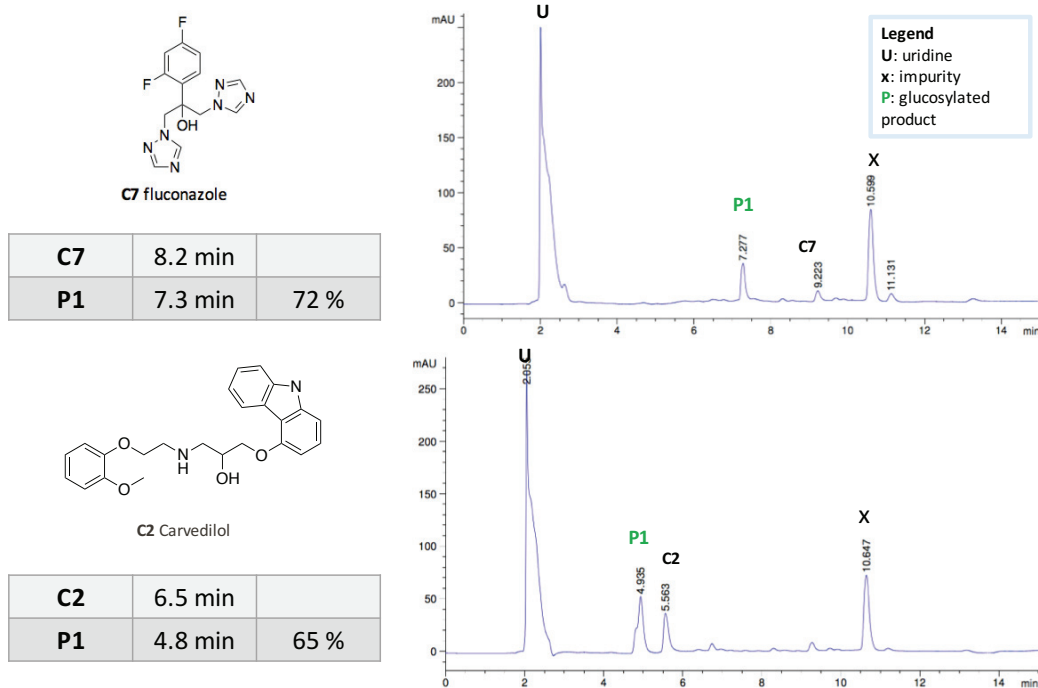


Figure 44. HPLC traces from secondary screen of Series C (selected examples).

2.5.6. Conclusions

In vitro analysis of Sv0189 established glycosyltransferase activity with UDP-Glc serving as an effective donor. Genetic analysis of secondary metabolite gene clusters in the host strain, *S. venezuelae*, did not clarify the identity of a physiological acceptor. Homologous glycosyltransferases have been associated with macrolide inactivation. Initial acceptor screening efforts have shown that a diverse series of molecules may serve as substrates, with a preference for phenolic scaffolds with at least two aromatic rings. Further clarification of the acceptor scope, determination of conversions to glucosylated analogues at the optimal pH (7.0), HRMS data of new compounds, and the determination of regioselectivity are required to further ascertain whether Sv1089 will serve as a potential glycodiversification tool, as was proposed as the aim of the study.

Chapter 3: Diversification of the Jadomycin Family Natural Products

3.1. Introduction to Jadomycin Family Natural Products

Excerpts from this section are adapted from S.M. Forget, A.W. Robertson, D.P. Overy, R.G. Kerr, D.L. Jakeman. *J. Nat. Prod.* (2017) 80, 1860-1866 and J.M. MacLoed, S.M. Forget, D.L. Jakeman. *Can. J. Chem.* (2017), Mini-review submitted to *Can. J. Chem.*

Actinobacteria, particularly the genus *Streptomyces*, are prolific producers of secondary metabolites, and natural products isolated from these bacteria or their derivatives have contributed significantly to the current arsenal of drugs.¹⁶¹⁻¹⁶³ While nature generates an array of complex structures, our ability to tweak the chemical functionality of bacterial metabolites for structure-activity studies or for lead optimization is typically narrow due to the challenges associated with either the synthesis of these complex molecules or due to the limited scope of genetic engineering.¹⁶⁴ Type II polyketide synthase (PKS-II) derived natural products, such as the chemotherapeutic doxorubicin, are an important subset of these bioactive bacterial secondary metabolites.¹⁶⁵ The jadomycins are a family of PKS-II secondary metabolites produced by *Streptomyces venezuelae* ISP5230 that are encoded within an inducible cryptic biosynthetic pathway.¹⁶⁶ An exploitable feature of the jadomycins invokes the non-enzymatic biosynthetic step in which an amino acid is incorporated into the structure, forming the E-ring (Figure 45).¹⁶⁷ Taking a precursor-directed approach, culturing *S. venezuelae* in the presence of selected

amino acids has generated a series of jadomycin analogues with structural diversity about the E-ring.¹⁶⁸⁻¹⁷¹

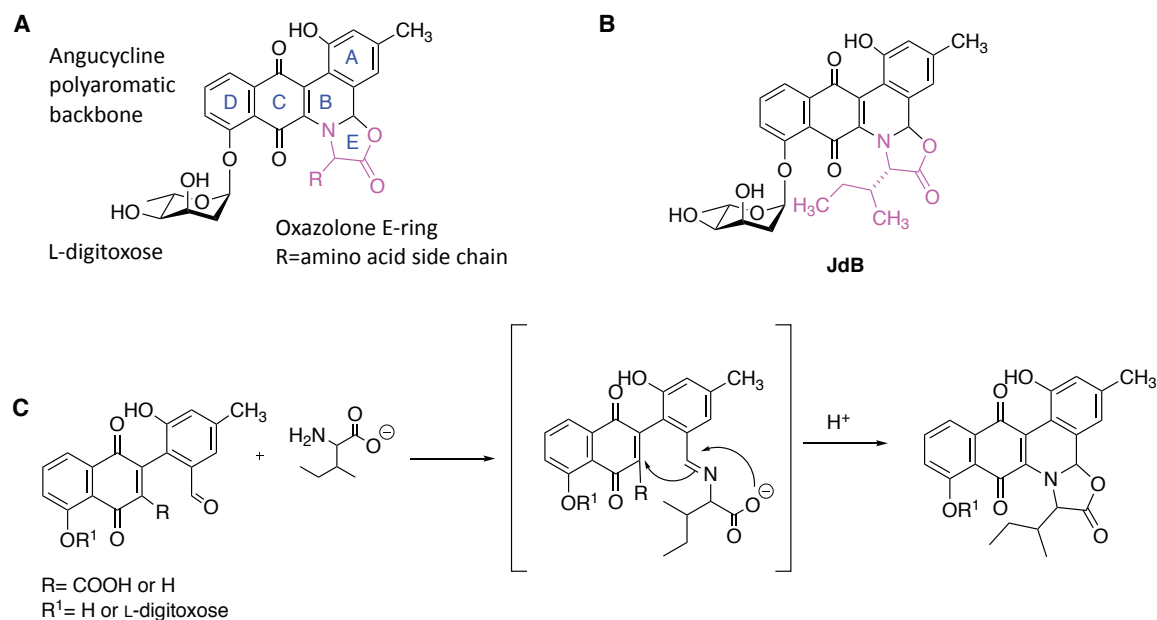


Figure 45. (A) Generic jadomycin structure with labelled ABCDE rings; (B) structure of **JdB**; (C) Proposed spontaneous mechanism for E-ring formation.

Since the first isolation of a jadomycin in the early 1990's, the L-isoleucine derived aglycone **JdA** and L-digitoxylated **JdB**, more than 70 jadomycins have been reported, though many have not been isolated and fully characterized, and not all amino acids that have been evaluated are incorporated in a jadomycin congener.^{166, 172, 173} The minimal culture media for jadomycin production utilizes only the selected amino acid to support primary metabolic functions requiring nitrogen.^{174, 175} Typically, failure of an amino acid to incorporate is accompanied by failure of *S. venezuelae* to grow in its presence, either due to toxicity or an inability to be assimilated as a nitrogen source. A recent study has reported that co-amino acid

supplementation can be implemented to facilitate incorporation of amino acids that do not otherwise support jadomycin production.¹⁷⁶

3.1.1. E-ring Variability in Jadomycin Family Natural Products

Cyclization about the E-ring is dictated by the incorporated amino acid. Recent studies have revealed that the default oxazolone ring often depicted in the literature may not be the major product when the amino acid precursor possesses multiple nucleophilic groups. Total synthesis of the jadomyicins incorporating serine and threonine revealed that the E-ring was cyclized from the side-chain hydroxyl, forming an oxazolidine ring, prompting a revision of the reported structures for D/L-serine (**JdD** and **JdDS**) and D/L-threonine derivatives (**JdT** and **JdDT**, Figure 46).^{177, 178} Given the spontaneous nature of amino acid incorporation and subsequent cyclization, the observation of different modes of incorporation may be expected.

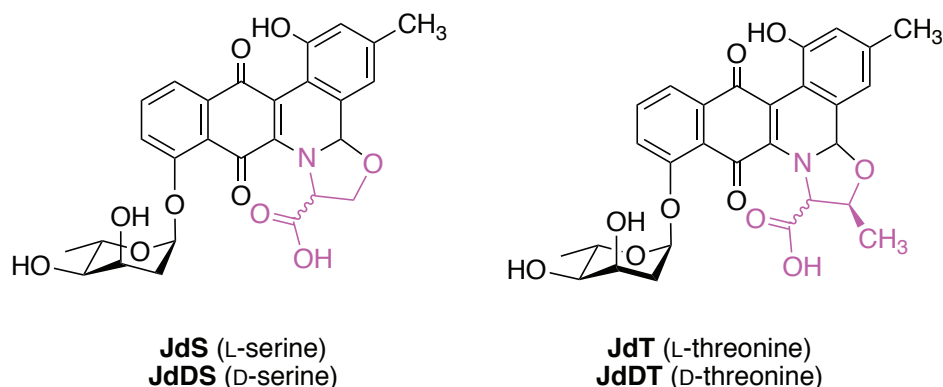


Figure 46. Structures of oxazolidine-ring containing jadomyicins **JdS**, **JdDS**, **JdT**, and **JdDT**.

The introduction of non-proteinogenic amino acids and amino acids bearing functionalized handles for semi-synthetic derivitization have also been reported

(Figure 47).^{169, 170, 179} More recently, the formation of larger E-ring containing jadomycins arising from cyclization of a primary amine have been reported, first by the isolation of **JdOct** from cultures with L-ornithine, and subsequently by isolation of a series of jadomycins with rings sizes up to ten-atoms.^{171, 172} In the study presented in Section 3.2 of this thesis, a culture with *N* ϵ -trifluoroacetyl-L-lysine (TFAL) resulted in the isolation of a series of new jadomycins.

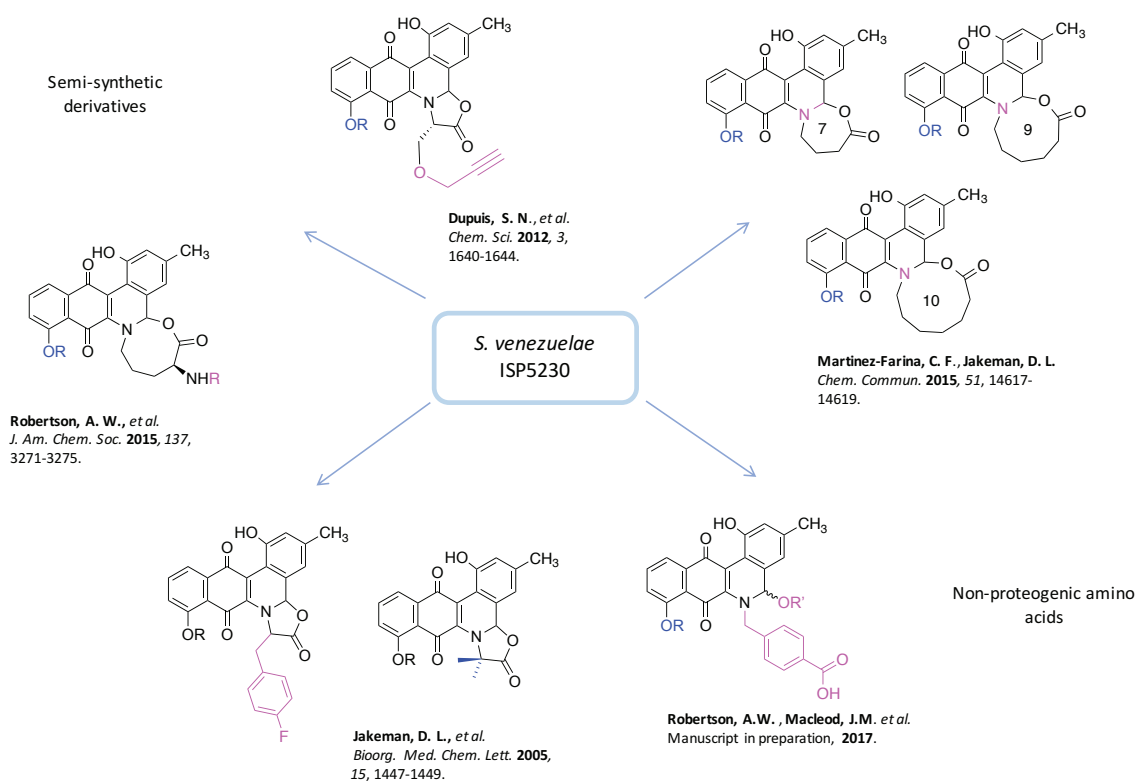


Figure 47. Scope of jadomycin analogues derived from precursor-directed amino acid incorporation.

3.1.2 Modification of the Jadomycin Sugar Moiety

In contrast to the extensive description of analogues arising from manipulation of the E-ring, there have been only a handful of studies in which modification of the

sugar moiety has been targeted. The L-digitoxyl deoxysugar biosynthetic gene cluster was annotated by Wang and co-workers in the early 2000s through sequence homology and by evaluation of disruption mutants.¹⁴¹ On entry into the pathway, Glc 1-P is converted by a nucleotidyltransferase, JadQ, into the activated donor, NDP- α -D-glucose. Subsequently, the hexose ring is transformed by JadTOPUV to provide the final donor, NDP-L-digitoxose, serving as a substrate for the pathway-specific glycosyltransferase JadS (Figure 48).

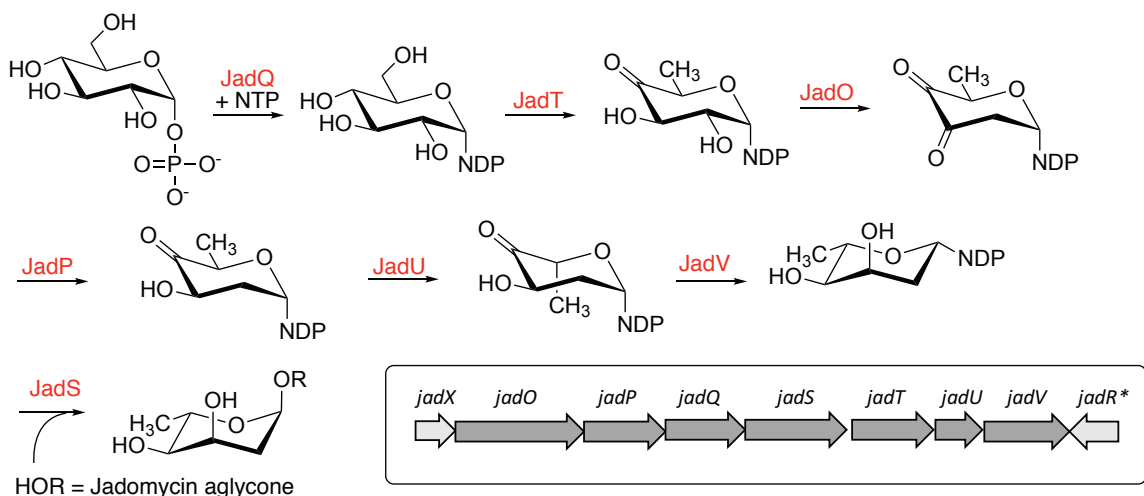


Figure 48. Genes related to L-digitoxyl biosynthesis in *S. venezuelae* (inset) and scheme depicting the reactions catalysed by pathway enzymes.

Jadomycins bearing sugars divergent from the usual L-digitoxose have been generated through genetic engineering of *S. venezuelae* and a synthetically prepared carbasugar-containing jadomycin B (**JdB-a**) has also been evaluated.¹⁸⁰ To date, such efforts have generated glycodiversified jadomycins with eight distinct sugar moieties (Figure 49).

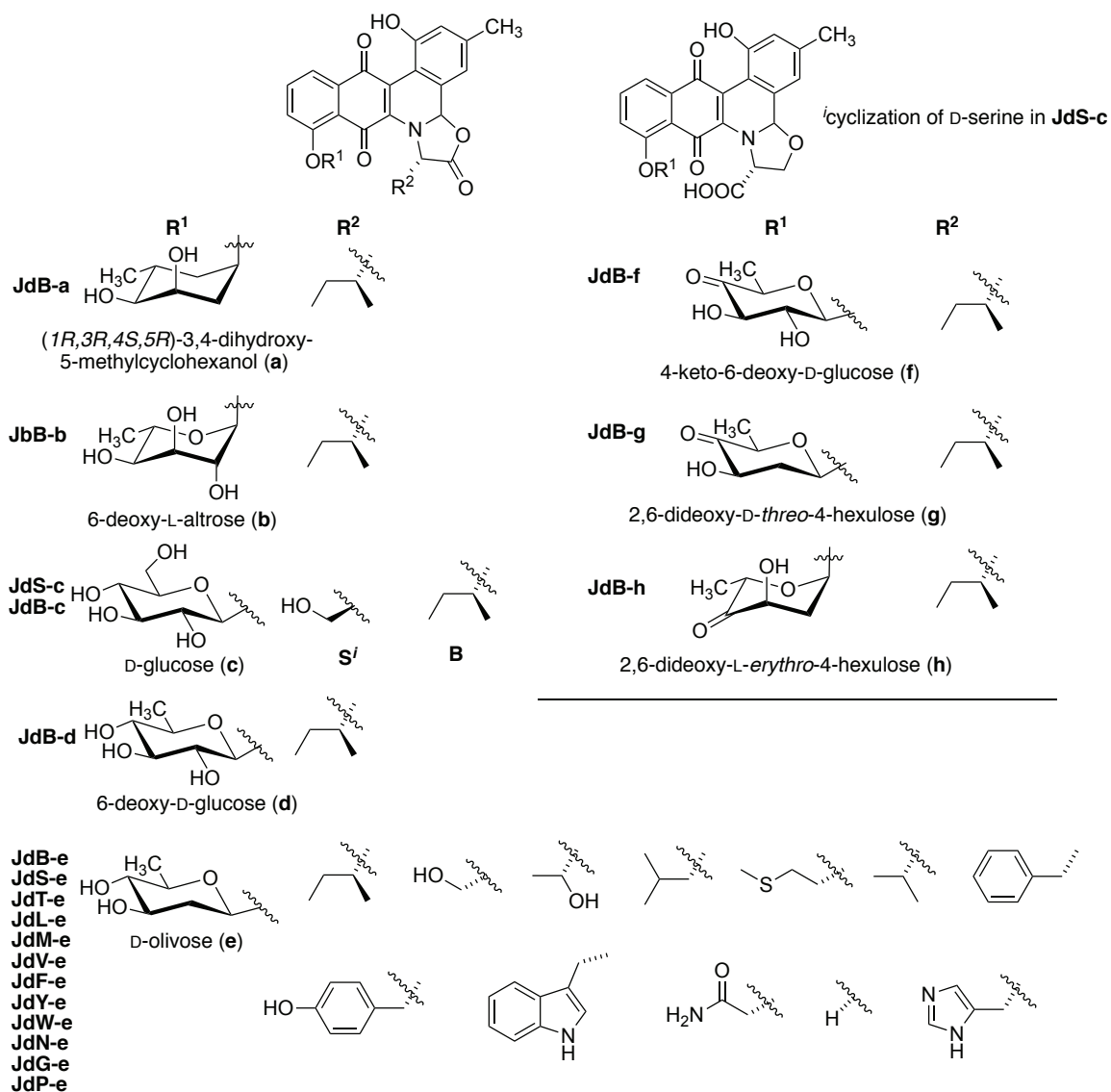


Figure 49. Jadomycins with modified sugar moieties.

On re-examination of a previously described *jadO* disruption mutant (strain ILEVS10801), producing a non-functional 2,3-dehydratase, Jakeman *et al.* identified a jadomycin B analogue (**JdB-b**) decorated by a sugar with the 2-hydroxy group intact.⁶⁰ Identification of the sugar as a 6-deoxy-L-altropyranoside through analysis of the NOESY correlations implicated that downstream enzymes JadU and JadV, a 5-epimerase and 4-ketoreductase, respectively, were able to act on the JadT

product, NDP-4-keto-6-deoxy-D-glucose. In addition to being the first report of a jadomycin congener with a sugar other than L-digitoxose, the study was the first to suggest that the glycosyltransferase, JadS, was flexible with respect to sugar donors. In a study presented in this thesis (Section 3.3), the mutant strain *S. venezuelae* Δ *jadT*, possessing a deletion of the gene encoding a 4,6-dehydratase, was found to produce a jadomycin D-serine congener appended with D-glucose (**JdS-c**).⁵⁹ Evaluation of a double gene deletion mutant, *S. venezuelae* Δ *jadST*, was not able to produce the glucosylated jadomycin, indicating that JadS was responsible for catalysis. Consistent with the above, *S. venezuelae* Δ *jadUTV* was evaluated by Li *et al.* and was found to produce a D-glucosyl jadomycin B analogue (**JdB-c**).¹⁸¹ In the same study, complementation of *S. venezuelae* Δ *jadTUV* with an expression vector encoding JadT and UrdR, the 4-keto-reductase generating D-olivose in urdamycin biosynthesis, was found to generate a D-olivoylated jadomycin B analogue (**JdB-e**).¹⁸² *S. venezuelae* Δ *jadTUV* and *S. venezuelae* Δ *jadOPQSTUV* served as a hosts for heterologous expression of various combinations of partially reconstituted L-digitoxose biosynthetic genes and/or *urdR* to produce jadomycin B analogues decorated with 6-deoxy-D-glucose (**JdB-d**), 4-keto-6-deoxy-D-glucose (**JdB-f**), 2,6-dideoxy-D-threo-4-hexulose (**JdB-g**) and 2,6-L-erythro-4-hexulose (**JdB-h**). Culture of the strain *S. venezuelae* Δ *jadUTV::jadTurdR*, which produces D-olivose, with different amino acids allowed detection of an additional eleven E-ring variant D-olivoylated jadomyicins. Of the compounds described, **JdB-e**, **JdS-e**, and **JdT-e** were produced in sufficient yields for isolation and full characterization by NMR, and the authors cite poor yield and compound instability as hindrances towards

isolation of the remaining analogues.¹⁸¹ In all cases, these genetically complemented systems were reliant on the relaxed specificity of native JadS to render the sugar-modified jadomycin analogues. These studies reveal JadS as a glycosyltransferase with notable tolerance to variation about the C-2, C-3, C-5, and C-6 positions of the donor hexose ring. In Section 3.4 of this thesis, efforts towards complementation of *S. venezuelae* with a putative iterative L-digitoxyltransferase (KijC4) are reported.

3.1.3. Biological Activities of Jadomycin Family Natural Products

A number of biological activities are reported for jadomyicins including anticancer, antimicrobial and antifungal, with some indication that structural modification has an effect on activity trends. Early screening with **JdA** and **JdB** against yeast demonstrated that the presence of the L-digitoxyl moiety of jadomycin B was necessary for antifungal activity.^{167, 174} Studies evaluating jadomycin family compounds against cancer cell lines have identified variability in potency depending on the amino acid side chain.^{168, 183} Jadomycin L-leucine (**JdL**) and the semi-synthetic triazole-containing jadomyicins have been the most bioactive in cancer cell screening in the 60-cell panel assay provided by the National Cancer Institute (NCI).^{184, 185} Large E-ring containing jadomyicins have reduced activity in the same 60-cell line screen.¹⁷¹ Jadomyicins incorporating 4-amino-L-phenylalanine displayed poor cytotoxicity profiles and poor DNA cleavage capabilities.¹⁷⁰ Two D-olivosylated jadomyicins, **JdT-e** and **JdL-e**, have been screened against a panel of cancer cell lines and were found to possess comparable potency to their L-digitoxylated counterparts.¹⁸¹ Work in the McFarland research group has examined a photo-induced mechanism for DNA cleavage in the presence of Cu(II), which may

represent an aspect of the mechanism of jadomycin cytotoxicity.^{186, 187} Studies examining the mechanisms of bioactivity in triple-resistant breast cancer lines reported that jadomyicins were resistant to export by the ABC transporters overexpressed in these cancer cell lines, enabling cytotoxicity in multi-drug resistant cancer cell lines, and a later study demonstrated that jadomycin cytotoxicity was enhanced by the presence of reactive oxygen species.^{188, 189} **JdB** has been identified as an Aurora kinase B-inhibitor, a protein that is overexpressed in tumour cells.¹⁹⁰ In an antimicrobial screening panel, it was found that jadomyicins incorporating L-isoleucine **JdB**, L-leucine **JdL**, and L-phenylalanine **JdF**, were the most potent, while jadomyicins derived from L-glycine **JdG**, which possesses no amino acid side chain, and structures not containing an oxazolone ring, including the jadomyicins derived from L-apharigine **JdN**, L or D-serine **JdS/JdDS**, and L or D-threonine **JdT/JdDT**, possessed reduced activity. Jadomyicins were most active against Gram-positive *Staphylococci*.¹⁹¹ Similarly, the study presented in section 3.2 of this thesis identified the oxazolone-containing **3.1** as the most active in an antimicrobial screen compared to E-ring modified analogues.¹⁹²

3.2. Furan and Lactam Jadomycin Biosynthetic Congeners Isolated from *Streptomyces venezuelae* ISP5230 Cultured with *N* ϵ -trifluoroacetyl-L-Lysine

Excerpts from this section are taken from: S.M. Forget, A.W. Robertson, D.P. Overy, R.G. Kerr, D.L. Jakeman. *J. Nat. Prod.* (2017) 80, 1860-1866. Fragmentation

studies with ^{15}N -lysine were performed by A.W. Robertson. Biological screening was performed by D.P. Overy and R.G. Kerr.

E-ring modification has proven to be a facile method for jadomycin diversification. In this study we have expanded the library of E-ring modified jadomycins, by culturing *S. venezuelae* with *N* ϵ -trifluoroacetyl-L-lysine (TFAL). Analysis of the culture media from the *S. venezuelae*/TFAL production revealed a number of unanticipated analogues (**3.1-3.4**), which were fully characterized and evaluated for antimicrobial, anticancer, and cytotoxic properties. The new analogues include an unprecedented lactam-containing jadomycin (**3.2**) and two furan analogues that did not contain an incorporated amino acid (**3.3** and **3.4**, Figure 50). A discussion of the plausible biochemical origins of these novel shunt products is presented.

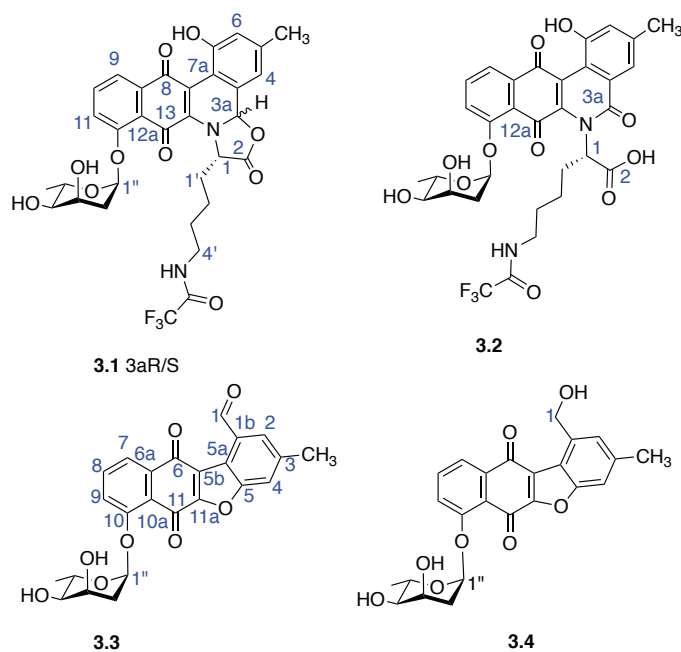


Figure 50. Jadomycins **3.1-3.4** isolated from a culture with TFAL.

3.2.1. Previous Studies on Jadomycin Lysine (**JdK**)

Prior studies have reported that the jadomycin derived from L-lysine, **JdK**, was unstable and therefore full characterization of this molecule has not been reported.^{171, 193} In other work, jadomycin productions with L-ornithine produced a jadomycin with an eight-membered E-ring (**JdOct**, Figure 51).¹⁷¹ In order to investigate whether a nine membered ring (**JdK ϵ**) was produced in cultures with L-lysine, a fragmentation study from cultures supplemented with ¹⁵N- α -L-lysine and ¹⁵N- ϵ -L-lysine as selectively labelled precursors was executed. Analysis of the fragmentation pattern of the ¹⁵N-incorporated **JdK** demonstrated formation of a “typical” oxazolone ring (5-membered) jadomycin **JdK α** was produced as the major product.¹⁹²

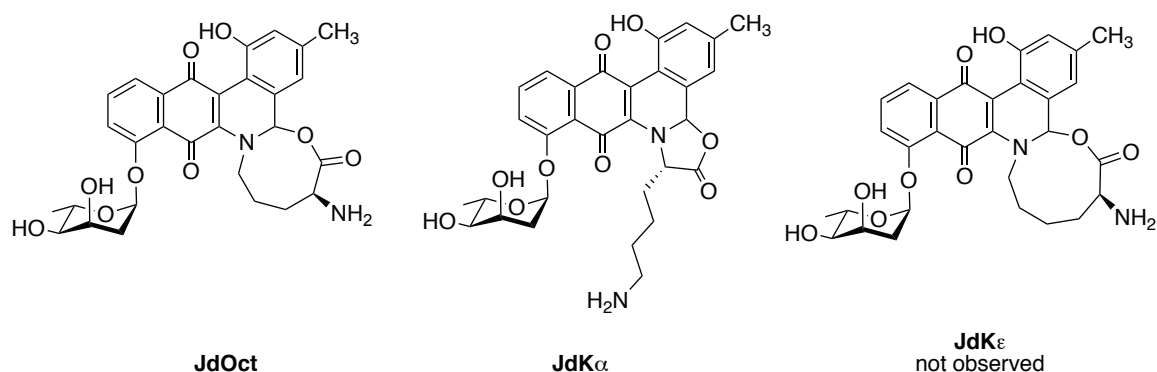


Figure 51. The jadomycin derived from L-ornithine, **JdOct**, and structures for the jadomycin derived from L-lysine, **JdK α** , and **JdK ϵ** .

Given that the instability of **JdK** likely arose from the nucleophilicity of the *N ϵ* amine group, protection of the amine was anticipated to furnish a stable analogue, and to select for the 5-membered oxazolone ring. TFAL was thus selected with the additional benefit of the inclusion of an NMR-sensitive ¹⁹F handle.

Furthermore, a large proportion of synthetically derived drugs are designed to include a fluorine substituent; by contrast, there are very few fluorine-containing natural products.^{194, 195}

3.2.2. Jadomycin Productions with TFAL

S. venezuelae VS1099 was cultured in the presence TFAL as the sole nitrogen source following standard procedures for jadomycin production.¹⁷⁵ Isolation of compounds was accomplished by a series of chromatographic steps. In the first step, clarified culture media was passed through a silica phenyl column, to which the jadomyicins bind tightly. Multiple washes of the column with water removed water-soluble and non-aromatic impurities. Elution of the jadomyicins into methanol provided an extract, and TLC analysis showed that several coloured compounds were present (Figure 52A). Fractionation of the material obtained in the first step using normal phase chromatography with methanol and dichloromethane was performed to separate the coloured compounds (Figure 52B). A final purification step by preparatory HPLC with a reversed-phase column was then performed, if necessary. Three fractions containing novel jadomyicins were obtained (Figure 52C).

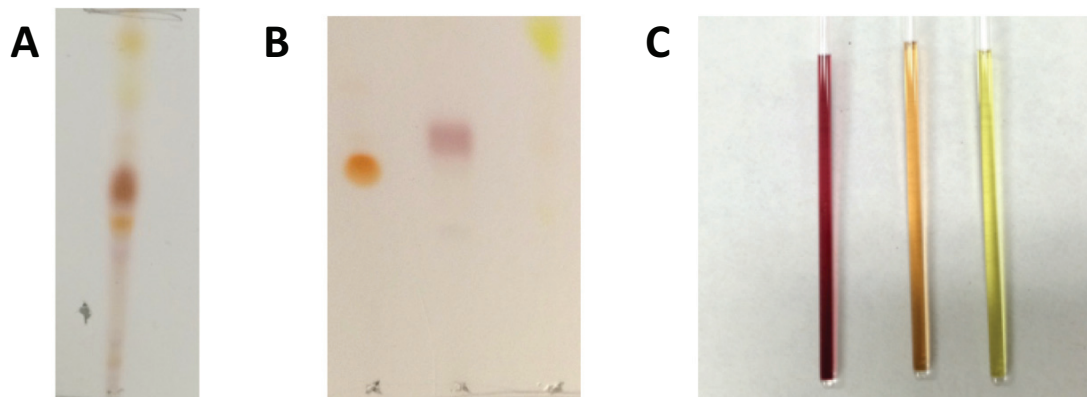


Figure 52. TLC plates from indicated purification steps for **3.1-3.4** and NMR tubes showing colour of isolated products in solution. (A) TLC of the methanol extract from the silica phenyl column step; (B) TLC after purification, from the right **3.2**, **3.1** and mixture of **3.3**. and **3.4**; (C) Purified **3.1** (purple) and **3.2** (orange) in methanol- d_4 , mixture of **3.3** and **3.4** (yellow) in chloroform- d_3 . TLC solvent: 5:5:1 ethyl acetate:acetonitrile:water.

Isolation of a reddish-purple compound that possessed spectroscopic and HRMS data consistent with the anticipated jadomycin TFAL **3.1** was achieved with an isolated yield of 4.5 mgL^{-1} . The $^1\text{H-NMR}$ spectrum showed two distinct sets of signals. Two sets of proton signals from diastereomers arising from the interconversion at the hemiaminal ether (3a) position. 1D-NOESY experiments (Figure 53) identified the major diastereomer as 3a*S* in a 1.7:1 ratio to 3a*R*. The same ratio was observed in the ^{19}F NMR spectrum, with $\delta -77.28$ and $\delta -77.29$ for the 3a*S* and the 3a*R* diastereomers, respectively (Figure 54). Cyclization of the α -

amino group of lysine to produce a five membered oxazolone ring (E ring) was confirmed by the observation of an HMBC correlation between H3a and C1.

A second compound appeared as an orange spot by TLC. It was initially isolated in quantities insufficient for full characterization (sub-milligram), but possessed a $^1\text{H-NMR}$ spectrum displaying features of a jadomycin family natural product: including the characteristic aromatic doublet-triplet-doublet pattern of the H9- H11 spin system, all of the L-digitoxose signals, as well as signals consistent with the presence of the amino acid side chain. A singlet ^{19}F NMR signal at $\delta -77.3$ was consistent with the expected chemical shift for the trifluoroacetamide group.

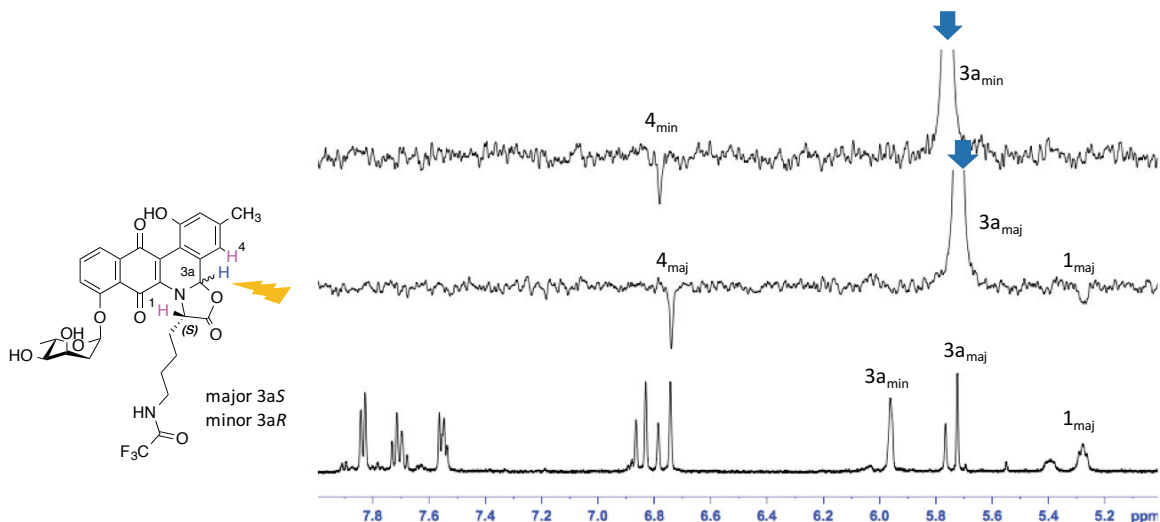


Figure 53. Irradiation of the 3a proton at 5.67 ppm of the major **3.1** diastereomer and at 5.72 ppm in the minor compound (500 MHz, methanol- d_4).

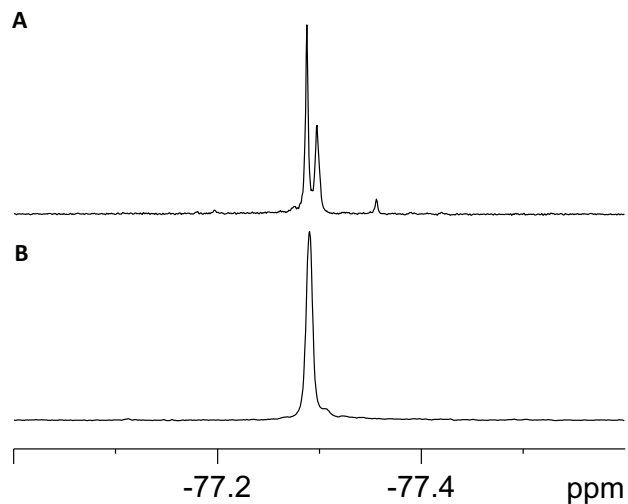


Figure 54. $^{19}\text{F}\{^1\text{H}\}$ NMR spectra (470 MHz) in methanol- d_4 (A) jadomycin TFAL **3.1**, a mixture of 3*aS*/3*aR* diastereomers; (B) jadomycin lactam **3.2**.

To obtain sufficient quantities of **3.2** for full characterisation, a 1.5-L culture supplemented with 33% isotopically labelled glucose, 1- ^{13}C glucose, was performed. 1- ^{13}C glucose is metabolised by glycolysis generating acetyl-coenzyme A (Ac-CoA), the polyketide synthase substrate for the jadomycin biosynthetic pathway (Figure 55).

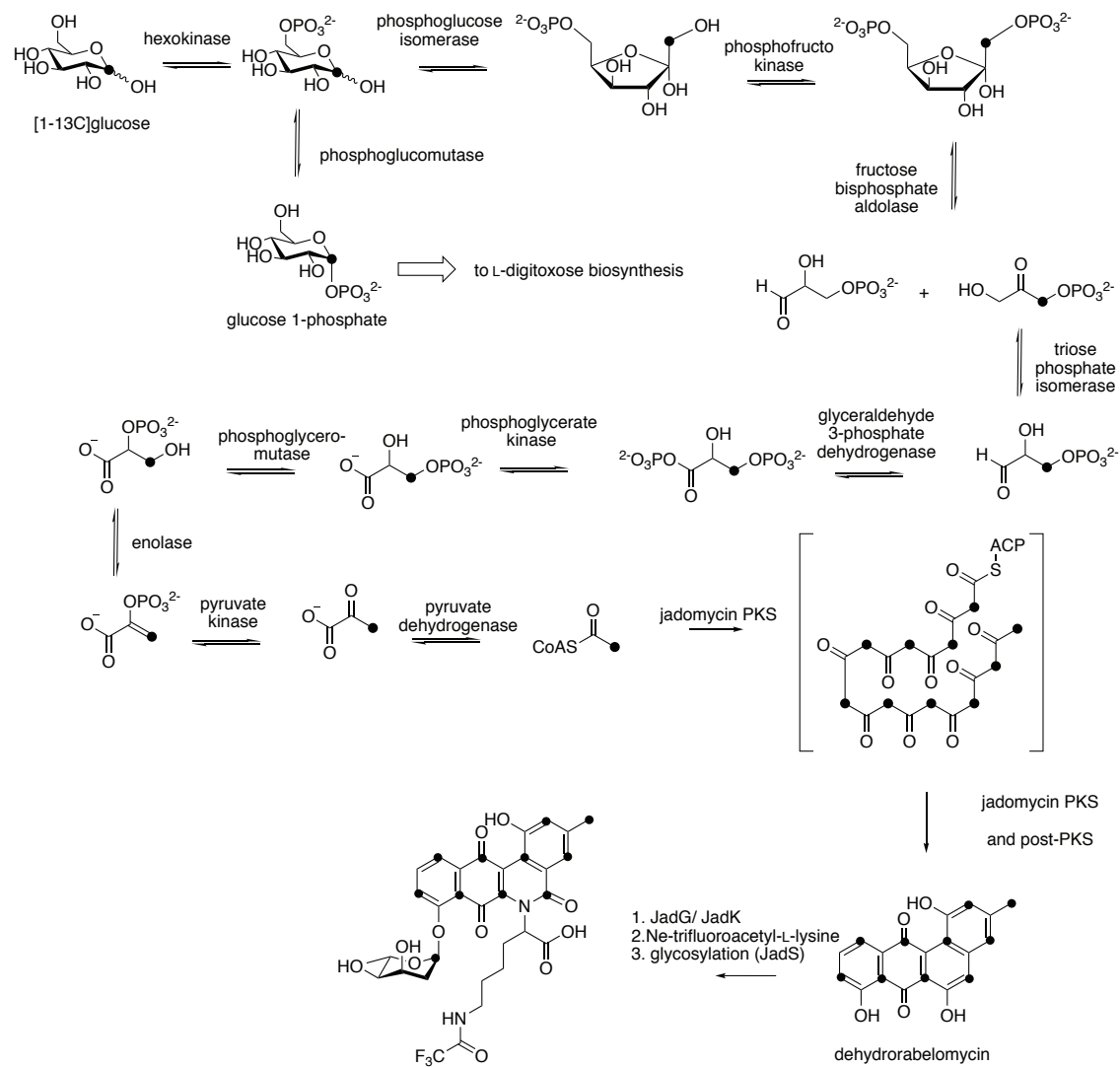


Figure 55. $1\text{-}^{13}\text{C}$ glucose metabolism by *S. venezuelae* and incorporation in jadomycins.

A more expedient purification procedure was developed for **3.2** using preparatory HPLC, resulting in a ten-fold improvement in isolated yield (5.9 mgL^{-1}). ^{13}C -enriched signals were found at the predicted positions in the ^{13}C NMR spectrum (Figure 56).

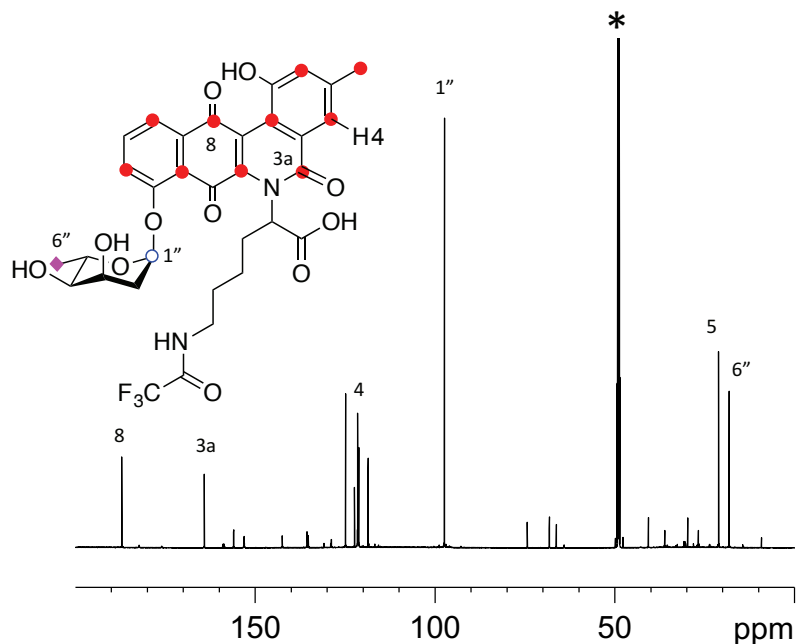


Figure 56. ¹³C incorporation in **3.2**; red circles (●) indicate positions with 14% isotopic incorporation, derived from the PKS-II substrate malonyl-CoA; a blue circle (○) indicates 27% incorporation derived from glucose 1-phosphate, and a pink diamond (◆) indicates 11% incorporation, arising from shuffling the isotopic label from C1 to C6 during glycolysis and gluconeogenesis. *solvent signal (methanol-*d*₄)

Percent ¹³C-incorporation, calculated from the ratio of the proton satellite signals to the corresponding uncoupled signal, was found to be 27% for the anomeric carbon (C1'') of L-digitoxose and 14% for the PKS-II assembled angucycline carbon C4, in close agreement to the predicted values. Spectroscopic data of ¹³C-labelled **3.2** showed signals characteristic of a jadomycin with an intact angucycline backbone (A-D rings), with evident deshielding of H4 and H6, indicating the presence of an electron-withdrawing group (EWG) associated with

the A ring. There was no doubling of signals corresponding to a diastereomeric pair observed in the ^1H -NMR spectrum, and, consistently, no signal corresponding to the hemiaminal ether proton (H3a). 2D-HMBC correlations from ^{13}C -labelled **3.2** showed a correlation between H1 of the amino acid side chain, and a ^{13}C -shift δ 165, consistent with an oxidized carbon at position 3a (Figure 57). The chemical shift data were similar to synthetic cyclic amides of similar architecture, possessing ^{13}C chemical shifts in this range (160-165 ppm).¹⁹⁶ These data supported oxidation of position 3a to give lactam **3.2**.

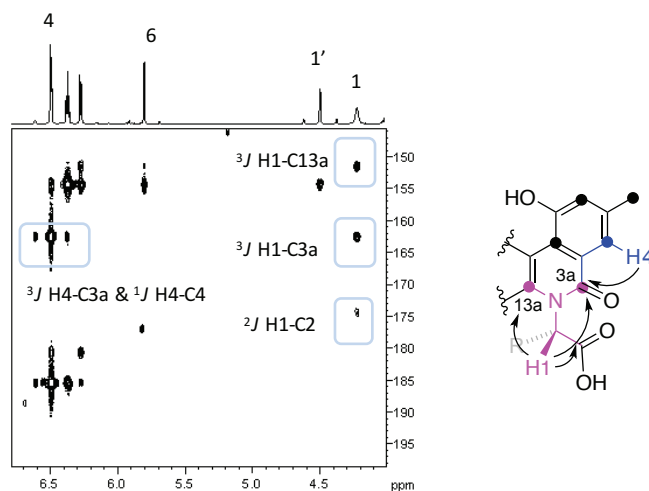


Figure 57. Key HMBC correlations showing amide connectivity in ^{13}C -labelled **3.2**. (700 MHz, methanol- d_4).

Isolation of a bright yellow solid, initially collected as precipitate from methanol- d_4 as described in the experimental section (Section 4.6.3), resulted in the discovery of compounds **3.3** and **3.4**, isolated as a mixture. Attempts to separate **3.3** and **3.4** were unsuccessful using our preparatory HPLC methods and as such these compounds were characterized and subsequently assayed as a mixture. The ^1H NMR

spectrum revealed that the mixture contained two compounds in a 2:1 ratio both possessing angucycline aromatic protons characteristic of jadomycin family natural products. The absence of side-chain methylene functionality in the ^1H and ^{19}F resonances in the NMR spectra indicated that the amino acid moiety was not incorporated. L-Digitoxylation on the D-ring was confirmed by ^1H NMR, HMBC analysis and HRMS. Furthermore, analysis of the NMR spectra showed that the two compounds were closely related structurally but were not diastereomers. The major compound **3.3** possessed a proton (H1) at δ 11.37 with a corresponding ^{13}C -signal (C1) at δ 195.2 (Figure 58), indicating an aldehyde group. 2D correlations positioned the aldehyde group on the A-ring; as was the case for compound **3.2**, the A-ring aromatic protons of **3.3** were deshielded in the ^1H NMR spectrum, due to the EWG effects of the aldehyde.

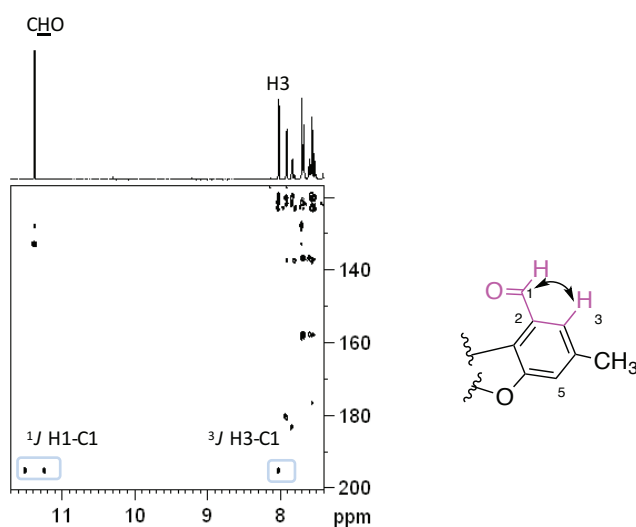


Figure 58. Key HMBC correlation demonstrating the presence of an aldehyde functional group in **3.3**. (700 MHz, chloroform-*d*3).

The minor compound **3.4**, however, did not appear to have an EWG at position-1 as the A-ring aromatic protons were between δ 7.2 and 7.4. An edited HSQC experiment identified a methylene unit, with a ^{13}C -chemical shift of δ 65.7 (Figure 59A), consistent with an analogue of **3.3** with reduction of the aldehyde to an alcohol. A COSY correlation between the CH_2 and a hydroxyl group confirmed the presence of a primary alcohol (Figure 59B). With the absence of an amino acid side chain in compounds **3.3** and **3.4**, a furan B ring was proposed as a structure consistent with both the NMR and HRMS data.

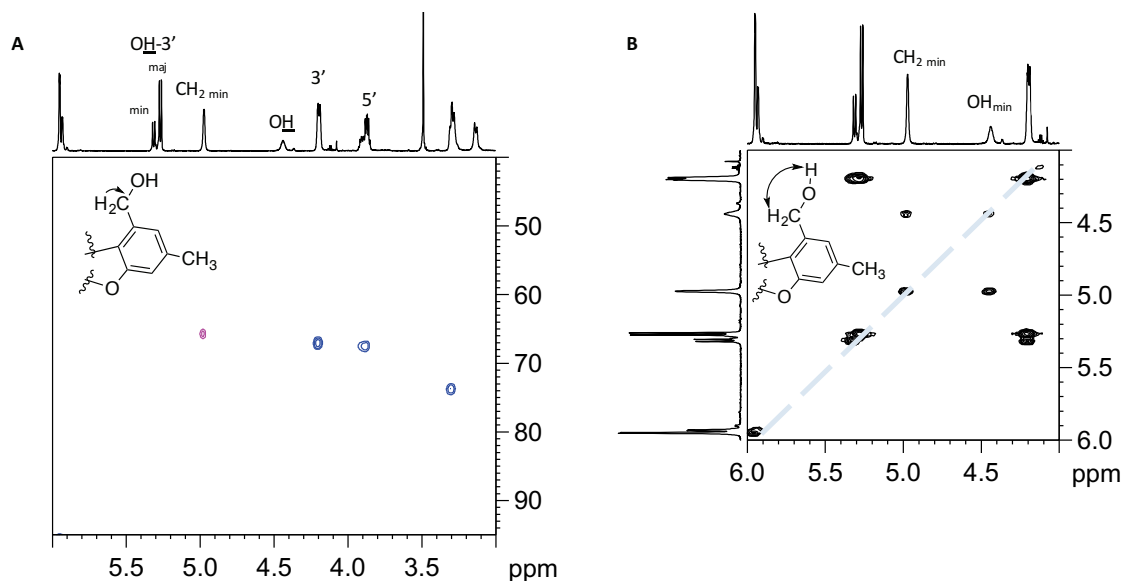


Figure 59. (A) Expansion of an edited-HSQC spectrum of the yellow precipitate containing compounds **3.3** and **3.4**; CH and CH_3 signals are colored in blue and CH_2 signals are colored in fushia; (B) expansion of a COSY NMR spectrum of the yellow precipitate showing the hydroxyl group present at C1 in the minor compound **3.4**. (700 MHz, chloroform- d_3)

3.2.3. Discussion of the Biosynthetic Origins of **3.2-3.4**

Jadomycin biosynthesis has been outlined through the use of blocked mutants and by sequence homology.¹⁴¹ We propose that **3.2**, **3.3** and **3.4** are derived from characterized intermediate **3.5** (Figure 60).¹⁹⁷ In the generally accepted mechanism, the B-ring of **3.5** is enzymatically cleaved to yield reactive intermediate **3.6**;¹⁹⁸ subsequently, the spontaneous reaction of aldehyde **3.6** with an amino acid generates the proposed intermediate **3.7** that forms either **3.1** or **3.2** through competing pathways. Remarkably, the isolated yields of **3.1** and **3.2** were comparable, although a precise explanation for the production of lactam **3.2** as a major product when cultured with TFAL remains speculative. Alternately, **3.2** may be a product of the oxidation of **3.1**, although our attempts to replicate this oxidation using H₂O₂ did not produce **3.2** (data not shown). Enzyme-mediated oxidation is also plausible. Cyclization initiated by conjugate addition of the A-ring OH to the quinone produced the furan (B-ring) present in **3.3** and **3.4**. The presence of compounds **3.2**, **3.3**, and **3.4** in these cultures, but not in detectable quantities in previous studies, suggests that the protected lysine plays a role directing product formation through the imine intermediate **3.7**, plausibly due to a conformation of **3.7** that limits facile E-ring cyclisation to give **3.1**, enabling the formation of **3.2**. A proposed long-lived imine intermediate **3.7**, may promote the production of **3.3** and **3.4** through a conjugate addition analogous to the chemistry that produces furan intermediate **3.8**, followed by hydrolysis of the imine to unmask the aldehyde yielding **3.3**. Studies observing the effect of trifluoroacetate on metabolic pathways are not reported, to the best of our knowledge, whilst fluoroacetate, a potent

pesticide, is known to interfere with biological pathways *in vivo* by inhibiting the citric acid cycle.¹⁹⁹ The effect of trifluoroacetate supplementation (30 mM final concentration) in a culture with a different amino acid, D-serine, was performed to investigate the effect on cell growth and natural product production in a well characterized system: however, no change in cell growth and no change in the natural product profile was observed (data not shown), and the production of compounds **3.3** and **3.4** was not observed.

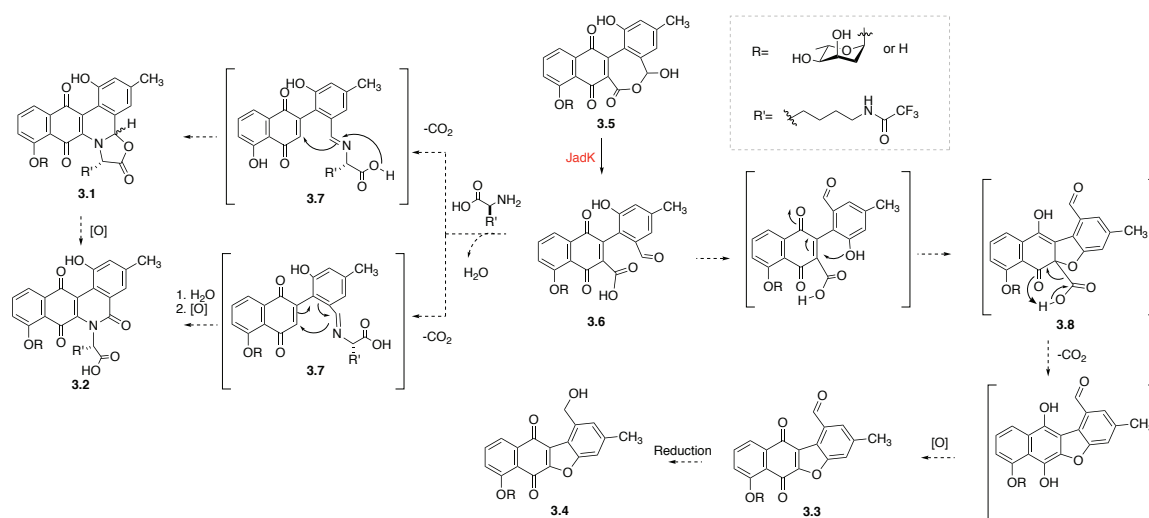


Figure 60. Proposed mechanistic origin of jadomycins **3.1-3.4** based on common biosynthetic intermediate **3.6**. It is plausible that **3.7** is the common biosynthetic intermediate for **3.1-3.4**.

3.2.4. Antimicrobial and Cancer Cell Line Bioassays

Compounds **3.1** and **3.2** were evaluated against a 5-strain antimicrobial panel with three Gram-positive bacteria, methicillin-resistant *Staphylococcus aureus* (MRSA), *Staphylococcus warneri* and vancomycin-resistant *Enterococcus faecium* (VRE); two Gram-negative bacteria, *Proteus vulgaris* and *Pseudomonas aeruginosa*; and a strain

of yeast, *Candida albicans* (Tables 8 and 9). Oxazolone-ring-containing **3.1** was active against Gram-positive MRSA (minimum inhibitory concentration (MIC), 3 $\mu\text{g mL}^{-1}$), *S. warneri* (3 $\mu\text{g mL}^{-1}$), and VRE (13 $\mu\text{g mL}^{-1}$), comparable to the activity of previously tested jadomycins against MRSA.¹⁹¹ In contrast, **3.2** was much less active (MIC $\geq 100 \mu\text{g mL}^{-1}$) against all three Gram-positive strains. The evaluated compounds were not active against Gram-negative bacteria or the yeast strain. Both compounds were not toxic against human fibroblast and kidney cells (MIC $> 128 \mu\text{g mL}^{-1}$, Table 10). The enhanced antibiotic activity of **3.1** in comparison to **3.2** implies that the hemiaminal ether functionality plays an important role in the antimicrobial properties of the jadomycins. Compounds **3.2-3.4**, were evaluated against the National Cancer Institute's 60 human cancer cell line panel, but did not show sufficient activity from the initial one-dose screen to warrant further evaluation.

Table 8. Antimicrobial assay results for **3.1** and **3.2** against Gram-positive MRSA, *S. warneri* and VRE.

	MRSA		<i>S. warneri</i>		VRE	
	MIC ₉₀ (µg/ml)	IC ₅₀ (µg/ml)	MIC ₉₀ (µg/ml)	IC ₅₀ (µg/ml)	MIC ₉₀ (µg/ml)	IC ₅₀ (µg/ml)
3.1	3.13	2.09 ± 0.2	3.13	2.84 ± 0.14	12.5	1.5 ± 0.3
3.2	100	47.4 ± 4.5	100	84.1 ± 0.01	>100	24.5 ± 0.3
Vancomycin	0.78	0.51 ± 0.08	0.39	0.24 ± 0.05		
Rifampicin					3.13	1.4

Table 9. Antimicrobial assay results for **3.1** and **3.2** against Gram-negative *P. aeruginosa* and *P. vulgaris*, and yeast strain *C. albicans*.

	<i>P. aeruginosa</i>		<i>P. vulgaris</i>		<i>C. albicans</i>	
	MIC ₉₀ (µg/ml)	IC ₅₀ (µg/ml)	MIC ₉₀ (µg/ml)	IC ₅₀ (µg/ml)	MIC ₉₀ (µg/ml)	IC ₅₀ (µg/ml)
3.1	>100	>100	>100	>100	>100	>100
3.2	>100	>100	>100	>100	>100	>100
Gentamicin	1.56	1.04				
Ciprofloxacin			0.004	0.0037		
Nystatin					1.56	0.87

Table 10. Cell toxicity assays for **3.1** and **3.2**.

	Fibroblast		Kidney	
	MIC ₉₀ ($\mu\text{g/ml}$)	IC ₅₀ ($\mu\text{g/ml}$)	MIC ₉₀ ($\mu\text{g/ml}$)	IC ₅₀ ($\mu\text{g/ml}$)
3.1	>128	>128	>128	>128
3.2	64	57.5 \pm 3.7	>128	>128
zinc pyrithione	16	7.8 \pm 0.4		
phenoxyethanol			0.63*	0.32 \pm 0.01*

*units are a% based on total well volume

3.2.5. Conclusions

In this study, the isolation and characterization of three novel jadomycin congeners differing in the functionality of the E-ring are described. This demonstrates that the non-enzymatic process to form the jadomycin oxazolone E-ring is amenable to different functional group manipulations. To the best of our knowledge, these are the first reports of amide- and furan-containing jadomycins, and demonstrate the surprising plasticity of the jadomycin biosynthetic machinery to deliver unanticipated derivatives. Furthermore, we demonstrate, using MS, the presence of a five-membered E-ring size in the jadomycin derived from L-lysine, which contrasts with the congeners isolated from L-ornithine, and utilize TFAL as a means to deliver and observe the L-lysine derived congener.

3.3. Biosynthetic 4,6-dehydratase Gene Deletion: Isolation of a Glucosylated Jadomycin Natural Product Provides Insight into the Substrate Specificity of Glycosyltransferase JadS

Excerpts from this section are taken from: S. M. Forget, J. Na, N. C. McCormick, D.L. Jakeman. *Org. Biomol. Chem.* (2017) 15, 2725-2729.

As touched upon in the introductory section, Wang and coworkers have previously outlined the L-digitoxyl biosynthetic gene cluster.¹⁴¹ The first committed step in the biosynthetic pathway is the formation of nucleoside diphospho glucose (NDP-Glc), where the nucleoside is likely thymidine, catalysed by nucleotidyltransferase JadQ (Figure 48). Five subsequent enzymes result in functional group interconversion of D-glucose into L-digitoxose in preparation for formation of the glycosidic linkage by the glycosyltransferase JadS. In this study, a 4,6-dehydratase gene deletion strain, *S. venezuelae* Δ *jadT*, was evaluated for its natural product profile. We have expanded on previous work in which evaluation of the strain bearing a disruption in the 2,3-dehydratase gene resulted in isolation of a sugar-modified jadomycin where the 2-hydroxyl was present in the final sugar, ILEVS1080 (**JdB-b**).⁶⁰

3.3.1. Isolation of Glucosylated Jadomycin 3.9 from *S. venezuelae* Δ *jadT*

S. venezuelae Δ *jadT*, a deletion strain prepared previously in the Jakeman lab,⁵⁹ was cultured using minimal media with D-serine as the sole nitrogen source and ethanol shock to induce jadomycin production using the standardized method.¹⁷⁵ One advantage of isolating the jadomycin congener incorporating D- (or L-) serine is the presence of only one observable diastereomer at position 3a, likely as a result of

preferential arrangement of the E-ring as an oxazolidine ring. As a consequence, the NMR spectrum is devoid of diastereomeric signals for several resonances, resulting in greater signal-to-noise and more ready elucidation of the natural product structure. Visual inspection of the growing *S. venezuelae* $\Delta jadT$ cultures for colour indicated that induction of natural products had occurred by production of deeply coloured pigments, giving cultures a muddy brown-red appearance. TLC analysis of the extracted natural products, obtained from a methanol elution after application of clarified culture media to a silica phenyl column, showed that a non-polar green material, jadomycin aglycon, was a major product. A second pink spot more polar than the wild-type product, jadomycin DS (**JdDS**), was also present. This second compound was subsequently isolated through a series of normal phase chromatographic separations to yield 3 mgL^{-1} of a new jadomycin congener. As a comparison, the wild type strain produces 50 mgL^{-1} of jadomycin DS, thus the total amount of glycosylated material isolated was roughly reduced by a factor of ten.²⁰⁰ The unanticipated jadomycin congener produced by the *S. venezuelae* $\Delta jadT$ strain was characterized using various MS and NMR spectroscopy experiments, including COSY, HSQC, and HMBC. ^1H NMR spectroscopy was utilized to assign the proton peaks, a COSY spectrum showed correlations between the carbohydrate protons to confirm the presence of a hexose, an HSQC spectrum was used to assign the carbon peaks, and an HMBC spectrum indicated that the carbohydrate moiety was appended at C12. The chemical shift of the anomeric centre at 5.01 ppm and a $^3J_{\text{H1}''\text{H2}''} = 7.5 \text{ Hz}$ was consistent with a β -configured, 1''-2''-trans glycosidic linkage (Figure 61). All spectroscopic data were consistent with the assignment of the

structure of this novel congener as glucosylated jadomyacin DS (**3.9**). The loss of 162 amu from a parent ion $[M+H]^+$ 566 in an LC-MS² experiment was consistent with fragmentation of a glucose moiety (Figure 62).

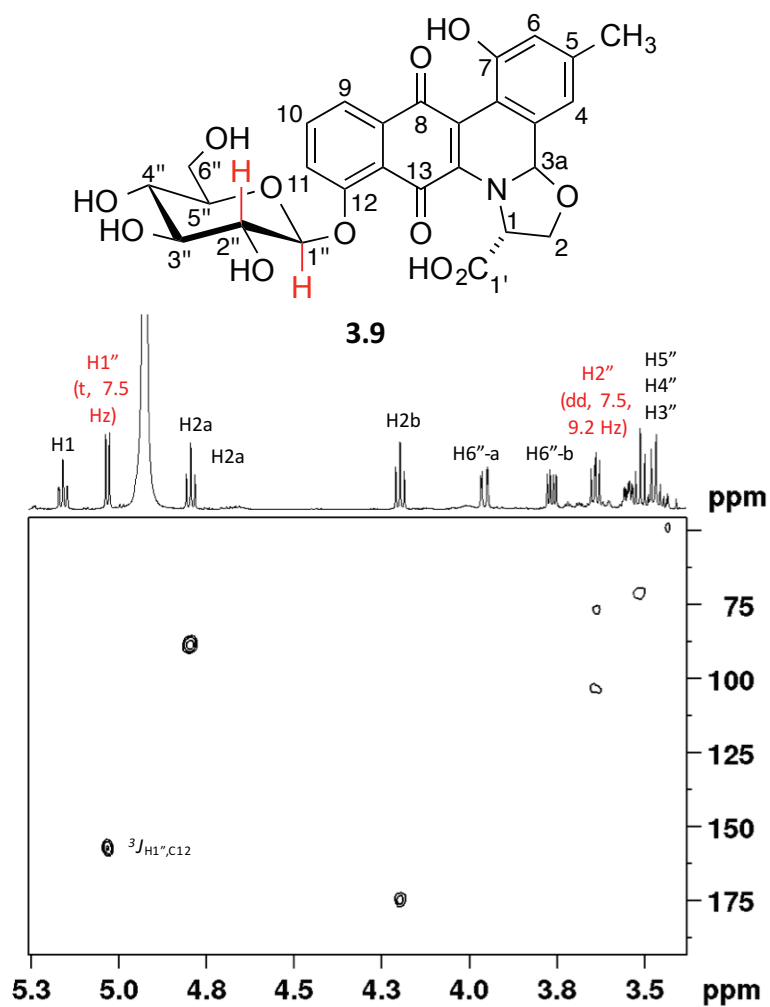


Figure 61. Structure of glucosylated jadomyacin DS (**3.9**) and HMBC expansion showing attachment of the glucose moiety at C12 of the angucycline ring.

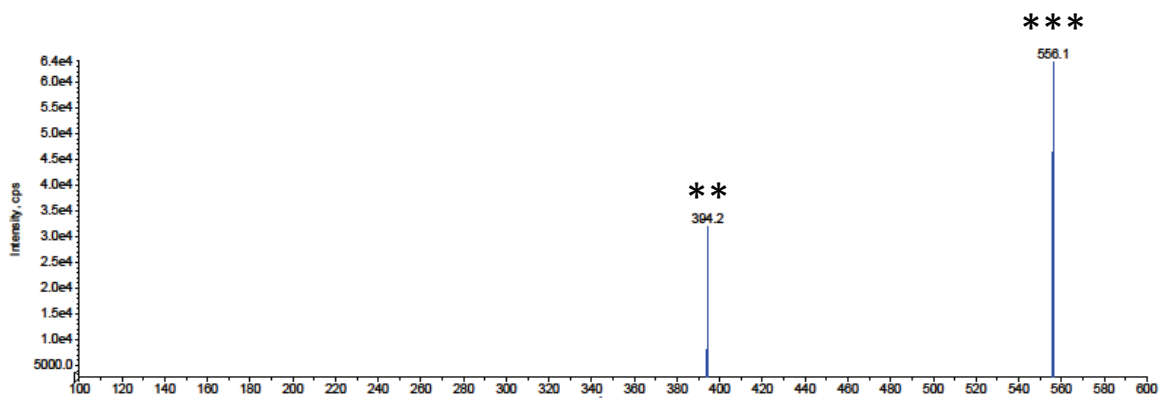


Figure 62. LC-MS² fragmentation of **3.9** (parent ion $[M+H]^+$ 556, showing $[M+H]^+$ (***) and cleavage of the sugar $[M+H-C_6H_{10}O_5]^+$ (**).

3.3.2. Identification of the Glycosyltransferase

The origin of the glucose and the biosynthetic catalyst responsible for its attachment was unclear. The deletion of the 4,6-dehydratase gene present in the *L*-digitoxose biosynthetic pathway was anticipated to furnish jadomycin aglycone. A second plausible outcome was that a 4,6-dehydratase could be recruited from an unrelated pathway to furnish **JdDS**, unmodified, i.e. with *L*-digitoxose appended. The recruitment of a 4,6-dehydratase from rhamnose biosynthesis has been reported in daunorubicin and doxorubicin biosynthesis.^{201, 202} However, this possibility was excluded, since no evidence of unmodified jadomycin DS was found by TLC or MS. We therefore turned to a bioinformatics analysis to provide insight into the biosynthetic catalyst responsible for appending D-glucose. Inspection of the CAZy database for natural product glycosyltransferases present in the genome of *S. venezuelae* ISP5230 (ATCC10712) identified 66 glycosyltransferases, which led us to examine the five GT1 family proteins present in the genome (Table 5).^{203, 204} Of

these five GT1 enzymes, two were shortlisted for further consideration, JadS (Sv5997) and Sv0189. That the JadS glycosyltransferase present in the jadomycin biosynthetic pathway, and which is responsible for appending L-digitoxose, would be amenable to appending D-glucose would be unprecedented for a 2,6-dideoxysugar transferase, given the different configurations at all positions on the hexose except C3. However, related natural product glycosyltransferases have demonstrated donor substrate non-specificity. For instance, the UrdGT2 catalyst, responsible for *S. fradiae* C-glycosylation in urdamycin biosynthesis, was not stereoselective with respect to the configuration at the 4- or 5-positions of the trideoxysugar donor substrate.⁵² Gene deletion of DesI resulted in the isolation of a macrolide bearing D-quinovose in lieu of D-desosamine, showing tolerance to modification at the 3- and 4- positions of the 6-deoxy sugar.⁵³ Similarly glucosyltransferase StaG⁵⁴ from staurosporine and rhamnosyltransferase ElmGT⁵⁵ from elloramycin biosynthetic pathways have been shown to transfer a variety of deoxy sugars to their respective aglycones. Rhamnosyltransferases CalG1²⁰⁵ and ElmGT⁵⁵ have been shown to process a variety of sugars, including D-glucose. A phylogenetic analysis of the five GT1 family glycosyltransferases and OleD based on sequence homology clustered JadS with Sv0189 and OleD. OleD has 75% identity with Sv0189, and Sv0189 is similarly located in a region of the *S. venezuelae* ISP5230 genome that is not associated with the biosynthesis of putative natural products (see Section 2.5), and may potentially function as a glucosylation catalyst within the organism. OleD is an enzyme initially discovered in *S. antibioticus* as being able to glucosylate oleandomycin with the same regio- and

stereochemical outcome as OleI, the glycosyltransferase present in the oleandomycin gene cluster that is responsible for protecting *S. antibioticus* against the effects of oleandomycin. By contrast, OleD is not associated with the oleandomycin biosynthetic gene cluster.^{142, 144}

3.3.3. Evaluation of *S. venezuelae* $\Delta sv0189\Delta jadT$ and *S. venezuelae* $\Delta jadS\Delta jadT$

To further investigate the putative roles of JadS and Sv0189, two double deletion strains *S. venezuelae* $\Delta sv0189\Delta jadT$ and *S. venezuelae* $\Delta jadS\Delta jadT$ were prepared by homologous recombination. See section 3.4 for a more detailed explanation of this method. *S. venezuelae* mutants were identified using PCR primers flanking the site of deletion, such that smaller amplification products compared to wild-type controls provided evidence of gene deletion (Figure 63).

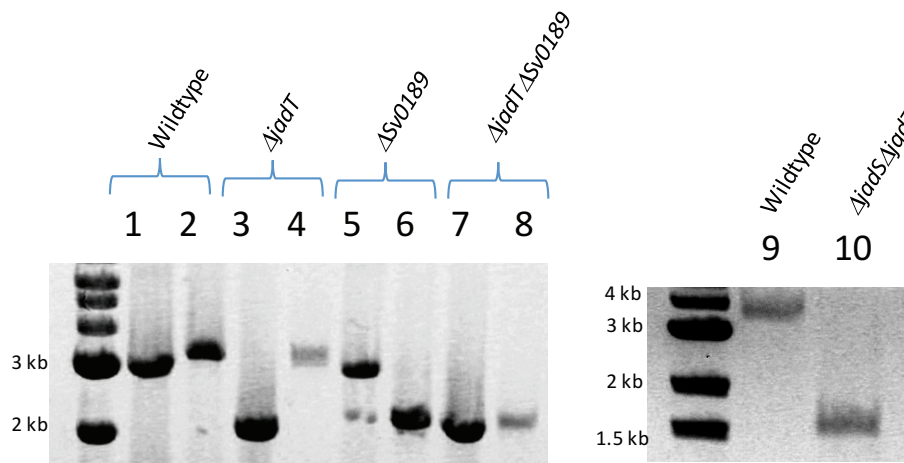


Figure 63. TAE-agarose gel (0.75%) showing PCR amplification products with appropriate flanking primers for *S. venezuelae* wild-type, $\Delta jadT$, $\Delta sv0189$, $\Delta jadT\Delta sv0189$ and $\Delta jadS\Delta jadT$.

S. venezuelae $\Delta sv0189$ was also analyzed given the function of Sv0189 within the organism was unknown and deletion of this gene was found to have no effect on either cell growth or jadomycin production. All three strains were cultivated under standard stress conditions for jadomycin production, and induced natural products were analyzed by TLC and HPLC after extraction by silica phenyl chromatography. All of the mutant strains evaluated in this study were observed to produce chloramphenicol, visible in the HPLC traces, which is typically not observed in cultures with the wild-type strain (Figure 64).²⁰⁶ The presence of chloramphenicol in extracts from the deletion mutants is consistent with earlier studies demonstrating cross-regulation between the respective biosynthetic pathways.^{206, 207} Otherwise, the TLC and HPLC traces of *S. venezuelae* $\Delta sv0189$ metabolite profiles were comparable to the wild-type strain.²⁰⁰ Evaluation of the secondary metabolites produced by the double deletion strain, *S. venezuelae* $\Delta sv0189\Delta jadT$, demonstrated that it produced glucosylated jadomycin (Figures 65), conclusively revealing that Sv0189 does not play a role in the formation of **3.9**. According to analysis using HPLC, *S. venezuelae* $\Delta jadS\Delta jadT$ did not produce glucosylated jadomycin DS but did produce jadomycin aglycone. The absence of glycosylated jadomycins in cultures with *S. venezuelae* $\Delta jadS\Delta jadT$ was confirmed by TLC and by HPLC. Thus, we conclude that JadS is able to transfer D-glucose to the jadomycin aglycone demonstrating a remarkable capacity to tolerate various sugar donors *in vivo*.

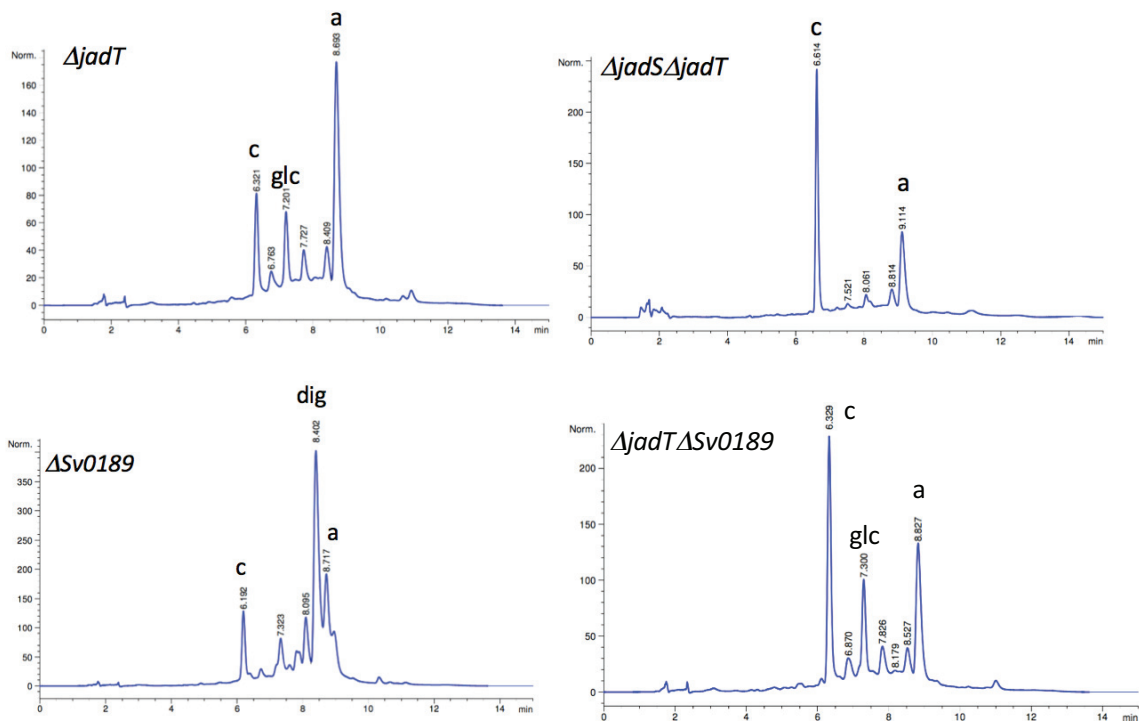


Figure 64. HPLC traces of the methanol extract from the phenyl column for *S. venezuelae* wild-type, $\Delta jadT$, $\Delta sv0189$, $\Delta jadT\Delta sv0189$ and $\Delta jadS\Delta jadT$. Symbol key: c, chloramphenicol; a, jadomycin aglycon; dig, JdDS; glc, 3.9.

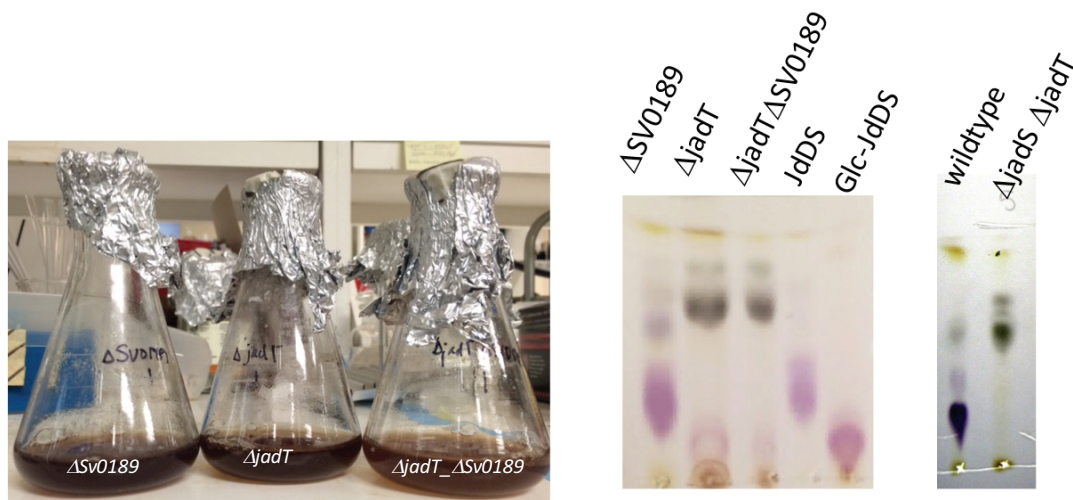


Figure 65. Left: Jadomycin production cultures after 48 h. Centre: TLC (20% methanol/dichloromethane) methanol extracts from indicated strains, alongside standards for jadomycin DS (**JdDS**) and glucosylated jadomycin DS (**3.9**); Right: TLC (20% methanol/dichloromethane), wild-type produces **JdDS** (major purple spot), and the $\Delta jadS \Delta jadT$ strain produces jadomycin aglycone (green spots) and no visible glucosylated **Jd** species (absence of polar purple spots).

3.3.4. Conclusions

In summary, an unanticipated natural product glycoside **3.9** was isolated as a result of deleting the 4,6-dehydratase gene present in the jadomycin L-digitoxose biosynthetic gene cluster. We have investigated the potential involvement of two GT1 family glycosyltransferase, JadS and Sv0189. JadS was identified as the glycosyltransferase responsible for transfer of the glucose. While several reports of glycosyltransferases with broad substrate specificity exist in the literature, to our knowledge this is the first example of a 2,6-dideoxy-L-sugar glycosyltransferase that is able to transfer D-glucose to its aglycone. Our results shed light on the expanding

body of work demonstrating that pathway-specific glycosyltransferases possess flexibility with respect to sugar donors, a feature which bears interesting possibilities for *in vitro* glycodiversification efforts. Sv0189 was not found to participate in the glucosylation and the physiological role for this enzyme remains undefined, although its similarity to OleD suggests it may play a function in defense specifically against macrolide antibiotics. Evaluation of Sv0189 *in vitro* is discussed in Section 2.5.

3.4. Introduction of a Non-Native L-digitoxyltransferase into *S. venezuelae*

Genetic engineering offers advantages over other approaches to glycodiversification, enabling complex chemical modification to occur *in vivo* that would be difficult to achieve using synthetic bench chemistry.²⁰⁸ *In vitro* approaches, involving isolation multiple biosynthetic enzymes, are limited by factors such as efficient expression of the requisite proteins by *E. coli*, protein instability and insolubility that may arise from heterologous expression and the availability of the required chemical intermediates to serve as substrates. Such obstacles are absent when engineering of the host strain is possible.⁴³ Drawbacks to *in vivo* methods include the ease with which the targeted bacterial species may be genetically manipulated, potential toxicity to the heterologous host, uncertainties relating to the regulation of secondary metabolite gene clusters by the host, lengthy time requirements to culture bacteria for natural product production, low yields of the target compound per liter (sub-milligram), and tedious purification of products from complex mixtures.²⁰⁹ Many examples of combinatorial biosynthesis have been

reported.²¹⁰⁻²¹² Glycodiversification of the anthracycline antibiotic, steffimycin, and of tetracycline and elloramycin, using genes from a heterologous dideoxy sugar pathway, oleodomycin, resulted in compounds that were more active against several cancer cell lines (Figure 66).^{213, 214} The disaccharide and trisaccharide analogues of doxorubicin, obtained by chemical synthesis, were found to reduce off-target cytotoxicity in comparison to the parent compound.²¹⁵ Supplementation of genes from landomycin biosynthesis into the urdamycin biosynthetic pathway resulted in the isolation of analogues with unnatural glycosylation patterns.²¹⁶ In another study, engineering of the urdamycin biosynthetic glycosyltransferases UrdGT1b and UrdGT1b enabled the isolation of a novel branched analogue, urdamycin P.²¹⁷

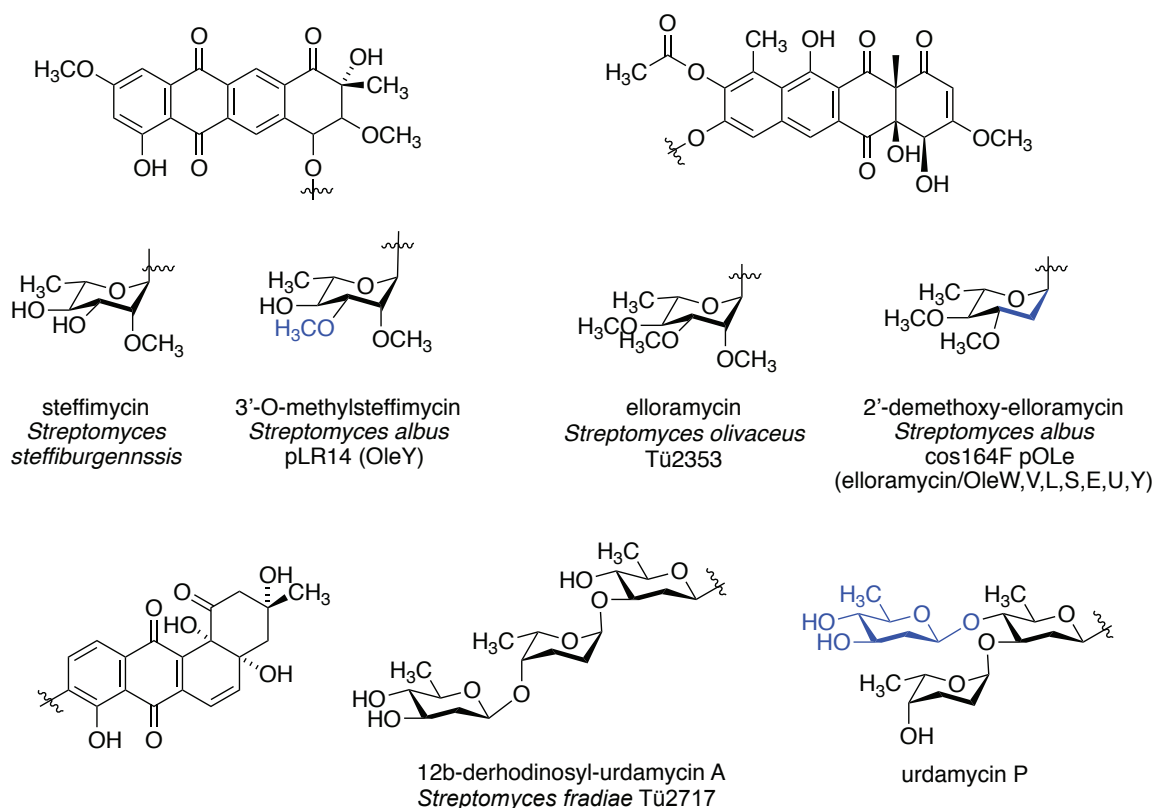


Figure 66. Examples of glycodivesification by combinatorial biosynthesis.

Over the past decade, *Streptomyces venezuelae* ISP5230 has emerged as a favourable strain for heterologous protein expression for combinatorial biosynthesis, due to a convenient fast growth rate, 2-3 days compared to 6-9 days for other *Streptomyces* species, and to being highly amenable to standard genetic editing techniques.²¹⁸⁻²²¹ Publication of the *S. venezuelae* genome in 2011 has resulted in the discovery and isolation of several new secondary metabolites by implementation of genomic editing techniques to express these silent pathways; these natural products are listed in Section 2.5.²⁰⁴

The aim of this project was to implement a combinatorial approach to jadomycin biosynthesis, by selecting a glycosyltransferase from a disparate biosynthetic gene cluster for complementation in *S. venezuelae*. On induction of jadomycin biosynthesis, which is turned on under stress conditions,^{166, 174, 175} we hypothesized that a glycosyl-modified jadomycin will be obtained. The first criterion taken into consideration for the selection of a suitable glycosyltransferase was utilization of NDP-L-digitoxose as a substrate, such that the sugar donor would not be a limiting factor. Additionally, selecting a catalyst that physiologically utilizes L-digitoxose would provide the best scenario to facilitate glycosylation of an unnatural acceptor. A handful of other characterized natural products contain L-digitoxose, including kijanimicin and lobophorin, lactonamycin Z, RK286-C, selvamicin, and the heptadecasaccharide saccharomicins (Figure 67).²²²⁻²²⁸

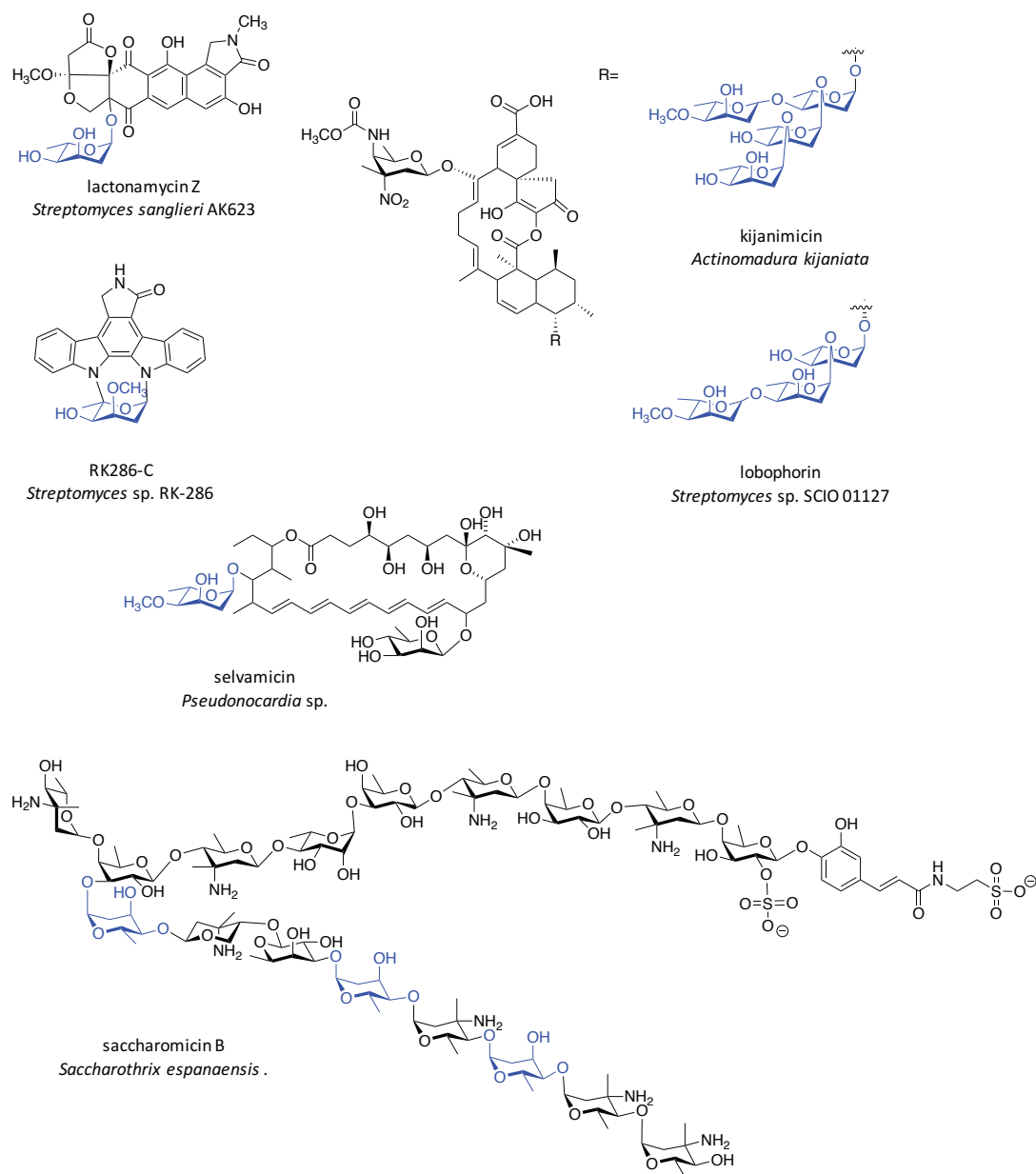


Figure 67. Structures of natural products decorated with α -L-digitoxose (blue).

Based on these criteria, the L-digitoxyl transferases involved in kijanimicin and lobophorin biosynthesis emerged as contenders, as the biosynthetic gene clusters for these macrolide antibiotics are partially elucidated.^{222, 224} Li *et al.* functionally assigned the glycosyltransferases involved in lobophorin biosynthesis through evaluation of deletion mutants. LobG3 was identified as an iterative

glycosyltransferase, responsible for appending the two α -linked L-digitoxose moieties, and LobG2 was assigned as the retaining glycosyltransferase, responsible for adding the third the β -linked L-digitoxose.²²⁴ Not having access to the lobophorin-producing strain, the corresponding genes in the kijanimicin gene cluster of *Actinomadura kijanita* were identified based on sequence similarity to LobG3 and LobG2, allowing us to assign putative functional assignments to KijC4 (74% identity to LobG3) and KijC3 (81% identity to LobG2, Figure 68).

1: Sv0189	100.00	23.50	19.45	21.74	21.87	22.67	21.54	25.54
2: Sv5997	23.50	100.00	32.50	29.20	31.37	32.98	31.65	31.20
3: kijC4	19.45	32.50	100.00	73.55	52.81	52.43	54.18	53.71
4: LobG3	21.74	29.20	73.55	100.00	52.28	52.93	54.52	56.74
5: kijC3	21.87	31.37	52.81	52.28	100.00	80.29	59.28	58.29
6: LobG2	22.67	32.98	52.43	52.93	80.29	100.00	58.70	57.68
7: kijA4	21.54	31.65	54.18	54.52	59.28	58.70	100.00	61.00
8: kijC1	25.54	31.20	53.71	56.74	58.29	57.68	61.00	100.00

Figure 68. Sequence identity alignments between biosynthetic glycosyltransferases in jadomycin (Sv5997), lobophorin, and kijanimicin gene clusters, and Sv0189 (*S. venezuelae* GT1 family glycosyltransferase). Alignment using Clustal Omega.

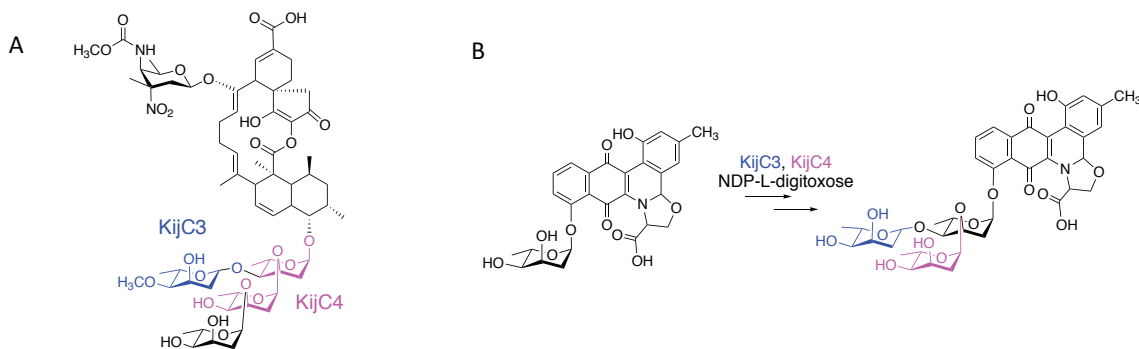


Figure 69. (A) Proposed glycosylation by KijC4 (pink) and KijC3 (blue); (B) Anticipated structure of a modified jadomycin.

The first objective was to define methodology for complementation of wild-type *S. venezuelae* with *kijC4* and *kijC3* and to evaluate complemented strains for the production of jadomycin congeners containing additional L-digitoxyl moieties (Figure 69). Three approaches to gene complementation are summarized in Table 11, along with some pros and cons associated with each method. While the first method listed (homologous recombination) has typically been applied in gene disruption and gene deletion experiments, methods two and three have routinely been employed for gene complementation in *Streptomyces*. The first approach is uncommon in the literature due to the risk of disrupting downstream gene expression, a phenomenon termed a polar effect in the genetic literature. By implementation of the first method, we anticipated that gene expression of the introduced gene would be under the same control as the jadomycin gene cluster. In the second approach the introduced gene is inserted after a strong constitutive promoter, such that its transcription is continuously turned on. The second approach is widely used for heterologous expression in *Streptomyces* but requires culture in the presence of a selective antibiotic to maintain the expression vector. Likewise, in the third approach, a strong promoter is utilized to ensure transcription of the gene and selective pressure is required to maintain the plasmid, although the plasmid is incorporated into the genome. CRISPR-Cas9 methods to perform the gene insertion were not considered at the outset of this project because the methods had not yet been developed for use with *Streptomyces*.^{229, 230}

Table 11. Methods for heterologous gene complementation in *Streptomyces*.

Description and vector used	Vector Gene insertion site	Advantages	Disadvantages
(1) Homologous recombination	pKC1139; insertion at any site in the genome as dictated by the regions of homology flanking the insert on the plasmid	<ul style="list-style-type: none"> • Markerless selection • Insetion of gene into dideoxy gene cluster allows regulation of gene transcription under same control • Conjugation between <i>E.coli</i> and <i>Streptomyces</i> to introduce gene 	<ul style="list-style-type: none"> • Gene knock-in strategies are uncommon in literature • Possibility of polar effects resulting from disruption of gene transcription • Selection of double crossover mutant takes a long time (~4 weeks)

(2) Integrative complementation	pSET152; ϕ C31 gene integrates with <i>attB</i> sites and highly homologous sites in the genome	<ul style="list-style-type: none"> • Literature precedent • Conjugation between <i>E. coli</i> and <i>Streptomyces</i> to insert plasmid • Selection of single crossover mutant is fast (~1-2 weeks) 	<ul style="list-style-type: none"> • Selective pressure is necessary (Apr) to maintain insertion • Uncertainty associated with integration site and number of insertions • The plasmid must be modified by introduction of a promoter (i.e. <i>ermE*</i>)
---------------------------------	--	---	--

Description and vector used	Vector Gene insertion site	Advantages	Disadvantages
(3) <i>Streptomyces</i> expression vector	pSE34; plasmid maintained under selective pressure	<ul style="list-style-type: none"> • Literature precedent • Contains a strong and well-characterized promoter (<i>ermE*</i>) • Selection of single crossover mutant is fast (~1 week) 	<ul style="list-style-type: none"> • Protoplast transformation procedure are tedious • Expression of gene not tunable • Thiostreptin required in all culture media to maintain plasmid • Some <i>Streptomyces</i> strains develop resistance to thiostreptin giving false positives

3.4.1. Homologous Recombination Using pKC1139 (Method 1)

For insertion by homologous recombination (method one), the site of gene insertion in the chromosome was controlled by the design of the knock-in cassette wherein the new gene is flanked by ~ 1 kb of the chromosomal DNA located immediately up and downstream of the selected site. This approach is routine in biosynthetic gene disruption experiments and for regulatory gene induction.^{231, 232} Despite the lack of precedent for this method in applications similar to ours, it was appealing given the opportunity to introduce the gene directly into the L-digitoxyl biosynthetic gene cluster of *S. venezuelae* ISP5230 (wild-type), given that the regulatory processes involved in jadomycin production would control gene expression. Wang and Vining demonstrated that insertion of apramycin (*Apr*, *aaa(3)IV*) disruption cassettes within the genes involved in dideoxy sugar biosynthesis did not produce polar effects.¹⁴¹ Another advantage to this approach was the generation of markerless mutants, which allowed for subsequent genetic engineering with standard selection techniques, given that the double crossover event that occurs effectively exchanges with genomic DNA for the homologous DNA on the plasmid that introduces the mutation. Due to the double crossover event, the mutation would be stable, and the bacteria could be cultured without selective antibiotics, which could be deleterious to bacterial growth and have unknown effects on secondary metabolite production. A site between *jadU* and *jadV*, situated near the end of the L-digitoxyl dideoxy gene cluster, was selected for insertions (Figure 70). As a control for possible disruption to the gene situated immediately downstream of the insertion

site, a *jadV* deletion mutant was also produced. A conjugal vector pKC1139 bearing *jadU* and *jadV* was constructed. Standard molecular biology techniques were used to assemble plasmids, as detailed in the experimental section. Inserts *kijC3*, *kijC4* and *kijC4kijC3* were ligated with linearized pKC1139::*jadUV*. pKC1139::*kijC4*(*XhoI*) was prepared by mutagenesis of pKC113::*kijC4* which effectively shifted *jadV* to the original reading frame relative to other genes in the cluster. However, an error was later found in the design of these plasmids, as discussed in detail in Section 3.4.4.2. The conjugal plasmid bearing the insert gene carried by *E. coli* ET12567 pUZ8002 was transferred to *S. venezuelae* by conjugation. A homologous recombination protocol outlined in the literature was followed.²³³ Screening for the insert was accomplished by colony PCR or by amplifying extracted genomic DNA to identify mutants *S. venezuelae*::*kijC3*, *S. venezuelae*::*kijC4*, *S. venezuelae*::*kijC4*(*XhoI*), and *S. venezuelae*::*kijC4kijC3*. Assembly of pKC1139 Δ *jadV* was accomplished by cloning the ~1 kb regions immediately up and downstream of *jadV* to give a *jadU-jadR** deletion cassette (Δ *jadV*), which was then ligated to linearized pKC1139. The same conjugation and screening protocols were employed to identify *S. venezuelae* Δ *jadV*.

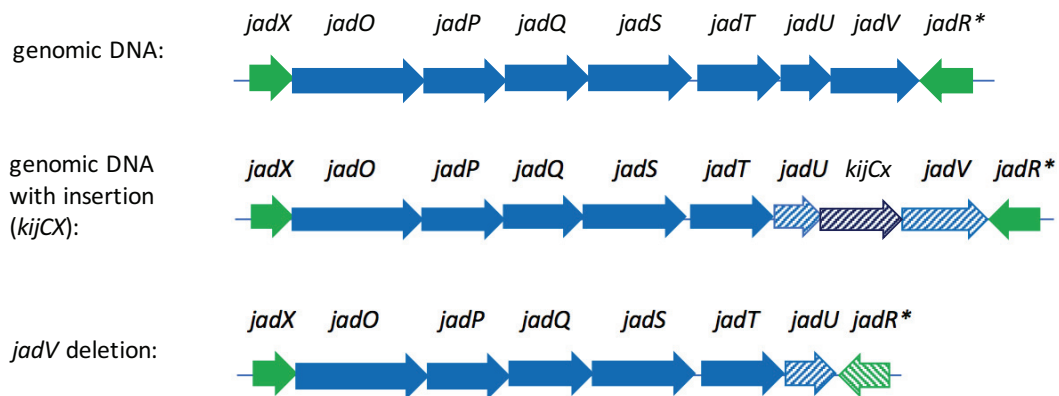


Figure 70. L-digitoxose biosynthetic gene cluster from the wild-type strain (top) with structural genes shaded in blue and regulatory genes in green. *kijCX*: *kijC3*, *kijC4*, *kijC4(XhoI)*, or *kijC4kijC3*. Hatched genes represent knock-in or deletion cassettes introduced by homologous recombination.

3.4.2. Integrative Insertion Using pSET152 (Method 2)

The vector pSET152 possesses a *Streptomyces* phage ϕ C31 integrase that recognizes *attB* sites in the chromosome, resulting in chromosomal insertion of the plasmid at these sites.²³⁴ This vector has been extensively used; Kobylansky *et al.* complemented various *Streptomyces* with the C-glycosyltransferase UrdGT2 for glycodiversification studies.^{235, 236} The Yoon research group has complemented the pikromycin producing strain of *Streptomyces venezuelae* ATCC 15439 with dideoxy sugar biosynthetic genes from other strains and achieved up-regulation of pikromycin biosynthesis through complementation with non-native transcriptional regulators.^{237, 238} BlastP search of the genome of *S. venezuelae* (ATCC10712) identified an *attB* site within the gene *sv3566* (NCBI FR845719.1, possible chromosome condensation protein), although studies have shown that secondary integration sites in homologous regions of the genome are possible.²³⁹ Integration of

pSET152 occurs as a result of a single crossover event, in which the entire plasmid is inserted into the *attB* site and is maintained under selective pressure. Continuous use of the selective antibiotic (Apr) is required to maintain the plasmid, thus limiting the potential for further genetic manipulation of the mutant strain. An advantage to this approach is the elimination of possible polar effects on the jadomycin gene cluster. On the other hand, cell growth and secondary metabolism may be affected by the required inclusion of antibiotic in the culture media. Assembly of a pSET152::*kijC4* vector is ongoing.

3.4.3. Heterologous Expression Using pSE34 (Method 3)

The third approach utilized the *Streptomyces* expression vector pSE34, which does not integrate into the genome. The plasmid is carried by the bacteria under selective pressure through culture in the presence thioestrepton.²¹⁸ A constitutive promoter (*ermE**) allows for overexpression of the inserted gene.²⁴⁰⁻²⁴² This plasmid has been used successfully in *S. venezuelae* for heterologous expression of the glycosyltransferase AknS from the aclacinomycin A gene cluster of *S. galilaeus* ATCC 31615.^{221, 236} A plasmid bearing *kijC4*, pSET34::*kijC4*, was assembled using standard molecular biology techniques. The plasmid pSE34 lacks the *oriT* gene necessary for genetic transfer by conjugation, therefore *Streptomyces* protoplasts were prepared to enable transformation by heat shock, following adapted literature procedures for *Streptomyces*.^{59, 233, 243} The protoplast transformation resulted in many exconjugants (hundreds) and from a screen of ~100 colonies the majority were not thioestrepton-resistant after patching. Two thioestrepton resistant colonies were identified during screening. Unfortunately, attempts to unambiguously confirm the

presence of the plasmid by PCR and plasmid isolation were unsuccessful. Some strains of *Streptomyces* may display pseudo-resistance to thiostrepton, resulting in a high number of false positives in selective screening.²³³ Given the challenges encountered in the screening process and a failure to identify *S. venezuelae* carrying pSET34::*kijC4*, this method was not pursued further.

3.4.4. Analysis of *kijC3*, *kiC4*, *kijC4kijC3* complemented *S. venezuelae* (Method 1)

The *Streptomyces* strains generated by homologous recombination (method one), *S. venezuelae*::*kijC3*, *S. venezuelae*::*kijC4*, *S. venezuelae*::*kijC4*(XhoI), *S. venezuelae*::*kijC4kijC3* and *S. venezuelae* Δ *jadV*, were cultured for jadomycin production using a standardized small-scale protocol employing triplicate (3 × 25 mL) jadomycin cultures with D-serine as the amino acid. D-Serine was selected as the amino acid for inclusion in the minimal media, because this culture has been well characterized and reported to produce good yields of jadomycin D-serine (**JdDS**).²⁰⁰ Culture growth was monitored by OD₆₀₀, for bacterial proliferation, and at A₅₂₆, as an estimate of jadomycin production. After 48 h, the cultures were subject to an initial purification step using silica phenyl column chromatography by applying clarified culture media to the column, followed by washes with several volumes of water. The deeply coloured band remaining at the top of the silica column was extracted with methanol. Throughout the discussion, use of “methanol extract” refers to the partially purified material extracted from the silica phenyl column chromatography step as described above. Methanol extracts, typically deeply coloured with a purple to brown hue, were analysed by HPLC, TLC and LCMS in an attempt to identify the natural products present.

3.4.4.1. Evaluation of *kijC3* Knock-In Strains: *S. venezuelae::kijC3*

A few of the strains identified as *S. venezuelae::kijC3* strains (1-5) were selected and cultured with D-serine alongside a wild-type control. Several strains were selected to determine whether all strains would possess the same natural product profile. The mutant strains grew at a rate comparable to the wild-type as reflected in the OD₆₀₀ curves, but only reached approximately half of the A₅₂₆ values (Figure 71AB). Quantitative differences in the A₅₂₆ measurements between strains were also visually observed by intensity of the pigment developed in the cultures after 48 hours (Figure 71C). The methanol extracts from mutant strains and the wild-type strain were evaluated by TLC (Figure 71D). Two of the knock-in strains (*kijC3*-1 and -2) produced both unmodified jadomycin D-serine (**JdDS**) and jadomycin aglycone by TLC, although no new spots were obvious on primary inspection. Some promising faint spots that did not match **JdDS** were present, also. The observation that some strains were producing **JdDS** was encouraging, as it demonstrated that insertion of *kijC3* did not have polar effect on expression of the dideoxy gene cluster, at least not in all of the strains. The remaining strains (*kijC3*-3, -4 and -5) produced jadomycin aglycone. Only a scarce amount, if any, **JdDS**, was observed by TLC, contrarily suggesting polar effects on the gene cluster. In an effort to clarify whether any new products were produced, an LCMS experiment using a precursor positive scan of *m/z* 306, corresponding to phenanthroviridine, a fragment arising from loss of the sugar and amino acid that is common to all jadomycins, was run on methanol extracts. The results obtained from the LCMS analysis supported that the natural products observed by TLC were present in the mixture, with either

jadomycin aglycone $[M+H]^+$ m/z 394 or **JdDS** m/z 525 as the major species detected in all cases. Additional screening for the di- L-digitoxylated jedomycin was performed by running an EPI (enhanced product ion, MS^2) experiment scanning for its mass $[M + H]^+$ m/z 654, which was found in the extracts from strains *kijC3-1* and -2. However, some care had to be taken in interpreting LCMS results, given that the mass of the di-L-digitoxylated jedomycin $[M + H]^+$ m/z 654 could be detected also in the extract from the wild-type strain. Analysis of natural products from a scaled-up D-serine production with strain *kijC3-2* after methanol extraction and fractionation using normal phase silica chromatography did not reveal any new products: only jedomycin aglycone (m/z 394) and **JdDS** (m/z 525) were detected. As such, detection of the ion m/z 654 was attributed to an artifact of the LCMS running conditions. The faint spots that are observed by TLC in extracts from *kijC3-3*, -4 and -5, but not *kijC3-1* and -2 may be related to disruption of *jadV*, due to polar effects, in those strains (Section 3.4.4.2).

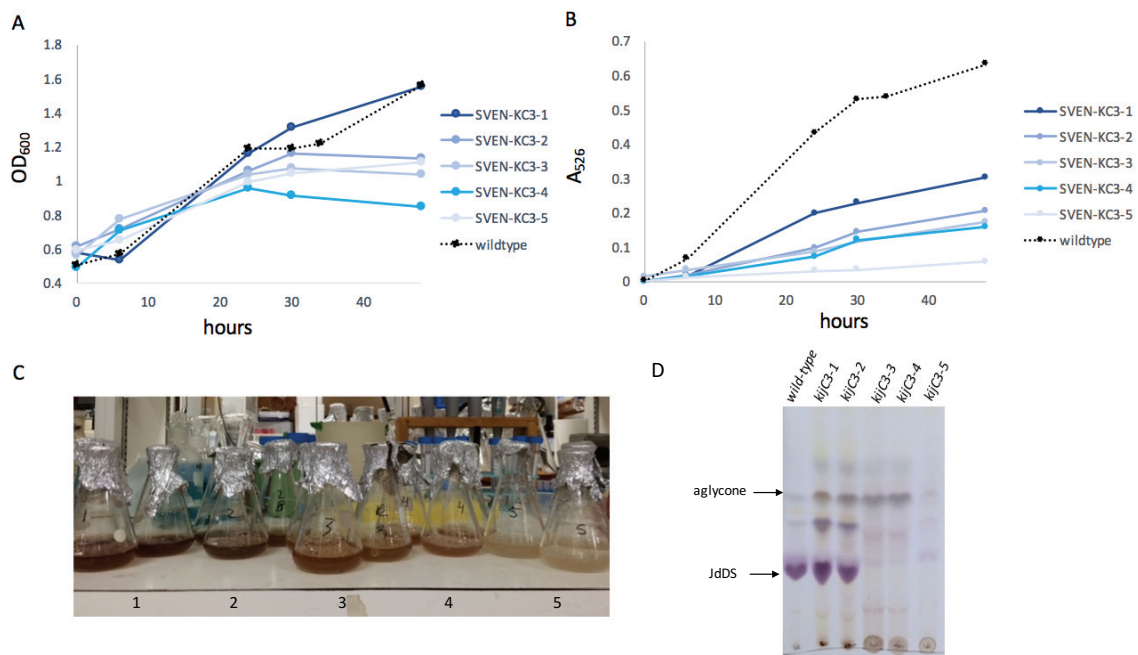


Figure 71. *S. venezuelae::kijC3* cultured with D-serine. (A) OD₆₀₀ growth curves; (B) A₅₂₆ measurements; (C) Cultures after 48 h of growth for *S. venezuelae* (1) *kijC3-1* (2) *kijC3-2*, (3) *kijC3-3*, (4) *kijC3-4*, (5) *kijC3-5*, (6) *kijC3-6*; (D) TLC of the methanol extracts for each strain developed with 5:5:1 ethyl acetate: acetone: water.

Two strains, *S. venezuelae::kijC3-2* and *kijC3-4*, each representative of the distinct natural product profiles observed in D-serine cultures, were cultured in the presence of other amino acids, *N* ϵ -trifluoroacetyl-L-lysine (TFAL) and 4-aminobutanoic acid (ABA) that have previously been for precursor directed biosynthesis of jadomycins.^{172, 192} The bacteria showed growth in the presence of both amino acids, although absorbance at A₅₂₆ was consistently depressed in comparison to the wild-type (Figure 72AB and Figure 73AB). For productions with TFAL, TLC analysis did not show any non-polar jadomycin products in extracts

from both strains (Figure 72C), and analysis of the methanol extracts by HPLC showed a prominent signal corresponding to chloramphenicol (Figure 72D). For productions with ABA, TLC analysis with strain *kijC3-2* showed production of the wild-type product jadomycin (**JdABA**), along with several interesting new polar spots (Figure 73CD). In the corresponding HPLC trace, a new, prominent peak at R_T 7.2 min was observed, in addition to the expected signal for **JdABA** at R_T 7.5 min (Figure 73E). In the HPLC trace of extract from strain *kijC3-4*, the most prominent peak (R_T 8 min) was tentatively assigned to the aglycone of **JdABA**, which would be consistent with the TLC profile.

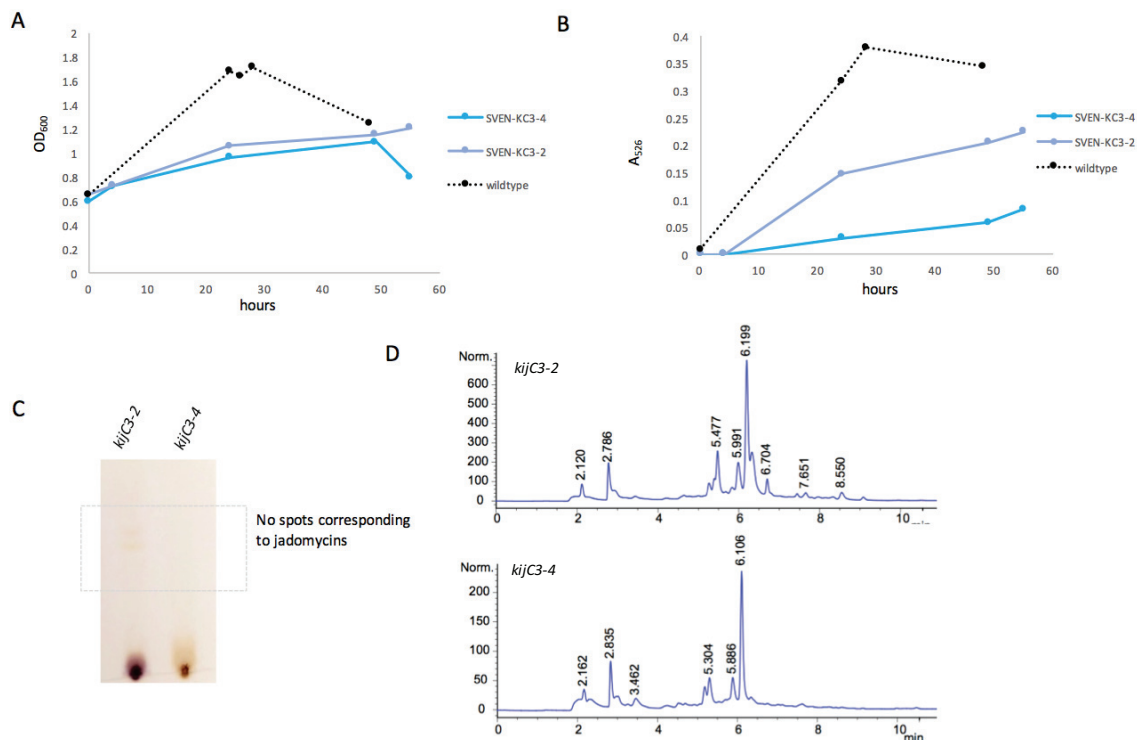


Figure 72. *S. venezuelae::kijC3-2*, *S. venezuelae::kijC3-4*, and wild-type cultures with TFAL. (A) OD₆₀₀ growth curves; (B) A₅₂₆ measurements; (C) TLC of the natural product extracts for each strain developed with 5:5:1 ethyl acetate: acetone: water; (D) HPLC traces of the methanol extracts showing chloramphenicol (Cam, R_T 6.1 min) as the major natural product. *Data used to plot wild-type curves taken from previous work.¹⁷²

Methanol extracts from the ABA cultures were evaluated using LCMS and a positive precursor scan of m/z 306. Unfortunately, in all cases, the masses $[M + H]^+$ of di-glycosylated jadomycin TFAL and ABA congeners were not found. Of interest was the identification by mass of open-ring analogues including C-C branched analogues (Figure 74), which are reminiscent of jadomycin congeners recently described by the Jakeman group. In that study, it was demonstrated that amino acids

that prohibit E-ring formation give rise to congeners with various addition products to the 3a position, including reversible solvolysis products and irreversible C-C bonded acetate and pyruvate products, likely arising from the encounter of the reactive intermediate with nucleophiles involved in primary metabolism.¹⁷⁶ The discovery of these analogues provides evidence of a general trend in which systems with an impeded ability to cyclize, or with unstable E-ring systems, can generate such C-C branched analogues.

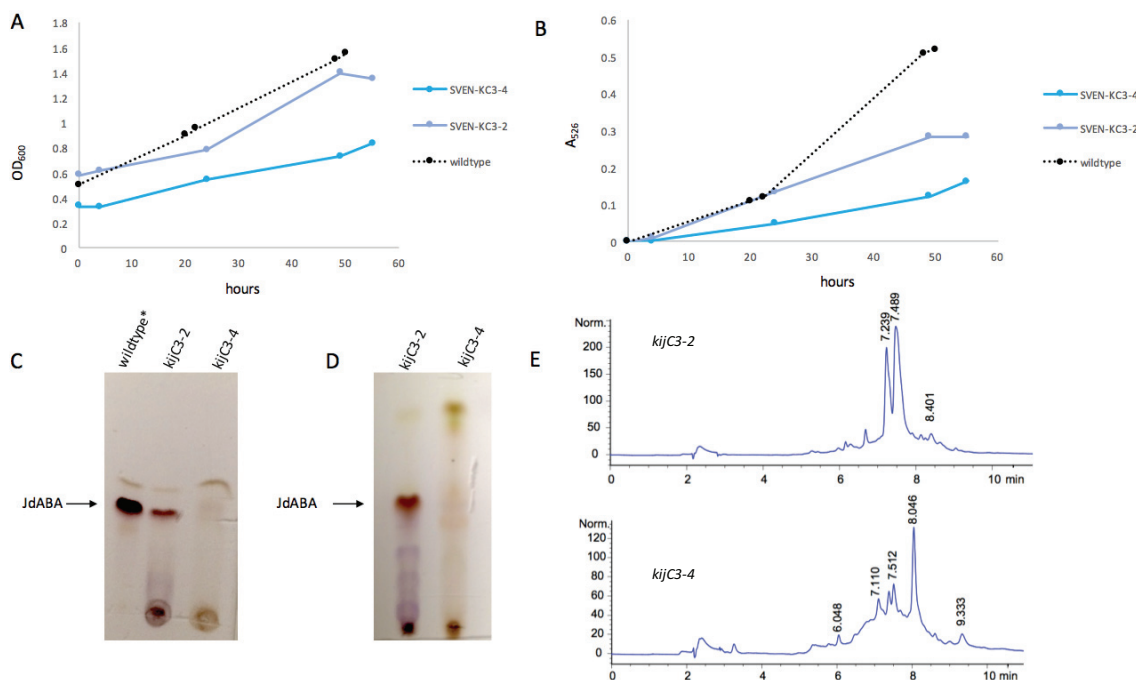


Figure 73. *S. venezuelae::kijC3-2*, *S. venezuelae::kijC3-4*, and wild-type cultures with ABA. (A) OD₆₀₀ growth curves; (B) A₂₆₆ measurements; (C) TLC of the methanol natural product extracts for each strain developed with 5:95 methanol: dichloromethane; (D) TLC of the methanol natural product extracts for each strain developed with 5:5:1 ethyl acetate: acetone: water (E) HPLC traces of the extracted natural products, showing **JdABA** as the major product in *S. venezuelae::kijC3-2* (R_T 7.5 min) and the corresponding aglycone in *S. venezuelae::kijC3-4* (R_T 8.0 min). *Data used to plot wild-type and the purified **JdABA** used to spot the TLC plates were taken from previous work.¹⁹²

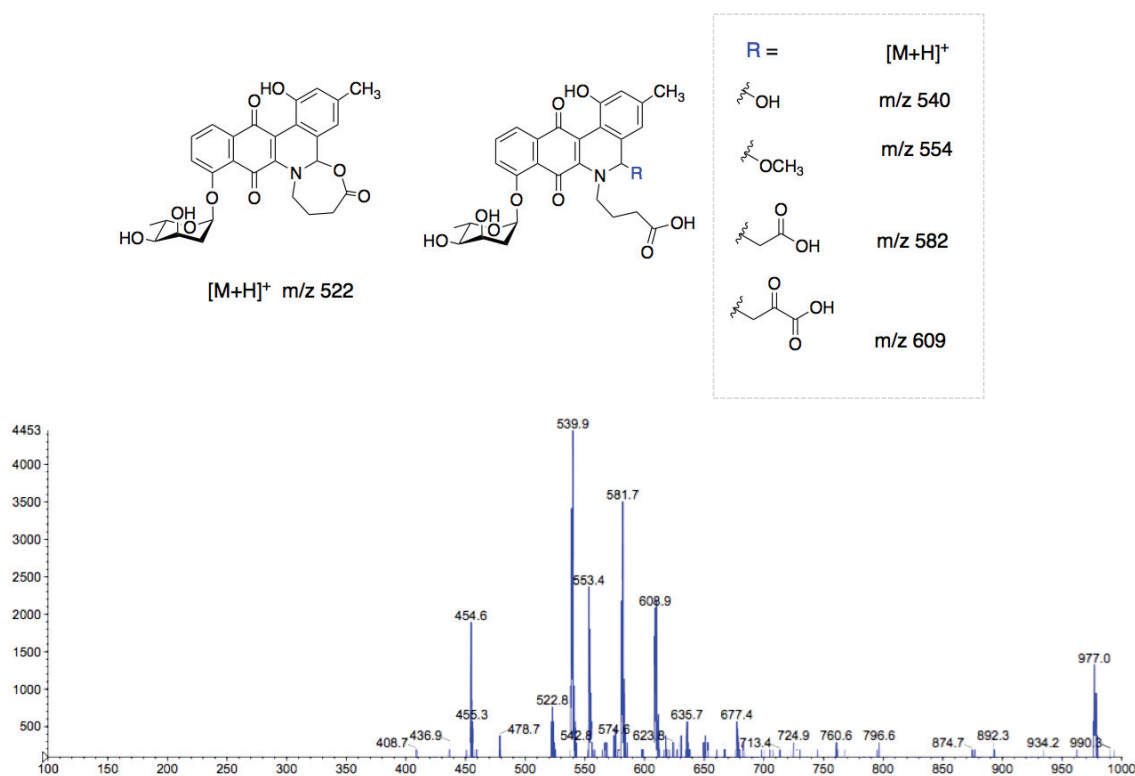


Figure 74. LCMS precursor 306 (positive) scan of the methanol extract from an *S. venezuelae::kijC3-2* culture with ABA and proposed structures corresponding to the observed m/z signals.

3.3.4.2. Evaluation of *kijC4* Knock-In Strains and *jadV* Deletion Strain: *S. venezuelae::kijC4*, *S. venezuelae::kijC4(XhoI)*, *S. venezuelae::kijC4kijC3*, and *S. venezuelae Δ jadV*

Strains complemented with *kijC4* were initially cultured with D-serine using the same methods. Three constructs with *kijC4* were evaluated: *S. venezuelae::kijC4*, *S. venezuelae::kijC4(XhoI)* and *S. venezuelae::kijC4kijC3*. The strain *S. venezuelae::kijC4(XhoI)* introduced a frame-shift that returns *jadV* to its usual transcription frame relative to the other genes as found in the wild-type cluster, and *S. venezuelae::kijC4kijC3* contained both *kijC4* and *kijC3*. Due to concerns

regarding the potential for polar effects, a strain with deletion of *jadV*, *S. venezuelae* Δ *jadV* was also evaluated. The *kijC4* knock-in mutants grew at a rate and to a final density comparable to the wild-type, reaching a fairly disperse range of A_{526} values (Figure 75AB). The Δ *jadV* strain also grew well and developed a similar deep colour to the other strains (Figure 75C). TLC analysis of the methanol extracts illustrated that these strains were not able to produce **JdDS**, although a new less polar spot was evident (Figure 75D). Rather discouragingly, the same new spot was also present in extracts from the Δ *jadV* strain. This suggested to us that a jadomycin with a modified sugar arising from disruption of the gene encoding the 4-ketoreductase, *jadV*, was being produced. An LCMS precursor-scan of the phenanthroviridine fragment m/z 306 identified a signal, m/z 522, corresponding to jadomycin bearing a sugar with a non-reduced 4-keto group. The strain *kijC4-3* was cultured with L-isoleucine and L-phenylalanine (Figure 76) and evaluation of the extracts was performed by LCMS in a precursor 306 experiments (positive). In the precursor scans from cultures with L-phenylalanine, the wild-type strain extract contained jadomycin-L-phenylalanine (**JdF**) with m/z 584 ($[M + H]^+$) as expected, while the *kijC4-3* strain extract contained the aglycone with m/z 454 and a second signal with m/z 582 as the most prominent peaks. Correspondingly, in the analysis from cultures with L-isoleucine, the wild-type strain extract contained jadomycin-L-isoleucine (**JdB**) with m/z 550 ($[M + H]^+$) as expected, while the *kijC4-3* strain extract contained the aglycone m/z 420 and m/z 548 as the most prominent peaks. The detection of products containing two mass units less than the usual jadomycin is consistent with the presence of an oxidized sugar, 2,6-dideoxy-D-*threo*-4-hexulose,

being produced by the *kijC4* mutant strain, and provides strong evidence for disruption of *jadV*. A trial NaBD₄ reduction was performed on a portion of the material isolated from *S. venezuelae* Δ *jadV* (D-serine production). Analysis showed the emergence of a new peak, *m/z* 525, by LCMS, providing additional evidence of a reducible keto group on the sugar (Figure 77). A recent study has shown that the L-digitoxyltransferase JadS is able to transfer a 4-keto sugar to the aglycone of jadomcyin B.¹⁸¹

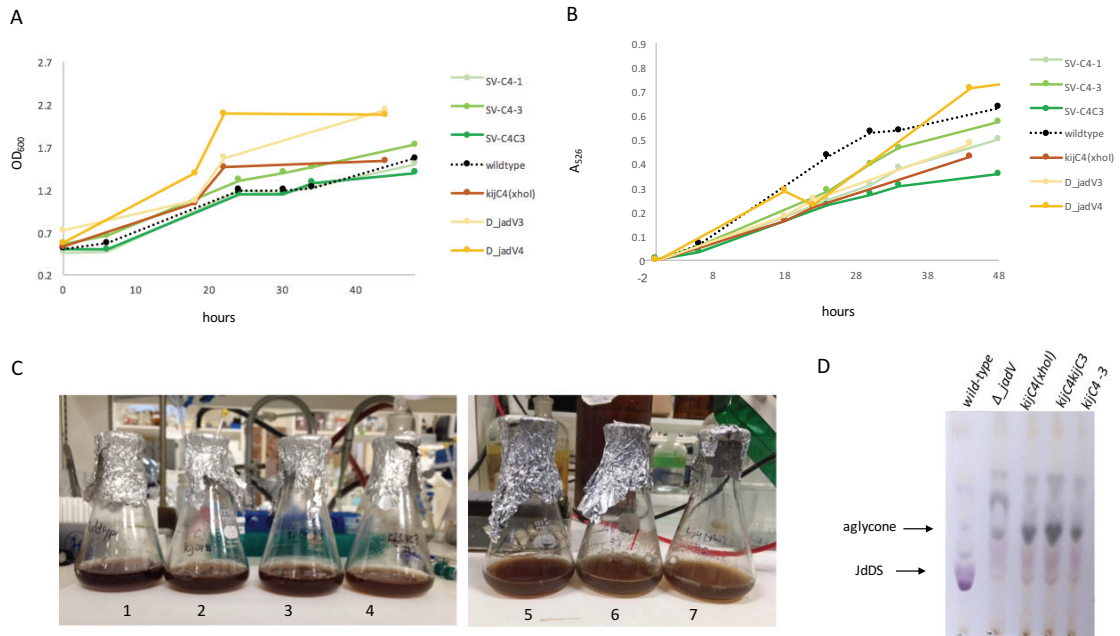


Figure 75. *S. venezuelae::kijC4-1*, *S. venezuelae::kijC4-2*, *S. venezuelae::kijC4kijC3*, wild-type *S. venezuelae::kijC4(XhoI)*, *S. venezuelae ΔjadV-1*, *S. venezuelae ΔjadV-2*, and wild-type cultures with D-serine. (A) OD₆₀₀ growth curves; (B) A₅₂₆ measurements; (C) Cultures after 48 h of growth for *S. venezuelae* (1) wild-type (2) *kijC4-1* (3) *kijC4-2*, (4) *kijC4kijC3*, (5) *ΔjadV-1*, (6) *ΔjadV-2*, (7) *kijC4(XhoI)*. (D) TLC of the methanol natural product extracts for each strain developed with 5:5:1 ethyl acetate: acetone: water.

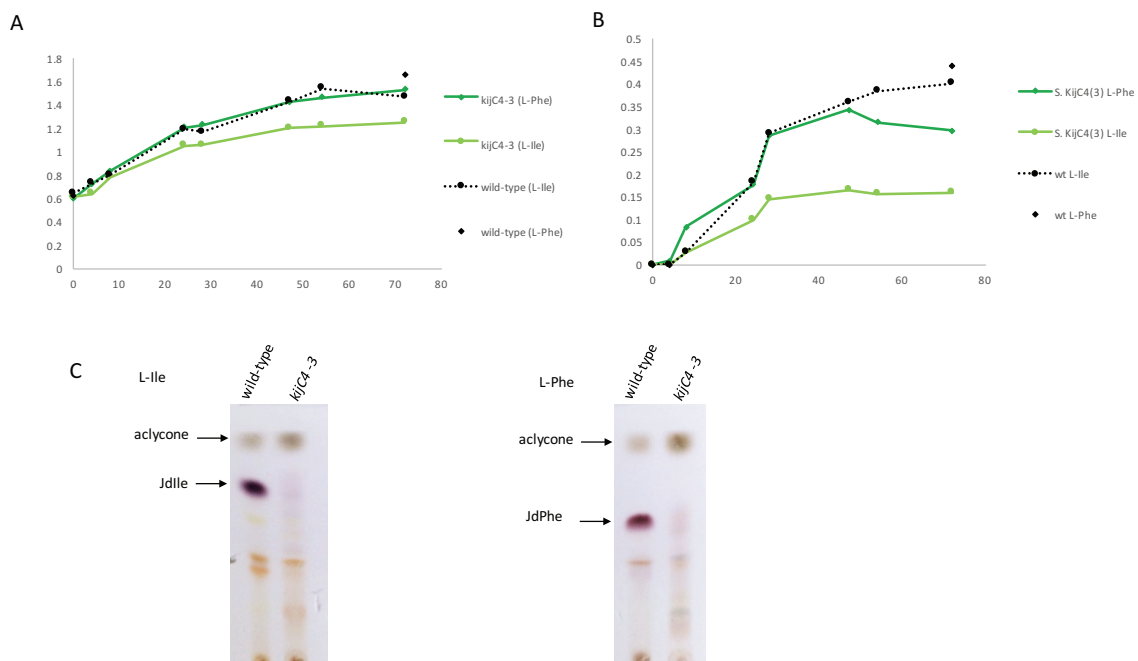


Figure 76. *S. venezuelae::kijC4-2* cultured with L-Ile and L-Phe. (A) OD₆₀₀ growth curves; (B) A₅₂₆ measurements; (C) TLC of the methanol natural product extracts developed with 2:8 methanol: dichloromethane, plate removed from solvent when solvent point reached half the distance of the silica plate, allowed to dry, followed by 5:95 methanol: dichloromethane.

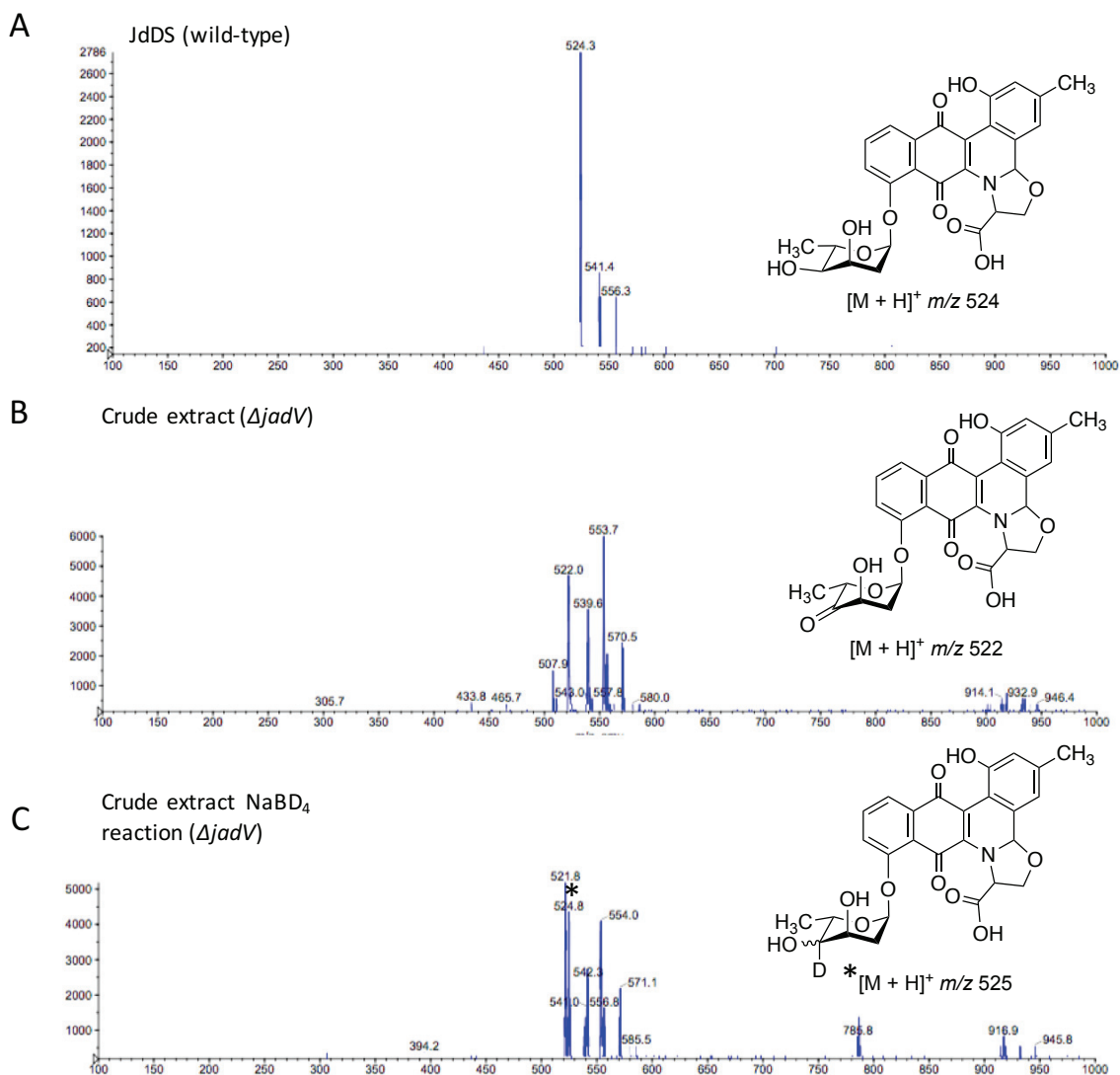


Figure 77. LCMS precursor scans with parent ion m/z 306 (positive) of (A) **JdDS** from wild-type strain; (B) methanol extract from $\Delta jadV$ strain, (C) reaction mixture of extract from $\Delta jadV$ strain with NaBD₄.

These results prompted a careful re-evaluation of the original plasmid used for complementation, to assess whether any error in design may have resulted in disruption of *jadV*. A potential source of such a disruption was found; the start codon of *jadV* was demarked differently in old, NCBI: AY026363.3, and new,

NCBI: NC_018750.1 (fully sequenced genome), annotations of the gene cluster. In the new annotation, the start codon overlaps with *jadU*, while in old annotation there is a gap between the stop codon of *jadU* and start of *jadV*. This had significant implications, as our construct was based on the older version, and was intended to insert the gene after *jadU*, but in “front” of *jadV*. The new annotation implied that we had removed the *jadV* start codon, very likely producing the observed polar effects. The old and new protein translation sequences of *jadV* were compared to 4-keto-reductase sequences from the literature, including a 4-keto-reductase that had been characterized *in vitro* (RubN6).²⁴⁴ It was found that the new annotation was a better match compared to known sequences (Figure 78). Future work may involve correcting this error through mutagenesis of the conjugal vectors, to observe whether it is possible to restore JadV function.



Figure 78. N-terminal protein sequence alignments of old and new JadV protein sequences against other 4-ketoreductases. Alignment performed using Clustal Omega.

3.4.4.3. Attempted Isolation and Characterization of the Jadomycin Produced by *S. venezuelae* Δ *jadV*

S. venezuelae::*kijC4* and *S. venezuelae* Δ *jadV* were each cultured at a 1-L scale with D-serine to obtain sufficient material to characterize the new product(s). Given the data collected from the small-scale cultures, we anticipated isolating a jadomycin congener bearing 2,6-dideoxy-D-*erythro*-4-hexulose, the sugar that would result from disruption, or deletion, of *jadV*. Standard culture and work-up procedures were used as detailed in the experimental section. The compound of interest, which appeared as a smear on the TLC plate, was challenging to purify using silica chromatography. The observed smearing may be the result of a mixture of 5-epimers, and the intermediate tautomer, arising from incomplete conversion of NDP-2,6-dideoxy-D-*threo*-4-hexulose to NDP-2,6-dideoxy-D-*erythro*-4-hexulose by JadU in the absence of JadV as a driving force for the forward reaction (Figure 79). The 3,5-epimerase, RmlC, involved in Rha biosynthesis, favours the substrates in the absence of the 4-ketoreductase, RmlD.¹⁰⁰

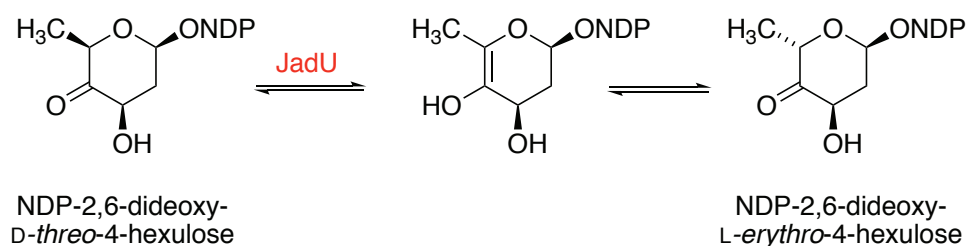


Figure 79. Possible sugar nucleotides produced as a result of *jadV* deletion.

The NMR spectra were insufficiently clean for characterization of the isolated compounds, and were challenging to interpret thoroughly due to signal overlap. A comparison of the ¹H NMR spectra revealed that the products isolated

from mutant strains, both $\Delta jadV$ and $kijC4$, were clearly different from the wild-type, as the proton signals associated with H-3 and H-5 of the L-digitoxose of **JdDS** were not present in the NMR spectra corresponding to the mutant strains (Figure 80). The similarities in the ^1H NMR spectra make it evident that the same products are found in the isolated material from both *S. venezuelae* $\Delta jadV$ and $kijC4$. By LC-MS² a mass of m/z 522 was identified in the extract from both mutant strains from a precursor scan (m/z 306, positive mode), consistent with the proposed structure.

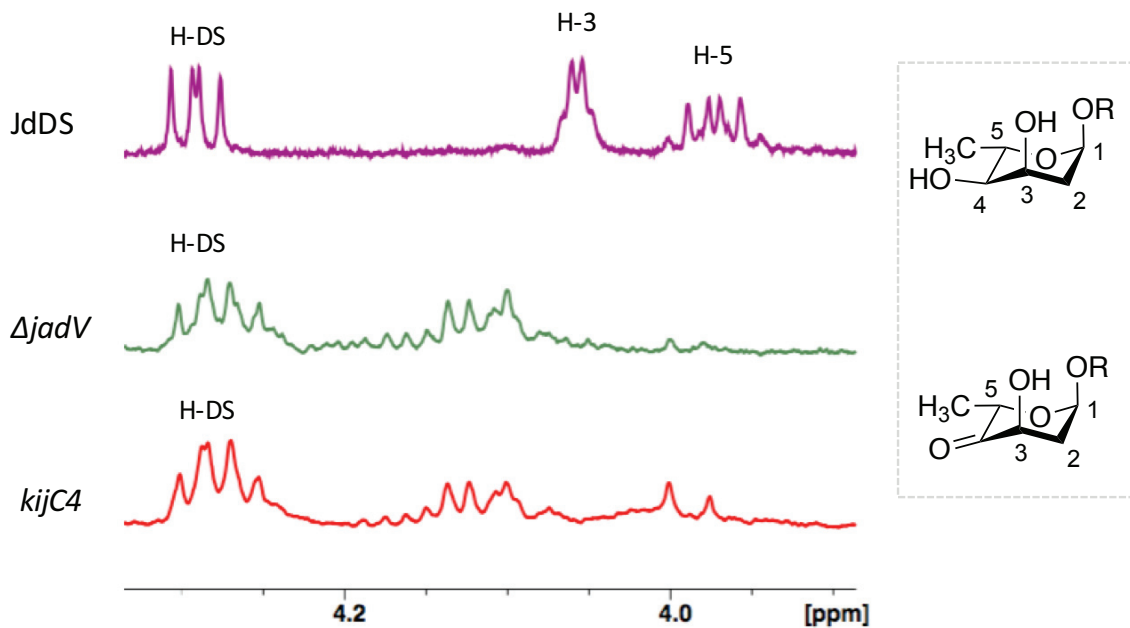


Figure 80. Expansion of ^1H NMR spectra (500 MHz, methanol- d_4) of **JdDS** from the wild-type strain (top, purple), of the purified material from *S. venezuelae* $\Delta jadV$ (middle, green) and of the purified material from the *S. venezuelae*:: $kijC4$ strain (bottom, red). L-digitoxose (top) and 2,6-dideoxy-D-erythro-4-hexulose (bottom) are shown in the panel. H-DS indicates a proton arising from the E-ring incorporated D-serine.

3.4.5. Conclusions and Future Work

Three methods to enable gene complementation were discussed. So far, our attempts to introduce *kijC3* and/or *kijC4* into the dideoxy gene cluster by homologous recombination (method 1) have caused polar effects, resulting in the disruption of *jadV*. Thus, in the absence of a functional 4-ketoreductase, the glycosylated jadomycins in these strains were found to contain a modified sugar, 2,6-dideoxy-D-*erythro*-4-hexulose. These results provide further evidence for the flexibility of JadS with respect to sugar donors.^{59, 60, 181} We identified that disruption of *jadV* may have arisen from deletion of the start codon. A list of future projects to elaborate this study include:

- Complete assembly of pSET152::*kijC4* (method 2) and conjugation to *S. venezuelae* for complementation, a approach that bypasses the possibility of polar effects.
- The reintroduction of the *jadV* start codon into the conjugal vector, pKC1139::*kijC4* or pKC1139::*kijC4kijC3*, by mutagenesis and evaluation of the corresponding mutant strain to observe whether JadV function was restored.
- Measurement of mRNA levels by quantitative PCR (qPCR) to confirm transcription of dideoxy sugar genes and of the complemented gene, as a surrogate marker for protein production.
- Isolation of the observed unknown products from jadomycin productions with ABA, which are anticipated to be C-linked acetate derivatives similar to those recently described.^{176, 245}

Chapter 4: Experimental

4.1. General Methods

All chemicals and reagents were purchased from commercial sources and were used as received, unless otherwise noted. Lyophilisation of samples was carried out using an Edward Freeze-Dryer. Visualization of pigmented compounds was performed using glass-backed TLC plates (SiliCycle, 250 μ M, F₂₅₄ silica) developed with an eluent system of 5:5:1 ethyl acetate: acetonitrile: water or methanol: dichloromethane, as indicated.

4.1.1. NMR Methods

NMR spectra acquired for studies in Chapter 2, and all ¹⁹F and ³¹P NMR spectra and nOe experiments were acquired at the Nuclear Magnetic Resonance Research Resource (NMR-3, Dalhousie University, Halifax, NS) using a Bruker AV500 MHz spectrometer equipped with an ATMA-BBFO SmartProbe. NMR spectra for jadomycins described in Chapter 3 and all waterLOGSY NMR spectra were recorded at the Canadian National Research Council Institute for Marine Bioscience (NRC-IMB, Halifax, NS) using a Bruker AV-III 700 MHz spectrometer equipped with an ATMA 5 mm or 1.7 mm TCI cryoprobe. ¹H and ¹³C chemical shifts are reported in ppm using, tetramethylsilane (δ 0.00) or the residual solvent signal [chloroform-*d* (¹H 7.26 ppm; ¹³C 77.16 ppm); D₂O (¹H 4.79 ppm); methanol-*d*₄ (¹H 3.31 ppm, ¹³C 49.50 ppm)]²⁴⁶ as the internal reference. ³¹P chemical shifts were calibrated to 85% aq. H₃PO₄ (δ 0.00) as an external reference. An external calibration to CCl₃F (δ 0.00) was used for ¹⁹F NMR spectra. Splitting patterns are

indicated as follows: br, broad; s, singlet; d, doublet; t, triplet; a, apparent; q, quartet; m, multiplet. Obscured (obs) may refer either to overlap of NMR signals from the same molecule, from a second species or from a solvent signal. All coupling constants (J) are reported in Hertz (Hz).

4.1.2. HRMS and LCMS Running Conditions

Low resolution mass spectra were obtained using an Applied Biosystems hybrid triple quadrupole linear ion trap (*Qtrap 2000*) mass spectrometer equipped with an electrospray ionization (ESI) source. Negative mode detection was used for sugar nucleotides. The capillary voltage was set to -4500 kV with a declustering potential of -60 V and the curtain gas was set to 10 (arbitrary units). Positive mode detection was generally used for natural product samples. For positive mode detection, the following settings were applied: capillary voltage $+4500$ kV, declustering potential $+80$ V, curtain gas 10 (arbitrary units). Enhanced product ionization (EPI) was performed with scans that were conducted over a range of 200-1000 m/z scanning for $[M+H]^+$ and the appropriate fragmentation. The mass spectrometer was coupled to an Agilent 1100 HPLC instrument fitted with a Phenomenex Kinetex 2.6 μ (150×2.10 mm) that was run using an isocratic method with 70:30 CH_3CN : 2 mM aqueous ammonium acetate (pH 5.5) at a flow rate of $120 \mu L \text{min}^{-1}$. Samples were prepared in methanol and 5 μL aliquots were injected onto the column. High resolution mass spectra were recorded using ion trap (ESI time-of-flight, TOF) instruments or recorded on an API Qstar XL pulsar hybrid LC/MS/MS (System Applied Biosystem/MDS Sciex).

4.1.3. UV Spectroscopy Methods

Ultraviolet-visible (UV-vis) spectroscopy measurements were carried out using a SpectraMax Plus Microplate Reader (Molecular Devices). Samples (500 μ L) were placed in a quartz cuvette (1 cm path length) and scanned at the indicated wavelength or over a range of 280-700 nm using 5 nm intervals in order to determine maximal absorbance wavelengths (λ_{max}). Jadomycin culture aliquots were withdrawn at indicated time points and recorded at λ 600 nm for the resuspended culture media, and at λ 526 nm for clarified aliquots (cell pelleted at 10000 rpm, 5-10 min). Kinetic reactions were performed in 96-well plates and were monitored using a SPECTRAmax Plus³⁸⁴ Microplate Reader spectrophotometer with SoftMax Pro version 4.8.

4.1.4. Analytical HPLC Method

A Hewlett Packard Series 1050 instrument was equipped with an Agilent Zorbax 5 μ M Rx-C18 column (150 \times 4.6 mm) with monitoring at λ 254 nm. A linear gradient from 90/10 A/B to 40/60 A/B over 8.0 min followed by a plateau at 40/60 A/B over 2.0 min at 1.0 mL/min⁻¹ was used, where A is an aqueous buffer containing 12 mM Bu₄NBr, 10 mM KH₂PO₄ and 5% HPLC grade CH₃CN and B is HPLC grade CH₃CN.

4.1.5. Normal Phase Chromatography

All normal phase column chromatography was performed using an SPI 1TM unit (Biotage), using pre-packed columns (SiliCycle, 12 g or 40 g) with wavelength monitoring at λ 254 nm. HPLC solvents were used with eluent systems as indicated.

4.1.6. Ion Pair Reversed-Phase Chromatography

This procedure was followed for the isolation of sugar nucleotides **2.8**, **2.9**, **2.11**, **2.15**, and dTDP-1C-Rha, with minor alterations to the gradient for **2.8** (Section 4.2.1) and **2.9** (Section 4.2.2). The following gradient on an SPI 1TM unit (Biotage) equipped with a C-18 pre-packed column (SiliCycle, 12 g or 24 g), was run using buffer A (10 mM tributylammonium (TBA) bicarbonate, pH ~5.5, prepared from bubbling CO₂ through a solution of tributylamine in water) and B (methanol), column volume (CV) of 24 mL, and a flow rate 15 mLmin⁻¹: 2 CV 0% B, 15 CV 0-40% B, 2 CV 40% B, 3 CV 100% B with wavelength monitoring at λ 254 nm. Sugar nucleotides (non-amine) eluted at ~30% B.

4.1.7. Preparatory HPLC Method

Preparatory scale HPLC was performed using a C-18 reversed phased column (Ultrasphere ODS, 5 μ m particle size, 10 mm \times 25 cm) with degassed methanol (A) and water (B) using the following method: a linear gradient from 5:95 A:B to 95:5 A:B over 30 min, followed by a hold at 95:5 A:B for 30 min at 5 mL min⁻¹ with wavelength monitoring at λ 254 nm.

4.1.8. SDS-PAGE Gel Running Conditions

SDS-PAGE gels were run using a Mini-Protean Tetra Cell (Bio Rad) apparatus using a Laemmli discontinuous buffer system. Gels were set in a 0.5 mm cast. A resolving gel (1.24 mL water, 1.35 mL resolving buffer (1.5 M Tris·HCl, pH 8.8), 2.75 mL 30% acrylamide solution (30% acrylamide, 2.67% *N*'*N*'-bis-methylene acrylamide), 27.5 μ L 10% SDS solutions, 110 μ L 10% ammonium persulfate (APS), 6 μ L tetramethylenediamine (TEMED)) was poured into the cast and allowed to set

for 30 min. A stacking gel (1.17 mL H₂O, 0.5 mL stacking buffer (0.5 M Tris·HCl pH 6.8), 0.33 mL 30% acrylamide solution, 10 µL 10% SDS, 60 µL 10% APS solution, 6 µL TEMED) was poured, then a sample comb was rapidly inserted into the template to create the loading wells. The gel was allowed to sit for at least 30 min prior to use and could be stored wrapped in plastic film up to one week at 4 °C. Protein samples were prepared by diluting 10 µL sample with 20 µL sample buffer (3.55 mL water, 1.25 mL 0.5 M Tris·HCl (pH 6.8), 2.5 mL glycerol, 2.0 mL 10% SDS, 200 µL 0.5% bromophenol blue 50 µL β-mercaptoethanol was added to 950 µL sample buffer prior to use), and heated at 95 °C for 5 min. Gels were run with electrode running buffer at 140 V for approximately 1 h. Gel staining was accomplished using commercial stain (EZBlue™ gel staining reagent, Sigma), following manufacturer protocols.

4.1.9. Bioinformatics Methods

BLASTP (protein-protein) analysis (<https://blast.ncbi.nlm.nih.gov>) was performed with the database “non-redundant protein sequence” and excluded models and uncultured samples. GT1 family glycosyltransferases were identified from the CAZy database (<http://www.cazy.org>). Sequence alignments and percent identities were determined by pairwise alignment (Emboss Needle global alignment tool, http://www.ebi.ac.uk/Tools/psa/emboss_needle/) or for multiple sequences by ClustalOmega (1.2.1, <https://www.ebi.ac.uk/Tools/msa/clustalo/>). ApE (A plasmid Editor, V 2.0.52a) software used for DNA sequence analysis.

4.1.10. General Bacterial Maintenance

E. coli cultures were grown overnight at 37 °C, 250 rpm in LB media with antibiotics as required, and stored as solutions supplemented with 25% glycerol at -70 °C. *Streptomyces venezuelae* and *Actinomadura kijaniata* strains were grown on malt yeast maltose (MYM) agar plates at 30 °C. A 1 × 1 cm² lawn was scraped from the plates to inoculate 250 mL liquid (MYM) cultures. Liquid cultures were grown at 30 °C and 250 rpm. *A. kijaniata* glycerol stocks were prepared from the addition glycerol (to 25%) to liquid cultures grown for several days until the liquid broth was cloudy, and stored in 1 mL aliquots at -70 °C. *S. venezuelae* spores were harvested from plates grown for 3-15 days, with a thick white to green coloured plaque indicative of sporulation. Sterile glass beads were used to loosen the bacterial plaque, followed by suspension of the bacterial fragments in sterile water (9 mL). The water suspension was collected in a falcon tube, vortexed for 30-60 seconds, and filtered through cotton wool. Inspection under the microscope confirmed the absence of mycelial fragments and presence of spores. This spore solution was pelleted at 4 °C, 5000 g, for 10 min and the supernatant decanted. The spore pellet was re-suspended in 4-10 mL 25% glycerol and stored at -70 °C in 1 mL aliquots. This same procedure was scaled down ten-fold to prepare spore stocks from single colonies when screening *S. venezuelae* mutant strains.

4.1.11. Methods for Primer and DNA Handling

DNA samples, including genomic DNA and plasmid isolates, were kept at -20 °C for long-term storage. All primers were purchased from Integrated DNA Technologies. All buffers and solution preparations used in molecular biology

procedures were prepared as described in Section 4.1.23. Those not listed were provided with the commercial kits described in the corresponding procedure.

4.1.12. Genomic DNA Extraction Protocols

Overnight (for *S. venezuelae*) and 4-5 day (for *A. kijaniata*) liquid cultures in MYM were used to collect bacteria for genomic DNA extractions using the Bio Basic EZ-10 spin column genetic kit for bacterial samples (catalogue B5624) following manufacturer guidelines. An aliquot (1.5 mL) from a cloudy culture was pelleted at 12000 rpm for 5 min, and the supernatant removed. The cell pellet was re-suspended in 200 μ L TE buffer. To this cell suspension was added 400 μ L of the Digestion solution and 3 μ L Proteinase K solution. The sample was heated at 55 $^{\circ}$ C for 1 h. Ethanol (260 μ L) was added, and the solution mixed well and applied to an EZ-10 spin column. The column was spun for 2 min (or longer as needed) at 10000 rpm. The column flow-through was discarded and 500 μ L of Wash solution was applied to the column, the column was spun once again, and the flow through decanted. The wash step was repeated. After decanting the wash solution, the column was spun for an additional minute to remove residual wash solution. To the dried column, 50 μ L of Elution buffer was applied and incubated for 2-3 min at 37 $^{\circ}$ C. The column was transferred to a clean 1.5 mL Eppendorf tube and then centrifuged to collect the genomic DNA extracted from the column.

4.1.13. PCR and Colony PCR methods

For use in PCR reactions, 10 μ M working solutions of primers in sterile water were prepared. A 10 mM dNTP stock solution in sterile water was prepared from biotech

grade dNTP stock solutions (100 mM, Bio Basic). The indicated manufacturers supplied other reagents. PCR reactions were performed using a BIOMETRA Tpersonal thermocycler with the program in the table below. PCR reactions contained 10 μ L NEB Q5 buffer (5 \times), 10 μ L NEB Q5 GC enhancer (5 \times), 1 μ L dNTP (10 mM), 5 μ L forward primer (10 μ M), 5 μ L reverse primer (10 μ M), 2 μ L template DNA, 0.5 μ L Q5 DNA polymerase, and 16.5 μ L sterile water. Colony PCR screening was carried out with Phusion DNA (NEB) polymerase with the following reaction composition: 10 μ L Phusion GC buffer (5 \times), 5 μ L DMSO, 1 μ L dNTP (1 mM), 5 μ L forward primer (10 μ M), 5 μ L reverse primer (10 μ M), 0.5 μ L Phusion DNA polymerase, and 23.5 μ L sterile water. For challenging templates, the polymerase was added to the other reaction components when the thermocycler reached 98 $^{\circ}$ C. PCR reactions without inclusion of GC enhancer or DMSO were typically unsuccessful. PCR products were visualized by running on a TAE-agarose gel (Section 4.1.16). For colony PCR, the colony of interest was scraped with a toothpick and dipped in a solution of 50 μ L DMSO in a microtube, then vortexed briefly, heated at 95 $^{\circ}$ C for 10 min, then briefly centrifuged to settle the cell debris. This DMSO, with extracted genomic DNA, was used directly as the DMSO component in the reaction for colony PCR applications.

PCR cycling program:

Step	Temp (°C)	Time (s)	Cycles
0	95	600	1
1	98	30	15 (steps 1-3)
2	82.6 - 0.5 per cycle	30	
3	72	30/ kb	
4	98	30	20 (steps 4-6)
5	55	30	
6	72	30/kb	
7	4	hold	1

4.1.14. Restriction Digestion Protocols

Restriction digestion of plasmids and PCR products for screening purposes and for ligation reactions followed the manufacturer suggestions (NEB Biolabs) for buffer selection and incubation times. A general restriction digest contained 7 μ L DNA, 1 μ L restriction enzyme A, 1 μ L restriction enzyme B, 1 μ L commercial buffer, with incubation at 37 °C for 1 h. As required, incubation times were extended and/or the concentration of restriction enzyme(s) increased.

4.1.15. Ligation Protocols

Prior to ligation reactions, linearized plasmids were treated with CIP (NEB Biolabs) by adding 1 μ L (10 EU) to heat-inactivated digest reactions, and incubated for 1 h at 37°C. Linearized and CIP-treated vectors were purified using a gel extraction kit (QIAquick® gel extraction kit, Qiagen). Digested PCR products were either purified using a PCR clean up kit (QIAquick® PCR purification kit, Qiagen) or using a gel

extraction kit (as above), following manufacturer protocols exactly. Prior to ligation, DNA concentrations of inserts and vectors were determined using densitometry. DNA samples were run alongside three dilutions of a standardized DNA ladder (NEB 1kb DNA ladder), and the intensity of the bands closest in size to the DNA band of interest was used to generate a standard curve using DocITLS 5.5.5 (UVP Inc). Ligation reactions were carried out using various ligand: vector ratios, usually between 2:1 and 7:1 depending on the concentrations of the vector and insert DNA. Reaction set up with T4 ligase followed manufacturer protocols (NEB Biolabs) and reactions were left either for two hours at room temperature or overnight at 16 °C. A typical ligation reaction contained 1 µL T4 ligase, 1 µL T4 ligase buffer, x µL linearized vector, and 8-x µL insert. Aliquots (2-5 µL) of ligation mixtures were directly used to transform NEB[®] 5-alpha or NEB[®] 10-beta competent *E. coli* (high efficiency, Section 4.1.17).

4.1.16. Agarose Gel Running Conditions and Visualization

Agarose (300 mg) was dissolved in 30 mL TAE-buffer in a microwave. The dissolved agarose was then poured into a cast and allowed to set for 30 min. DNA samples were prepared by the addition of 2 µL loading dye (6 ×) to 10 µL of the sample. Samples were run alongside 3 µL of a 1-kb reference ladder (NEB 1kb DNA ladder). The running buffer (TAE) contained 30 µL of 1 mg/mL ethidium bromide and gels were run with an applied current of 120 V. Developed gels were visualised under a UV light (λ 302 nm) and images captured using an Olympus C-4000 Zoom camera and DOC ITLS 5.5.5 software (UVP, Inc). Adobe Photoshop

Elements 2.0 used for manipulation of images such as colour inversion and contrast adjustments.

4.1.17. Transformation of NEB® 5-alpha and NEB® 10-beta Competent *E. coli*

Plasmid transformation to NEB® 5-alpha and 10-beta competent *E. coli* (high efficiency) followed manufacturer protocols exactly. A tube containing 50 µL aliquot of competent cells was thawed on crushed ice for about 10 min. To the thawed competent cells 2-5 µL of the incoming plasmid or ligation mixture was added, and the contents gently mixed. The solution was kept on ice for 30 min, then heat shocked by placing the tube in a hot water bath at 42 °C for 30 seconds, and returned to the ice bath. After 5 min on ice, 950 µL SOC (supplied by NEB) media was added to the cell mixture and incubated 1 h at 37 °C with shaking. The solution was spread onto LB selection plates and the plates incubated overnight at 37 °C.

4.1.18. Miniprep Plasmid Isolation from *E. coli*

Isolation of plasmids was accomplished using EZ-10 spin column plasmid DNA miniprep kit (Bio Basic, catalogue B5614). A single *E. coli* colony was grown overnight in 25 mL LB with the appropriate selective antibiotic(s). An aliquot (1-2 mL) was spun down at 12000 rpm, and the supernatant decanted. To the cell pellet was added 200 µL Solution I. Following a one minute incubation, 200 µL Solution II was added and the tube gently inverted to mix, and incubated another minute. Solution III (350 µL) was added and the solution was mixed gently and thoroughly, and then incubated once again for one minute. The suspension was centrifuged for 5-10 min at 12000 rpm. The supernatant was then transferred to an EZ-10 spin

column, and centrifuged for 2 min at 10,000 rpm. The column was then washed twice with 750 μ L Wash buffer, discarding the flow through after each step. After the second wash, the column was spun down once again for an additional minute to remove residual wash buffer. Elution buffer (50 μ L) was then added to the column and incubated for 2 min at 37 °C. The column flow through was then collected in a clean 1.5 mL Eppendorf tube and stored at -20 °C.

4.1.19. Protocol for Competent *E. coli*

This procedure was used to prepare competent cells for the following strains in the presence of the indicated antibiotics; *E. coli* BL21(DE3) (no antibiotics), *E. coli* BL21(DE3) pLysS (Cam 25 μ g/mL), and *E. coli* ET12567 pUZ8002 (Cam 25 μ g/mL and Kan 50 μ g/mL). *E. coli*, either a single colony from an LB-agar plate or 25 μ L from a glycerol stock, was cultured overnight in 25 ml LB with selective antibiotics (if applicable) at 37 °C, 250 rpm. LB (25 mL with antibiotics) and 20 mM MgCl₂ was inoculated with 1 mL of the overnight culture, and the subculture was grown until an OD₆₀₀ 0.4-0.6 was reached. At this point, the culture was kept on crushed ice for 10 min, and then transferred to a chilled 50 mL falcon tube. The culture was pelleted at 4 °C, 4000 rpm for 10 min and the supernatant discarded. The cell pellet was re-suspended in 10 mL cold 0.1 M CaCl₂, and then incubated on crushed ice for 20 min, then centrifuged as before. After discarding the supernatant, the cell pellet was re-suspended in 5 mL chilled 0.1 M CaCl₂ and 50 μ L aliquots were dispensed into chilled 1.5 mL Eppendorf tubes containing 50 μ L 50% glycerol.

Frozen competent cells were kept at -70 °C until use and were viable for up to eight months.

4.1.20. *E. coli* Transformation Protocol

E. coli competent cells (Section 4.1.19) were transformed with the appropriate plasmid for use in protein expression, conjugation experiments, or protoplast transformations. A 100 µL aliquot of the competent cells was thawed on ice. To the competent cells 2-5 µL of incoming plasmid was added and the tube gently flicked to mix the solution. The cell mixture was kept on ice for 30 min, then heat shocked at 42 °C for 90 s, and returned to the ice bath for 2-3 min. At this point 950 µL room temperature SOC or LB media was added to the competent cell solution, and then incubated with shaking at 37°C for 1 h. 100 µL aliquots of the cultures (10^0 and 10^{-1} dilutions) were plated to selective LB-agar. Plates were kept at 37 °C overnight, then stored in the fridge for up to three weeks.

4.1.21. *E. coli*-*Streptomyces* Conjugation Protocol

This protocol was used to prepare deletion and complementation *S. venezuelae* mutants by homologous recombination, following a literature method with minor alterations.²³³ Conjugal vectors (i.e. pKC1139::*kijC4*) were transformed to methylation deficient *E. coli* ET12567 pUZ8002 according to the procedure in Section 4.2.20. A 250 µL aliquot from an overnight *E. coli* ET12567 pUZ8002 culture with an appropriate shuttle vector was sub-cultured in 25 mL LB with appropriate selective antibiotics (i.e. Cam 25 µg/mL, Kan 50 µg/mL, Apr 50 µg/mL for strains carrying pKC1139::*kijC4*). At the point where the culture reached an

OD₆₀₀ of 0.4-0.6 (~4-7 h), the culture was transferred to a falcon tube and centrifuged (3 min, 5000 rpm). The supernatant was decanted, and the cell pellet re-suspended in 10 mL LB without antibiotics, and pelleted again. This procedure was repeated two additional times, after which the pellet was suspended in 1 mL LB and set aside until needed. Concurrently, the *Streptomyces* spores were prepared. An MYM agar plate of *S. venezuelae* ISP5230 (3 -21 days old) with a white plaque was scraped using sterile glass beads, and the material re-suspended in 2 × 4.5 mL sterile Millipore water. The suspension was filtered through cotton wool, to remove mycelial fragments. The filtered solution was examined under a microscope to confirm the presence of spores, and absence of mycelial fragments. The solution was diluted to an OD₄₅₀ of 0.04-0.06, and one mL of the spore suspension at this concentration was heated at 50 °C for 10 min. The spore suspension was then allowed to cool to room temperature. To 500 µL of the *E. coli* solution described above was added 500 µL of the *Streptomyces* spore suspension. The solution was then centrifuged at 4 °C, 13000 rpm for 3 min, followed by removal of the supernatant. The cell pellet was re-suspended in 100 µL LB, and this stock solution (10⁰) was used to make a 10⁻¹ and 10⁻² dilution series. These solutions (100 µL) were plated on MS-agar with 10 mM MgCl₂. The plates were left to dry for 10-20 min in the sterile hood, then transferred to a 30 °C incubator overnight. After 16 h incubation, 1 mL of a soft nutrient agar overlay containing naladixic acid (Nal) and Apr was applied to each of the plates. When the agar was set, the plates were returned to 30 °C. Exconjugant *Streptomyces* colonies were visible after 3-4 days. Exconjugant colonies (at least 40) were patched to MYM-Nal-Apr agar plates and

grown at 37°C. This step is selective for single crossover mutants, which grew within 3 days. The colonies that grew (~ 20/40) were patched to MYM-Apr plates and grown at 30 °C. After 2 days, the colonies that grew were patched to MYM and grown at 30 °C for two days. All colonies were retained, and patched twice more on MYM plates for two additional rounds of sporulation. After this time, the colonies from the third round of MYM growth were patched to MYM-Apr plates and grown at 30 °C. Colonies showing sensitivity to Apr (a highly variable number of colonies were retained at this step, from a third to three quarters) were likely to have undergone a double crossover recombination event, and as such the colonies corresponding to Apr sensitive colonies from the third round were screened for the insertion. Spore preparations from colonies found to be Apr sensitive were streaked for single colonies. Single colonies were screened by colony PCR or grown in liquid culture (MYM) for genomic extraction for PCR screening (Sections 4.1.12 and 4.1.13). Primers flanking the insert were used to identify knock-in mutants.

4.1.22. List of Plasmids and Strains

Table 12. Strains and plasmids in this thesis.

Strain	Description	Source
NEB [®] 5-alpha competent <i>E. coli</i> 5 (high efficiency)	Commercial cloning strain	New England Biolabs
NEB [®] 10-beta competent <i>E. coli</i> (high efficiency)	Commercial cloning strain	New England Biolabs
<i>E. coli</i> BL21(DE3)	Protein expression strain	New England Biolabs
<i>E. coli</i> BL21(DE3) pLysS	Protein expression strain, pLysS plasmid carries Cam ^R	New England Biolabs
<i>E. coli</i> BL21(DE3) psK001	Cps2L production strain, Kan ^R	80
<i>E. coli</i> BL21(DE3) hPNP	hPNP production strain, Kan ^R	247
<i>E. coli</i> BL21(DE3) RmlB	RmlB production strain, Kan ^R	100
<i>E. coli</i> BL21(DE3) RmlC	RmlC production strain, Kan ^R	100
<i>E. coli</i> BL21(DE3) RmlD	RmlD production strain, Kan ^R	100
<i>E. coli</i> BL21(DE3) pLysS Sv0189	Sv0189 production strain, Kan ^R , Cam ^R	This work
<i>E. coli</i> ET12567 pUZ8002	Produces non methylated DNA (<i>dam</i> ⁻ <i>dcm</i> ⁻ <i>hdsS</i> ⁻); Cam ^R , Kan ^R	240
<i>Streptomyces venezuelae</i> ISP5230 ATCC 10721	Wild-type jadomycin and chloramphenicol producing strain	241
<i>Actinomadura kijaniata</i> SCC1256 ATCC 31588	Wild-type kijanimicin producing strain	American Type Culture Collection (ATCC)
<i>S. venezuelae</i> VS1099	Δ <i>jadW2::aac(3)IV</i> , Apr ^R	248

Strain	Description	Source
<i>S. venezuelae</i> $\Delta jadT$	<i>jadT</i> deletion mutant	⁵⁹
<i>S. venezuelae</i> $\Delta jadT\Delta jadS$	<i>jadS</i> and <i>jadT</i> deletion mutant	This work
<i>S. venezuelae</i> $\Delta sv0189$	<i>sv0189</i> deletion mutant	This work
<i>S. venezuelae</i> $\Delta sv0189\Delta jadT$	<i>sv0189</i> and <i>jadT</i> deletion mutant	This work
<i>S. venezuelae</i> :: <i>kijC3</i>	Knock-in strain with <i>kijC3</i> gene inserted into dideoxy gene cluster between <i>jadU</i> and <i>jadV</i>	This work
<i>S. venezuelae</i> :: <i>kijC4</i>	Knock-in strain with <i>kijC4</i> gene inserted into dideoxy gene cluster between <i>jadU</i> and <i>jadV</i>	This work
<i>S. venezuelae</i> :: <i>kijC4(XhoI)</i>	Knock-in strain with <i>kijC4</i> gene inserted into dideoxy gene cluster between <i>jadU</i> and <i>jadV</i>	This work
<i>S. venezuelae</i> :: <i>kijC4kijC3</i>	Knock-in strain with <i>kijC3</i> and <i>kijC4</i> genes inserted into dideoxy gene cluster between <i>jadU</i> and <i>jadV</i> .	This work
<i>S. venezuelae</i> $\Delta jadV$	<i>jadV</i> deletion mutant	This work

Plasmids	Description	Source
pET28a(+)	<i>E. coli</i> expression vector, T7 promoter, N-and C- His ₆ -tag, Kan ^R	Invitrogen
pET28a::NHis ₆ <i>sv0189</i>	<i>E. coli</i> Sv0189 expression vector, includes N-His ₆ tag, Kan ^R	This work
pKC1139	<i>E. coli-Streptomyces</i> conjugation vector; <i>oriT</i> RK2, <i>ori</i> PSG5, Apr ^R	^{233, 234}
pKC1139 $\Delta jadS\Delta jadT$	Vector bearing a <i>jadS</i> and <i>jadT</i> deletion cassette	This work

Plasmids	Description	Source
pKC1139 Δ <i>sv0189</i>	Vector bearing an <i>sv0189</i> deletion cassette	This work
pUC57:: <i>kijC3</i>	Synthetic <i>kijC3</i> gene with codon optimization for <i>Streptomyces</i>	Bio Basic Inc.
pKC1139:: <i>jadUV</i>	pKC1139 with <i>jadUjadV</i> recombination cassette (flanking regions)	This work
pKC1139:: <i>kijC3</i>	Vector bearing a <i>kijC3</i> gene knock-in cassette with <i>jadU</i> and <i>jadV</i> flanking regions	This work
pKC1139:: <i>kijC4kijC3</i>	Vector bearing a <i>kijC4kijC3</i> gene knock-in cassette with <i>jadU</i> and <i>jadV</i> flanking regions	This work
pKC1139:: <i>kijC4</i>	Vector bearing a <i>kijC4</i> gene knock-in cassette with <i>jadU</i> and <i>jadV</i> flanking regions	This work
pKC1139:: <i>kijC4(XhoI)</i>	Vector bearing a <i>kijC4</i> gene knock-in shuttle vector with restored frame of downstream genes with <i>jadU</i> and <i>jadV</i> flanking regions	This work
pKC1139 Δ <i>jadV</i>	Vector bearing a <i>jadV</i> deletion cassette	This work
pSE34	<i>Streptomyces</i> expression vector; <i>ori</i> PIJ101, <i>ori</i> pUC19, <i>ermE*</i> , Tsr ^R	218
pSE34:: <i>kijC4</i>	<i>kijC4</i> expression vector	This work
pSET152	Integrative vector; <i>oriT</i> RK2, <i>ori</i> pUC18, <i>int</i> ϕ C31, Apr ^R	233, 234

4.1.23. Media Recipes

All media, unless stated otherwise, was sterilized by autoclaving at 120 °C for 20 min. Unless otherwise indicated, water was distilled and deionized. Agar (15 g/L), apramycin (Apr, 50 μ g/mL), chloramphenicol (Cam, 25 μ g/mL), kanamycin (Kan,

50 µg/mL), thiostrepton (Tsr, 50 µg/mL), ampicillin (Amp, 100 µg/mL), and/or naladixic acid (Nal, 25 µg/mL), were added when required. Solutions and buffers provided in commercial kits are not included here.

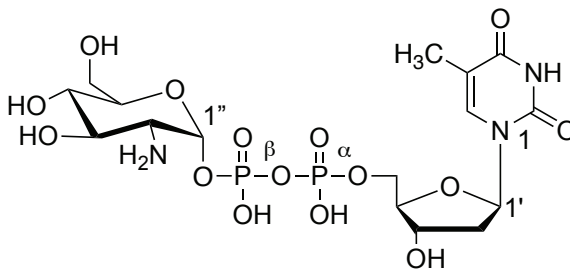
Electrode running buffer (10 ×): 30.3 g Tris base, 144.0 g glycine, 10.0 g SDS, to 1000 mL water. **Lysogeny broth (LB):** 5 g yeast extract, 10 g NaCl, 10 g tryptone, to 1000 mL distilled water, pH 7.5; **Malt yeast maltose (MYM):** 1 g malt extract, 4 g yeast extract, 4 g maltose, to 1000 mL distilled water, pH 7.5; **Mannitol soya flour medium (MS):** 1 g mannitol, 1 g soya flour, 50 mL tap water; **Minimal Salt media (MSM):** MgSO₄ (0.4 g), MOPS (1.9 g) salt solution (9 mL of 1% w/v NaCl and 1% w/v CaCl₂), FeSO₄·7H₂O (4.5 mL of 0.2% w/v), trace mineral solution (4.5 mL), to 1000 mL distilled water, pH 7.5; **MYEME medium:** 3 g yeast extract, 5 g peptone, 3 g malt extract, 10 g maltose, 103 g sucrose, to 1000 mL distilled deionized water, pH 7.5. After autoclaving, the solution was supplemented with glycine to 1% and MgCl₂ to 50 mM; **P buffer:** 0.25 g K₂SO₄, 103 g sucrose, 2.02 g MgCl₂·6H₂O, 2 mL trace element solution, 800 mL distilled water, aliquot into 10 × 80 mL solutions and autoclave. To each 80 mL autoclaved solution add the following filter-sterilized solutions 1 mL 0.5% KH₂PO₄, 10 mL 3.68% CaCl₂, 10 mL 5.73% TES, 15 mL 0.5% KH₂PO₄, 150 mL 3.68% CaCl₂ 2H₂O, 150 mL 5.73% TES pH 7.2; **R5N Medium:** 103 g sucrose, 0.25 g K₂SO₄, 10 g maltose, 5.0 g yeast extract, 0.1 g casamino acids, 5.73 g TES buffer, to 1000 mL double distilled water, pH 7.0. Autoclave 10 × 100 mL aliquots. To each autoclaved aliquot add 0.02 mL Trace element solution, 1 mL 0.5% KH₂B₄, 0.4 mL 5.0 M CaCl₂, 1.5 mL 20% proline; **Soft nutrient agar (SNA):** 0.8 g Difco nutrient broth powder, 0.5 g agar,

100 mL distilled water; **Tris-Acetate-EDTA buffer (TAE, 50 ×)**: 242 g Tris, 57.1 mL glacial CH₃COOH, 18.6 g disodium ethylenediaminetetraacetic acid (EDTA), to 1000 mL water; **Tris-EDTA Buffer (TE)**: 10 mL 1 M Tris (60.6 g in 500 mL water, pH 7.5), 2 mL 0.5 M EDTA (18.6 g EDTA in 100 mL water, pH 8.0), to 1000 mL water; **Trace mineral solution**: (1 L aqueous solution) ZnSO₄·7H₂O (880 mg), CuSO₄·5H₂O (39 mg), MnSO₄·4H₂O (6.1 mg), H₃BO₃ (5.7 mg), (NH₄)₆Mo₇O₂₄·4H₂O (3.7 mg).

4. 2. Experimental Chapter 2.2

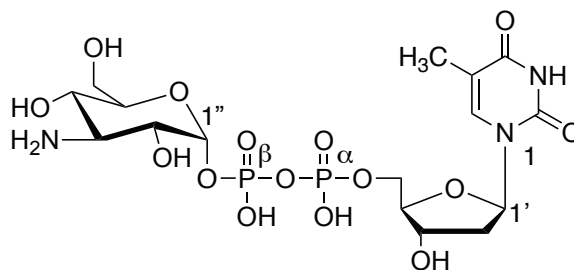
Compounds **2.1-2.4** were prepared by the Palmer (University of Saskatchewan) research group; synthetic methods are described elsewhere.¹³⁰ Synthesis of **2.5** was performed by S.A. Beaton (Dalhousie University) as described previously.⁸⁷ Cps2L and PNP were overexpressed, isolated, and quantified following the procedures outlined in the literature.^{80, 247} Microbial xanthine oxidase (XO) and IPP expressed in *Escherichia coli* were obtained from Sigma-Aldrich. IPP stock solutions (0.1 EU/μL) were prepared in Millipore water; thawed aliquots were kept in a fridge and were used for up to 1 month after thawing. XO stock solutions (120 EU/mL) were prepared in Tris·HCl (pH 7.5, 25 mM) and stored at -30 °C; aliquots were used immediately after thawing. Non-linear regression analysis was performed using GraFit 5.0.4., Erathacus Software.

4.2.1. Disodium Uridine 5'-(2-amino-2-deoxy- α -D-glucopyranosyl bisphosphate) (**2.8**)



A reaction containing **2.1** (2.5 mg, 9.6 μ mol), UTP (10.1 mg, 18.4 μ mol), MgCl_2 (2.2 mM), IPP (5 EU), in TRIS·HCl (final volume of 550 μ L, 25 mM, pH 7.4) was initiated by the addition of Cps2L (725 EU). Complete conversion to product was observed by HPLC at 20 h (Section 4.1.4). The quenching and purification procedure was the same as described for **2.9** (Section 4.2.2). The following modified gradient for ion-pair chromatography (Section 4.1.6.) was used: 100/0 A/B over 2 CV, linear increase to 80/20 A/B over 18 CV, and finally 0/100 A/B for 2 CV. Desalting was accomplished on an Sephadex® LH-20 column. Sugar nucleotide **2.8** (1.5 mg) was obtained as the disodium salt (2.5 μ mol, 26%; ^1H and ^{31}P NMR matched previously reported data.²⁴⁹

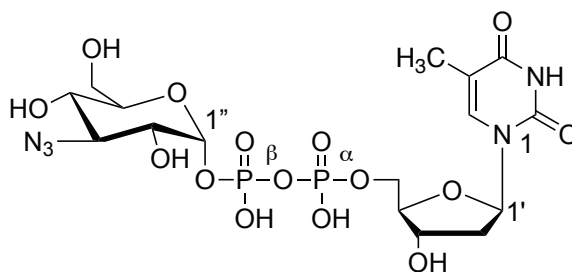
4.2.2. Disodium Deoxythymidine 5'-(3-amino-3-deoxy- α -D-glucopyranosyl bisphosphate) (2.9)



A reaction containing **2.2** (3.3 mg, 12.6 μ mol), dTTP (6.1 mg, 12.6 μ mol), MgCl_2 (2.2 mM final concentration), and 18 EU IPP was initiated by the addition of Cps2L (150 EU) in Tris·HCl buffer (50 mM, pH 7.5, 1 mL reaction volume). The enzymatic reaction was performed at 37 °C and reaction progress was monitored by HPLC (Section 4.1.4). No product breakdown was observed over the incubation period. Additional Cps2L (25 EU after 18 h, 25 EU after 32 h) was added to the enzymatic reaction mixture. Additional IPP (10 EU after 32 h) was added at 50% conversion. The enzymatic reaction was stopped once 100% conversion was reached (72 h). CIP (2 EU) was subsequently added to the mixture, and allowed to incubate for 1.5 h at 37 °C. After the set time, the protein was precipitated with an equivalent volume of methanol (1.5 mL) and the precipitate was washed with two 1 mL portions of methanol. The supernatants were combined, concentrated and re-dissolved in aqueous TBA bicarbonate buffer (10 mM, ~2 mL) for purification by C18 ion-pair reversed-phase chromatography (Section 4.1.6). All UV fractions containing sugar nucleotides, as judged by HPLC, were combined and concentrated to ~2 mL in volume and passed through a cation-exchange column (Dowex® 50W-X8 cation exchange resin 100-200 mesh, Na^+ form, 18 mm \times 18 cm) in order to

generate the sodium salt of the desired sugar nucleotide. Further desalting of the product mixture was performed by gel filtration using a Sephadex® G10 column (1.5 cm × 100 cm) with water as the eluent to afford **2.9** with an isolated yield of 6.1 mg (0.011 mmol, 86%). ¹H NMR (D₂O, 500 MHz): δ 8.34 (s, 1H, NH-3), 7.63 (s, 1H, H-6), 6.24 (t, 1H, *J* 7 Hz, H-1), 5.54 (dd, 1H, *J* 7.5, 3 Hz, H-1''), 4.51 (dt, 1H, *J* 6, 3 Hz, H-3'), 4.08-4.11 (m, 3H, H-4', H-5'a and H-5'b), 3.81-3.85 (m, 1H, H-2''), 3.76 (dd, 1H, *J* 12.2, 2.5 Hz, H-6''b), 3.70 (dd, 1H, *J* 12.2, 4 Hz, H-6''a), 3.64 (ddd, 1H, *J* 10.1, 4.5, 3 Hz, 5''-H), 3.53 (t, 1H, *J* 10.4 Hz, H-3''), 3.38 (t, 1H, *J* 9.4 Hz, H-4''), 2.21-2.33 (m, 2H, H-2'a and H-2'b), 1.82 (br s, 3H, CH₃) ppm; ¹³C (125 MHz, D₂O): δ 167.7 (C-4), 152.9 (C-2), 138.3 (C-6), 113.9 (C-5), 85.3 (d, *J* 8.8 Hz, C-4'), 85.0 (C-1'), 73.2 (C-3''), 72.8 (d, *J* 12.4 Hz, C-2''), 72.0 (d, *J* 4.5 Hz, C-1''), 71.1 (C-3'), 68.8 (C-5''), 65.7 (C-4''), 65.5 (d, *J* 5.4 Hz, C-5'), 59.5 (C-6''), 38.9 (C-2'), 12.7 (CH₃) ppm; ³¹P {¹H} (202.5 MHz, D₂O): δ -13.1 (d, 1P, *J*_{Pβ,Pα} 21 Hz, P-α), -11.3 (d, 1P, *J*_{Pα,Pβ} 21 Hz, P-β); HRMS (ESI⁻): found [M-H]⁻ 562.0821, C₁₆H₂₆N₃O₁₅P₂ requires [M-H]⁻ 562.0845.

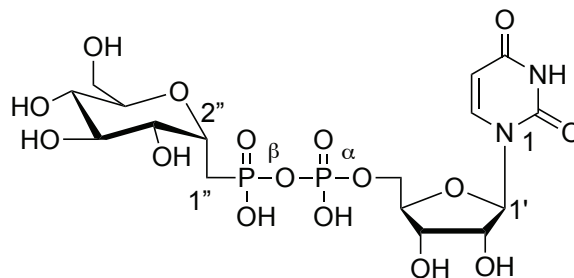
4.2.3. Tributylammonium deoxythymidine 5'-(3-azido-3-deoxy- α -D-glucopyranosyl) bisphosphate) (**2.11**)



A reaction containing **2.5** (6.0 mg, 21.2 μ mol), dTTP (18.8 mg, 32.1 μ mol), $MgCl_2$ (2.2 mM), and 5 EU IPP in Tris·HCl buffer (50 mM, pH 7.5, 1.5 mL final volume) was initiated by the addition of Cps2L (250 EU). Additional Cps2L (100 EU at 18 h, 100 U at 24 h, and 100 U at 32 h) and additional IPP (5 EU at 18, and 5 EU at 24 h) were added at the indicated times. The reaction was observed to plateau at 70% conversion after 24 h by HPLC (Section 4.1.4), with no further product formation after this time although additional Cps2L had been added to the reaction mixture. At 48 h, with no further reaction progress, CIP (8 EU) was added and the reaction incubated at room temperature for 20 h. A SiliaSep™ 12 g C-18 column (SiliCycle) was used with an altered gradient for the reverse phase chromatography (Section 4.1.6); the gradient was 20/80 A/B over 2 CV, linear increase to 80/20 A/B over 20 CV, and finally 0/100 A/B for 3 CV, where A is 10 mM aqueous tributylammonium bicarbonate buffer (pH 6.5) and B is HPLC-grade methanol. The combined fractions containing sugar nucleotide, as judged by HPLC analysis, were concentrated to a volume of \sim 2 mL and passed through a Sephadex® LH-20 gel filtration column (3.5 \times 22 cm) with water as the eluent for desalting. Sugar nucleotide **2.11** was isolated with 0.5 equivalents of TBA salt (4.6 mg, 7.3 μ mol, 33%). 1H NMR (D_2O ,

500 MHz): δ 7.65 (br d, 1H, J 1.1 Hz, H-6), 6.24 (t, 1H, J 7.0 Hz, H-1'), 5.48 (dd, 1H, J 7.2, J 3.2 Hz, H-1''), 4.52 (m, 1H, H-3'), 4.04-4.10 (m, 3H, H-5'a, H-5'b, H-4'), 3.81 (m, 1H, H-5''), 3.73 (dd, 1H, J 12.5, 2.2 Hz, H-6''a), 3.61-3.68 (m, 2H, H-3'' and H-6''b), 3.45 (dt, 1H, J 10.3, 3.1 Hz, H-2''), 3.35 (t, 1H, J 9.9 Hz, H-4''), 2.21-2.31 (m, 2H, H-2'a and H-2'b), 1.82 (br d, 3H, J 1.0 Hz, CH₃) ppm; ¹³C (D₂O 125, MHz): δ 166.5 (C-4), 151.6 (C-2), 137.2 (C-6), 111.7 (C-5), 94.8 (d, J 6.8 Hz, C-1''), 85.3 (d, J 8.9 Hz, C-5'), 84.9 (C-1''), 72.5 (C-5''), 70.9 (C-3'), 70.5 (d, J 8.9 Hz, C-2''), 67.8 (C-4''), 65.7 (C-3''), 65.4 (d, J 6.4 Hz, C-4'), 59.9 (C-6''), 38.6 (C-2'), 11.6 (CH₃) ppm; ³¹P{¹H} (D₂O, 202.5 MHz): δ -13.0 (d, 1P, $J_{P\beta, P\alpha}$ 21 Hz, P- β), -11.3 (d, 1P $J_{P\alpha, P\beta}$ 21 Hz, P- α); HRMS (ESI⁻): found [M-H]⁻ 588.0731, C₁₆H₂₄N₅O₁₅P₂ requires [M-H]⁻ 588.0750.

4.2.4. Tributylammonium deoxyuridine C-(1-deoxy- α -D-glucopyranosyl bisphosphate)methane (2.15)



2.5 (4 mg, 0.076 mM), UTP (0.114 mM), MgCl₂ (5 mM), IPP (20 EU), Cps2L (50 μ M) and TRIS-HCl (to 2 mL total volume, 50 mM, pH 7.5) were incubated at 37°C with shaking. Reaction progress was monitored by HPLC (Section 4.1.4). After 5 h, additional Cps2L (50 μ L of stock 917 μ M solution) and IPP (25 EU) was added to the reaction mixture. At 24 h, an additional (50 μ L of 917 μ M stock solution) and

IPP (10 EU). After 5 additional hours, CIP (10 EU) was added to the solution, and then shaken at room temperature overnight. After ion-pair reverse phase chromatography (Section 4.1.6) followed by LH20 size exclusion chromatography (Section 4.2.3), **2.15** was isolated with 0.7 equivalents TBA as determined by integration of the ^1H NMR spectrum. A yield of 1.1 mg (13%) was obtained as determined by UV absorbance at λ_{max} 262 nm, ϵ 9.7 $\text{mM}^{-1}\text{cm}^{-1}$. $^{250} \delta$ ^1H (500 MHz; D_2O) 8.01 (d, 8.0 Hz, 1H, H-6), 6.04-6.01 (m, 2H, H-1', H-5), 4.48 (m, 1H, H-2''), 4.44-4.42 (m, 2H, H-2', H-3'), 4.35 (m, 1H, H-4'), 4.29 (1H, ddd, 12.0, 4.7, 2.9 Hz, H-5'a), 4.25 (1H, ddd, 12.0, 5.6, 2.9 Hz, H-5'b), 3.89 (1H, dd, 12.0, 1.8 Hz, H-7''a), 3.79-3.74 (2H, m, H-7''b, H-3''), 3.71 (1H, m, H-6''), 3.66 (1H, t, 9.1 Hz, H-5''), 3.44 (1H, t, 9.1 Hz, H-4''), 2.34-2.13 (2H, m, H-1''a, H-1''b); ^{13}C (125 MHz; D_2O) δ 166.4 (C-4), 151.9 (C-2), 141.6 (C-6), 102.6 (C-5), 88.4 (C-1'), 83.2 (d, 9.1 Hz, C-4'), 73.7 (C-2'), 73.1 (C-5''), 72.7 (C-6''), 72.0 (d, 4.1 Hz, C-2''), 71.1 (d, 12.2 Hz, C-3''), 70.1 (C-4''), 69.6 (C-3'), 64.6 (d, 5.5 Hz, C-5'), 60.8 (C-7''), 24.3 (d, 139.8 Hz, C-1''); $^{31}\text{P}\{^1\text{H}\}$ (202 MHz; D_2O) δ 14.6 (d, 26 Hz, P- β), -11.3 (d, 26 Hz, P- α). HRMS-ESI m/z 563.0680 (calculated $\text{C}_{16}\text{H}_{25}\text{N}_2\text{O}_{16}\text{P}_2$, 563.0685).

4.2.5. IPP-PNP-XO Coupled Kinetic Assays

Stock solutions containing Tris·HCl (pH 7.5, 25 mM), Glc 1-P or compounds **2.1-2.6** (25-750 μM), dTTP (1 mM), MgCl_2 (5.7 mM), inosine (1 mM), IPP (1.7 EU/mL), PNP (1 μM), and XO (1.5 EU/mL), were allowed to pre-incubate at room temperature for five minutes, in order to consume contaminating P_i present in the solutions. The concentrations of substrate varied within the indicated range to be maintained at a level in which the change in absorbance could be detected by UV

spec (typically ≥ 25 mM), and keeping the concentrations lower than that of the co-substrate (<1 mM). Higher concentrations of dTTP made accurate quantification more challenging due to the presence of background phosphate. An appropriate concentration of Cps2L was then added to initiate the reaction. In all cases, initial reaction velocity was monitored spectrophotometrically over 10 min at a wavelength of 290 nm. Typically, rates were linear for these initial 10 min. Observed initial kinetic rates were halved to account for the 2 equivalents of P_i derived from each PP_i unit produced in the Cps2L reaction. Rates were converted from absorbance units (mAu) to concentration units (μM) using a phosphate standard curve. The standard curve was generated using identical conditions to those described for kinetic assays, except with variable P_i (10-100 μM $\text{NaH}_2\text{PO}_4 \cdot \text{H}_2\text{O}$) instead of sugar phosphate. λ_{290} values were taken once the reaction had reached completion (after approximately 7 min) and plotted against phosphate concentration producing data that was fit by linear regression, providing a slope that was used as the conversion factor between mAu and μM units. Inhibition assays were run using the same techniques as described above, using variable Glc 1-P (25-250 mM), except with an appropriate concentration of inhibitor included in the stock solution.

4.2.6. K_d Determination Using waterLOGSY NMR Spectroscopy

Aliquots (1-8 μL) of a 100 mM ethylphosphonate **2.6** solution were titrated into a solution containing dTTP (2 mM), MgCl_2 (1.3 mM), $d\text{Tris} \cdot \text{HCl}$ (pH 7.5, 20 mM), D_2O (10% v/v), Cps2L (60 μM), and ethylphosphonate **2.6** (initial concentration of 400 μM). After each addition, a waterLOGSY NMR spectrum was recorded (128 scans, relaxation delay ($d1$) 5 s, mixing time ($d9$) 0.12 s). WaterLOGSY NMR

spectra were also acquired without Cps2L to generate a correction curve for the contribution of free ligand to the observed signal intensities; these samples contained dTTP (2 mM), MgCl₂ (1.3 mM), *d*Tris·HCl (pH 7.5, 20 mM), D₂O (10% *v/v*), and ethylphosphonate **2.6** (400, 600, or 1600 μM). Corrected signal intensities were plotted as function of **2.6** concentration and fitted by a standard dose response curve by non-linear regression to determine K_d values, where I_{max} is the maximum waterLOGSY signal, K_d is the dissociation constant, and L is the concentration of free ligand.¹¹²

$$I = \frac{-I_{max}}{1 + \left(\frac{L}{K_D}\right)} + I_{Max}$$

L in the presence of protein is determined by subtracting the value observed in the absence of protein.¹¹² Values of 17 (±4) and 23 (±8) mM were obtained from the signal intensities corresponding to H-4 and H-6, respectively.

4.3. Experimental Chapter 2.3

The synthesis of p₄dT, by Dr. Smithen (Dalhousie University), was reported elsewhere.²⁵¹ A Hach H160 portable pH meter equipped with a PH47-SS probe was used to measure pH of solutions in NMR tubes.

4.3.1. p₄dT HPLC Assays and Specific Activity with Cps2L

Specific activity was measured from a reaction containing p₄dT or dTTP (1 mM), Glc 1-P (2 mM), MgCl₂ (1.1 mM), Cps2L (0.95 μM) and IPP (0.5 EU). The volume was brought up to 50 μL using Tris-HCl (stock solution of 20 mM, pH 7.5). The final sample pH was 7.5. Reactions were quenched by the addition of methanol (10

μL) to withdrawn reaction aliquots ($10 \mu\text{L}$) at 1, 2, and 5 min. Specific activity was defined in terms of enzyme units (EU) as the amount of product produced (μmol) per unit time (minutes) per unit volume ($1 \mu\text{L}$) of enzyme solution. Percent conversion was determined by integration of the HPLC (Section 4.1.4) trace as follows: % conversion = (area under product peak) / (area under product peak + area under p_4dT peak).

4.3.2. ^{31}P NMR Experiments with p_4dT

A reaction contained p_4dT (5 mM), Glc 1-P (5 mM), MgCl_2 (100 μM), D_2O (10% v/v) and Cps2L (95 μM). The volume was brought up to 500 μL using Tris·HCl (stock solution of 20 mM, pH 7.5). The final sample pH was 7.0. For reaction progress determination using HPLC (Section 4.1.4) analysis at λ_{254} , 10 μL of the reaction mixture was quenched with 10 μL of methanol, then centrifuged at 14,000 rpm for 5 min. After 5 h of incubation at 37 °C, conversion of 25% to dTDP-Glc was achieved. The production of dTDP-Glc was confirmed by LC-MS² analysis. The reaction mixture was transferred to a Shigemi NMR tube. $^{31}\text{P}\{^1\text{H}\}$ NMR spectra were recorded for 256 scans at various acidities (pH 7, 8.7, 9.2, 9.6, and 10 (3200 scans)); the pH of the solution was adjusted by titration with aqueous NaOH (0.2 M). Finally, the reaction was spiked with P_3 (2 mM) and an additional NMR spectrum was recorded.

4.4. Experimental Chapter 2.4

Synthesis of C-(1-Deoxy- α - D-glucopyranosyl)methane phosphonate (Glc 1C-P) and dTDP-C-(1-deoxy- α - D-glucopyranosyl)methane (dTDP-1C-Glc) was carried out

as previously described.⁸⁷ Compounds **2.16-2.20** were synthesized by Dr. J. S. Zhu (Dalhousie University) and methods are published elsewhere.¹²⁷

4.4.1. Expression and Purification of Recombinant Enzymes

E. coli BL21(DE3) bearing pET30 with *rmlB*, *rmlC* or *rmlD* were used to inoculate overnight cultures (25 mL LB medium with 50 µg/mL kanamycin, 37 °C or 30 °C, 250 rpm). After 16-18 h, 1 L of media (4 × 250 mL LB-kan) was inoculated with 2.5 mL of the overnight culture and shaken (37 °C, 250 rpm). IPTG was added to the cultures to a final concentration of 1 mM when OD₆₀₀ 0.6-0.8 was reached (3-6 h), and then shaking resumed for 18-20 h at 18 °C, 250 rpm. The cells were pelleted (4°C, 3750 rpm, 1 h) and stored at -70 °C until purification. Lysis was achieved by re-suspending cells in buffer (3 mL glycerol, 1 mL 10% Triton™ X-100, 16 mL wash buffer (W: 20 mM P_i, 300 mM NaCl, 10 mM imidazole, pH 7.5), lysozyme (10 mg) and deoxyribonuclease (Dnase, 20 µg). The cell suspension was stirred for 1 h at 0 °C, and then sonicated with 5 × 5 s pulses (50% amplitude). The cell debris was pelleted (13000 rpm, 10 min, 4 °C) and the supernatant collected and immediately purified by nickel-affinity chromatography. Manual elution was accomplished with a HisTrap HP 5 g Nickel affinity column (GE-healthcare) with wash buffer (W: recipe as above) and elution buffer (E: 20 mM P_i, 300 mM NaCl, 250 mM imidazole, pH 7.5) as the eluents. To a column pre-equilibrated with buffer W the combined supernatant was applied. Flow through was collected as fraction 1 (F1). Next, 3 × 20 mL (F2-4) buffer W was used to wash the column. A 50 mL fraction with 20:80 buffer W:E was collected (F5), and then 3 mL of buffer E was applied to the column and kept at 4 °C for 15-25 min. Three fractions (3 × 10

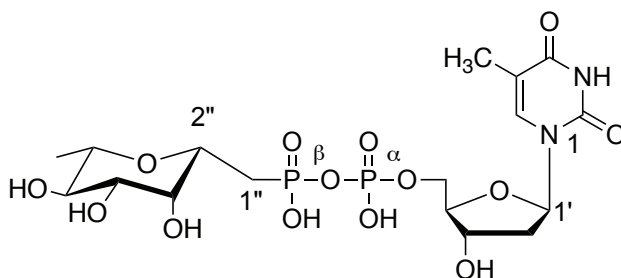
mL, F5-7) with buffer E were collected. Fractions containing pure protein as determined by SDS-PAGE (usually F5-F7) were concentrated using 10 k molecular weight cut-off (MWCO) filters, then buffer exchanged into 3.5 mL Tris·HCl (25 mM, pH 7.5) using a PD-10 desalting column (GE healthcare) following manufacturer protocols. Purified enzyme concentrations were determined by absorbance A_{280} using extinction coefficients calculated the using ExPASy ProtParam tool (<http://web.expasy.org/protparam/>). Final concentrations were 250 μ M RmlB, 1000 μ M RmlC, and 50 μ M RmlD. Cps2L was expressed using from *E. coli* BL21(DE3) pSK001 and purified as described before to yield a 900 μ M final solution.⁸⁰ Protein solutions were aliquoted (200 μ L) and kept frozen at -70 °C until use.

4.4.2. General Conditions for Analytical Cps2L, RmlB-D Assays

The nucleotidyltransferase reaction was set up as Step 1: Glc 1-P or analogue (4 mM), Mg^{2+} (8 mM), dTTP or UTP (2 mM), Cps2L (9 μ M), and Tris·HCl (to 50 μ L, 50 mM, pH 7.5). After 1 h, 10 μ L of the reaction mixture was withdrawn for analysis, quenched with 20 μ L methanol and centrifuged (10000 rpm, 5 min) to remove protein. The following components were added to the indicated concentrations, Step 2: ammonium formate (20 mM), NAD (0.1 mM), formate dehydrogenase (0.2 EU), RmlB (6.3 μ M) and Tris·HCl (to 80 μ L, 50 mM, pH 7.5). After another hour 20 μ L of the reaction mixture was withdrawn, quenched and centrifuged as above, and Step 3 components were added: RmlC (25 μ M), RmlD (10 μ M) and Tris·HCl (to 100 μ L, 50 mM, pH 7.5). Aliquots were taken as above at

indicated time points, and analysed by HPLC (Section 4.1.4) and/or LCMS (Section 4.1.2).

4.4.3. Tributylammonium 5'-deoxythymidine-C-(1-deoxy- β -L-rhamnopyranosyl bisphosphate) methane (dTDP-1C-Rha)



A reaction containing dTDP-1C-Glc (2.5 mg, 2.2 mM), NAD (0.025 mM), ammonium formate (20 mM), formate dehydrogenase (2 EU), RmlB (10 μ M), RmlC (10 μ M), and RmlD (10 μ M) in Tris·HCl (to 2 mL total volume, 50 mM, pH 7.5) was shaken (320 rpm) at room temperature for four hours. A negative mode LCMS experiment was run on an aliquot of the reaction mixture to confirm the presence of the product and absence of the starting material. The reaction was kept at -70 $^{\circ}$ C until purification. After thawing, methanol (2 mL) was added to the reaction and then centrifuged. The supernatant was collected and the pellet was washed with 2 mL 1:1 methanol: buffer A (Section 4.1.6), and centrifuged. The combined extracts were concentrated by rotary evaporation, taking care not to allow the material reduce to dryness. When 1-2 mL remained, the solution was immediately applied to a C-18 pre-packed column (SiliCycle, 12 g) that was pre-equilibrated with buffer A. Fractions showing UV absorbance were screened for the presence of TDP-1C-Rha by HPLC, and positive fractions were pooled and concentrated to a reduced volume

of ~4 mL. This concentrated solution was passed through a gel filtration column (50 g Sephadex® LH-20, 10 mLmin⁻¹, eluent H₂O) in multiple batches (1 mL), and UV active fractions were combined, concentrated by rotary evaporation, and finally lyophilized to dryness. This procedure significantly reduces the amount of residual TBA to ~2-5 equivalents, however repeated lyophilisation cycles further reduce the concentration of TBA present in the sample. The yield was 1.1 mg TDP-1C-Rha (46%) as determined from the UV absorbance (ϵ 9.5 mM⁻¹cm⁻¹, λ_{\max} 267 nm).⁸⁷ The sample contained 1.6 equivalent TBA as determined by integration of the ¹H NMR spectrum. $\delta^1\text{H}$ (500 MHz; D₂O) 7.78 (s, 1H, H-6), 6.38 (t, 6.8 Hz, H-1'), 4.66 (m, 1H, H-3'), 4.23-4.18 (m, 2H, H-5', H-4'), 2.07 (app d, 3.1 Hz, H-3''), 3.90 (td, 8.6, 5.6 Hz, 2H, H-2''a,b), 3.65 (dd, 9.0, 3.3 Hz, 1H, H-4''), 3.44-3.25 (m, 2H, H-6'', H-5''), 2.45-2.36 (m, 2H, H-2'a,b), 2.25 (ddd, 18.0, 15.1, 8.3 Hz, 1H, H-1''a), 2.06 (app ddd, 20.0, 15.0, 5.2, 1H, H-1''b), 1.97 (s, 3H, CH₃-5), 1.30 (d, 5.7 Hz, 3H, CH₃-6''); $\square^1\text{C}$ (125 MHz; D₂O) δ 166.6 (C-4), 151.7 (C-2), 137.3 (C-6), 111.7 (C-2), 85.4 (d, 9.1 Hz, C-4'), 84.9 (C-1'), 76.0 (C-6''), 74.4 (C-2''), 73.9 (C-4''), 72.4 (C-5''), 71.0 (C-3'), 70.8 (d, 4.6 Hz, C-3''), 65.2 (d, 5.7 Hz, C-5'), 38.6 (C-2'), 30.1 (d, 138 Hz, C-1''), 17.1 (CH₃-5''), 11.7 (CH₃-5); $\square^1\text{P}\{^1\text{H}\}$ (202 MHz; D₂O) δ 12.7 (d, 26 Hz, P- β), -11.5 (d, 26 Hz, P- α). HRMS-ESI⁻ m/z 545.0956 (calculated C₁₇H₂₇N₂O₁₄P₂, 545.0943).

4.5. Experimental for Chapter 2.5

4.5.1. AntiSMASH Analysis

AntiSMASH V4.0 was used to predict putative secondary metabolite gene clusters in the *S. venezuelae* genome (NCBI GCA_000253235.1) with the following settings: ClusterFinder 'on', BGC border prediction 'on', minimum cluster size in CDS '5', minimum number of biosynthesis-related PFAM domains '3', minimum cluster probability '60%', extra features 'all on'. The output summary can be found in Appendix D.

4.5.2. Assembly of pET28a::sv0189

The gene *sv0189* was amplified from *S. venezuelae* ISP5230 genomic DNA by PCR using primers P1 and P2.

P1: 5'-CTGGTGCCGCGCGGCAGCCCATATGACCACCACCGCGTCC-3' (NdeI site is underlined)

P2: 5'-GGTGCTCGAGTGCGGCCGCAAAGCTTCGATCCGGCGAGTTCGGC-3'
(HindIII site is underlined).

The resulting 1.3 kb PCR product was purified from agarose by gel extraction following manufacturer protocols (QIAquick® gel extraction kit, Qiagen). The *E. coli* expression vector, pET28a(+), was treated with NdeI and HindIII restriction digest enzymes, heated at 80 °C for 20 min, and treated with CIP (1 uL), at 37 °C for 1 h. The CIP-treated vector was then purified using a gel extraction kit (QIAquick® gel extraction kit, Qiagen). The insert and vector fragments were ligated using a Gibson Assembly® cloning kit (New England Bioscience)²⁵²

following manufacturer instructions; 2 μ L pET28a (50 ng), 8 μ L PCR product (40 ng), and 10 μ L Gibson assembly master mix. The reaction was incubated for 60 min at 50 °C. NEB® 5-alpha competent *E. coli* were transformed (Section 4.1.17) with 2 μ L of the reaction mixture. The plasmid was isolated using a miniprep kit (Section 4.1.18). Isolated plasmids were treated with restriction digest enzymes NdeI and HindIII to confirm pET28a::sv0189.

4.5.3. Preparation of pET28a::NHis₆sv0189

Complementary primers P3 and P4 (EcoRI underlined) were used to introduce a stop codon (bold) by site directed mutagenesis using the QuikChange Lightning Site-Directed Mutagenesis Kit (Agilent, catalogue 210518).

P3: 5'-CCGAACTCGCCGGATCG**TGAATTC**GCGGCCGCACTCGAGC-3'

P4: 5'-GCTCGAGTGCGGCCG**CGAATTC**ACGATCCGGCGAGTTCGG-3'

Reactions were set up as suggested by the manufacturer; 5 μ L QCL 10 \times buffer, 5 μ L pET28a::sv0189, 125 ng P3, 125 ng P4, 1 μ L QCL dNTP mix, 1.5 μ L Quick solution reagent, 1 μ L QCL enzyme, 34 μ L ddH₂O. The reaction was then subject to the following cycling program:

Step	Temp (°C)	Time (s)	cycles
1	95	120	1
2	90	20	18 (steps 2-4)
3	60	10	
4	68	360*	
5	68	300	1

*30 sec/kb

After completion of the cycling protocol, 2 μ L DpnI restriction enzyme was added to the reaction and incubated at 37 °C for 5 min. NEB® 5-alpha competent *E. coli* cells were transformed with 2 μ L of the DpnI treated reactions (Section 4.1.17). Plasmids were isolated using a Miniprep kit (Section 4.1.18). Plasmids were screened by restriction digestion with EcoRI and NdeI to confirm pET28a::NHis_{6sv0189}.

4.5.4. Transformation of *E. coli* BL21(DE3) pLysS

E. coli BL21(DE3) pLysS competent cells were prepared by the standard procedure (Section 4.1.19). To a 100 μ L aliquot of cells was added 2 μ L of pET28a::NHis_{6sv0189} following the general transformation protocol (Section 4.1.20). Plates with transformed colonies were kept at 4 °C for 2-3 weeks, and individual colonies were used to inoculate LB for protein production. Agar plates and culture media were supplemented with 1% glucose when working with *E. coli* bearing pET28a::NHis_{6sv0189}, which reduces basal expression of T7 polymerase prior to IPTG induction.^{253, 254}

4.5.5. Expression and Purification of Sv0189

A 2.5 mL of an overnight starter culture of *E. coli* BL21(DE3) pLysS pET28a::NHis_{6sv0189} in 25 mL LB with 1% glucose, Kan (50 μ g/mL) and Cam (25 μ g/mL) was used to inoculate each 4 \times 250 mL LB with 1% glucose and antibiotics. The cultures were grown at 37 °C until an OD₆₀₀ values of 0.6 \pm 0.1 was reached, about 5-7 h. At this point, the cultures were supplemented with 0.4 mM IPTG (250 μ L of a 400 mM stock solution) and an aliquot (1 mL) was withdrawn for SDS-

PAGE analysis and kept aside (Section 4.1.8). Cultures supplemented with IPTG were grown overnight at 18 °C with shaking at 250 rpm. A second sample of the cultures was withdrawn at this stage for SDS-PAGE analysis post-IPTG induction. The cells were pelleted (4 °C, 3750 rpm, 1 h) and stored at -70 °C until purification. Lysis was achieved by re-suspending cells in lysis buffer (3 mL glycerol, 1 mL 10% Triton™ X-100, 16 mL wash buffer (W: 20 mM P_i , 300 mM NaCl, 10 mM imidazole, pH 7.5), lysozyme (10 mg) and Dnase (20 µg). The cell suspension was stirred for 1 h at 0 °C, and then sonicated with 5 × 5 s pulses (50% amplitude). The cell debris was pelleted (13000 rpm, 10 min, 4 °C) and the supernatant collected and immediately purified by nickel-affinity chromatography. Manual elution was accomplished with a His Trap HP 5 g Nickel affinity column (GE-healthcare) with wash buffer (W: recipe as above) and elution buffer (E: 20 mM P_i , 300 mM NaCl, 250 mM imidazole, pH 7.5) as the eluents. To a column pre-equilibrated with buffer W the combined supernatant was applied. Flow through was collected as fraction 1 (F1). Next, 3 × 20 mL (F2-4) buffer W was used to wash the column. A 50 mL fraction with 20:80 buffer W:E was collected (F5), and then 3 mL of buffer E was applied to the column and kept at 4°C for 15-25 min. Three fractions (3 × 10 mL, F5-7) eluted with buffer E were collected. Fractions containing pure protein, as determined by SDS-PAGE (F5-F7) were concentrated using 10 k MWCO filters, then buffer exchanged into 3.5 mL Tris·HCl (50 mM, pH 8.0) using a PD-10 desalting column (GE healthcare) following manufacturer protocols. Purified enzyme concentrations were determined by absorbance A_{280} using a calculated extinction coefficient of $56045 \text{ M}^{-1}\text{cm}^{-1}$, determined using the ExPASy ProtParam

tool (<http://web.expasy.org/protparam/>). A final concentration of 200 μM was determined. Protein solutions were aliquoted (200 μL) and kept frozen at -70°C until use.

4.5.6. Determination of Kinetic Parameters

For kinetics with constant UDP and variable 2-chloro-4-nitro-phenol- β -D-glucopyranoside, reactions contained 2.5 mM UDP, 1 mM MgCl_2 , 2.5 μM Sv0189 and 0-7.5 mM 2-chloro-4-nitro-phenol- β -D-glucopyranoside. For kinetics with constant 2-chloro-4-nitro-phenol- β -D-glucopyranoside and variable UDP, reactions contained 5 mM 2-chloro-4-nitro-phenol- β -D-glucopyranoside, 1 mM MgCl_2 , 2.5 μM Sv0189 and 0-1 mM UDP. Reaction set up was performed in a 96-well plate to enable monitoring at λ 410 nm on a UV spectrometer over 20 min (Section 4.1.3). A standard curve of 2-chloro-4-nitro-phenol (1-100 μM in 50 mM Tris·HCl, pH 8.0) was used to convert rates from mAu/min to $\mu\text{M}/\text{min}$ using the equation from a linear fit.

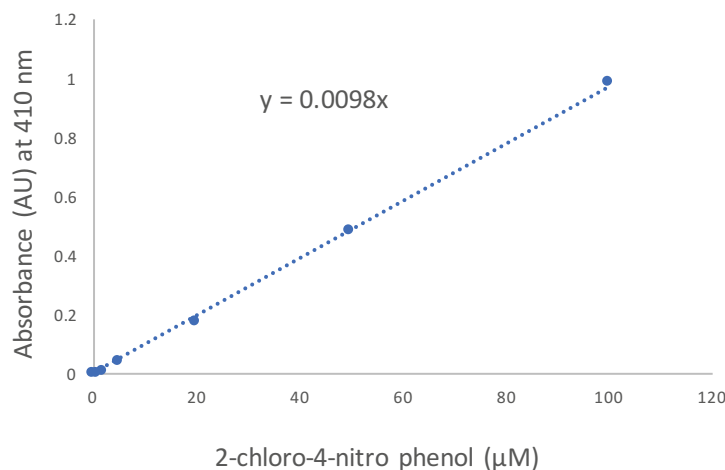


Figure 81. Standard curve used to convert absorbance units (AU) to concentration (μM).

4.5.7. First Round of Acceptor Screening

Three series A, B, and C comprising 72 compounds in total were screened with Sv0189 (Figures 82-84). Reactions set up in 96 well plates contained 1 mM 2-chloro-4-nitro-phenol- β -D-glucopyranoside, 1 mM acceptor, 0.01 mM UDP, 1 mM MgCl_2 , 20 μM Sv0189 and Tris·HCl (50 mM, pH 8.0) to a final volume of 100 μL . Acceptor stock solutions were 10 mM in DMSO. Initial reaction rates were monitored in 10 s intervals over the first 30 min at λ 410 nm (Section 4.1.13). End-point plate readings were taken at 0, 1 and 3 h. The rate observed with acceptor 4-methylumbelliferone (**A11**), having been established as an acceptor in initial screening, served as a positive control, and the rate observed with all components except with substitution of DMSO (5% final v/v) instead of and acceptor served as a negative control. Positive hits were those with initial rates greater than observed for

A11, putative hits were those greater than DMSO, and negative hits those with rates less than the DMSO negative control. For HPLC analysis, reactions were quenched at 24 h by the addition of methanol and DMSO (50 μ L each), then centrifuges at 10,000 rpm for 5 min prior to analysis by HPLC (Section 4.1.4).

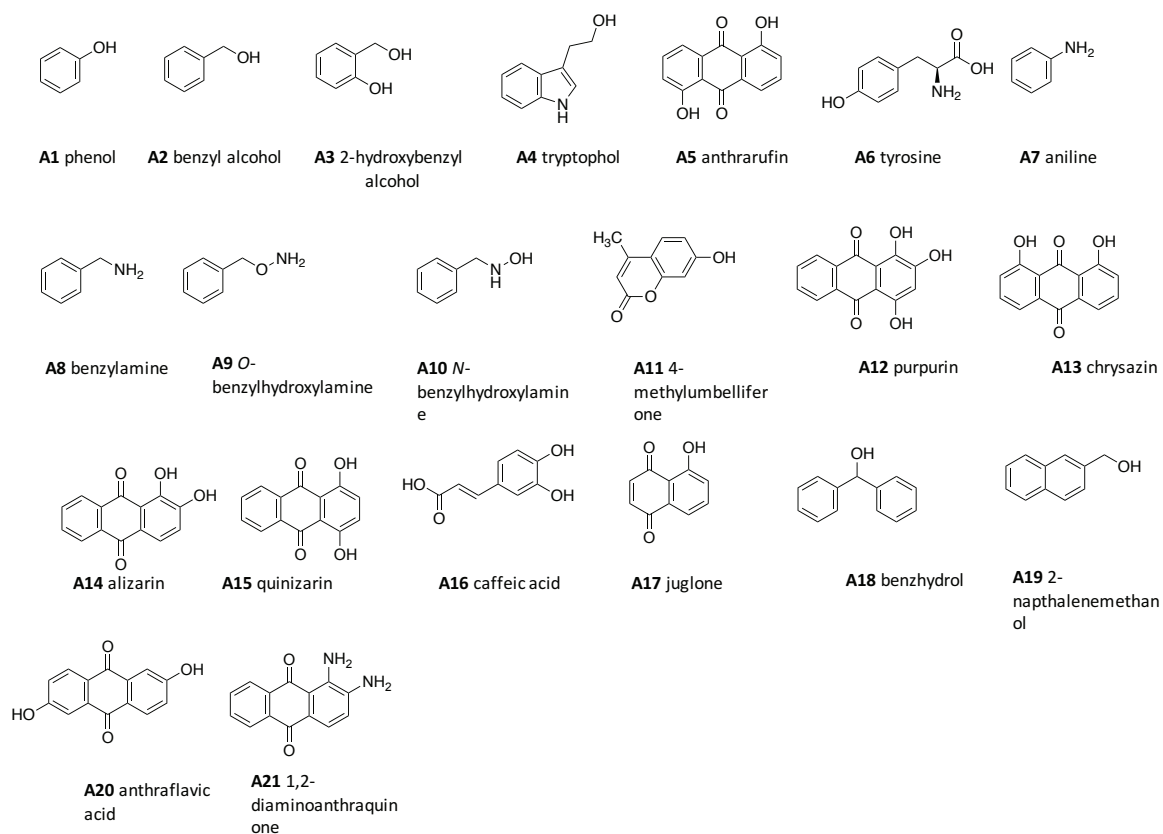


Figure 82. Series A chemical structures for Sv0189 acceptor screening.

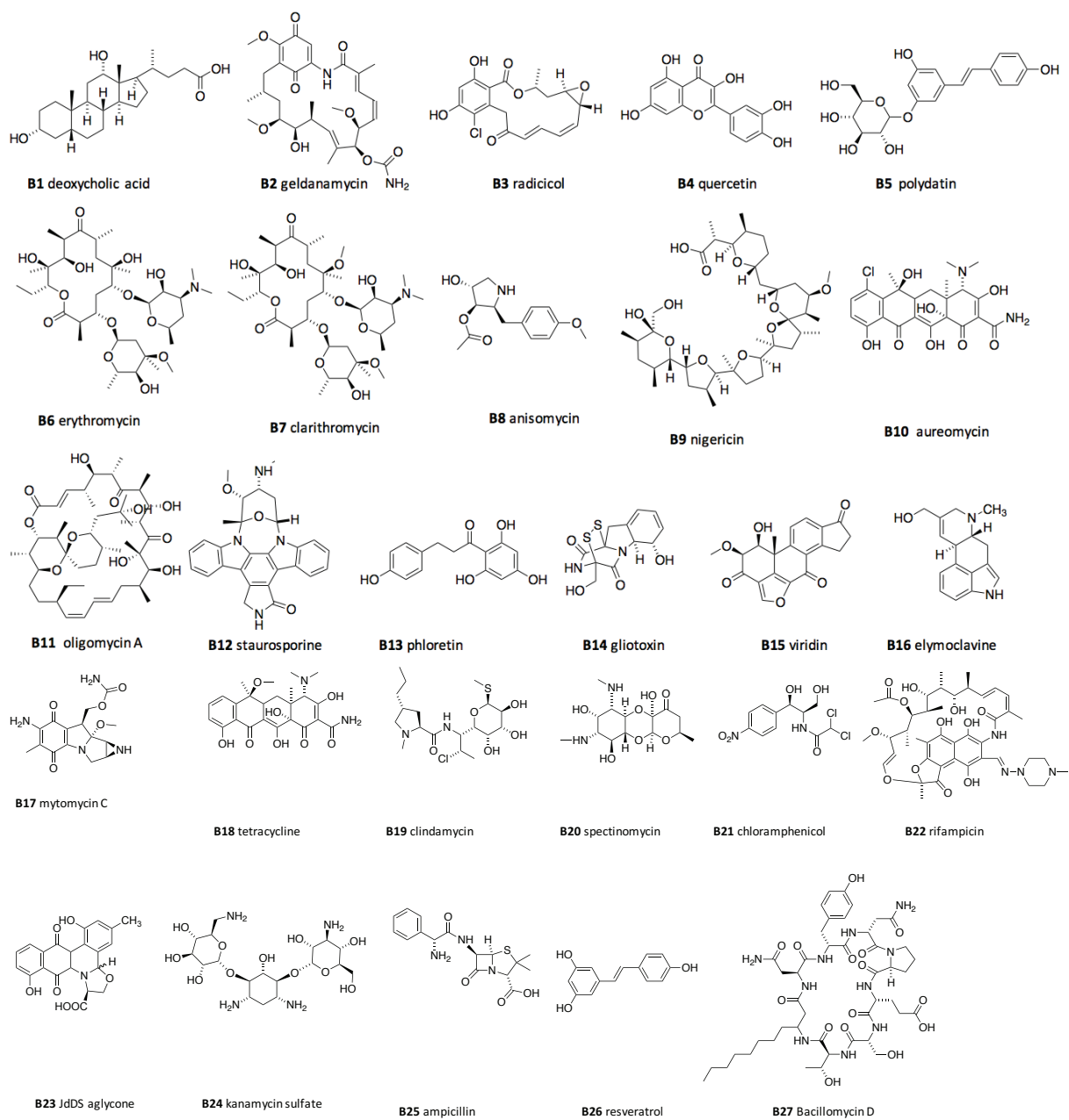


Figure 83. Series B chemical structures for Sv0189 acceptor screening.

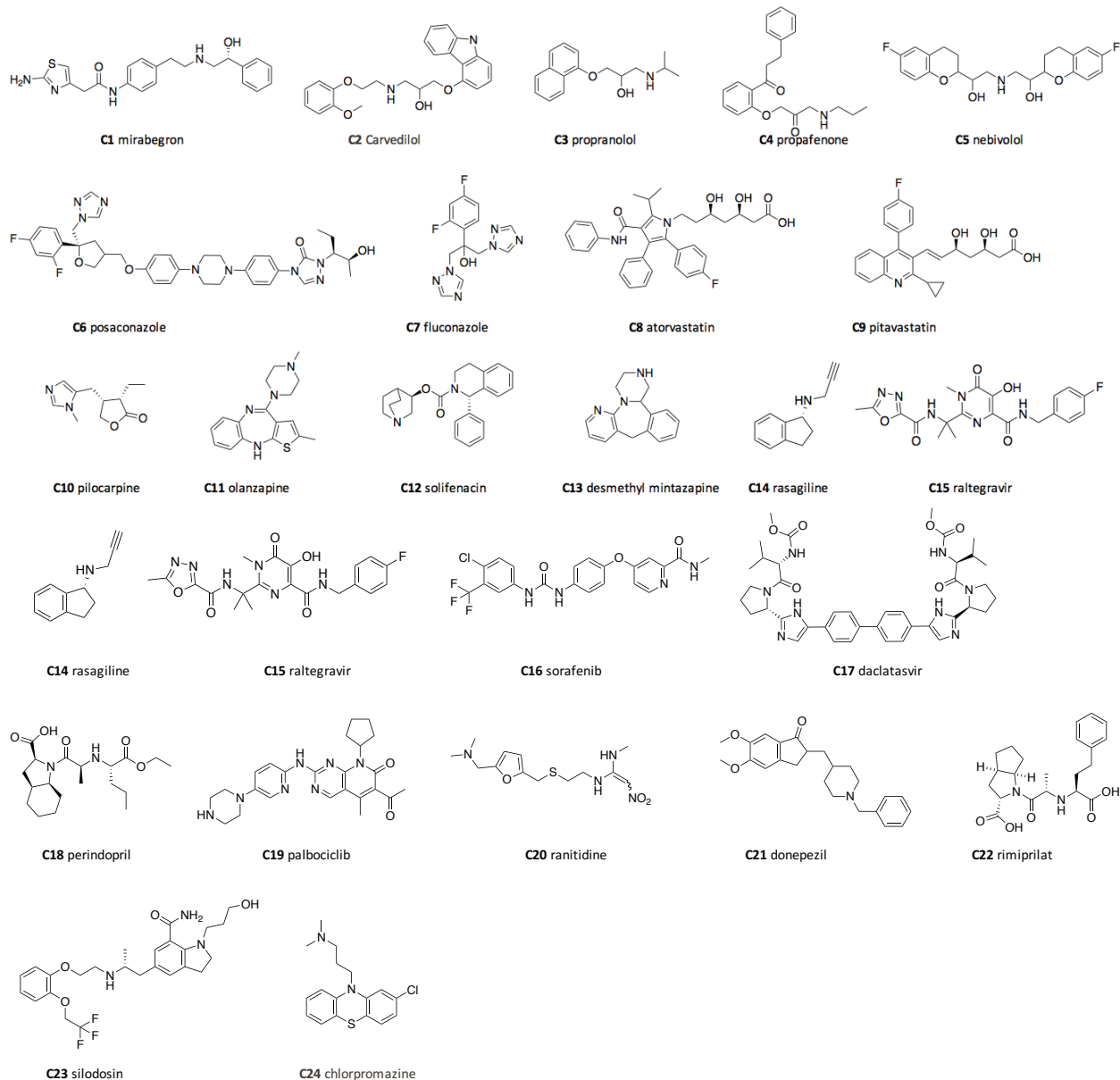


Figure 84. Series C chemical structures for Sv0189 acceptor screening.

4.5.8. Secondary Acceptor Screening

Compounds selected for secondary screening from the initial round were anthrarrufin (A5), alizarin (A14), benzhydrol (A18), resveratrol (B26), fluconazole (C7), purpurin (A12), posaconazole (C6), quinzarin (A15), carvedilol (C2), geldanamycin

(B3), sorafenib (C16), chlorpromazole (C24), tryptophol (A4), 2-naphthalene methanol (A19), desmethyl mirtazapine (C13), phloretin (B13), aureomycin (B10), 4-methylumbelliferone (A11), elymoclavine (B16), staurosporine (B12), quercetin (B4), chrysazin (A13), and anthraflavic acid (A20). Reactions set up in a 96 well plate contained 0.25 mM acceptor, 0.5 mM UDP-Glc, 1 mM MgCl₂, 20 μM Sv0189, 0.002 U CIP, Tris·HCl (50 mM, pH 8.0) to 100 μL. The plates were shaken at room temperature for 40 h. The solutions in the wells were transferred to a 96-well 10 kD MWCO filter, and centrifuged at 3750 rpm, 4 °C, and the flow-through collected in a clean 96 well plate. The filter was washed with 100 μL each methanol and DMSO, collected into the same plate as the initial extract, in an attempt to extract precipitated acceptors from the filter. The filtrate was analysed by HPLC (40 uL injection) using the general method (Section 4.1.4).

4.6. Experimental for Chapter 3.2

4.6.1. *S. venezuelae* Cultures with TFAL

Streptomyces venezuelae ISP5230 VS1099 (genotype $\Delta jadW2::aac(3)IV$)²⁴⁸ spores were stored as 25% glycerol stock at -70 °C (Section 4.1.10); 100 μL of a thawed aliquot was plated to MYM agar with 50 μg mL⁻¹ Apr and incubated at 30 °C for 1-2 weeks. A 1 cm² lawn of *S. venezuelae* VS1099 from these plates was used to inoculate MYM broth and grown overnight at 30 °C with shaking (250 rpm). After 16-18 h, the cloudy culture was centrifuged at 3750 rpm, the supernatant decanted, and the cell pellet re-suspended in MSM broth. This process (pelleting, decanting, and re-suspension) was repeated twice in order to remove traces of nutrient rich media. Finally, the cells were re-suspended in ~20 mL MSM and this cell

suspension was used to subculture MSM supplemented with 9 mM phosphate, 120 mM glucose, and 60 mM TFAL to an OD₆₀₀ value 0.6 ± 0.1 . Autoclaving the MSM media supplemented with TFAL resulted in partial hydrolysis of the amino acid to L-lysine and trifluoroacetate, as observed by ¹⁹F NMR. Cultures were inoculated in triplicate, 3 × 25 mL for small-scale productions, or 8 × 250 mL or 6 × 250 mL for large-scale productions, as indicated. Ethanol was added (7 mL to 250 mL media) immediately to induce jadomycin production, and the cultures were shaken at 30 °C (250 rpm) for a period of two days. At 16 h, the pH of the solution was readjusted to 7.5 by titration with 5 M NaOH. Growth curves were generated by withdrawing 200 μL aliquot from triplicate small-scale production (25 mL) at the indicated time intervals, and measuring OD₆₀₀ values and A₅₂₆. Cells were removed by centrifugation prior to A₅₂₆ readings (Section 4.1.3).

4.6.2. ¹³C-Supplemented Cultures with TFAL Productions

All jadomycin production procedures were as described in Section 4.6.1 with 33.3% of the glucose content of the MSM media substituted with 1-¹³C D-glucose. This fermentation was performed on a 1.5 L scale.

4.6.3. Isolation of Natural Products from TFAL Production

Large-scale (1.5 or 2 L) productions, initiated as described in Sections 4.6.1 and 4.6.2., were left for 30 h prior to work-up, the point at which A₅₂₆ values plateaued. At this time, cells were removed by centrifugation (8500 rpm). The supernatant was filtered through 0.45 and then 0.22 μM Millipore filters. The clarified culture media was passed through a pre-conditioned (methanol followed by H₂O) silica-phenyl column (12 g, SiliCycle). The column was washed with water (1 L total) to remove

water-soluble impurities. Organic material was stripped from the column by washing with 50 mL methanol. The highly pigmented methanol extract was concentrated to ~ 2 mL, and the solution diluted with ethyl acetate (500 mL). The solution was extracted with water (3 × 300 mL). Both the aqueous and organic layers retained a similar pigmented maroon color. Concentration of the aqueous layer yielded 54 mg and the organic layer yield 67 mg. The organic-soluble material, containing the compounds of interest as determined by TLC was fractionated using normal phase silica chromatography (40 g column, Section 4.1.5) using a gradient of methanol: dichloromethane as follows: 5:95 1 CV, linear gradient increase to 50:50 over 5 CV, hold at 50:50 over 2 CV, and final stepwise increase to 100:0 for 2 CV. Two fractions of interest were obtained: A less polar fraction, fraction 1, containing **3.3** and **3.4** was eluted at 95:5 methanol: dichloromethane, and the more polar fraction 2 eluting at 20:80 contained compounds **3.1** and **3.2**. The material from fraction 2 was resolved further by preparatory HPLC using the method outlined in general methods. This produced 9.0 mg **3.1** (from a 2 L production) and 8.8 mg **3.2** (from a 1.5 L ¹³C-supplemented production). The material from fraction 1 was concentrated and taken up in 600 μL methanol-*d*₄. By NMR, there were multiple species present and it was not possible to characterize this mixture. After time, a yellow precipitate formed. The yellow precipitate was collected and washed with cold methanol, to yield 1.3 mg of a mixture of **3.3** and **3.4**. When the fermentation was repeated with 1-¹³C D-glucose, material from fraction 1 was instead purified using the preparatory HPLC method (Section 4.1.7), to yield 0.5 mg of a less pure mixture of the same compounds.

4.6.4. Jadomycin TFAL (**3.1**)

Compound **3.1** was isolated as a dark purple amorphous solid; $^{19}\text{F}\{^1\text{H}\}$ NMR (methanol- d_4 , 470 Hz) δ -77.28 (s, **3.1** 3a*S*), -77.29 (s, **3.1** 3a*R*) ppm; HRMS-ESI⁺ m/z 683.1808 (calculated $\text{C}_{32}\text{H}_{31}\text{F}_3\text{N}_2\text{NaO}_{10}$, 683.1823 found (error 2.13 ppm); TLC R_f 0.7 (5:5:1 ethyl acetate: acetonitrile: water). ^1H and ^{13}C NMR characterization data can be found in Table 13.

4.6.5. Jadomycin TFAL Lactam (**3.2**)

Compound **3.2** was isolated as a deep red-orange amorphous solid; $^{19}\text{F}\{^1\text{H}\}$ NMR (methanol- d_4 , 470 Hz) δ -77.3 ppm; HRMS-ESI⁺ m/z 699.1748 (calculated $\text{C}_{32}\text{H}_{31}\text{F}_3\text{N}_2\text{NaO}_{11}$, 699.1772); TLC R_f 0.6 (5:5:1 ethyl acetate: acetonitrile: water). ^1H and ^{13}C NMR characterization data can be found in Table 14.

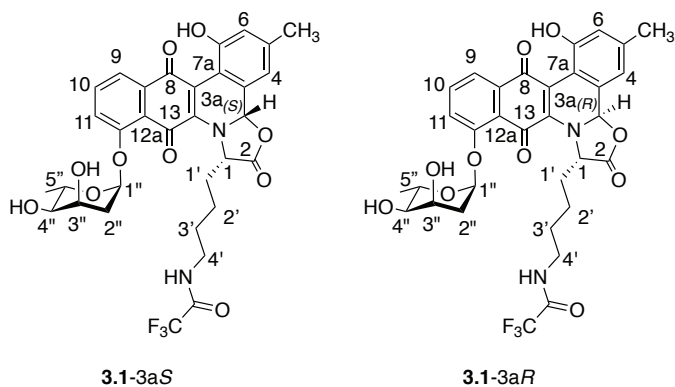
4.6.6. Jadomycin Furan Aldehyde (**3.3**)

Compound **3.3**, isolated in a mixture with **3.4**, was isolated as a bright yellow amorphous solid; HRMS; HRMS-ESI⁺ m/z 459.1050 (calculated $\text{C}_{24}\text{H}_{20}\text{NaO}_8$, 459.1050); TLC R_f 0.42 (5:95 methanol:dichloromethane). ^1H and ^{13}C NMR characterization data can be found in Table 15.

4.6.7. Jadomycin Furan Alcohol (**3.4**)

Compound **3.4**, isolated in a mixture with **3.3**, was isolated as a yellow colored solid; HRMS-ESI⁺ m/z 461.1189 (calculated $\text{C}_{24}\text{H}_{22}\text{NaO}_8$, 461.1207); TLC R_f 0.36 (5:95 methanol: dichloromethane). ^1H and ^{13}C NMR characterization data can be found in Table 16.

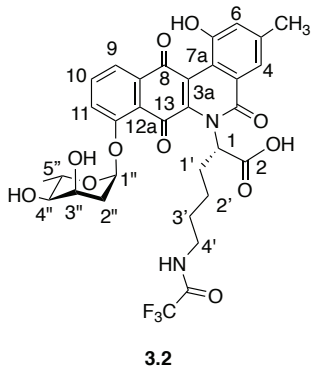
Table 13. NMR characterization data for **3.1**.



3.1 3aS (major)				3.1 3aR (minor)	
position	δC , type	δH (<i>J</i> in Hz)	HMBC	δC	δH (<i>J</i> in Hz)
1	67.7, CH	5.26, bs		64.4	5.37, bs
2	176.3, C			177.4	
3a	89.4, CH	5.67, s	1, 1', 3b, 4, 7, 7a	85.8	5.72, s
3b	130.7, C			130.6	
4	120.5, CH	6.71, s	3a, 3b, 5-CH ₃ , 6, 7	120.1	6.76, s
5	141.4, C			141.4	
					2.36, s
5-CH ₃	20.8, CH ₃	2.34, s		20.8	
6	120.3, CH	6.8, s	4, 5-CH ₃ , 7, 7a	120.5	6.83, s
7	155.9, C			154.5	
7a	114.2, C			114.3	
7b	^a 130.8, C			^a 130.6	
8	183.5, C			183.9	
8a	136.1, C			136.2	
9	120.4, CH	7.52, (8.3)	^d 8, 8a, 10, 12	121.2	7.52, obs
10	136.1, CH	7.69, t (8.3)	8a, 9, 11, 12	135.7	7.66, t (8.0)

3.1 3aS (major)				3.1 3aR (minor)	
position	δC , type	$\delta\text{H}(J$ in Hz)	position	δC	$\delta\text{H}(J$ in Hz)
11	121.0, CH	7.80, (8.3) d	8a, 10, 12, 13	121.2	7.8, obs
12	155.5, CH			155.5	
12a	^a 136.7 C			^a 136.5	
13	185.6, C			183.9	
13a	^a 155.7, C			^a 155.5	
1'	29.8, CH ₂	2.36, 2.14, m	2, 2'	29.5	1.96, 2.24
2'	25.05, CH ₂	1.41, obs	1', 3', 4'	25.25	2.24, obs
3'	29.75, CH ₂	1.61, obs	1', 2', 4'	29.5	1.55, obs
4'	40.6, CH ₂	3.34, t (7.5)	2', 3', 5'	40.5	1.58, obs
5'	158.8, C			158.8	3.31, obs
6'	^b CF ₃			^b CF ₃	
1"	96.5, CH	5.93, bm	3", 12	96.2	5.93, bm
2"	36.2, CH ₂	2.43, (15.2, 2.2); 2.21, (15.2, 3.5) dd dt	3", 4", 1"	33.5	2.55, obs; 2.35, obs
3"	68.2, CH	4.07, m	1", 5"	68.5	4.11, m
4"	73.9, CH	3.27, (9.9, 3.2) dd	5", 5" CH ₃	73.7	3.31, obs
5"	66.1, CH	3.95, m	4", 5"-CH ₃	65.7	4.02, m
5"-CH ₃	18.2, CH ₃	1.21, (6.2) d	1", 4", 5"	18.2	1.19, d (6.1)

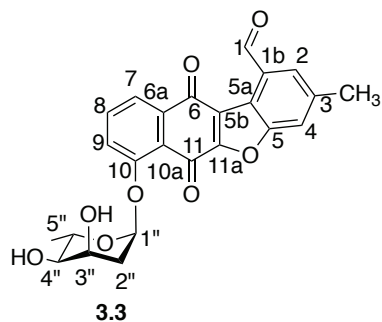
^aassignment by ¹³C-NMR only, resonances may be interchangeable; ^bsignal not identified.

Table 14. NMR characterization data for **3.2**.

position	δ C, type	δ H(<i>J</i> in Hz)	HMBC
1	64.0, CH	5.57, bs	2, 3a, 7
2	176.1, C		
3a	165.0, C		
3b	^a 135.6, C		
4	^c 121.5, CH	7.83, obs	3a, 6, 7, 8
5	142.6, C		
5-CH ₃	21.1, CH ₃	2.44, s	4, 5, 6, 7a
6	^c 124.9, CH	7.15, d (1.5)	4, 5-CH ₃ , 7, 7a
7	153.0, C		
7a	^c 118.7, C		
7b	^a 130.0, C		
8	^c 187.1, C		
8a	135.5, C		
9	^c 121.5, CH	7.83, obs	8, 8a, 10, 11
10	135.6, CH	7.71, t (8.3)	8a, 9, 11, 12
11	^c 121.2, CH	7.6, d (8.3)	8a, 9, 10, 12, 13
12	153.0, CH		
12a	^{a, c} 122.3, C		
13	182.3, C		
13a	^{a, c} 118.7, C		
1'	35.4, CH ₂	2.74, m; 2.15, obs	2

position	δC , type	δH (J in Hz)	HMBC
2'	26.7, CH ₂	1.57, obs; 1.72, obs	3', 4'
3'	29.7, CH ₂	1.67, m	2', 4'
4'	40.5, CH ₂	3.31, obs	2', 3', 5'
5'	156, C		
6'	159, CF ₃		
1''	^c 97.3, CH	5.84, d (2.8)	3'', 12
2''	36.2, CH ₂	2.67, bd(14.8); 2.14, obs	1'', 3'', 4''
3''	68.2, CH	4.08, q (3.1)	4'', 5''
4''	74.4, CH	3.25, dd (9.6, 2.7)	3'', 5'', 5''-CH ₃
5''	66.2, CH	4.00, dq (10.2, 6.4)	1'', 3'', 4'', 5''-CH ₃
5''-CH ₃	^c 18.2, CH ₃	1.19, d (6.2)	1'', 4'', 5''
2-OH		^d 11.92, bs	

^aassignment by ¹³C-NMR only, resonances may be interchangeable; ^b signal not identified; ^c indicates a ¹³C-enriched position when cultured with 1-¹³C glucose; ^d acetone-*d*₆ solvent

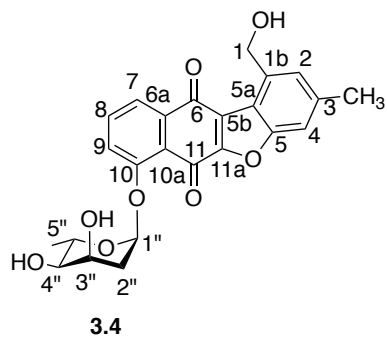
Table 15. NMR characterization data for **3.3**.

position	δ C, type	δ H(J in Hz)	HMBC
1	195.2, C	11.37, s	1b, 2
1b	132.8, C		
2	127.8, CH	8.02, s	1, 4, 3, 5a, 5-CH ₃
3	142.2, C		
3-CH ₃	22.9, CH ₃	2.60, s	2, 3, 4
4	119.5, CH	7.69, s	2, 3, 5, 5a, 5-CH ₃
5	157.8, C		
5a	123.1, C		
5b	116.4, C		
6	180.6, C		
6a	119.9, C		
7	123.1, CH	7.91, d (7.5)	5b, 6, 6a, 8, 9
8	137.3, CH	7.67, t (8.1)	7, 9, 10, 10a
9	121.7, CH	7.55, d (8.4)	6a, 7, 8, 10, 11
10	157.7, C		
10a	136.4, C		
11	177, C		
11a	^a C		
1''	95.2, CH	5.94, d (2.9)	3'', 10
2''	36.6, CH ₂	2.55, obs; 2.24, obs	1'', 3'', 4''
3''	67, CH	4.19, obs	1''

position	δC , type	δH (J in Hz)	HMBC
4"	73.7, CH	3.28, obs	
5"	67.5, CH	3.87, m	
5"-CH ₃	19.0, CH ₃	1.30, d (6.2)	3", 4"
1-OH			
3"-OH		5.26, d (10.0)	
4"-OH		3.13, d (10.4)	

^asignal not identified.

Table 16. NMR characterization data for **3.4**.



position	δC , type	δH (J in Hz)	HMBC
1	65.7, CH ₂	4.97, bs	1b, 2
1b	119.4, C		
2	130, CH	7.25, s	1, 3, 4, 5a, 5-CH ₃
3	142.3, C		
3-CH ₃	23.1, CH ₃	2.52, s	2, 3, 4
4	113.8, CH	7.37, s	2, 3, 5, 5a, 5-CH ₃
5	158.6, C		
5a	118.4, C		
5b	^a C		
6	183.2, C		
6a	119.9, C		
7	123.2, CH	7.83, d (7.5)	6a, 9
8	137.1, CH	7.59, t (8.0)	10, 10a
9	121.6, CH	7.52, d (8.5)	6a, 7, 10, 10a, 11
10	157.6, C		
10a	136.2, C		
11	176.6, C		
11a	^a C		
1''	95.2, CH	5.93, d (3.0)	3'', 10
2''	36.3, CH ₂	2.56, obs; 2.26, obs	
3''	67, CH	4.19, obs	

position	δC , type	$\delta H(J$ in Hz)	HMBC
4"	73.7, CH	3.29, obs	
5"	67.0, CH	3.90, obs	
5"-CH ₃	19.0, CH ₃	1.32, d (6.2)	3", 4"
1-OH		4.44, s	
3"-OH		5.31, d (10.2)	
4"-OH		3.13, obs	

^asignal not identified.

4.6.8. Microbroth Antimicrobial Assay

All microbroth antibiotic susceptibility testing was carried out in 96 well plates in accordance with Clinical Laboratory Standards Institute testing standards²⁵⁵ using the following pathogens: methicillin-resistant *Staphylococcus aureus* ATCC 33591 (MRSA), *S. warneri* ATCC 17917, vancomycin-resistant *Enterococcus faecium* EF 379 (VRE), *Pseudomonas aeruginosa* ATCC 14210, *Proteus vulgaris* ATCC 12454, and *Candida albicans* ATCC 14035. Compounds were tested in three replicates against each organism. Compounds were serially diluted to generate a range of concentrations in a final well volume concentration of 2% DMSO. Each plate contained eight uninoculated positive controls (media with 2% DMSO), eight untreated negative controls (Media with 2% DMSO + organism), and one column containing a concentration range of a control antibiotic (vancomycin for MRSA and *S. warneri*, rifampicin for VRE, gentamycin for *P. aeruginosa*, ciprofloxacin for *P. vulgaris*, or nystatin for *C. albicans*). The optical density of the plate was recorded on a BioTek Synergy HT plate reader at 600nm at time zero and then again after incubation of the plates for 22 h at 37 °C. After subtracting the time zero OD₆₀₀

from the final reading the percentages of microorganism survival relative to vehicle control wells were calculated and the IC₅₀ was determined.

4.6.9. Cell Toxicity Assay

Human foreskin BJ fibroblast cells (ATCC CRL-2522) and *Cercopithecus aethiops* kidney epithelial cells (Vero, ATCC CCL-81) were grown and maintained in 15 mL of Eagle's minimal essential medium (Sigma M5650) supplemented with 10% fetal bovine serum (VWR) and 100 µU penicillin and 0.1 mg/mL streptomycin (VWR) in T75cm² cell culture flasks (VWR) at 37 °C in a humidified atmosphere of 5% CO₂. Culture medium was refreshed every two to three days and cells were not allowed to exceed 80% confluency. At 80% confluency, the cells were counted, diluted and plated into 96 well treated cell culture plates (VWR) at a cell density of 10000 cells per well in 90 µL of growth medium (minus the addition of antibiotics). The plates were incubated at 37 °C in a humidified atmosphere of 5% CO₂ to allow cells to adhere to the plates for 24 h before treatment. DMSO was used as the vehicle at a final concentration of 1% in the wells. All tested compounds were resolubilized in sterile DMSO (Sigma) and a dilution series was prepared for each cell line, added to the respective assay plate, and plates were incubated at 37 °C in a humidified atmosphere of 5% CO₂ for 24 h. All samples were tested in triplicate. Each plate contained eight un-inoculated positive controls (media with 1% DMSO), eight untreated negative controls (media with 1% DMSO + cells), and a concentration range of a positive cytotoxin control (zinc pyrithione for fibroblast cells and phenoxyethanol for kidney cells). Alamar blue (Invitrogen) was added 24 h after treatment, to each well at 10% of the culture volume (11µL in 100 µL).

Fluorescence was monitored using a BioTek Synergy HT plate reader at 530/25 excitation, 590/35 emission at both time zero and 4 h after Alamar blue was added. After subtracting the time zero emission 590 nm measurements from the final reading, the inferred percentage of microorganism survival relative to vehicle control wells were calculated and the IC₅₀ was determined.

4.6.10. NCI-60 Cancer Cell Line Screening

Compounds **3.1**, **3.2**, and the mixture of **3.3** and **3.4** were submitted to the National Cancer Institute's Developmental Therapeutics NCI-60 Human Tumor cell lines screen. See https://dtp.cancer.gov/discovery_development/nci-60/methodology.htm (accessed May 31 2016) for detailed experimental procedures. **3.1** was rejected for screening. Compounds **3.2** and the mixture **3.3** and **3.4** were not selected for further screening after the one-dose NC-60 cell panel. The results of the initial one-dose screen are included in Appendix E.

4.7. Experimental for Chapter 3.3

4.7.1. Culture Conditions for Small Scale Jadomycin Productions

A small path of cells from a well-sporulated plate (1 week of growth) was used to inoculate MYM (2 × 25 mL) and grown overnight at 30 °C with agitation (250 rpm). The cells were pelleted in a 50 mL falcon tube by centrifugation at 3750 rpm (4 °C) for 10-30 min. The cells were washed twice with MSM (~30 mL), and re-suspended in 5 mL MSM. This cell suspension was used to inoculate MSM (3 × 25 mL) supplemented with D-serine (60 mM), D-glucose (33 mM) and phosphate (50 μM) to an initial optical density (OD₆₀₀) value of ~0.6. Immediately, ethanol (750 μL per 25

mL) was added to each flask to stimulate jadomycin production. Cultures were kept at 30 °C with agitation (250 rpm) for 48 h. Growth curves were generated by withdrawing 200 µL aliquot from triplicate small-scale production (25 mL) at the indicated time intervals, and measuring OD₆₀₀ values and A₅₂₆. Cells were removed by centrifugation prior to A₅₂₆ readings (Section 4.1.3).

4.7.2. Work-up for Small Scale Jadomycin Productions

For each strain evaluated, 50 mL of the culture media was collected at 48 h. The cells were pelleted at 8000 rpm for 10-15 min and the supernatant passed through 0.45 µM filters. Cells were discarded. The supernatant was applied to a 2 g silica phenyl column (SiliCycle) that had been preconditioned with methanol (10 mL), followed by water (30 mL). The column was then washed with water (50 mL), and subsequently the coloured material bound to the column was eluted with methanol (10 mL). The methanol extract was concentrated and the recovered mass was determined for each strain: 10.4 mg material was obtained from the *ΔjadT* strain, 5.7 mg from the *S. venezuelae ΔjadSΔjadT* strain 7.2 mg from the *S. venezuelae Δsv0189* strain, and 3.0 mg from the *S. venezuelae ΔjadTΔsv0189* strain. The extracts were analyzed by TLC (Section 4.1) and HPLC (Section 4.1.4).

4.7.3. Scale-Up Jadomycin Production with *S. venezuelae ΔjadT*

A 1 × 1 cm lawn of *S. venezuelae ΔjadT* was used to inoculate 250 mL MYM media (2 × 250 mL in 1 L flasks). Growths were incubated at 30 °C with agitation (250 rpm) for 16-24 hours. The cell suspension was centrifuged at 3750 rpm (4 °C) for 30-45 min. The supernatant was removed and the cell pellet was washed with 60 mL

MSM without amino acid. The washing step was repeated more than twice to remove all of the nutrient rich MYM. The cell pellet was re-suspended in 100 mL MSM without amino acid. Autoclaved MSM media containing D-serine (60 mM, 4 × 250 mL in 1 L flasks) were supplemented with glucose (to a final concentration of 33 mM) and phosphate (to a final concentration of 50 μM) before being inoculated with the pre-growth *S. venezuelae* Δ *jadT* cell suspension to an initial OD₆₀₀ of 0.6. Growths were ethanol shocked using 100% ethanol (3% v/v) and incubated at 30 °C with agitation (250 rpm) for 48 hours. The pH of the media was readjusted to 7.5 after 24 hours with 5 M NaOH.

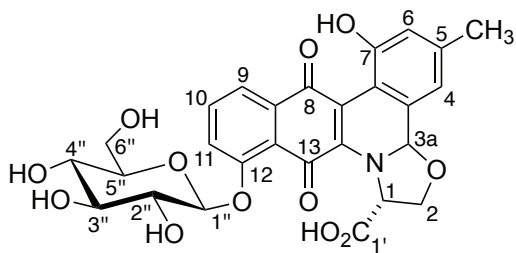
4.7.4. Extraction of Natural Products from Bacterial Cultures

Bacterial cells were removed by suction filtration through Whatman No. 5 filter paper, followed by 0.45 μm then 0.22 μm Millipore Durapore[®] membrane filters. The clear media was then passed through a reversed-phase SiliCycle[®] phenyl column (20 g), and washed with distilled water until flow-through was colorless (~2-4 L) to remove all water-soluble material. Material was eluted from the column with 100% methanol and dried *in vacuo* to yield 20 mg crude material.

4.7.5. Purification of Glucosylated Jadomycin DS (3.9)

A new purple compound of interest was observed by TLC analysis ($R_f = 0.2$, dichloromethane: methanol 8:2) when compared to previously isolated jadomycin DS ($R_f = 0.5$). The compound was isolated using normal phase chromatography (Section 4.1.5). The crude extract was brought up in a minimal volume of methanol and dichloromethane, and applied to a 40 g silica column preconditioned with methanol and dichloromethane. Isolation of the compound was accomplished using

a gradient system comprised of methanol and dichloromethane with a flow rate of 30 mL/min with collection of 6 mL fractions. To start, an initial isocratic gradient step using dichloromethane (4 column volumes (CV)) was performed. This was followed by a linearly increasing gradient of 0% to 20% methanol over 5 CV, which was then followed by an flat gradient of 40% methanol over 5 CV. Fractions of interest were identified visually for colour, and combined based on TLC analysis for the presence of the compound of interest. Combined fractions were concentrated to yield 3 mg of crude glucosylated jadomycin **3.9**. TLC analysis ($R_f = 0.2$, dichloromethane: methanol, 8:2).; LRMS (ESI⁺): MS/MS (556) found 556 [M+H]⁺, 394 [M+H-C₆H₁₀O₅]⁺; HRMS (ESI⁻): C₂₇H₂₄NO₁₂ requires 554.1304, found 554.1286. UV-Vis (1.6 × 10⁻³ and 2.0 × 10⁻⁴ M, methanol): λ_{max} = 285, 380, 520. ¹H and ¹³C NMR characterization data can be found in Table 17.

Table 17. NMR characterization data for **3.9**.**3.9**

Position	δC , type	δH (<i>J</i> in Hz)	HMBC
1	63.8, CH	5.14, dt (8.2, 1.3)	2a, 2b
2-a	72.4, CH ₂	4.77, t (8.5)	1, 2b
2-b		4.18, t (8.5)	1, 2a
3a	89.8, CH	5.78, s	
3b	130.5, C ^a		
4	120.6 CH	6.72, s	5,6
5	141.6, C		
5-CH ₃	21.4, CH ₃	2.31, s	4,6
6	116.6, CH	6.80, s	4,5
7	154.4, C		4
7a	112.8, C		4,6
7b	130.5, C ^a		
8	180.7, C		9
8a	136.5, C		10
9	122.0, CH	7.82, d (7.5)	10, 11
10	136.9, CH	7.68, t (8.1)	9, 11, 1''
11	121.5, CH	7.47, d (8.4)	9, 10
12	157.7, C		10, 11, 1''
12a	137.1, C		9
13	181.2, C ^a		
13b	C ^b		
1'	175.0, C		1, 2b
1''	104.7, CH	5.01, d (7.5)	10, 11
2''	75.3, CH	3.62, t (8.4)	3''
3''	71.4, CH	3.43, t (9.2)	2''

Position	δC , type	δH (<i>J</i> in Hz)	HMBC
4"	77.9, CH	3.48, t (9.2)	5"
5"	78.6, CH	3.52, ddd (9.2, 5.8, 2.2)	4"
6"-a	63.1, CH ₂	3.96, dd (12.1, 5.8)	5"
6"-b		3.74, dd (12.1 2.2)	3"

^aAssigned by ¹³C NMR only; ^bSignal not identified.

4.7.6. Preparation of conjugation vector pKC1139 $\Delta sv0189$

A 0.9 kb region upstream of *sv0189* was amplified from *S. venezuelae* (ISP5230) genomic DNA using primers P5 and P6.

P5: 5'-GGTGGTAAGCTTGTGTCCACGACCACCGAAAG-3' (HindIII site is underlined)

P6: 5'-CTGGATCTCCCGTGCGGAccacagtagacgagacgatacgTATC-3' (32 bp overlap region is underlined)

A 1.3 kb downstream region was similarly amplified using P7 and P8.

P7: 5'-CTCGTCTACTGTGGTCCGCACGGGAGATCCAGGAGTCCATG-3' (32 bp overlap region is underlined)

P8: 5'-GGTGGTCTAGACGGTGAAGGGATTCGGCGTGAC-3' (XbaI site is underlined)

The upstream and downstream PCR fragments were used as the template for overlap extension PCR amplification with the outer primers (P5 and P8) to produce the 2.2 kb deletion cassette. The deletion cassette was digested with HindIII and XbaI in preparations for ligation with linearized (HindIII/XbaI) pK1139 (Section 4.1.15). The plasmid was isolated using a miniprep kit (Section 4.1.18). Screening by

restriction digestion with HindIII and XbaI was used to confirm conjugal vector pKC1139 $\Delta sv0189$.

4.7.7. Preparation of conjugation vector pKC1139 $\Delta jadS\Delta jadT$

Regions upstream and downstream of the genes *jadS* and *jadT* site were amplified from *S. venezuelae* (ISP5230) genomic DNA. The 1.3 kb upstream fragment was amplified using primers P9 and P10.

P9: 5'-GCAGAAAGCTTGACCAGGTCCGCAACACG-3' (HindIII site is underlined)

P10: 5'-CCTGCATGGTCGTCGTCACTTCTAGACATGGTTCTCTCTCCGC-3'
(XbaI site is underlined)

A 1.1 kb downstream region was similarly amplified using primers P11 and P12:

P11: 5'-GCGGAGAGAGAACCATGTTCTAGAAGTGACGACGACCATGCAGG-3'
(XbaI site is underlined)

P12: 5'-GCTGATGAATTCGGTCGTACTCGCCCTGC-3' (EcoRI site is underlined)

Cloning procedures were identical to those described for the assembly of pKC1139 $\Delta sv0189$ (Section 4.7.6), with the following exception: the upstream and downstream PCR fragments were successively ligated to pKC1139 using XbaI/EcoRI and XbaI/HindIII restriction sites, respectively.

4.7.8. Generation of *S. venezuelae* $\Delta jadS\Delta jadT$, *S. venezuelae* $\Delta jadT\Delta sv0189$, and *S. venezuelae* $\Delta sv0189$ strains

S. venezuelae $\Delta jadT$ ⁵⁹ or *S. venezuelae* ISP5230 served as recipients and *E. coli* ET12567 pUZ8002 harbouring pKC1139 $\Delta sv0189$ or pKC1139 $\Delta jadS\Delta jadT$ as the

conjugal donor. See Section 4.1.21 for conjugation protocol. Colonies identified as having acquired sensitivity to Apr were screened by PCR using isolated genomic DNA extraction (Section 4.1.12) with primer pairs P5 and P8, and P1 and P4 to identify single deletion mutants (*S. venezuelae* $\Delta sv0189$) and double deletion mutants (*S. venezuelae* $\Delta jadT\Delta sv0189$), respectively, and P13 and P12 were used for identifying *S. venezuelae* $\Delta jadS\Delta jadT$ double deletion mutants.

P13: 5'-CTGGAGGAGAAGCCGGAGCACC-3'

4.8. Experimental for Chapter 3.4

Streptomyces-E. coli conjugation experiments (Sections 4.1.21) were carried out as described in the general methods.

4.8.1. Assembly of pKC1139::*jadUV*

The 1 kb upstream region “*jadU*” was amplified by PCR using primers P14 and P15.

P14: 5'-GGTGGTGAATTCATCACCCGCTGCTCCAACAACACTAC-3' (EcoRI site underlined)

P15:

5'GGTGGTAGGCCTCATATGTCTAGATCACAGCAGTTCCTCCAGCTTGC-3'
(NdeI, XbaI, StuI sites underlined)

The downstream 1.1 kb region “*jadV*” was amplified using P16 and P17.

P16: 5'-GGTGGTTCTAGACATATGAGGCCTCCGCCACCACCGGACAGAC-3'
(NdeI, XbaI, StuI sites underlined)

P17: 5'-GGTGGTAAGCTTGGCTGTTCTCGGCCTTCGACAGCTT-3' (HindIII site underlined)

The PCR products were purified using a gel extraction kit (QIAquick® gel extraction kit, Qiagen). An overlap extension PCR reaction to unify the “*jadU*” and “*jadV*” fragments was performed using the purified PCR products as template DNA with the outermost primers, P14 and P17. The resulting 2.5 kb *jadUV* PCR product was ligated (Section 4.1.15) with pCK1139 using restriction sites EcoRI and HindIII. The plasmid was isolated using a miniprep kit (Section 4.1.18). Plasmids were screened by EcoRI and HindIII double restriction digests to confirm pKC1139::*jadUV*.

4.8.2. Assembly of pKC1139::*kijC3*

The *kijC3* gene was retrieved from pUC57::*kijC3* (BioBasic) by restriction digest with StuI and XbaI. The 1.2 kb band was excised using a gel extraction kit (BioBasic), following manufacturer protocols exactly. Because the XbaI site in pKC1139_*jadUV* is blocked by methylation, the plasmid was passed through methylation deficient *E. coli* ET12567 pUZ8002 prior to digestion with XbaI and StuI. Ligation was performed following the general protocol (Section 4.1.15). The plasmid was isolated using a miniprep kit (Section 4.1.18). The plasmid was treated with EcoRI and NcoI restriction digest enzymes to confirm pKC1139::*kijC3*.

4.8.3. Assembly of pKC1139::*kijC4*

The gene *kijC4* was cloned from *A. kijaniata* genomic DNA using P18 and P19.

P18: 5'-GATGATGCTAGCCGGAGCTCCTTCGGTGGGAGG-3' (NheI site underlined)

P19: 5'-GATGATCATATGATGCGCATCCTGTTCACCCCGCTCC-3' (NdeI site underlined)

The 1.3 kb PCR product and vector pKC1139::*jadUV* were digested with NdeI and NheI in preparation for ligation following the usual procedure (Section 4.1.15). The plasmid was isolated using a miniprep kit (Section 4.1.18). The plasmid was using an FspI restriction digest to confirm pKC1139::*kijC4kijC3*.

4.8.4. Assembly of pKC1139::*kijC4kijC3*

The sequential genes *kijC4* and *kijC3* were cloned from *A. kijaniata* genomic DNA using P20 and P21.

P20: 5'-GATGATGCTAGCTCAGACCAGGGCTTCGAGGG-3' (NheI site underlined)

P21: 5'-GATGATCATATGATGCGCATCCTGTTCACCCCGCTCC-3' (NdeI site underlined)

The 2.5 kb PCR product and vector pKC1139::*jadUV* were digested with NdeI and NheI in preparation for ligation (Section 4.1.15). Evaluation of the isolated plasmid (Section 4.1.18) by restriction digest with FspI confirmed successful assembly of pKC1139::*kijC4kijC3*.

4.8.5. Assembly of pKC1139::*kijC4*(*XhoI*)

A QuikChange Lightning Site-Directed Mutagenesis Kit (Agilent, catalogue 210518) was used to introduce a two-base pair frame shift restoring the natural frame of *jadV* relative to the other genes in the dideoxy biosynthetic gene cluster using primers P22 and P23.

P22: 5'-CGAAGGAGCTCCGGCTAGCTCGAGAGGCCTCCGCCACCACC-3'

P23: 5'-GGTGGTGGCGGAGGCCTCTCGAGCTAGCCGGAGCTCCTTCG-3'

(*XhoI* site is underlined)

Methylated pKC1139::*kijC4* was used as the template. Protocols for mutagenesis were as suggested by the manufacturer with reaction conditions as follows: 5 μ L QuickChange Lightning buffer (10 \times), 5 μ L pKC1139::*kijC4* (various dilutions; 10^0 , 10^{-1} , 10^{-2}), 125 ng P22, 125 ng P23, 1 μ L dNTP mix, 1.5 μ L Quick solution reagent, 1 μ L QuickChange Lightning enzyme, and water to 50 μ L. The cycling protocol used was described in Section 4.5.3. After completion of the cycling protocol, 2 μ L DpnI restriction enzyme was added to the reaction and incubated at 37 $^{\circ}$ C for 5 min. NEB[®] 5-alpha competent *E. coli* cells were transformed with 2 μ L of the reaction mixture (Section 4.1.17). Screening of isolated plasmids (Section 4.1.18) was performed by restriction digestion with *XhoI* to confirm the desired construct, pKC1139::*kijC4*(*XhoI*) .

4.8.6. Assembly of pKC1139 Δ *jadV*

For construction of a deletion cassette, a 1.1 kb region *jadR** region downstream of *jadV* was amplified by PCR using primers P24 and P25.

P24: 5'-GATGATTCTAGATTCAGCGCGAGCGGCGCGGAGGAGCACTTCG-3'
(XbaI site underlined)

P25: 5'-GATAAAGCTTCCACTCGGCGTACAGGTAGTCGATGGCGTTC-3'
(HindIII site underlined)

The PCR product was then digested with HindIII and XbaI. pKC1139::*jadUV* was digested with HindIII and XbaI to prepare the vector. The linearized vector and 1.1 kb insert were ligated following the standard protocol (Section 4.1.15). Plasmids were isolated using a Miniprep kit (Section 4.1.18). Isolated plasmids were digested with EcoRI and HindIII to confirm successful assembly of pKC1139 Δ *jadV*.

4.8.7. Assembly of pSE34::*kijC4*

The gene *kijC4* was cloned from genomic *A. kijaniata* DNA using primers P26 and P27.

P26: 5'-GATTCTAGAAAGGAGGTAGGCCATGCGCATCCTG-3' (XbaI site underlined)

P27: 5'-GATAAAGCTTTCAGGCGGTCAGTTCCTGG-3' (HindIII site underlined)

The 1.2 kb PCR product and vector, pSE34, were each digested with HindIII and XbaI. Standard ligation procedures (Section 4.1.15) were followed. Plasmids were isolated using a miniprep kit (Section 4.1.18). Screening of plasmids was performed by restriction digestion with HindIII and XbaI to confirm assembly of pSE34::*kijC4*.

4.8.8. Protoplast Formation Protocol

Protoplast transformation procedures are adapted from the literature.^{233, 243} A 25 mL overnight *S. venezuelae* culture in MYEME was harvested by centrifugation at 4 °C, 5000 rpm for 10 min. The pellet was washed with 2 × 10 mL 7.32% mannitol. The pellet was suspended in 4 mL P buffer with 2 mg/mL lysozyme and then incubated for 2 h at 30 °C with gentle shaking every half hour. The protoplast solution was diluted with 6 mL B buffer, filtered through cotton wool and collected in a sterile 50 mL falcon tube. The filtered solution was pelleted by centrifugation at 4 °C, 5000 rpm, 10 min, and the cell pellet washed twice with 5 mL P buffer. The protoplast pellet was re-suspended in 400 µL P buffer.

4.8.9. *S. venezuelae* ISP5230 Protoplast Transformation with pSE34::*kijC4*

Prior to use in protoplast transformations, the incoming vector (pSE34::*kijC4*) was passed through *E. coli* ET12567 pUZ80002. To 100 µL protoplast suspension was added 10 µL of pSE34::*kijC4* (various dilutions 10⁰, 10⁻¹, 10⁻²) and 100 µL 25% polyethylene glycol-1000 in P buffer. The mixture was incubated at room temperature for 2 min. Aliquots (150 µL) of this solution were spread on R5N agar plates that were pre-dried in the sterile hood for four hours. The plates were incubated over night at 30 °C, and then a 1 mL of a soft nutrient agar overlay containing 25 µg/mL Tsr was applied to the plates. Exconjugants were visible within four days, with some evidence of sporulation (white plaque formation) along with deeply coloured red-brown diffusible pigment in the agar. Twenty colonies were patched to MYM-Tsr, and incubated again at 30 °C. One colony showed

growth after this time, and this colony was patched to MYM-Tsr again and incubated for 2 days. Due to the low number of hits from the initial screen, colonies from the original protoplast transformation were scraped, suspended in 100 μ L sterile water, and streaked onto MYM-Tsr, which yielded 12 colonies after four days. Spores were isolated and streaked for single colonies from the colonies grew well on MYM-Tsr. Two of the resulting strains possessed a sporulating phenotype, and were screened using colony PCR, however a strain carrying pSET34::*kijC4* was not identified.

4.8.10. Small-Scale Jadomycin Production with Complemented Mutants (Method 1)

The same procedures described in Section 4.7.1 and 4.7.2 were followed for cultures of *S. venezuelae* complementation mutants with the indicated amino acid: *S. venezuelae*::*kijC3* with DS, ABA, TFAL; *S. venezuelae*::*kijC4* with DS, L-Ile, L-Phe; *S. venezuelae*::*kijC4(XhoI)* with DS; *S. venezuelae*::*kijC3kijC4* with DS; *S. venezuelae* Δ *jadV* with DS. The concentrated methanol extracts after the silica-phenyl column step from 50 mL of culture gave 2-7 mg of material that was further evaluated by TLC (Section 4.1), HPLC (Section 4.1.4.), and LCMS (Section 4.1.2.).

4.8.11. Scaled-Up Production with *S. venezuelae*::*kijC4*

MYM (2 \times 250 mL) was inoculated with *S. venezuelae*::*kijC4* and grown overnight at 30 $^{\circ}$ C, 250 rpm. The cells were pelleted and washed with MSM as described for the small-scale cultures (Section 4.7.1). The washed cells were used to inoculate MSM (3 \times 333 mL) supplemented with 33 mM glucose, 50 μ M phosphate and 60 mM D-serine to an initial OD₆₀₀ \sim 0.6. Ethanol (9.3 mL) was added to each flask and then then cultures were grown at 30 $^{\circ}$ C, 250 rpm. The pH of the culture media

was readjusted to pH 7.5 with 5 M NaOH at 24 h. After 48 h, the cells were pelleted at 8500 rpm. The supernatant was then filtered through 0.45 μ M then 0.22 μ M filters, to remove residual cellular debris. The clarified media was then applied to a 12 g silica phenyl column (SiliCycle) that was pre-conditioned with methanol and then with water. After application the media, the column was washed with 600 mL water, which retained an orange colour. Elution of the remaining material into 50 mL methanol gave an extract that was a deep red-burgundy colour. After concentration, 43 mg of material was recovered. A Biotage (Section 4.1.5) normal-phase silica column (40 g SiliCycle column, 1 CV= 66 mL, 20 mL/min) column was run with the following gradient 1 CV 10:90, 5 CV gradient to 50:50, 1 CV 50:50, 1 CV 100:0 CH₃OH: CH₂Cl₂. The material of eluting at 30:70 CH₃OH: CH₂Cl₂ was concentrated to give 13 mg of material. A second normal-phase column was run using the Biotage (12 g SiliCycle column, 1 CV= 24 mL, 10 mL/min) with the following gradient; 0.2 CV 10:90, 2 CV gradient to 30:70, 2 CV 30:70, 2 CV gradient to 60:40 CH₃OH: CH₂Cl₂. Two fractions of interest were separately combined and purified further using the preparatory HPLC method (Section 4.1.7). After concentration, the concentrated fractions (1 mg each) were analyzed by LCMS (Section 4.1.2) and ¹H NMR spectroscopy, however the purity of the samples was insufficient for full characterization. Both fraction contained the purple material of interest, and the ¹H NMR showed a similar product profile. On standing in water, the solutions turned from purple to green, and when spotted by TLC an aglycone signal (green, non-polar) was apparent, suggesting instability of the isolated product(s).

4.8.12. Scaled-Up Production with *S. venezuelae* Δ jadV

MYM (2×250 mL) was inoculated with *S. venezuelae* Δ jadV and grown overnight at 30 °C, 250 rpm. The cell pellets were collected and washed with MSM as described for the small-scale cultures (Section 4.7.1). The washed cells were used to inoculate MSM (4×250 mL) supplemented with with 33 mM glucose, 50 μ M phosphate and 60 mM D-serine to an initial OD₆₀₀ ~ 0.6. Ethanol (7.5 mL) was added to each flask. The cultures were grown at 30 °C, 250 rpm. The pH of the culture media was readjusted to pH 7.5 with 5 M NaOH at 24 h. After 52 h, the cells were pelleted at 8500 rpm. The supernatant was then filtered through 0.45 μ M then 0.22 μ M filters, to remove residual cellular debris. The clarified media was then applied to a 12 g silica phenyl column (SiliCycle) that was pre-washed with water. After application the media, the column was washed with 600 mL water, which retained an orange colour. Elution of the remaining material into 50 mL methanol gave an extract that was a deep red-burgundy colour. After concentration, 137 mg of material was recovered. The recovered material was fractionated by normal phase chromatography on the Biotage (Section 4.1.5) in two batches; the material was applied to a 40 g biotage column (SiliCycle, 1 CV= 66 mL, 20 mL/min flow rate) and the following method was run 10:90 methanol: dichloromethane 2 CV, gradient increase to 30:70 methanol: dichloromethane over 3 CV, 30:70 methanol 2 CV. The fraction containing the material of interest (~ 20 mg) were combined and subject to a second normal phase column (40 g, SiliCycle) with the following method: 0:100 methanol: dichloromethane 1.5 CV, gradient increase to 12:88 methanol: dichloromethane 1.5 CV, 12:88 methanol: dichloromethane 1 CV, gradient increase

to 30:70 methanol: dichloromethane 1.5 CV. Combining the material containing the spot of interest gave 3.4 mg of material. The material was analyzed by TLC (Section 4.1), LCMS (Section 4.1.2), and ^1H NMR spectroscopy but was not fully characterized due to insufficient purity and significant signal overlap.

4.8.13. NaBD_4 reaction with Product from up *S. venezuelae* ΔjadV

One milligram (~ 0.002 mM based on molecular weight of jadomycin DS-2,6-dideoxy-D-erythro-4-hexulose 521.48 g/mol) of the material obtained from the scaled-up *S. venezuelae* ΔjadV production was taken up in 100 μL methanol. To the sample was added 100 μL methanol with NaBD_4 (~ 0.002 mM). An identical control reaction without NaBD_4 was set up. In the sample with added NaBD_4 , an immediate colour change from purple to reddish brown was observed. The reactions were shaken at room temperature for 1 h and then analyzed by LCMS (Section 4.1.2) using a precursor m/z 306 (pos) experiment.

Chapter 5: Conclusions and Future Directions

In Chapter 2, a number of studies related to carbohydrate recognizing enzymes were discussed. In Sections 2.2 and 2.3, studies on the thymidyltransferase Cps2L demonstrated the application of this enzyme as a tool for chemoenzymatic synthesis through its use in the isolation of dT/UDP-sugars **2.8** (from **2.1** and UTP), **2.9** (**2.2** and dTTP), **2.11** (**2.3** and dTTP) and **2.15** (**2.5** and UTP) on a milligram scale. Isolation of **2.8** and **2.15** illustrated that Cps2L can utilize two unnatural substrates with sufficient yield for isolation. This study also delineated limitations in terms of substrate scope, showing that extended α -1C-phosphonate analogues (**2.6**) and an inositol-based scaffold (**2.4**), the latter anticipated to act as a substrate based on analysis of the active site in RmlA (a Cps2L homologue) crystal structure, were found not to be substrates, which will inform future inhibitor design. A summary of all sugar phosphate analogues evaluated with Cps2L can be found in Figure 85,^{80, 87, 111, 127, 130, 256} not including a series of furanose 1-phosphates that were found to be moderate substrates (~7-58% conversion over 24 h).¹¹⁰

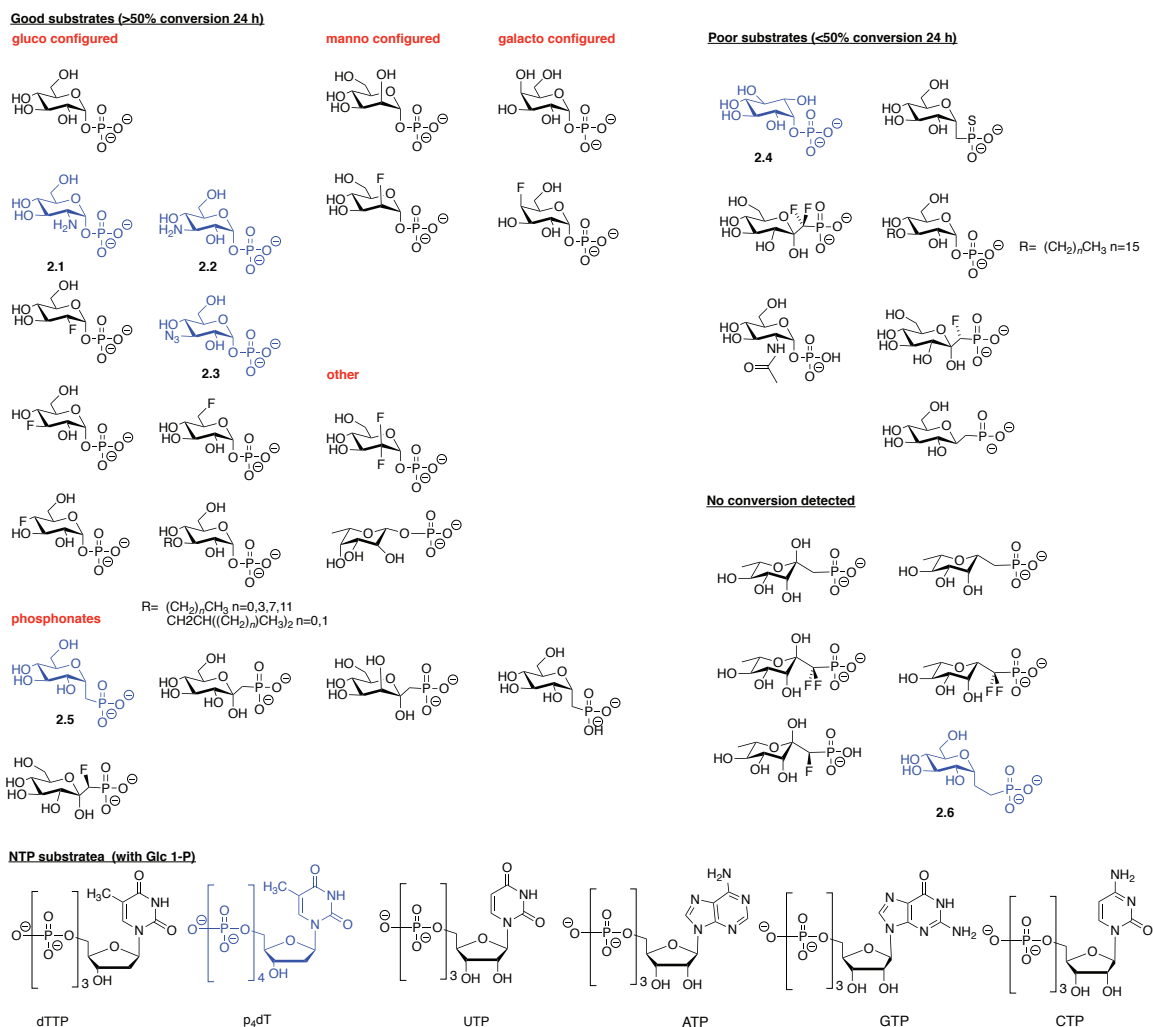


Figure 85. Summary of hexose 1-phosphate and NTP substrates evaluated with Cps2L. Compounds in blue were evaluated in this thesis.

Cps2L was able to use Glc 1-P analogues with modifications on the hexose ring, including functional group changes at positions C2, C3, C4, and C6. Cps2L possessed tolerance to changes at the anomeric position, including phosphonate substitutions, β -configuration, the addition of steric bulk such as with ketose-phosphonates and fluoro-methylene analogues (only one diastereomer).³ The Cps2L active site was found to tolerate additional charge as p₄dT was found to act as a

substrate. In a related study by Smithen *et al.*, the evaluation of dTDP-Glc analogues with three and four phosphates linking the glucose to the thymidine deoxyribose moieties were identified as micromolar Cps2L inhibitors, with a trend of improved inhibition correlating to increasing number of phosphates.²⁵⁷ Efforts to further examine the substrate scope included a previous study employing rational design of a Cps2L mutant (Q24S) by site-directed mutagenesis, which enabled more rapid turn over with UTP.²⁵⁸ The NDP-sugar analogues produced in these studies will be evaluated as inhibitors of bacterial biosynthetic enzymes.

In Section 2.4, the RmlB, RmlC and RmlD enzymes that modify the product of the Cps2L reaction, dTDP-Glc, to generate dTDP-Rha were evaluated. The first enzyme acting in the sequence, RmlB, was found to tolerate amino group at positions C-2 (dTDP-**2.1**) and C-3 (dTDP-**2.2**) of the hexose ring, generating the corresponding 4-keto-6-deoxy- analogues, as detected by LCMS (Figure 86). The predicted final pathway products were not observed after incubation with RmlC and RmlD. The fluoro sugar analogues (dTDP-**2.16-2.20**) were not turned over by any of the enzymes, suggesting that the electronegativity of the fluorine may interfere with enzyme mechanisms. The phosphonate analogue (dTDP-1C-Glc) was found to be a good substrate and the final pathway product dTDP-1C-Rha was isolated and fully characterized.

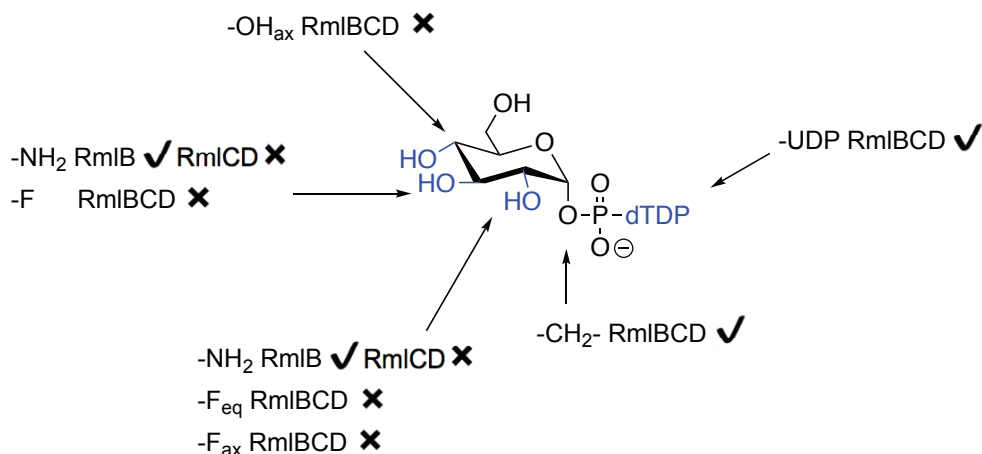


Figure 86. Summary of substrate scope study with RmlB, RmlC and RmlD.

In Section 2.5, a glycosyltransferase, Sv0189, from *S. venezuelae* ISP5230 was cloned and expressed as a recombinant protein. The physiological role of the enzyme remained undetermined, although homologous enzymes have been proposed to serve a role in xenobiotic resistance.^{145, 148} Sv0189 glycosyltransferase activity was established using UDP-Glc and 4-methylumbelliferone, and was evaluated in kinetic assays with 2-chloro-4-nitro-phenol- β -D-glucopyranoside and UDP. A preliminary assay to establish the acceptor scope was performed, identifying 25 compounds as putative hits. Phenolic and bis-aromatic compounds were generally well tolerated, which was also observed in studies with a homologous enzyme, OleD.¹⁵⁸ Future work involves modifications to the assay to address analytical detection issues arising from insolubility of the acceptors and confirmation of the glucosylated products by HRMS. The isolation of glucosylated compounds derived from natural products (Series B hits) and from synthetic drugs (Series C hits), demonstrating methods for late stage functionalization of these complex molecules, is of particular interest. Isolation of glucosylated products will additionally enable

an assessment of regioselectivity of Sv0189 on compounds with multiple hydroxyl and/or amine groups. Another avenue of research involves the evaluation the donor specificity for Sv0189, and exploration of the application of this substrate in aglycone exchange experiments (Figure 87).^{56, 259, 260}

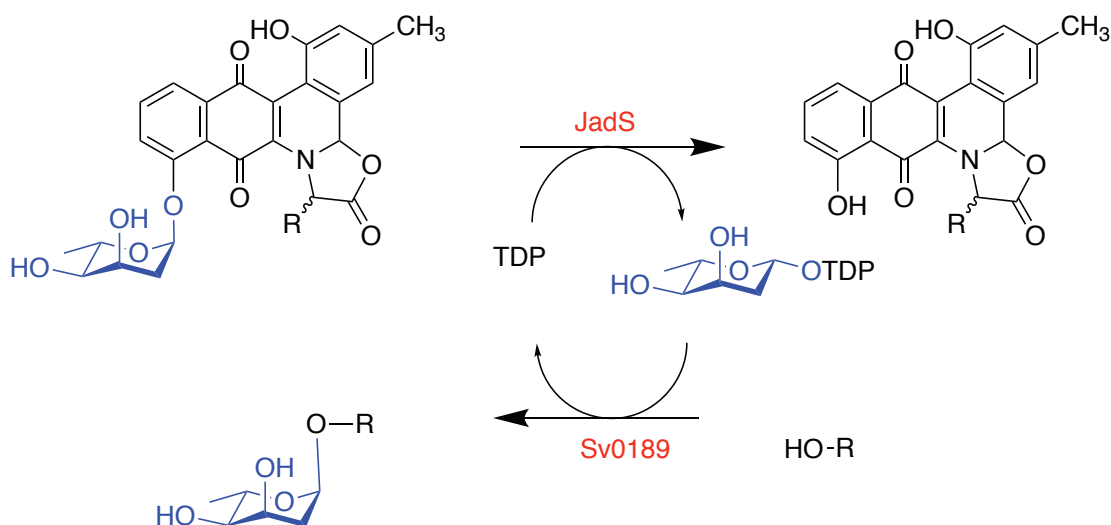


Figure 87. Conceptual example of aglycone exchange using JadS, the glycosyltransferase from jadomycin biosynthesis, and Sv0189.

Chapter 3 described a series of studies on the jadomycin of family natural products. In Section 3.2, a series of jadomycins were isolated from a culture with TFAL was discussed. This provided the first report of a lactam containing jadomycin (**3.2**) and of jadomycins with a furan ring (**3.3** and **3.4**). Since the discovery of the lactam analogues derived from TFAL, two more amide analogues have been described from cultures utilizing 4-aminobenzoic acid (4AMBA) and 3-aminobenzoic acid (3AMBA) as precursors (Figure 88).^{176, 245} The isolation of these compounds demonstrate the plasticity of bacterial biosynthetic platforms, however these new derivatives lacking the 3a-hemi-aminal were found to be less active in

antimicrobial screens or against cancer cell lines (NCI Developmental Therapeutics NCI-60 Human Tumor cell lines screen) in comparison to jadomycins with the usual oxazolone scaffold, suggesting that this position is important for the SAR.

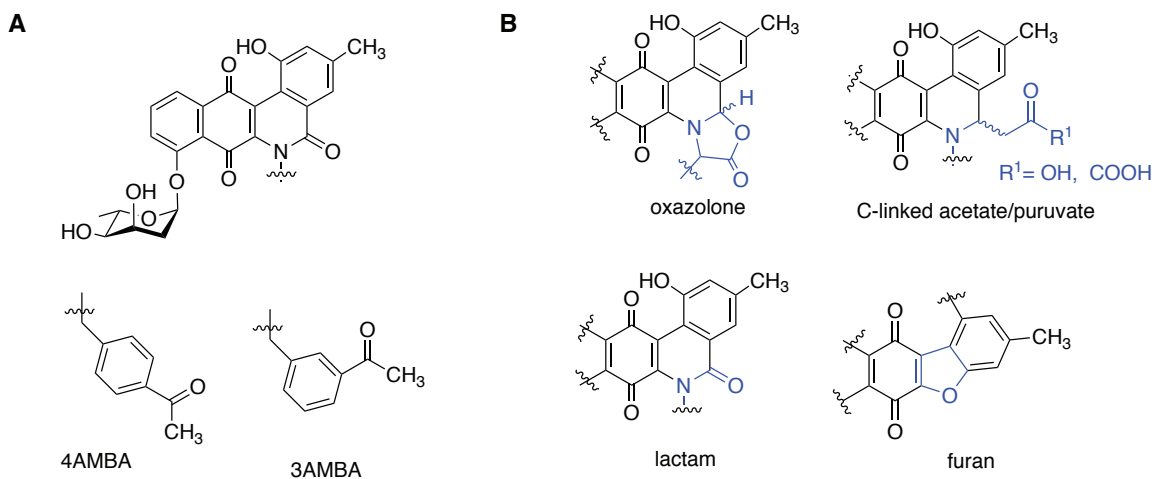


Figure 88. (A) Recently described jadomycin lactam congeners; (B) jadomycin ring scaffolds.

In Section 3.3, the deletion of the 4,6-dehydratase (*jadT*) from the L-digitoxose biosynthetic pathway of *S. venezuelae* resulted in the isolation of a glucosylated jadomycin (**3.9**). The absence of this product in a double deletion mutant, *S. venezuelae* Δ *jadSjadT*, demonstrated that JadS was able to transfer D-glucose in the absence of the physiological substrate, dTDP- β -L-digitoxose. This expands on a previous study that identified JadS as being flexible with respect to its sugar donor, and was corroborated in a recent study that used a combinatorial approach to glycodiversify JadS, resulting in the detection of a series of sugar-modified jadomycins.^{60, 181} This result sets the stage for future glycodiversification efforts on the jadomycins, including the introduction of sugar analogue precursors into the jadomycin biosynthesis pathway. Glc 1-P analogues with biolabile

phosphate protecting groups that are cleaved by esterases upon take-up by the bacteria, such as bis-diisopropylloxycarbonyloxymethyl (POC), bis-pivaloyloxymethyl (POM) or phosphoramidite,²⁶¹⁻²⁶³ could be used in cultures with either wild-type or deletion mutants to generate new derivatives (Figure 89).

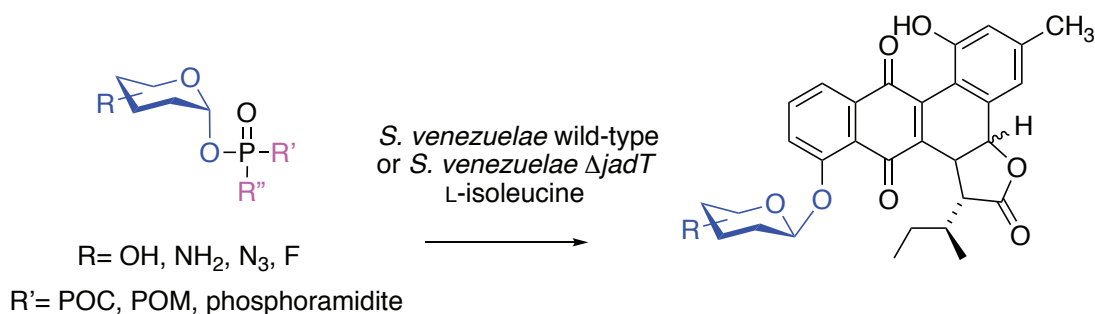


Figure 89. Proposed general scheme for precursor-directed approach to jadomycin glycodiversification.

Progress towards an alternate approach for jadomycin glycodiversification was discussed in Section 3.4 involving complementation of *S. venezuelae* with glycosyltransferase genes *kijC4* and *kijC3* from the kijanimicin gene cluster. This work was inspired by a number of reports demonstrating that bacterial secondary metabolite glycosyltransferases possess remarkable promiscuity with respect to donors and/or acceptors. The *kijC4* gene was presumed to encode an iterative L-digitoxyltransferase, and therefore we proposed that KijC4 would recognize jadomycins as a substrate, possessing one L-digitoxose installed by JadS. A number of *kijC4* and *kijC3* complementation mutants were generated using homologous recombination to introduce genes directly into the L-digitoxose gene cluster, however evaluation of these knock-in strains did not produce L-digitoxylated analogues. It was established that inadvertent disruption of *jadV*, a biosynthetic

gene that encoded the catalyst for 4-ketoreduction in the final step of L-digitoxose biosynthesis, was occurring in these complemented strains. As a next step, generation of complemented strains using a well-studied integrative vector (pSET152) will be attempted. The use of qPCR methods to ascertain whether successful transcription of the biosynthetic genes has occurred would also serve as a valuable tool in these studies, and would inform whether an absence of anticipated products was due to the genetic platform or due to incompatibility of KijC4 to use jadomycins as an acceptor.

References

- (1) Boons, G.; Wu, P. *Glycobiology* **2016**, *26*, 788-788.
- (2) Trang, V. H.; Senter, P. D. *Proc. Natl. Acad. Sci. U. S. A.* **2016**, *113*, 10228-10230.
- (3) Forget, S. M.; Bhattasali, D.; Hart, V. C.; Cameron, T. S.; Syvitski, R. T.; Jakeman, D. L. *Chem. Sci.* **2012**, *3*, 1866-1878.
- (4) Poulin, M. B.; Zhou, R.; Lowary, T. L. *Org. Biomol. Chem.* **2012**, *10*, 4074-4087.
- (5) Wiederschain, G. Y. *Biochemistry (Moscow)* **2009**, *74*, 1056-1056.
- (6) Elshahawi, S. I.; Shaaban, K. A.; Kharel, M. K.; Thorson, J. S. *Chem. Soc. Rev.* **2015**, *44*, 7591-7697.
- (7) Wright, G. D. *Can. J. Microbiol.* **2014**, *60*, 147-154.
- (8) Willyard, C. *Nature News* **2017**, *543*, 15.
- (9) Maki, M.; Renkonen, R. *Glycobiology* **2004**, *14*, 1R-15R.
- (10) Thibodeaux, C. J.; Melancon, C. E.; Liu, H. *Nature* **2007**, *446*, 1008-1016.
- (11) Leloir, L. F. *Science* **1971**, *172*, 1299-1303.
- (12) Lin, C.; McCarty, R. M.; Liu, H. *Chem. Soc. Rev.* **2013**, *42*, 4377-4407.
- (13) Blair, J. M.; Webber, M. A.; Baylay, A. J.; Ogbolu, D. O.; Piddock, L. J. *Nat. Rev. Microbiol.* **2015**, *13*, 42-51.
- (14) Tra, V. N.; Dube, D. H. *Chem. Commun.* **2014**, *50*, 4659-4673.
- (15) Kohanski, M. A.; Dwyer, D. J.; Collins, J. J. *Nat. Rev. Microbiol.* **2010**, *8*, 423-435.
- (16) Müller, A.; Klöckner, A.; Schneider, T. *Nat. Prod. Rep.* **2017**, *34*, 909-932.
- (17) Breukink, E.; de Kruijff, B. *Nat. Rev. Drug Discov.* **2006**, *5*, 321-332.
- (18) Stone, K. J.; Strominger, J. L. *Proc. Natl. Acad. Sci. U. S. A.* **1971**, *68*, 3223-3227.
- (19) Tamura, G.; Sasaki, T.; Matsushashi, M.; Takatsuki, A.; Yamasaki, M. *Agric. Biol. Chem.* **1976**, *40*, 447-449.
- (20) Brandish, P. E.; Kimura, K. I.; Inukai, M.; Southgate, R.; Lonsdale, J. T.; Bugg, T. D. *Antimicrob. Agents Chemother.* **1996**, *40*, 1640-1644.

- (21) Heifetz, A.; Keenan, R. W.; Elbein, A. D. *Biochemistry* **1979**, *18*, 2186-2192.
- (22) Elbein, A. D. *Trends Biochem. Sci.* **1981**, *6*, 219-221.
- (23) Thibodeaux, C. J.; Melancon, C. E.; Liu, H. W. *Angew. Chem. Int. Ed.* **2008**, *47*, 9814-9859.
- (24) Saxon, E.; Bertozzi, C. R. *Science* **2000**, *287*, 2007-2010.
- (25) King, M.; Wagner, A. *Bioconjug. Chem.* **2014**, *25*, 825-839.
- (26) Baskin, J. M.; Prescher, J. A.; Laughlin, S. T.; Agard, N. J.; Chang, P. V.; Miller, I. A.; Lo, A.; Codelli, J. A.; Bertozzi, C. R. *Proc. Natl. Acad. Sci. U. S. A.* **2007**, *104*, 16793-16797.
- (27) McKay, C. S.; Finn, M. *Chem. Biol.* **2014**, *21*, 1075-1101.
- (28) Bertozzi, C. R.; Kiessling, L. L. *Science* **2001**, *291*, 2357-2364.
- (29) Laughlin, S. T.; Bertozzi, C. R. *Nature protocols* **2007**, *2*, 2930-2944.
- (30) Haltiwanger, R. S.; Lowe, J. B. *Annu. Rev. Biochem.* **2004**, *73*, 491-537.
- (31) Paulson, J. C.; Blixt, O.; Collins, B. E. *Nat. Chem. Biol.* **2006**, *2*, 238-248.
- (32) Gloster, T. M.; Zandberg, W. F.; Heinonen, J. E.; Shen, D. L.; Deng, L.; Vocadlo, D. *J. Nat Chem Biol* **2011**, *7*, 174-181.
- (33) Rillahan, C. D.; Antonopoulos, A.; Lefort, C. T.; Sonon, R.; Azadi, P.; Ley, K.; Dell, A.; Haslam, S. M.; Paulson, J. C. *Nat Chem Biol* **2012**, *8*, 661-668.
- (34) Lairson, L. L.; Henrissat, B.; Davies, G. J.; Withers, S. G. *Annu. Rev. Biochem.* **2008**, *77*, 521-555.
- (35) Atanasov, A. G.; Waltenberger, B.; Pferschy-Wenzig, E.; Linder, T.; Wawrosch, C.; Uhrin, P.; Temml, V.; Wang, L.; Schwaiger, S.; Heiss, E. H. *Biotechnol. Adv.* **2015**, *33*, 1582-1614.
- (36) Newman, D. J.; Cragg, G. M.; Snader, K. M. *Nat. Prod. Rep.* **2000**, *17*, 215-234.
- (37) Newman, D. J.; Cragg, G. M. *J. Nat. Prod.* **2012**, *75*, 311-335.
- (38) Wright, G. D. *Nat. Prod. Rep.* **2017**, *34*, 694-701.
- (39) Cox, G.; Sieron, A.; King, A. M.; De Pascale, G.; Pawlowski, A. C.; Koteva, K.; Wright, G. D. *Cell Chem Biol* **2017**, *24*, 98-109.
- (40) Katz, L.; Baltz, R. H. *J. Ind. Microbiol. Biotechnol.* **2016**, *43*, 155-176.

- (41) Cimermancic, P.; Medema, M. H.; Claesen, J.; Kurita, K.; Brown, L. C. W.; Mavrommatis, K.; Pati, A.; Godfrey, P. A.; Koehrsen, M.; Clardy, J. *Cell* **2014**, *158*, 412-421.
- (42) Bachmann, B. O.; Van Lanen, S. G.; Baltz, R. H. *J. Ind. Microbiol. Biotechnol.* **2014**, *41*, 175-184.
- (43) Park, J. W.; Nam, S.; Yoon, Y. J. *Biochem. Pharmacol.* **2017**, *134*, 56-73.
- (44) Song, M. C.; Kim, E.; Ban, Y. H.; Yoo, Y. J.; Kim, E. J.; Park, S. R.; Pandey, R. P.; Sohng, J. K.; Yoon, Y. J. *Appl. Microbiol. Biotechnol.* **2013**, *97*, 5691-5704.
- (45) Weymouth-Wilson, A. C. *Nat. Prod. Rep.* **1997**, *14*, 99-110.
- (46) Di Marco, A.; Casazza, A. M.; Gambetta, R.; Supino, R.; Zunino, F. *Cancer Res.* **1976**, *36*, 1962-1966.
- (47) Arcamone, F.; Animati, F.; Berettoni, M.; Bigioni, M.; Capranico, G.; Casazza, A. M.; Caserini, C.; Cipollone, A.; De Cesare, M.; Franciotti, M. *J. Natl. Cancer Inst* **1997**, *89*, 1217-1223.
- (48) O'Byrne, K.; Dunlop, D.; Eberhardt, W.; Gillissen, A.; Wagner, T.; Capriati, A.; Dickgreber, N. *J. Clin. Oncol* **2008**, *26*, 19043-19043.
- (49) Gantt, R. W.; Peltier-Pain, P.; Thorson, J. S. *Nat. Prod. Rep.* **2011**, *28*, 1811-1853.
- (50) Lin, H.; Walsh, C. T. *J. Am. Chem. Soc.* **2004**, *126*, 13998-14003.
- (51) Langenhan, J. M.; Griffith, B. R.; Thorson, J. S. *J. Nat. Prod.* **2005**, *68*, 1696-1711.
- (52) Hoffmeister, D.; Drager, G.; Ichinose, K.; Rohr, J.; Bechthold, A. *J. Am. Chem. Soc.* **2003**, *125*, 4678-4679.
- (53) Borisova, S. A.; Zhao, L.; Sherman, D. H.; Liu, H. *Org. Lett.* **1999**, *1*, 133-136.
- (54) Salas, A. P.; Zhu, L.; Sanchez, C.; Brana, A. F.; Rohr, J.; Mendez, C.; Salas, J. A. *Mol. Microbiol.* **2005**, *58*, 17-27.
- (55) Fischer, C.; Rodríguez, L.; Patallo, E. P.; Lipata, F.; Braña, A. F.; Méndez, C.; Salas, J. A.; Rohr, J. *J. Nat. Prod.* **2002**, *65*, 1685-1689.
- (56) Zhang, C. S.; Griffith, B. R.; Fu, Q.; Albermann, C.; Fu, X.; Lee, I. K.; Li, L. J.; Thorson, J. S. *Science* **2006**, *313*, 1291-1294.
- (57) Zhang, C.; Albermann, C.; Fu, X.; Peters, N. R.; Chisholm, J. D.; Zhang, G. S.; Gilbert, E. J.; Wang, P. G.; Van Vranken, D. L.; Thorson, J. S. *ChemBioChem* **2006**, *7*, 795-804.

- (58) Pandey, R. P.; Parajuli, P.; Gurung, R. B.; Sohng, J. K. *Enzyme Microb. Technol.* **2016**, *91*, 26-33.
- (59) Forget, S. M.; Na, J.; McCormick, N. E.; Jakeman, D. L. *Org. Biomol. Chem* **2017**, *15*, 2725-2729.
- (60) Jakeman, D. L.; Borissow, C. N.; Reid, T. R.; Graham, C. L.; Timmons, S. C.; Syvitski, R. T. *Chem. Commun.* **2006**, *35*, 3738-3740.
- (61) Olano, C.; Gomez, C.; Perez, M.; Palomino, M.; Pineda-Lucena, A.; Carbajo, R. J.; Brana, A. F.; Mendez, C.; Salas, J. A. *Chem. Biol.* **2009**, *16*, 1031-1044.
- (62) Xie, K.; Zhang, Y.; Chen, R.; Chen, D.; Yang, L.; Liu, X.; Dai, J. *Tetrahedron Lett.* **2017**, *58*, 2118-2121.
- (63) Song, C.; Gu, L.; Liu, J.; Zhao, S.; Hong, X.; Schulenburg, K.; Schwab, W. *Plant Cell Physiol.* **2015**, *56*, 2478-2493.
- (64) Dewitte, G.; Walmagh, M.; Diricks, M.; Lepak, A.; Gutmann, A.; Nidetzky, B.; Desmet, T. *J. Biotechnol.* **2016**, *233*, 49-55.
- (65) Chen, D.; Sun, L.; Chen, R.; Xie, K.; Yang, L.; Dai, J. *Chem. Eur. J.* **2016**, *22*, 5873-5877.
- (66) Härtl, K.; Huang, F.; Giri, A. P.; Franz-Oberdorf, K.; Frotscher, J.; Shao, Y.; Hoffmann, T.; Schwab, W. *J. Agric. Food Chem.* **2017**, *65*, 5681-5689.
- (67) Chen, D.; Chen, R.; Wang, R.; Li, J.; Xie, K.; Bian, C.; Sun, L.; Zhang, X.; Liu, J.; Yang, L.; Ye, F.; Yu, X.; Dai, J. *Angew. Chem. Int. Ed.* **2015**, *54*, 12678-12682.
- (68) Xie, K.; Chen, R.; Chen, D.; Li, J.; Wang, R.; Yang, L.; Dai, J. *Adv. Synth. Catal.* **2017**, *359*, 603-608.
- (69) Chiu, H.; Shen, M.; Liu, Y.; Fu, Y.; Chiu, Y.; Chen, Y.; Huang, C.; Li, Y. *Appl. Microbiol. Biotechnol.* **2016**, *100*, 4459-4471.
- (70) Ahn, B. C.; Kim, B. G.; Jeon, Y. M.; Lee, E. J.; Lim, Y.; Ahn, J. H. *J. Microbiol. Biotechnol.* **2009**, *19*, 387-390.
- (71) Kim, J. H.; Kim, B. G.; Kim, J. A.; Park, Y.; Lee, Y. J.; Lim, Y.; Ahn, J. *J. Microbiol. Biotechnol.* **2007**, *17*, 539-542.
- (72) Williams, G. J.; Zhang, C.; Thorson, J. S. *Nat. Chem. Biol.* **2007**, *3*, 657-662.
- (73) Zhou, M.; Hamza, A.; Zhan, C.; Thorson, J. S. *J. Nat. Prod.* **2013**, *76*, 279-286.
- (74) Gantt, R. W.; Peltier-Pain, P.; Cournoyer, W. J.; Thorson, J. S. *Nat. Chem. Biol.* **2011**, *7*, 685-691.

- (75) Liang, C.; Zhang, Y.; Jia, Y.; Wang, W.; Li, Y.; Lu, S.; Jin, J.; Tang, S. *Sci. Rep.* **2016**, *6*, DOI: 10.1038/srep21051.
- (76) Pallares, R.; Viladrich, P. F.; Linares, J.; Cabellos, C.; Gudiol, F. *Microb. Drug Resist.* **1998**, *4*, 339-347.
- (77) Strateva, T.; Yordanov, D. *J. Med. Microbiol.* **2009**, *58*, 1133-1148.
- (78) Mistou, M.; Sutcliffe, I. C.; van Sorge, N. M. *FEMS Microbiol. Rev.* **2016**, *40*, 464-479.
- (79) Dong, C.; Beis, K.; Giraud, M. F.; Blankenfeldt, W.; Allard, S.; Major, L. L.; Kerr, I. D.; Whitfield, C.; Naismith, J. H. *Biochem. Soc. Trans.* **2003**, *31*, 532-536.
- (80) Timmons, S. C.; Mosher, R. H.; Knowles, S. A.; Jakeman, D. L. *Org. Lett.* **2007**, *9*, 857-860.
- (81) Alphey, M. S.; Pirrie, L.; Torrie, L. S.; Boulkeroua, W. A.; Gardiner, M.; Sarkar, A.; Maringer, M.; Oehlmann, W.; Brenk, R.; Scherman, M. S.; McNeil, M.; Rejzek, M.; Field, R. A.; Singh, M.; Gray, D.; Westwood, N. J.; Naismith, J. H. *ACS Chem. Biol.* **2013**, *8*, 387-396.
- (82) Barton, W. A.; Lesniak, J.; Biggins, J. B.; Jeffrey, P. D.; Jiang, J. Q.; Rajashankar, K. R.; Thorson, J. S.; Nikolov, D. B. *Nat. Struct. Biol.* **2001**, *8*, 545-551.
- (83) Zuccotti, S.; Zanardi, D.; Rosano, C.; Sturla, L.; Tonetti, M.; Bolognesi, M. *J. Mol. Biol.* **2001**, *313*, 831-843.
- (84) Blankenfeldt, W.; Asuncion, M.; Lam, J. S.; Naismith, J. H. *EMBO J.* **2000**, *19*, 6652-6663.
- (85) Errey, J. C.; Mukhopadhyay, B.; Kartha, K. P.; Field, R. A. *Chem. Commun.* **2004**, *23*, 2706-2707.
- (86) Moretti, R.; Chang, A.; Peltier-Pain, P.; Bingman, C. A.; Phillips, G. N., Jr.; Thorson, J. S. *J. Biol. Chem.* **2011**, *286*, 13235-13243.
- (87) Beaton, S. A.; Huestis, M. P.; Sadeghi-Khomami, A.; Thomas, N. R.; Jakeman, D. L. *Chem. Commun.* **2009**, 238-240.
- (88) Ko, K. S.; Zea, C. J.; Pohl, N. L. *J. Am. Chem. Soc.* **2004**, *126*, 13188-13189.
- (89) Huestis, M. P.; Aish, G. A.; Hui, J. P.; Soo, E. C.; Jakeman, D. L. *Org. Biomol. Chem.* **2008**, *6*, 477-484.
- (90) Rahim, R.; Burrows, L. L.; Monteiro, M. A.; Perry, M. B.; Lam, J. S. *Microbiology* **2000**, *146*, 2803-2814.
- (91) Ma, Y.; Pan, F.; McNeil, M. *J. Bacteriol.* **2002**, *184*, 3392-3395.

- (92) Giraud, M. F.; Naismith, J. H. *Curr. Opin. Struct. Biol.* **2000**, *10*, 687-696.
- (93) Giraud, M. F.; Leonard, G. A.; Field, R. A.; Berlind, C.; Naismith, J. H. *Nat. Struct. Biol.* **2000**, *7*, 398-402.
- (94) Dong, C.; Major, L. L.; Srikannathasan, V.; Errey, J. C.; Giraud, M. F.; Lam, J. S.; Graninger, M.; Messner, P.; McNeil, M. R.; Field, R. A.; Whitfield, C.; Naismith, J. H. *J. Mol. Biol.* **2007**, *365*, 146-159.
- (95) Beis, K.; Allard, S. T.; Hegeman, A. D.; Murshudov, G.; Philp, D.; Naismith, J. H. *J. Am. Chem. Soc.* **2003**, *125*, 11872-11878.
- (96) Blankenfeldt, W.; Kerr, I. D.; Giraud, M. F.; McMiken, H. J.; Leonard, G.; Whitfield, C.; Messner, P.; Graninger, M.; Naismith, J. H. *Structure* **2002**, *10*, 773-786.
- (97) Tsukioka, Y.; Yamashita, Y.; Nakano, Y.; Oho, T.; Koga, T. *J. Bacteriol.* **1997**, *179*, 4411-4414.
- (98) Tsukioka, Y.; Yamashita, Y.; Oho, T.; Nakano, Y.; Koga, T. *J. Bacteriol.* **1997**, *179*, 1126-1134.
- (99) Graninger, M.; Nidetzky, B.; Heinrichs, D. E.; Whitfield, C.; Messner, P. *J. Biol. Chem.* **1999**, *274*, 25069-25077.
- (100) Graninger, M.; Kneidinger, B.; Bruno, K.; Scheberl, A.; Messner, P. *Appl. Environ. Microbiol.* **2002**, *68*, 3708-3715.
- (101) Kang, Y.; Yang, Y.; Lee, K.; Lee, S.; Sohng, J. K.; Lee, H. C.; Liou, K.; Kim, B. *Biotechnol. Bioeng.* **2006**, *93*, 21-27.
- (102) Poon, K. K. H.; Westman, E. L.; Vinogradov, E.; Jin, S.; Lam, J. S. *J. Bacteriol.* **2008**, *190*, 1857-1865.
- (103) Webb, M. R. *Proc. Natl. Acad. Sci. U. S. A.* **1992**, *89*, 4884-4887.
- (104) Upson, R. H.; Haugland, R. P.; Malekzadeh, M. N.; Haugland, R. P. *Anal. Biochem.* **1996**, *243*, 41-45.
- (105) Vazquez, M. J.; Rodriguez, B.; Zapatero, C.; Tew, D. G. *Anal. Biochem.* **2003**, *320*, 292-298.
- (106) Guillen Suarez, A. S.; Stefan, A.; Lemma, S.; Conte, E.; Hochkoeppler, A. *BioTechniques* **2012**, *53*, 99-103.
- (107) Tagiri-Endo, M. *Anal. Biochem.* **2003**, *315*, 170-174.
- (108) Wagner, G. K.; Pesnot, T.; Field, R. A. *Nat. Prod. Rep.* **2009**, *26*, 1172-1194.
- (109) Jiang, J. Q.; Biggins, J. B.; Thorson, J. S. *J. Am. Chem. Soc.* **2000**, *122*, 6803-6804.

- (110) Timmons, S. C.; Hui, J. P.; Pearson, J. L.; Peltier, P.; Daniellou, R.; Nugier-Chauvin, C.; Soo, E. C.; Syvitski, R. T.; Ferrieres, V.; Jakeman, D. L. *Org. Lett.* **2008**, *10*, 161-163.
- (111) Loranger, M. W.; Forget, S. M.; McCormick, N. E.; Syvitski, R. T.; Jakeman, D. L. *J. Org. Chem.* **2013**, *78*, 9822-9833.
- (112) Dalvit, C.; Pevarello, P.; Tato, M.; Veronesi, M.; Vulpetti, A.; Sundstrom, M. J. *Biomol. NMR* **2000**, *18*, 65-68.
- (113) Dalvit, C.; Fogliatto, G.; Stewart, A.; Veronesi, M.; Stockman, B. J. *Biomol. NMR* **2001**, *21*, 349-359.
- (114) Melo, A.; Glaser, L. *J. Biol. Chem.* **1965**, *240*, 398-405.
- (115) Fielding, L.; Rutherford, S.; Fletcher, D. *Magn. Reson. Chem.* **2005**, *43*, 463-470.
- (116) Fielding, L. *Prog. Nucl. Magn. Reson. Spectrosc.* **2007**, *51*, 219-242.
- (117) Huang, R.; Bonnichon, A.; Claridge, T. D. W.; Leung, I. K. H. *Sci. Rep.* **2017**, *7*, DOI: 10.1038/srep43727.
- (118) Fraga, H.; Fontes, R. *Biochim. Biophys. Acta-Gen. Subj.* **2011**, *1810*, 1195-1204.
- (119) McLennan, A. G. *Pharmacol. Ther.* **2000**, *87*, 73-89.
- (120) McLennan, A. G.; Barnes, L. D.; Blackburn, G. M.; Brenner, C.; Guranowski, A.; Miller, A. D.; Rovira, J. M.; Rotllan, P.; Soria, B.; Tanner, J. A.; Sillero, A. *Drug Dev. Res.* **2001**, *52*, 249-259.
- (121) Toelle, M.; Jankowski, V.; Schuchardt, M.; Wiedon, A.; Huang, T.; Hub, F.; Kowalska, J.; Jemielity, J.; Guranowski, A.; Loddenkemper, C.; Zidek, W.; Jankowski, J.; van der Giet, M. *Circ. Res.* **2008**, *103*, 1100-1108.
- (122) Retaillieu, P.; Weinreb, V.; Hu, M.; Carter Jr, C. W. *J. Mol. Biol.* **2007**, *369*, 108-128.
- (123) Guranowski, A.; Starzynska, E.; Pietrowska-Borek, M.; Jemielity, J.; Kowalska, J.; Darzynkiewicz, E.; Thompson, M.; Blackburn, G. *FEBS J.* **2006**, *273*, 829-838.
- (124) Coste, H.; Brevet, A.; Plateau, P.; Blanquet, S. *J. Biol. Chem.* **1987**, *262*, 12096-12103.
- (125) Singh, S.; Phillips, G. N., Jr.; Thorson, J. S. *Nat. Prod. Rep.* **2012**, *29*, 1201-1237.
- (126) Guranowski, A.; de Diego, A.; Sillero, A.; Günther Sillero, M. A. *FEBS Lett.* **2004**, *561*, 83-88.

- (127) Zhu, J.; McCormick, N. E.; Timmons, S. C.; Jakeman, D. L. *J. Org. Chem.* **2016**, *81*, 8816-8825.
- (128) Stein, A.; Kula, M.; Elling, L. *Glycoconj. J.* **1998**, *15*, 139-145.
- (129) Marumo, K.; Lindqvist, L.; Verma, N.; Weintraub, A.; Reeves, P. R.; Lindberg, A. A. *FEBS J.* **1992**, *204*, 539-545.
- (130) Forget, S. M.; Jee, A.; Smithen, D. A.; Jagdhane, R.; Anjum, S.; Beaton, S. A.; Palmer, D. R.; Syvitski, R. T.; Jakeman, D. L. *Org. Biomol. Chem.* **2015**, *13*, 866-875.
- (131) Stein, A.; Kula, M.; Elling, L.; Verseck, S.; Klaffke, W. *Angew. Chem. Int. Ed.* **1995**, *34*, 1748-1749.
- (132) Jin, Y.; Bhattasali, D.; Pellegrini, E.; Forget, S. M.; Baxter, N. J.; Cliff, M. J.; Bowler, M. W.; Jakeman, D. L.; Blackburn, G. M.; Waltho, J. P. *Proc. Natl. Acad. Sci. U. S. A.* **2014**, *111*, 12384-12389.
- (133) Baxter, N. J.; Bowler, M. W.; Alizadeh, T.; Cliff, M. J.; Hounslow, A. M.; Wu, B.; Berkowitz, D. B.; Williams, N. H.; Blackburn, G. M.; Waltho, J. P. *Proc. Natl. Acad. Sci. U. S. A.* **2010**, *107*, 4555-4560.
- (134) Allard, S. T.; Giraud, M. F.; Whitfield, C.; Graninger, M.; Messner, P.; Naismith, J. *H. J. Mol. Biol.* **2001**, *307*, 283-295.
- (135) Engel, R. *Chem. Rev.* **1977**, *77*, 349-367.
- (136) Zhao, Z. B.; Hong, L.; Liu, H. W. *J. Am. Chem. Soc.* **2005**, *127*, 7692-7693.
- (137) Partha, S. K.; Sadeghi-Khomami, A.; Slowski, K.; Kotake, T.; Thomas, N. R.; Jakeman, D. L.; Sanders, D. A. R. *J. Mol. Biol.* **2010**, *403*, 578-590.
- (138) Gordon, R. D.; Sivarajah, P.; Satkunarajah, M.; Ma, D.; Tarling, C. A.; Vizitiu, D.; Withers, S. G.; Rini, J. M. *J. Mol. Biol.* **2006**, *360*, 67-79.
- (139) Armstrong, R. N.; Andre, J. C.; Bessems, J. G. M. In *Mechanistic and stereochemical investigations of UDP-glucuronosyltransferases*; Siest, G., Magdalou, J. and Burchell, B., Eds.; Cellular and molecular aspects of glucuronidation; INSERM/ John Libbey Eurotext Ltd.: 1988; Vol. 173, pp 51-58.
- (140) Liang, D.; Liu, J.; Wu, H.; Wang, B.; Zhu, H.; Qiao, J. *Chem. Soc. Rev.* **2015**, *44*, 8350-8374.
- (141) Wang, L.; White, R. L.; Vining, L. C. *Microbiology* **2002**, *148*, 1091-1103.
- (142) Quiros, L. M.; Carbajo, R. J.; Brana, A. F.; Salas, J. A. *J. Biol. Chem.* **2000**, *275*, 11713-11720.

- (143) Gantt, R. W.; Goff, R. D.; Williams, G. J.; Thorson, J. S. *Angew. Chem. Int. Ed.* **2008**, *47*, 8889-8892.
- (144) Quiros, L. M.; Aguirrezabalaga, I.; Olano, C.; Mendez, C.; Salas, J. A. *Mol. Microbiol.* **1998**, *28*, 1177-1185.
- (145) Bolam, D. N.; Roberts, S.; Proctor, M. R.; Turkenburg, J. P.; Dodson, E. J.; Martinez-Fleites, C.; Yang, M.; Davis, B. G.; Davies, G. J.; Gilbert, H. J. *Proc. Natl. Acad. Sci. U. S. A.* **2007**, *104*, 5336-5341.
- (146) Sasaki, J.; Mizoue, K.; Morimoto, S.; Omura, S. *J. Antibiot.* **1996**, *49*, 1110-1118.
- (147) Zhao, L.; Beyer, N. J.; Borisova, S. A.; Liu, H. W. *Biochemistry* **2003**, *42*, 14794-14804.
- (148) Strobel, T.; Schmidt, Y.; Linnenbrink, A.; Luzhetskyy, A.; Luzhetska, M.; Taguchi, T.; Brotz, E.; Paululat, T.; Stasevych, M.; Stanko, O.; Novikov, V.; Bechthold, A. *Appl. Environ. Microbiol.* **2013**, *79*, 5224-5232.
- (149) Blin, K.; Wolf, T.; Chevrette, M. G.; Lu, X.; Schwalen, C. J.; Kautsar, S. A.; Duran, S.; Hernando, G.; de los Santos, E. L. C.; Kim, H. K.; Nave, M.; Dickschat, J. S.; Mitchell, D. A.; Shelest, E.; Breitling, R.; Takano, E.; Lee, S. Y.; Weber, T.; Medeman, M. H. *Nucleic Acids Res.* **2017**, *45*, W36-W41.
- (150) Sidda, J. D.; Song, L.; Poon, V.; Al-bassam, M.; Lazos, O.; Buttner, M. J.; Challis, G. L.; Corre, C. *Chem. Sci.* **2014**, *5*, 86-89.
- (151) Goto, Y.; Li, B.; Claesen, J.; Shi, Y.; Bibb, M. J.; van der Donk, W. A. *PLoS Biol.* **2010**, *8*, e1000339-e1000339.
- (152) Kodani, S.; Komaki, H.; Suzuki, M.; Kobayakawa, F.; Hemmi, H. *Biometals* **2015**, *28*, 791-801.
- (153) Rabe, P.; Rinkel, J.; Klapschinski, T. A.; Barra, L.; Dickschat, J. S. *Org. Biomol. Chem.* **2015**, *14*, 158-164.
- (154) Thanapipatsiri, A.; Gomez-Escribano, J. P.; Song, L.; Bibb, M. J.; Al-Bassam, M.; Chandra, G.; Thamchaipenet, A.; Challis, G. L.; Bibb, M. J. *ChemBioChem* **2016**, *17*, 2189-2198.
- (155) Inahashi, Y.; Zhou, S.; Bibb, M. J.; Song, L.; Al-Bassam, M.; Bibb, M. J.; Challis, G. L. *Chem. Sci.* **2017**, *8*, 2823-2831.
- (156) He, J.; Magarvey, N.; Pirae, M.; Vining, L. C. *Microbiology* **2001**, *147*, 2817-2829.
- (157) Hernandez, C.; Olano, C.; Mendez, C.; Salas, J. A. *Gene* **1993**, *134*, 139-140.
- (158) Gantt, R. W.; Peltier-Pain, P.; Singh, S.; Zhou, M.; Thorson, J. S. *Proc. Natl. Acad. Sci. U. S. A.* **2013**, *110*, 7648-7653.

- (159) Williams, G. J.; Yang, J.; Zhang, C. S.; Thorson, J. S. *ACS Chem. Biol.* **2011**, *6*, 95-100.
- (160) Hughes, R. R.; Shaaban, K. A.; Zhang, J.; Cao, H.; Phillips, G. N.; Thorson, J. S. *ChemBioChem* **2017**, *18*, 363-367.
- (161) Bérdy, J. *J. Antibiot.* **2012**, *65*, 385-395.
- (162) Moloney, M. G. *Trends Pharmacol. Sci.* **2016**, *37*, 689-701.
- (163) Butler, M. S.; Robertson, A. A. B.; Cooper, M. A. *Nat. Prod. Rep.* **2014**, *31*, 1612-1661.
- (164) Hillenmeyer, M. E.; Vandova, G. A.; Berlew, E. E.; Charkoudian, L. K. *Proc. Natl. Acad. Sci. U. S. A.* **2015**, *112*, 13952-13957.
- (165) Hertweck, C.; Luzhetskyy, A.; Rebets, Y.; Bechthold, A. *Nat. Prod. Rep.* **2007**, *24*, 162-190.
- (166) Ayer, S. W.; McInnes, A. G.; Thibault, P.; Wang, L.; Doull, J. L.; Parnell, T.; Vining, L. C. *Tetrahedron Lett.* **1991**, *32*, 6301-6304.
- (167) Rix, U.; Zheng, J.; Remsing Rix, L. L.; Greenwell, L.; Yang, K.; Rohr, J. *J. Am. Chem. Soc.* **2004**, *126*, 4496-4497.
- (168) Borissow, C. N.; Graham, C. L.; Syvitski, R. T.; Reid, T. R.; Blay, J.; Jakeman, D. L. *ChemBioChem* **2007**, *8*, 1198-1203.
- (169) Jakeman, D. L.; Farrell, S.; Young, W.; Doucet, R. J.; Timmons, S. C. *Bioorg. Med. Chem. Lett.* **2005**, *15*, 1447-1449.
- (170) Martinez-Farina, C. F.; Robertson, A. W.; Yin, H.; Monroe, S. M. A.; McFarland, S. A.; Syvitski, R. T.; Jakeman, D. L. *J. Nat. Prod.* **2015**, *78*, 1208-1214.
- (171) Robertson, A. W.; Martinez-Farina, C.; Smithen, D. A.; Yin, H.; Monroe, S.; Thompson, A.; McFarland, S. A.; Syvitski, R. T.; Jakeman, D. L. *J. Am. Chem. Soc.* **2015**, *137*, 3271-3275.
- (172) Martinez-Farina, C. F.; Jakeman, D. L. *Chem. Commun.* **2015**, *51*, 14617-14619.
- (173) Doull, J. L.; Ayer, S. W.; Singh, A. K.; Thibault, P. *J. Antibiot.* **1993**, *46*, 869-871.
- (174) Doull, J. L.; Singh, A. K.; Hoare, M.; Ayer, S. W. *J. Ind. Microbiol.* **1994**, *13*, 120-125.
- (175) Jakeman, D. L.; Graham, C. L.; Young, W.; Vining, L. C. *J. Ind. Microbiol. Biotechnol.* **2006**, *33*, 767-772.

- (176) Robertson, A. W.; MacIntyre, L. W.; MacLeod, J. M.; Forget, S. M.; Jakeman, D. L. *Chem. Sci.* **2017**, , Manuscript under review.
- (177) Tajima, T.; Akagi, Y.; Kumamoto, T.; Suzuki, N.; Ishikawa, T. *Tetrahedron Lett.* **2012**, *53*, 383-387.
- (178) Yang, X.; Yu, B. *Chem. Eur. J.* **2013**, *19*, 8431-8434.
- (179) Dupuis, S. N.; Veinot, T.; Monro, S. M. A.; Douglas, S. E.; Syvitski, R. T.; Goralski, K. B.; McFarland, S. A.; Jakeman, D. L. *J. Nat. Prod.* **2011**, *74*, 2420-2424.
- (180) Shan, M.; Sharif, E. U.; O'Doherty, G. A. *Angew. Chem. Int. Ed.* **2010**, *49*, 9492-9495.
- (181) Li, L.; Pan, G.; Zhu, X.; Fan, K.; Gao, W.; Ai, G.; Ren, J.; Shi, M.; Olano, C.; Salas, J. A. *Appl. Microbiol. Biotechnol.* **2017**, *101*, 5291-530.
- (182) Hoffmeister, D.; Ichinose, K.; Domann, S.; Faust, B.; Trefzer, A.; Drager, G.; Kirschning, A.; Fischer, C.; Kunzel, E.; Bearden, D. W.; Rohr, J.; Bechthold, A. *Chem. Biol.* **2000**, *7*, 821-831.
- (183) Zheng, J. T.; Rix, U.; Zhao, L.; Mattingly, C.; Adams, V.; Quan, C.; Rohr, J.; Yang, K. Q. *J. Antibiot.* **2005**, *58*, 405-408.
- (184) Dupuis, S. N.; Robertson, A. W.; Veinot, T.; Monro, S. M. A.; Douglas, S. E.; Syvitski, R. T.; Goralski, K. B.; McFarland, S. A.; Jakeman, D. L. *Chem. Sci.* **2012**, *3*, 1640-1644.
- (185) Jakeman, D. L.; Dupuis, S. N.; Graham, C. L. *Pure Appl. Chem.* **2009**, *81*, 1041-1049.
- (186) Monro, S. M. A.; Cottreau, K. M.; Spencer, C.; Wentzell, J. R.; Graham, C. L.; Borissow, C. N.; Jakeman, D. L.; McFarland, S. A. *Bioorg. Med. Chem.* **2011**, *19*, 3357-3360.
- (187) Cottreau, K.; Spencer, C.; Wentzell, J.; Graham, C. L.; Borissow, C. N.; Jakeman, D. L.; McFarland S.A. *Org. Lett.* **2010**, *12*, 1172-1175.
- (188) Issa, M. E.; Hall, S. R.; Dupuis, S. N.; Graham, C. L.; Jakeman, D. L.; Goralski, K. B. *Anti-Cancer Drug* **2014**, *25*, 255-269.
- (189) Hall, S. R.; Blundon, H. L.; Ladda, M. A.; Robertson, A. W.; Martinez-Farina, C.; Jakeman, D. L.; Goralski, K. B. *Pharmacol. Res. Perspect.* **2015**, *3*, e00110.
- (190) Fu, D. H.; Jiang, W.; Zheng, J. T.; Zhao, G. Y.; Li, Y.; Yi, H.; Li, Z. R.; Jiang, J. D.; Yang, K. Q.; Wang, Y.; Si, S. Y. *Mol. Cancer Ther.* **2008**, *7*, 2386-2393.
- (191) Jakeman, D. L.; Bandi, S.; Graham, C. L.; Reid, T. R.; Wentzell, J. R.; Douglas, S. E. *Antimicrob. Agents Chemother.* **2009**, *53*, 1245-1247.

- (192) Forget, S. M.; Robertson, A. W.; Overy, D. P.; Kerr, R. G.; Jakeman, D. L. *J. Nat. Prod.* **2017**, *80*, 1860-1866.
- (193) Fan, K.; Zhang, X.; Liu, H.; Han, H.; Luo, Y.; Wang, Q.; Geng, M.; Yang, K. *J. Antibiot.* **2012**, *65*, 449-452.
- (194) Wang, J.; Sánchez-Roselló, M.; Aceña, J. L.; del Pozo, C.; Sorochinsky, A. E.; Fustero, S.; Soloshonok, V. A.; Liu, H. *Chem. Rev.* **2013**, *114*, 2432-2506.
- (195) Zhu, X. M.; Hackl, S.; Thaker, M. N.; Kalan, L.; Weber, C.; Urgast, D. S.; Krupp, E. M.; Brewer, A.; Vanner, S.; Szawiola, A.; Yim, G.; Feldmann, J.; Bechthold, A.; Wright, G. D.; Zechel, D. L. *ChemBioChem* **2015**, *16*, 2498-2506.
- (196) Khodade, V. S.; Sharath Chandra, M.; Banerjee, A.; Lahiri, S.; Pulipeta, M.; Rangarajan, R.; Chakrapani, H. *ACS Med. Chem. Lett.* **2014**, *5*, 777-781.
- (197) Tibrewal, N.; Pahari, P.; Wang, G.; Kharel, M. K.; Morris, C.; Downey, T.; Hou, Y.; Bugni, T. S.; Rohr, J. *J. Am. Chem. Soc.* **2012**, *134*, 18181-18184.
- (198) Fan, K.; Pan, G.; Peng, X.; Zheng, J.; Gao, W.; Wang, J.; Wang, W.; Li, Y.; Yang, K. *Chem. Biol.* **2012**, *19*, 1381-1390.
- (199) Goncharov, N. V.; Jenkins, R. O.; Radilov, A. S. *J. Appl. Toxicol.* **2006**, *26*, 148-161.
- (200) Forget, S. M.; Mcvey, J.; Vining, L. C.; Jakeman, D. L. *Front. Microbiol.* **2017**, *8*, doi: 10.3389/fmicb.2017.00432.
- (201) Gallo, M. A.; Ward, J.; Hutchinson, C. *Microbiology* **1996**, *142*, 269-275.
- (202) Malla, S.; Prasad Niraula, N.; Singh, B.; Liou, K.; Kyung Sohng, J. *Microbiol. Res.* **2010**, *165*, 427-435.
- (203) Lombard, V.; Ramulu, H. G.; Drula, E.; Coutinho, P. M.; Henrissat, B. *Nucleic Acids Res.* **2014**, *42*, D490-D495.
- (204) Pullan, S. T.; Chandra, G.; Bibb, M. J.; Merrick, M. *BMC Genomics* **2011**, *12*, doi.org/10.1186/1471-2164-12-175.
- (205) Griffith, R. R.; Thorson, J. S. *Nat. Chem. Biol.* **2006**, *2*, 659-660.
- (206) Robertson, A. W.; Forget, S. M.; Martinez-Farina, C. F.; McCormick, N. E.; Syvitski, R. T.; Jakeman, D. L. *J. Am. Chem. Soc.* **2016**, *138*, 2200-2208.
- (207) Xu, G. M.; Wang, J. A.; Wang, L. Q.; Tian, X. Y.; Yang, H. H.; Fan, K. Q.; Yang, K. Q.; Tan, H. R. *J. Biol. Chem.* **2010**, *285*, 27440-27448.
- (208) Nah, H.; Pyeon, H.; Kang, S.; Choi, S.; Kim, E. *Front. Microbiol.* **2017**, *8*, doi: 10.3389/fmicb.2017.00394.

- (209) Bekiesch, P.; Basitta, P.; Apel, A. K. *Arch. Pharm. Chem. Life Sci.* **2016**, *349*, 594-601.
- (210) Olano, C.; Méndez, C.; Salas, J. A. *Nat. Prod. Rep.* **2009**, *26*, 628-660.
- (211) Kim, E.; Moore, B. S.; Yoon, Y. J. *Nat. Chem. Biol.* **2015**, *11*, 649-659.
- (212) Weissman, K. J. *Nat. Prod. Rep.* **2016**, *33*, 203-230.
- (213) Wohler, S. E.; Blanco, G.; Lombo, F.; Fernandez, E.; Brana, A. F.; Reich, S.; Udvarnoki, G.; Mendez, C.; Decker, H.; Frevert, J.; Salas, J. A.; Rohr, J. *J. Am. Chem. Soc.* **1998**, *120*, 10596-10601.
- (214) Olano, C.; Abdelfattah, M. S.; Gullón, S.; Braña, A. F.; Rohr, J.; Méndez, C.; Salas, J. A. *ChemBioChem* **2008**, *9*, 624-633.
- (215) Binaschi, M.; Bigioni, M.; Cipollone, A.; Rossi, C.; Goso, C.; Maggi, C.; Capranico, G.; Animati, F. *Curr. Med. Chem. Anticancer Agents* **2001**, *1*, 113-130.
- (216) Trefzer, A.; Fischer, C.; Stockert, S.; Westrich, L.; Kunzel, E.; Girreser, U.; Rohr, J.; Bechthold, A. *Chem. Biol.* **2001**, *8*, 1239-1252.
- (217) Hoffmeister, D.; Wilkinson, B.; Foster, G.; Sidebottom, P. J.; Ichinose, K.; Bechthold, A. *Chem. Biol.* **2002**, *9*, 287-295.
- (218) Yoon, Y. J.; Beck, B. J.; Kim, B. S.; Kang, H.; Reynolds, K. A.; Sherman, D. H. *Chem. Biol.* **2002**, *9*, 203-214.
- (219) Jung, W.; Kim, E.; Kang, H.; Choi, C.; Sherman, D. H.; Yoon, Y. J. *J. Microbiol. Biotechnol.* **2003**, *13*, 823-827.
- (220) Maharjan, S.; Park, J. W.; Yoon, Y. J.; Lee, H. C.; Sohng, J. K. *Biotechnol. Lett.* **2010**, *32*, 277-282.
- (221) Kim, E.; Song, M. C.; Kim, M. S.; Beom, J. Y.; Jung, J. A.; Cho, H. S.; Yoon, Y. J. *ACS Comb. Sci.* **2017**, *19*, 262-270.
- (222) Zhang, H.; White-Phillip, J.; Melancon, C. E.; Kwon, H.; Yu, W.; Liu, H. *J. Am. Chem. Soc.* **2007**, *129*, 14670-14683.
- (223) Holtzel, A.; Dieter, A.; Schmid, D. G.; Brown, R.; Goodfellow, M.; Beil, W.; Jung, G.; Fiedler, H. *J. Antibiot.* **2003**, *56*, 1058-1061.
- (224) Li, S.; Xiao, J.; Zhu, Y.; Zhang, G.; Yang, C.; Zhang, H.; Ma, L.; Zhang, C. *Org. Lett.* **2013**, *15*, 1374-1377.
- (225) Takahashi, H.; Osada, H.; Uramoto, M.; Isono, K. *J. Antibiot.* **1990**, *43*, 168-173.

- (226) Van Arnam, E. B.; Ruzzini, A. C.; Sit, C. S.; Horn, H.; Pinto-Tomas, A. A.; Currie, C. R.; Clardy, J. *Proc. Natl. Acad. Sci. U. S. A.* **2016**, *113*, 12940-12945.
- (227) Zielinski, J.; Golik, J.; Pawlak, J.; Borowski, E.; Falkowski, L. *J. Antibiot.* **1988**, *41*, 1289-1291.
- (228) Kong, F.; Zhao, N.; Siegel, M. M.; Janota, K.; Ashcroft, J. S.; Koehn, F. E.; Borders, D. B.; Carter, G. T. *J. Am. Chem. Soc.* **1998**, *120*, 13301-13311.
- (229) Zhang, M. M.; Wong, F. T.; Wang, Y.; Luo, S.; Lim, Y. H.; Heng, E.; Yeo, W. L.; Cobb, R. E.; Enghiad, B.; Ang, E. L. *Nat. Chem. Biol.* **2017**, *13*, 607-609.
- (230) Li, L.; Jiang, W.; Lu, Y. *Biotechnol. Adv.* **2017**, ,
[dx.doi.org/10.1016/j.biotechadv.2017.03.007](https://doi.org/10.1016/j.biotechadv.2017.03.007).
- (231) Xiao, J.; Li, H.; Wen, S.; Hong, W. *J. Gen. Applied. Microbiol.* **2014**, *60*, 256-261.
- (232) Ni, X.; Zong, T.; Zhang, H.; Gu, Y.; Huang, M.; Tian, W.; Xia, H. *Microbiol. Res.* **2016**, *185*, 36-44.
- (233) Kieser, T.; Bibb, M. J.; Buttner, M. J.; Chater, K. F.; Hopwood, D. A. In *Practical Streptomyces Genetics*; The John Innes Foundation: Norwich, England, 2000; Vol. 2, pp 613.
- (234) Bierman, M.; Logan, R.; O'Brien, K.; Seno, E. T.; Rao, R. N.; Schoner, B. E. *Gene* **1992**, *116*, 43-49.
- (235) Kobylansky, A.; Ostash, B.; Fedorenko, V. *Cytol. Genet.* **2009**, *43*, 194-200.
- (236) Han, A. R.; Park, J. W.; Lee, M. K.; Ban, Y. H.; Yoo, Y. J.; Kim, E. J.; Kim, E.; Kim, B. G.; Sohng, J. K.; Yoon, Y. J. *Appl. Environ. Microbiol.* **2011**, *77*, 4912-4923.
- (237) Mo, S.; Yoon, Y. J. *J. Mol. Microbiol. Biotechnol.* **2016**, *26*, 66-71.
- (238) Hong, J. S. J.; Park, S. H.; Choi, C. Y.; Sohng, J. K.; Yoon, Y. J. *FEMS Microbiol. Lett.* **2004**, *238*, 391-399.
- (239) Combes, P.; Till, R.; Bee, S.; Smith, M. C. *J. Bacteriol.* **2002**, *184*, 5746-5752.
- (240) Bibb, M. J.; Janssen, G. R.; Ward, J. M. *Gene* **1986**, *41*, E357-E368.
- (241) Bibb, M. J.; White, J.; Ward, J. M.; Janssen, G. R. *Mol. Microbiol.* **1994**, *14*, 533-545.
- (242) Schmitt-John, T.; Engels, J. W. *Appl. Microbiol. Biotechnol.* **1992**, *36*, 493-498.
- (243) Okanishi, M.; Suzuki, K.; Umezawa, H. *J. Gen. Microbiol.* **1974**, *80*, 389-400.

- (244) Lamichhane, J.; Liou, K.; Lee, H. C.; Kim, C.; Sohng, J. K. *Biotechnol. Lett.* **2006**, *28*, 545-553.
- (245) MacLeod, J. M.; Robertson, A. W.; Hall, S. R.; Bennett, L. G.; Kerr, R. G.; Goralski, K. B.; Jakeman, D. L. *J. Nat. Prod.* **2017**, Manuscript in preparation.
- (246) Gottlieb, H. E.; Kotlyar, V.; Nudelman, A. *J. Org. Chem.* **1997**, *62*, 7512-7515.
- (247) Lewandowicz, A.; Schramm, V. L. *Biochemistry* **2004**, *43*, 1458-1468.
- (248) Wang, L.; Vining, L. C. *Microbiology* **2003**, *149*, 1991-2004.
- (249) Morais, L. L.; Yuasa, H.; Bennis, K.; Ripoche, I.; Auzanneau, F. I. *Can. J. Chem.* **2006**, *84*, 587-596.
- (250) Cavaluzzi, M. J.; Borer, P. N. *Nucleic Acids Res.* **2004**, *32*, 10.1093/nar/gnh015.
- (251) Forget, S. M.; Smithen, D. A.; Jee, A.; Jakeman, D. L. *Biochemistry* **2015**, *54*, 1703-1707.
- (252) Gibson, D. G.; Young, L.; Chuang, R.; Venter, J. C.; Hutchison, C. A.; Smith, H. O. *Nat. Methods* **2009**, *6*, 343-345.
- (253) Pan, S. H.; Malcolm, B. A. *BioTechniques* **2000**, *29*, 1234-1238.
- (254) Grossman, T. H.; Kawasaki, E. S.; Punreddy, S. R.; Osburne, M. S. *Gene* **1998**, *209*, 95-103.
- (255) Methods for dilution antimicrobial susceptibility test for bacteria that grow aerobically *National Committee for Clinical Laboratory Standards* **2003**, *6th ed.*, Approved standard M7-A6.
- (256) Loranger, M. W.; Beaton, S. A.; Lines, K. L.; Jakeman, D. L. *Carbohydr. Res.* **2013**, *379*, 43-50.
- (257) Smithen, D. A.; Forget, S. M.; McCormick, N. E.; Syvitski, R. T.; Jakeman, D. L. *Org. Biomol. Chem.* **2015**, *13*, 3347-3350.
- (258) Jakeman, D. L.; Young, J. L.; Huestis, M. P.; Peltier, P.; Daniellou, R.; Nugier-Chauvin, C.; Ferrieres, V. *Biochemistry* **2008**, *47*, 8719-8725.
- (259) Bode, H. B.; Müller, R. *Angew. Chem. Int. Ed.* **2007**, *46*, 2147-2150.
- (260) Minami, A.; Kakinuma, K.; Eguchi, T. *Tetrahedron Lett.* **2005**, *46*, 6187-6190.
- (261) Jessen, H.; Schulz, T.; Balzarini, J.; Meier, C. *Angew. Chem. Int. Ed.* **2008**, *47*, 8719-8722.
- (262) Pertusati, F.; Serpi, M.; McGuigan, C. *Antivir. Chem. Chemother.* **2012**, *22*, 181-203.

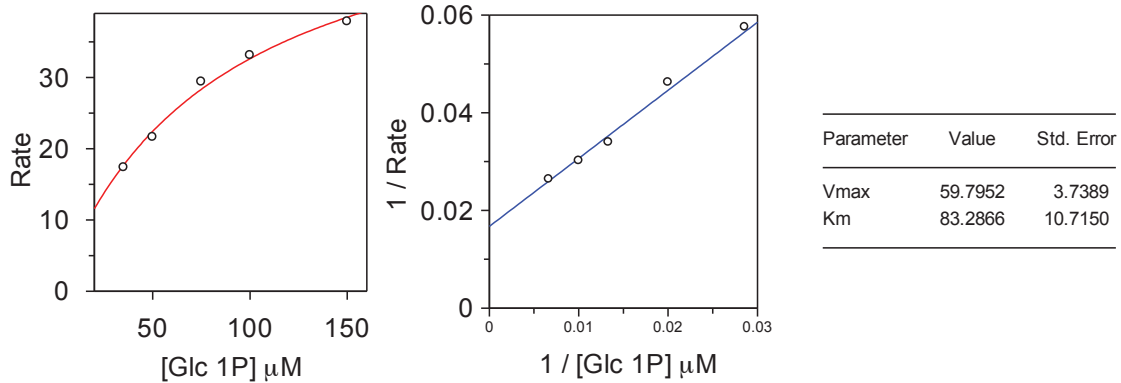
(263) Rautio, J.; Kumpulainen, H.; Heimbach, T.; Oliyai, R.; Oh, D.; Jarvinen, T.; Savolainen, J. *Nat. Rev. Drug Discov.* **2008**, *7*, 255-270.

Appendix A: Supplementary materials for Chapter 2.2.

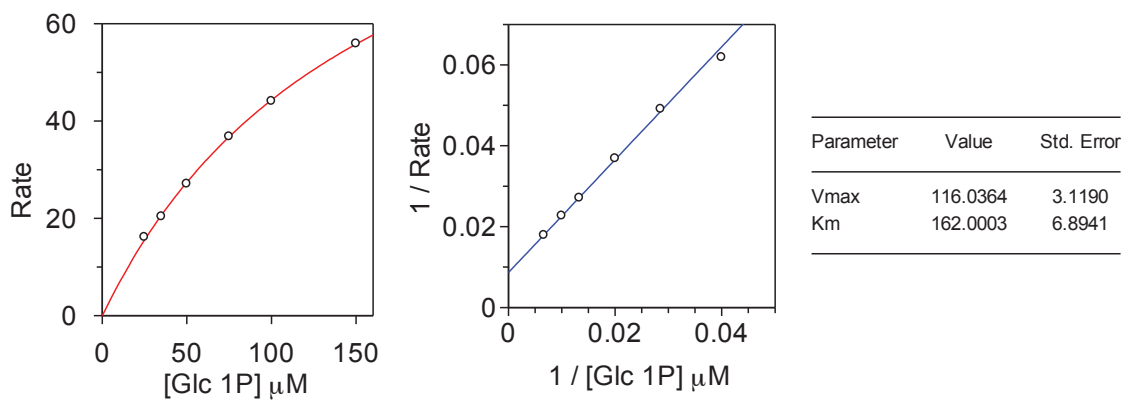
Cps2L reaction sugar nucleotide product retention times and EPI fragmentation.

NDP-sugar product	HPLC retention time (min) ^a	EPI (<i>m/z</i>)
dTTP	7.52	-
UTP	7.43	-
dTDP-GlcN 2.7 ^b	2.60 ^b	562,383,357 ^b
UDP-GlcN 2.8	2.34	564, 385, 320
dTDP-kan 2.9	2.87	562, 321, 273
UDP-Kan 2.10	2.34	564,385,323
dTDP-3AzGlc 2.11	6.45	589, 321, 266
UDP-3azGlc 2.12	5.75	590, 323
dTDP- <i>myo</i> -Ino 2.13	5.46	563, 321, 241
dTDP-Glc1CP 2.14 ^c	5.47 ^c	561,321 ^c
UDP-Glc1CP 2.15 ^c	5.27 ^c	563, 323 ^c

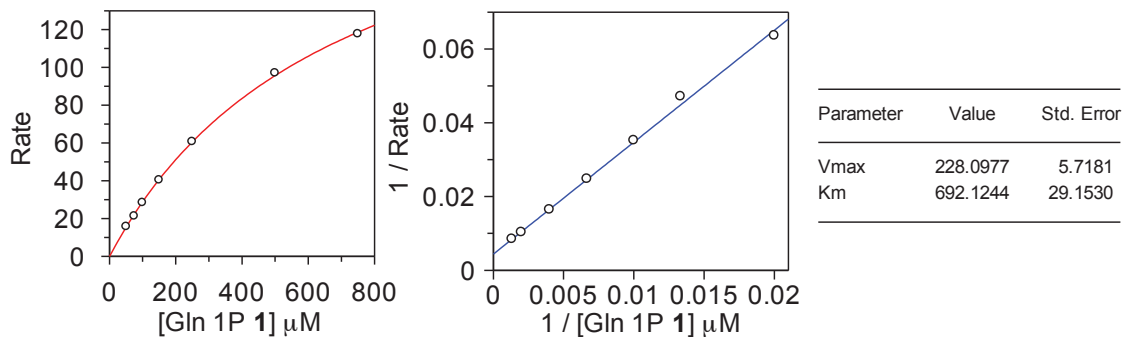
^aThe provided retention times are representative, as some variability in the retention times (+/- 0.2 min) was observed due to instrument variability; ^{b,c}Previous work^{80,87}



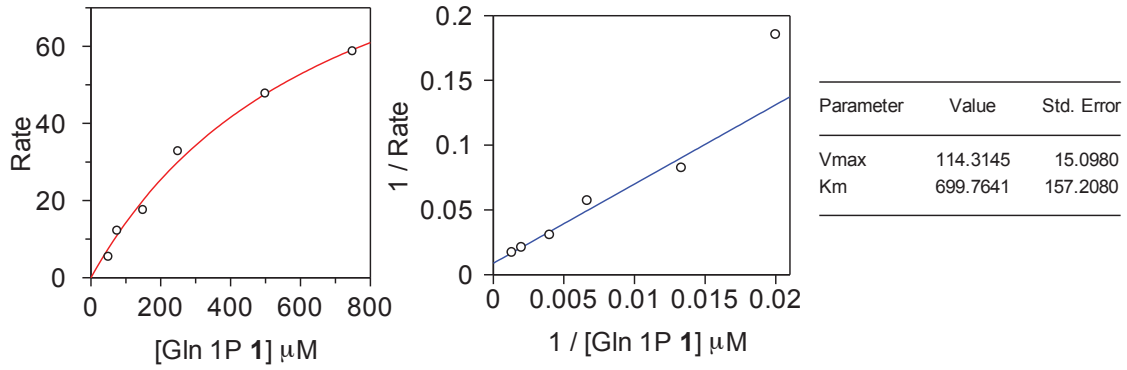
Variable Glc 1-P in the presence of constant dTTP (1 mM) and 0.003 μM Cps2L.



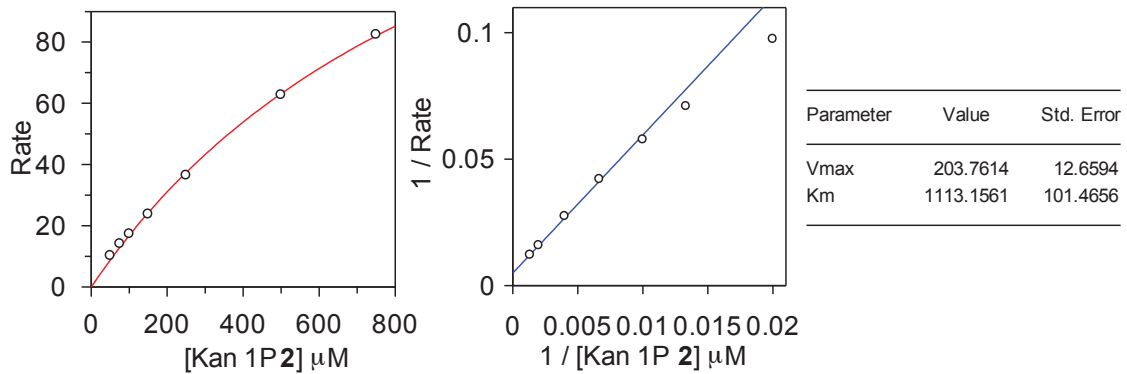
Variable Glc 1-P in the presence of constant UTP (1 mM) and 0.0925 μM Cps2L.



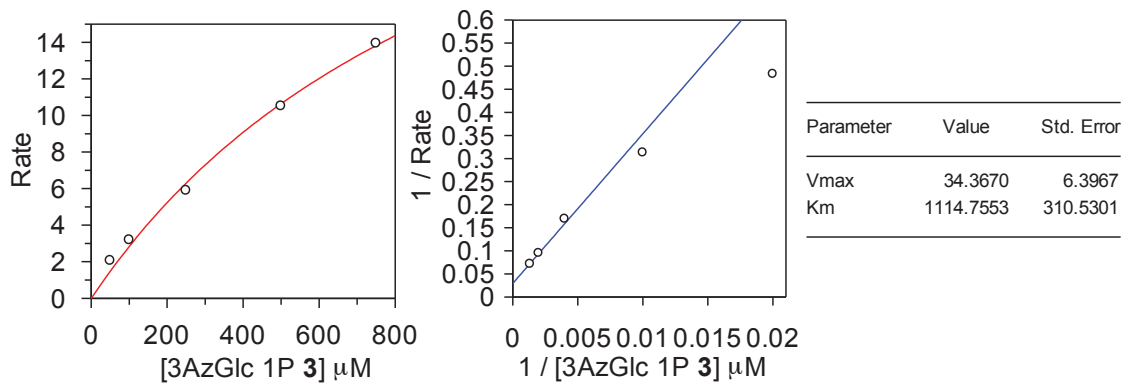
Variable GlcN 1-P **2.1** in the presence of constant dTTP (1 mM) and 0.06 μM Cps2L.



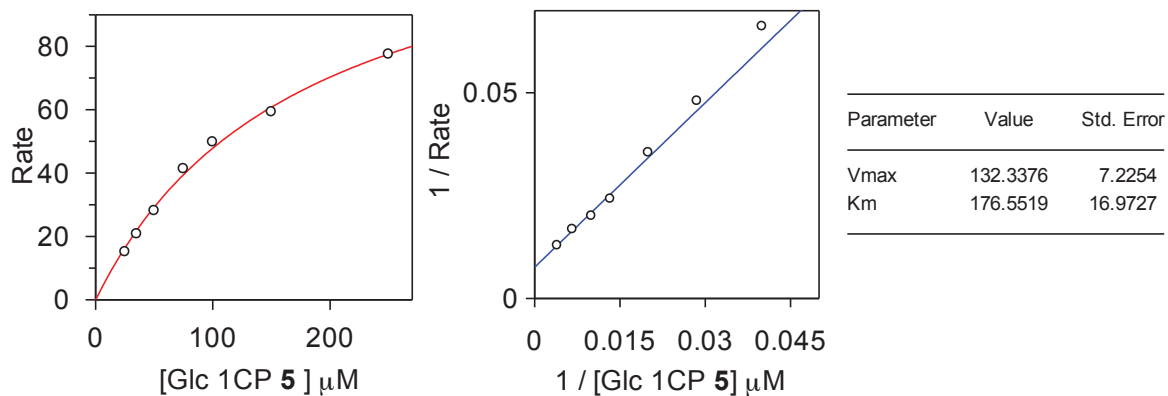
Variable GlcN 1-P **2.1** in the presence of constant UTP (1 mM) and 1.34 μM Cps2L.



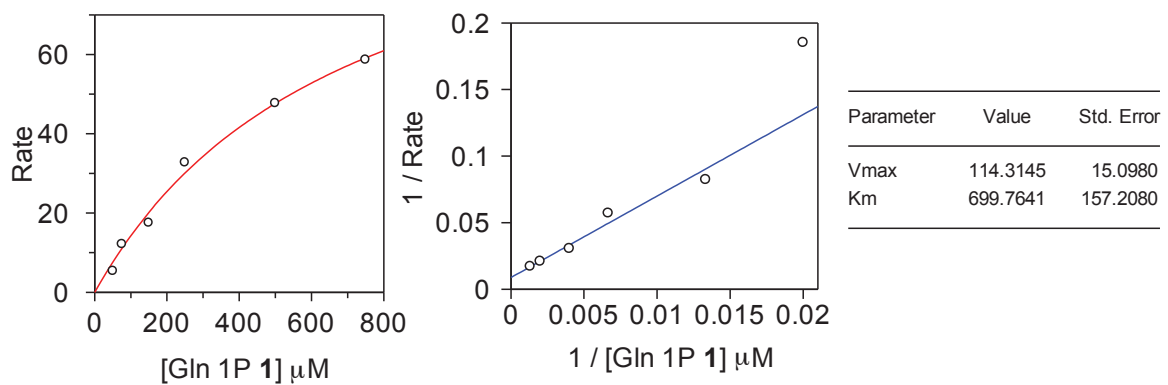
Variable Kan 1-P **2.2** in the presence of constant dTTP (1 mM) and 3 μM Cps2L.



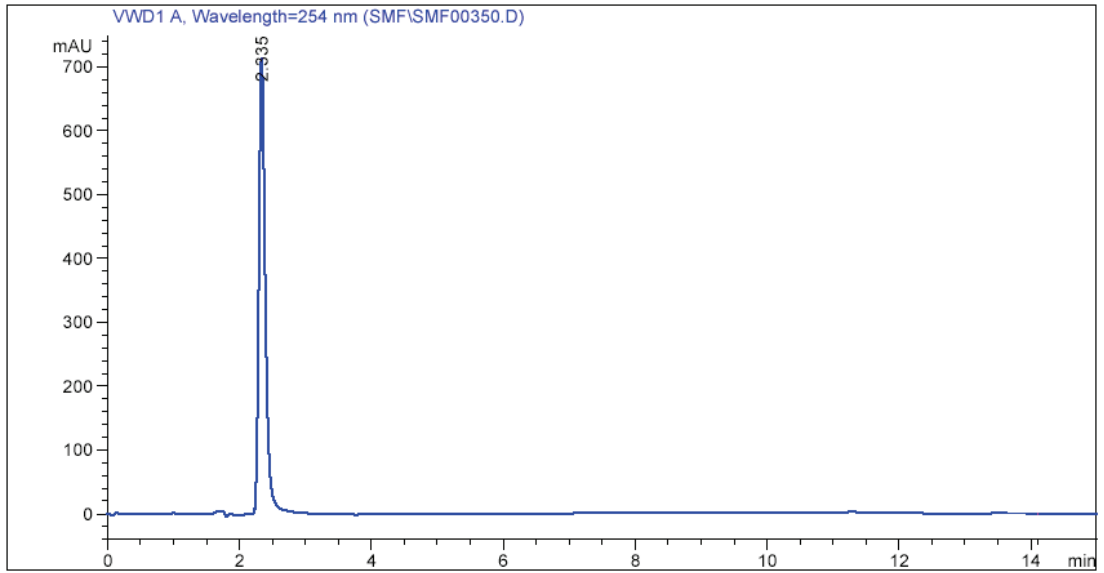
Variable 3Az-Glc 1-P **2.3** in the presence of constant dTTP (1 mM) and 134 μM Cps2L.



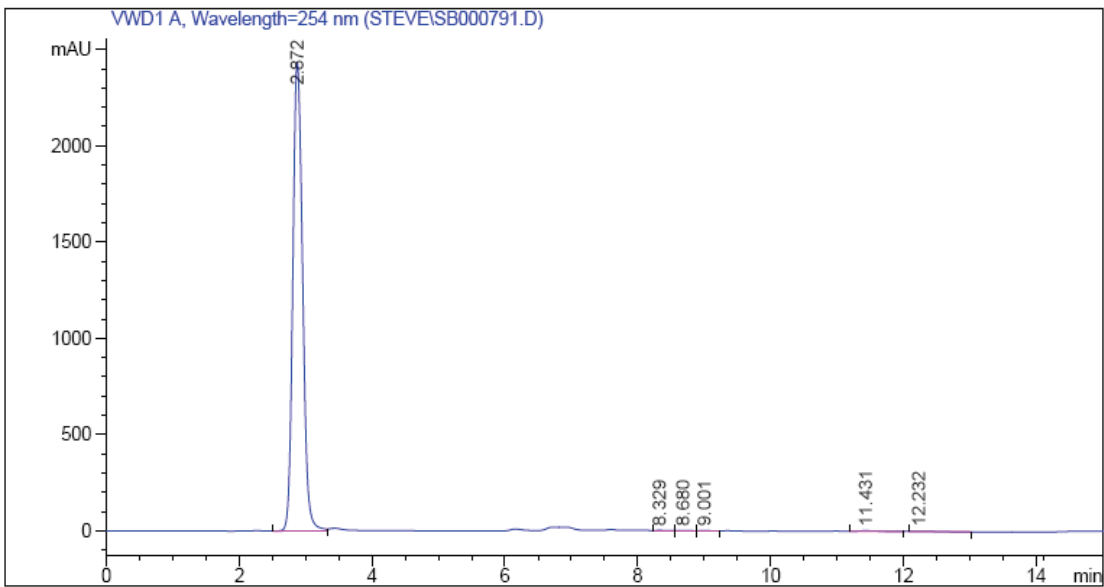
Variable Glc 1C-P **2.5** in the presence of constant dTTP (1 mM) and 0.03 μM Cps2L.



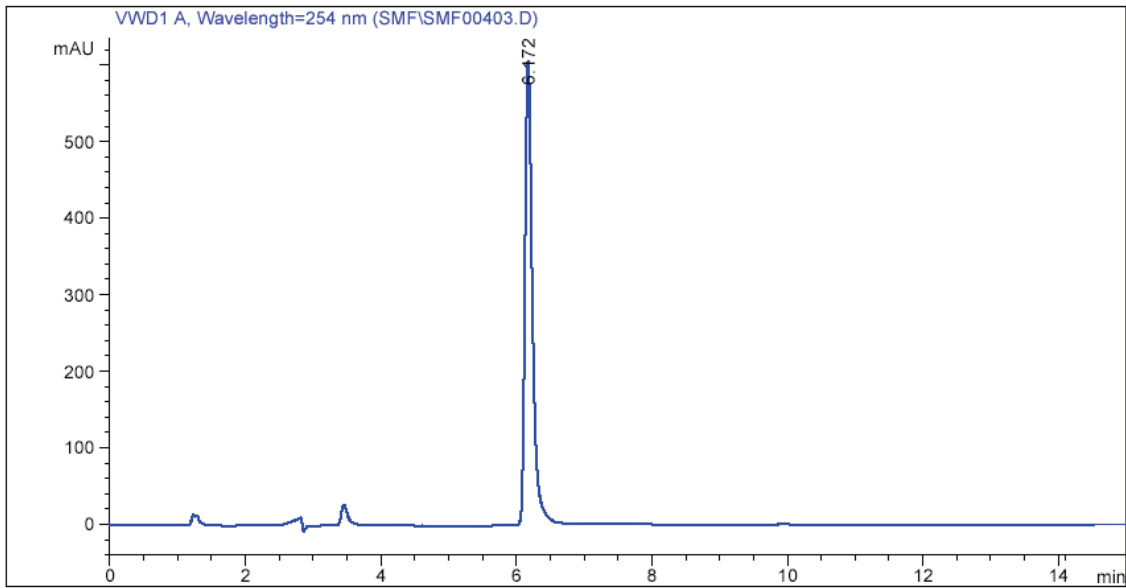
Variable Glc 1C-P **2.5** in the presence of constant UTP (1 mM) and 1.85 μM Cps2L.



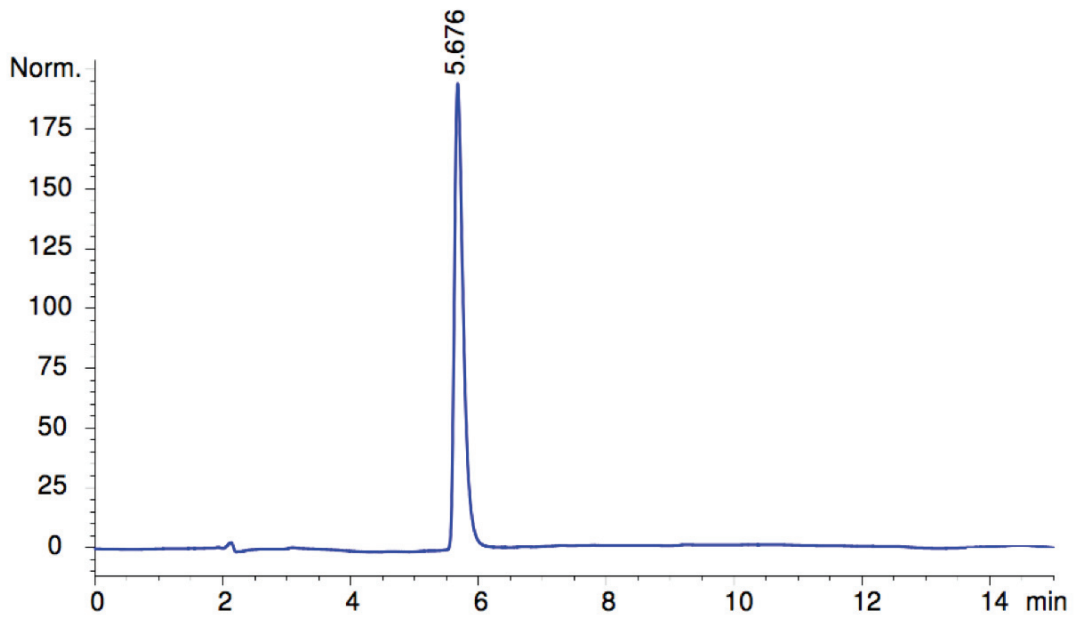
HPLC trace of purified UDP-GlcN **2.8**.



HPLC trace of purified dTDP-Kan **2.9**.

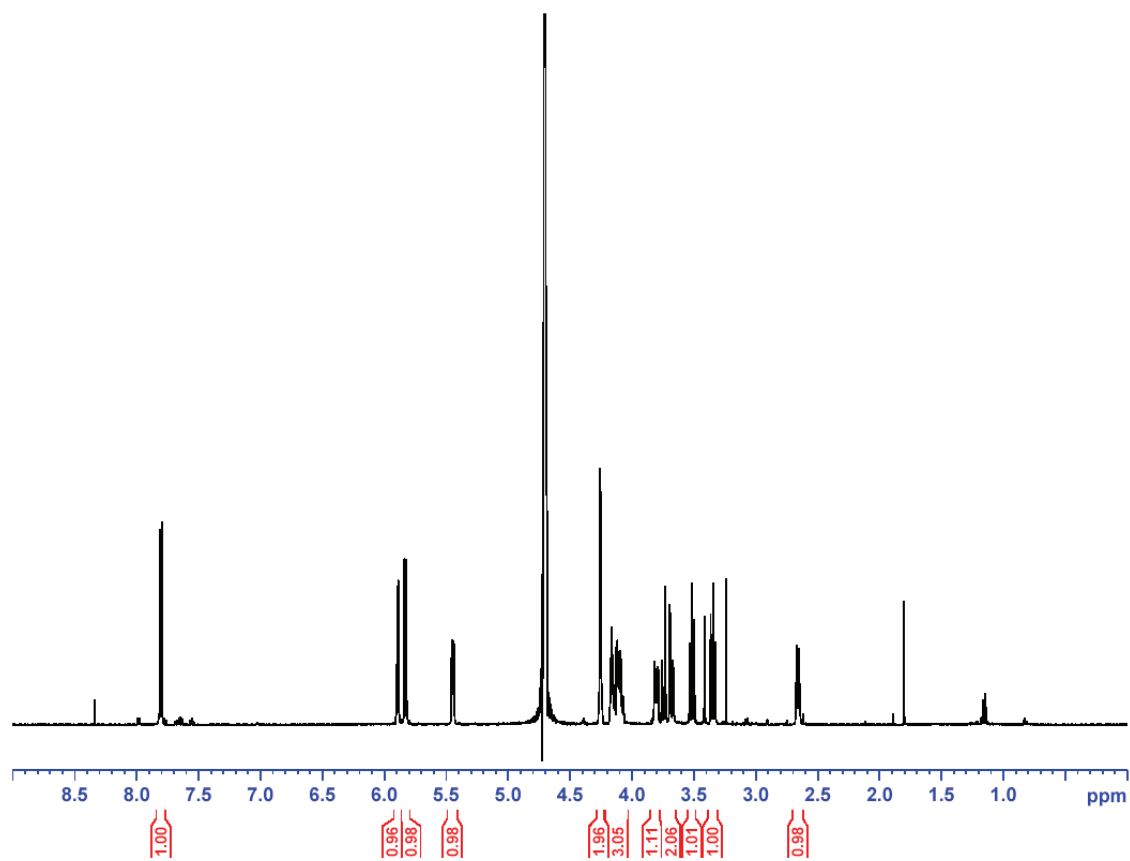


HPLC trace of purified dTDP-3AzGlc **2.11**.

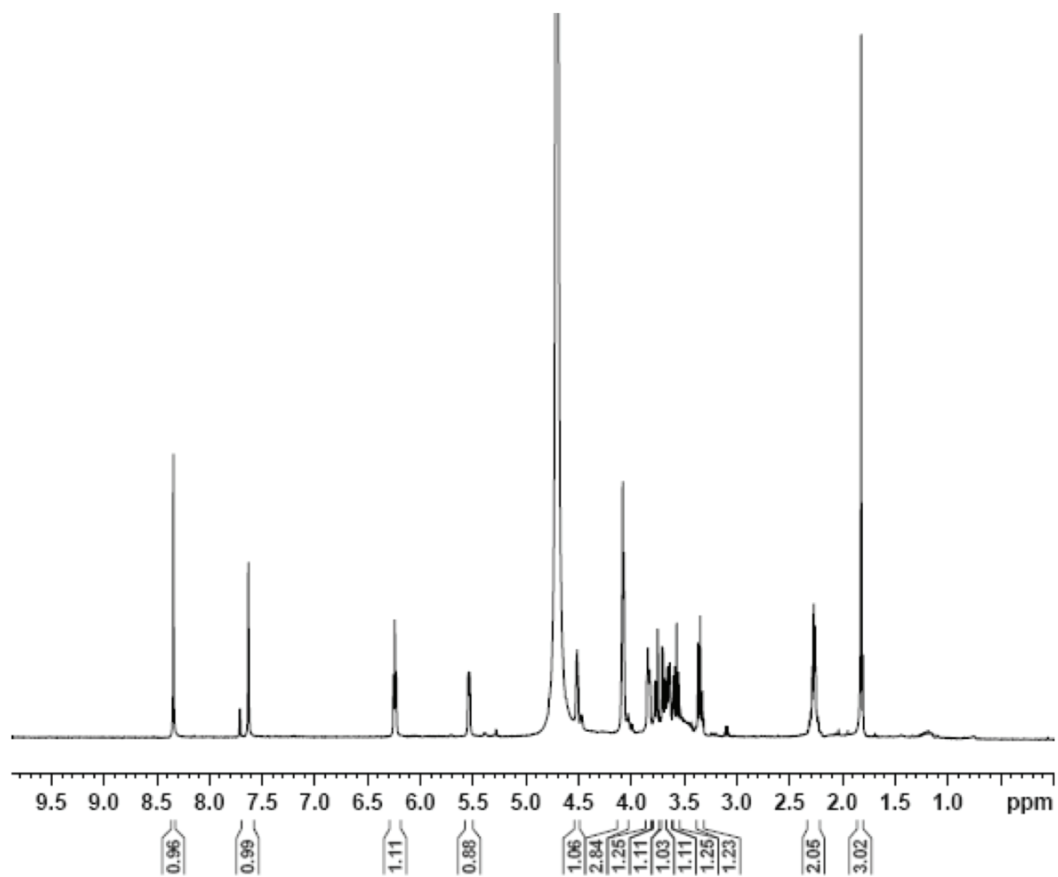


HPLC trace of UDP-1C-glc **2.15**.

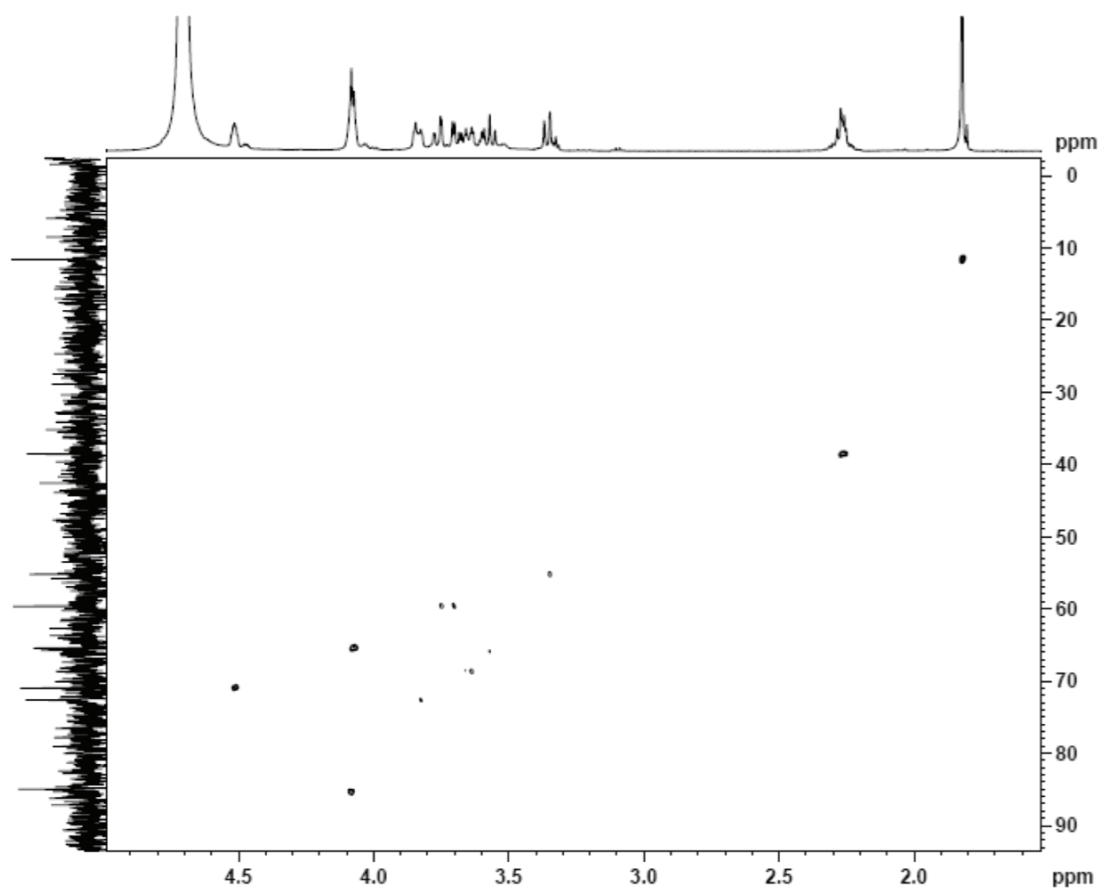
^1H NMR (D_2O , 500 MHz) spectrum of UDP-GlcN **2.8**.



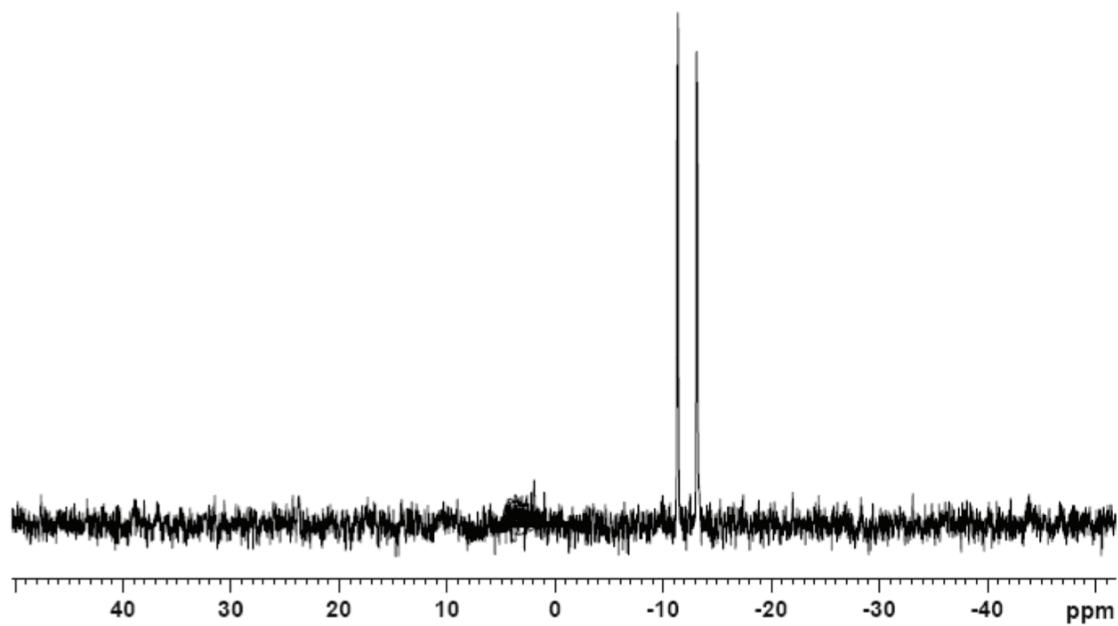
^1H NMR (D_2O , 500 MHz) spectrum of dTDP-kanosamine **2.9**.



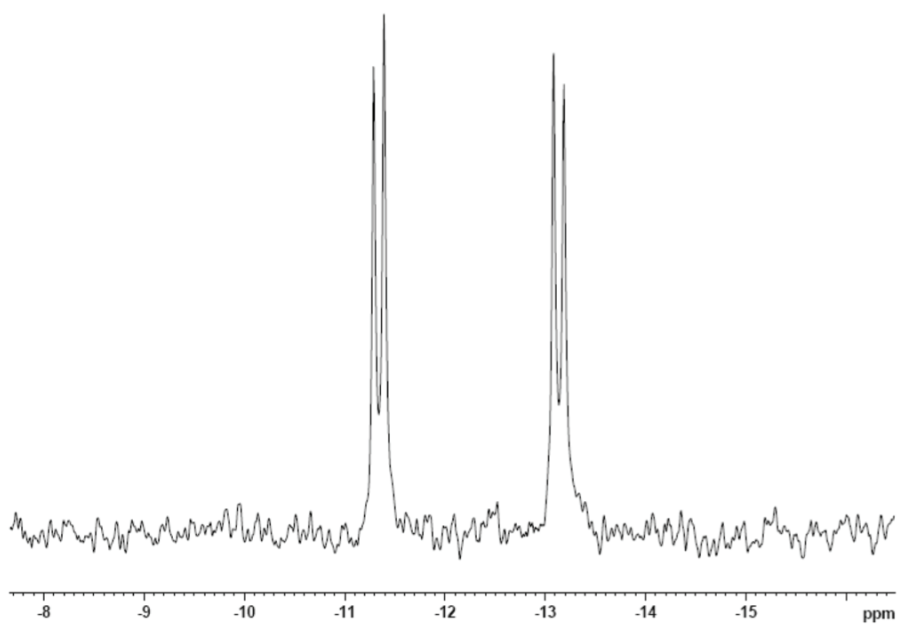
2D HSQC (D_2O , 500 MHz) spectrum of dTDP-kanosamine **2.9**.



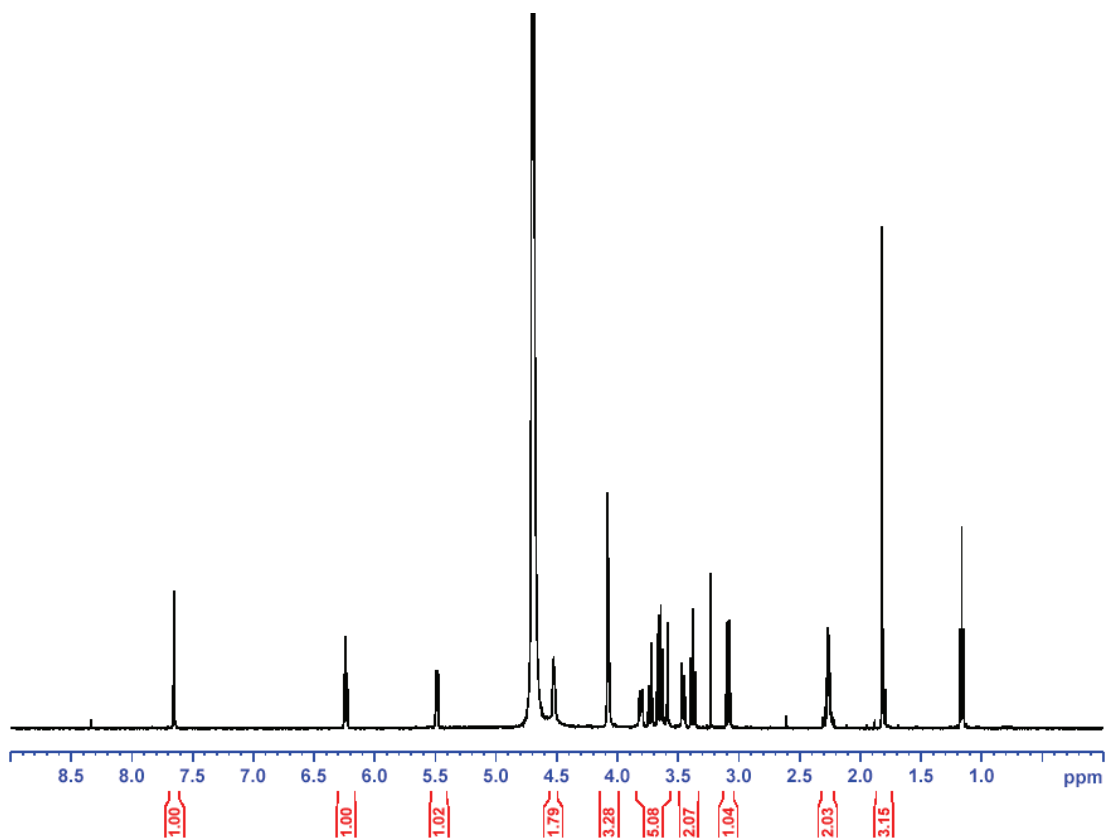
$^{31}\text{P} \{^1\text{H}\}$ NMR (D_2O , 202 MHz) spectrum of dTDP-kanosamine **2.9**.



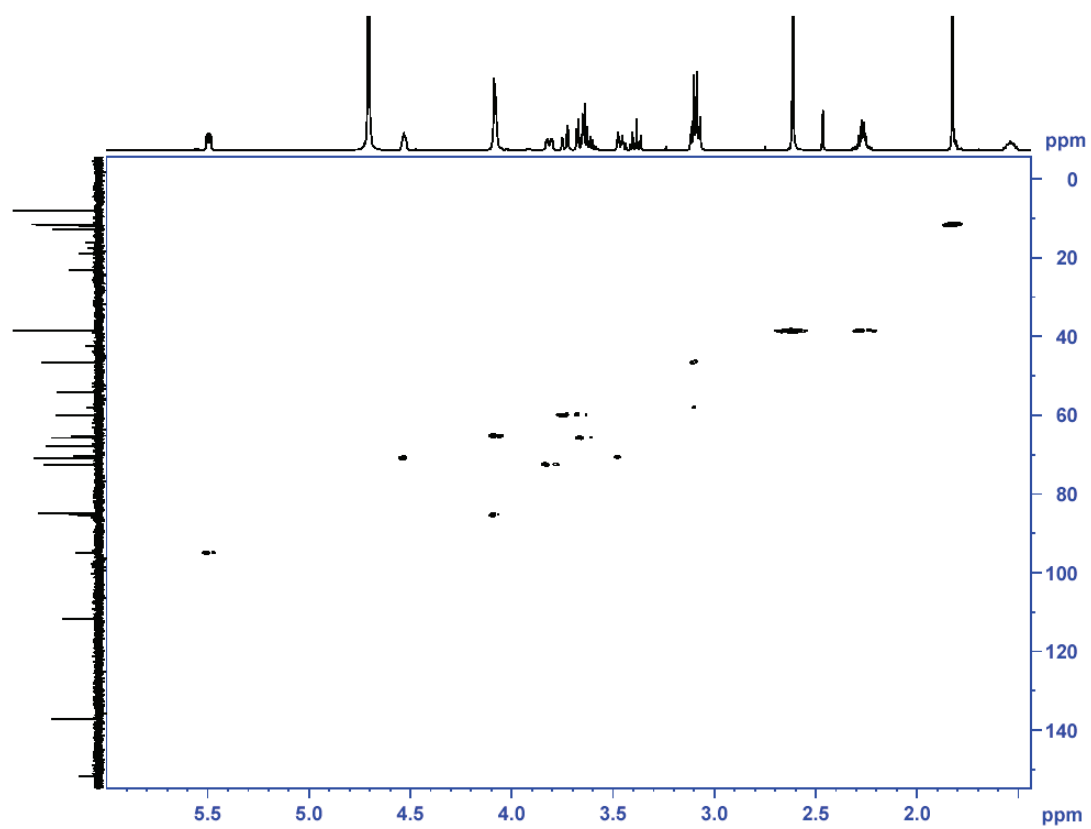
Expansion of above spectrum:



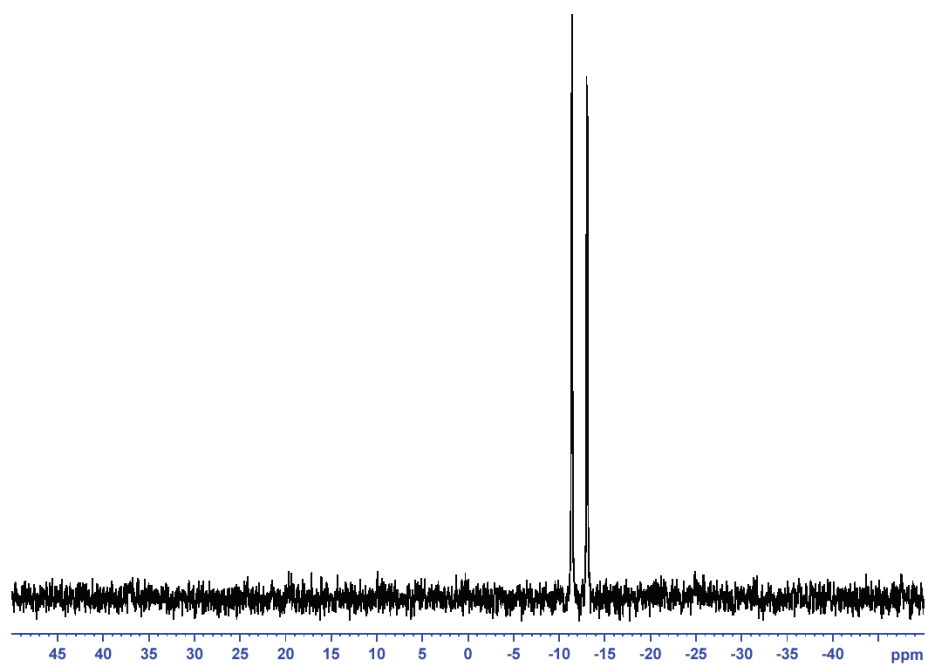
^1H NMR (D_2O , 500 MHz) spectrum of dTDP-3AzGlc **2.11**.



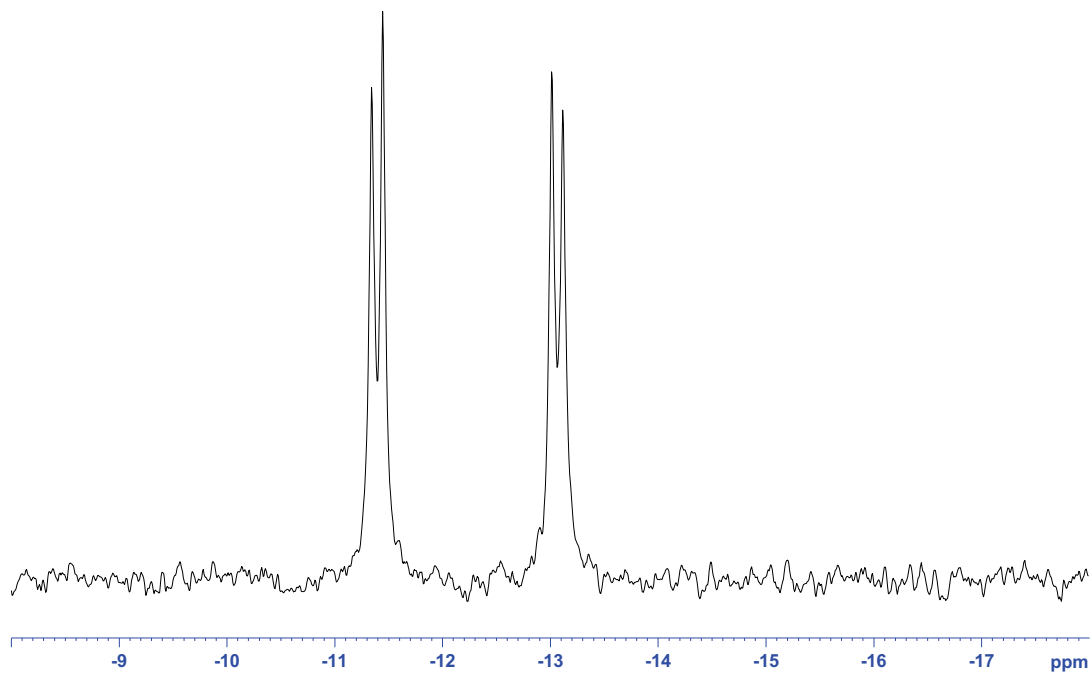
HSQC (D₂O, 500 MHz) spectrum of dTDP-3AzGlc **2.11**.



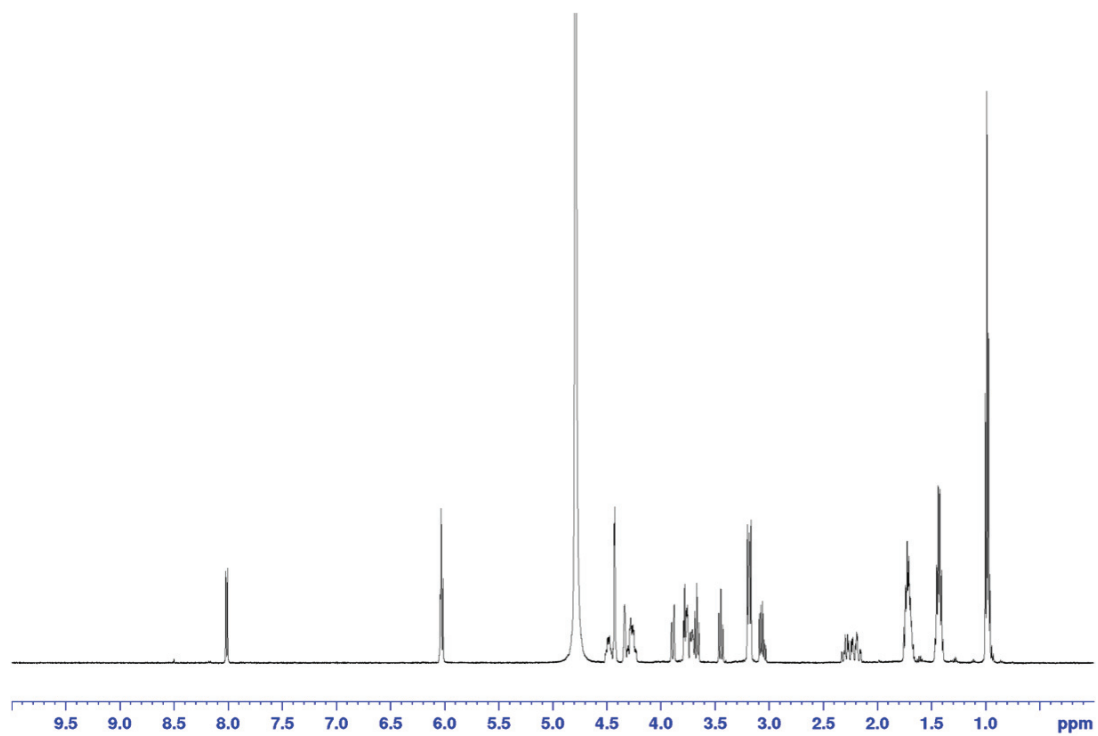
$^{31}\text{P} \{^1\text{H}\}$ NMR (D_2O , 202 MHz) spectrum of dTDP-3AzGlc **2.11**.



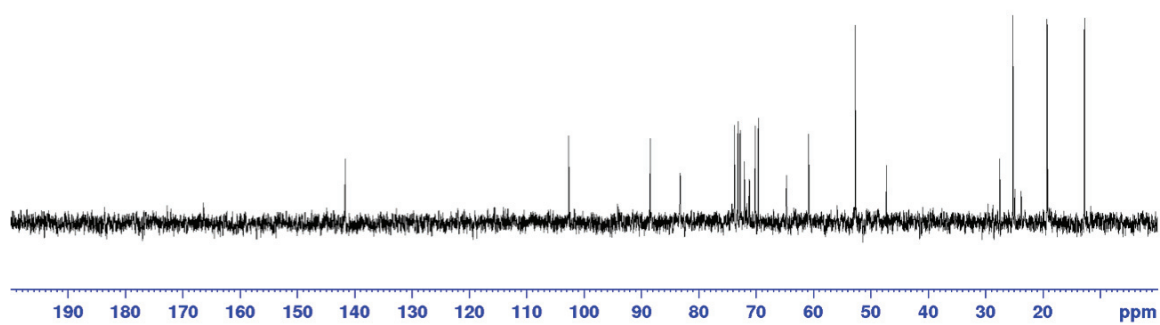
Expansion of above spectrum:



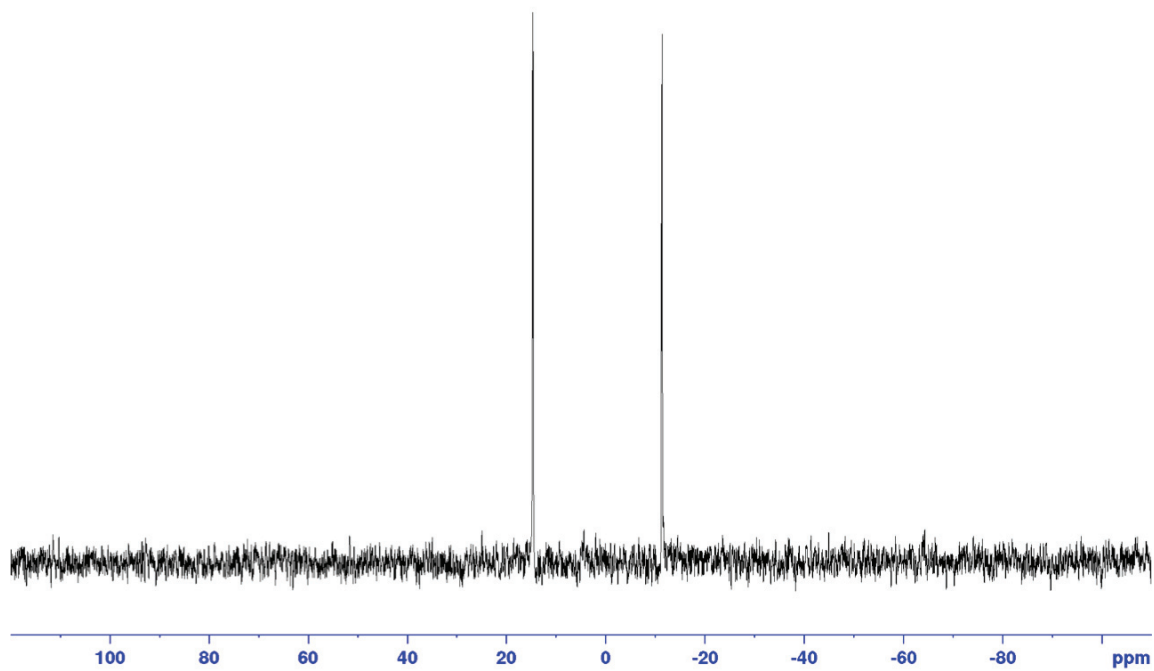
^1H NMR (D_2O , 500 MHz) spectrum of UDP-1C-glc **2.15**.



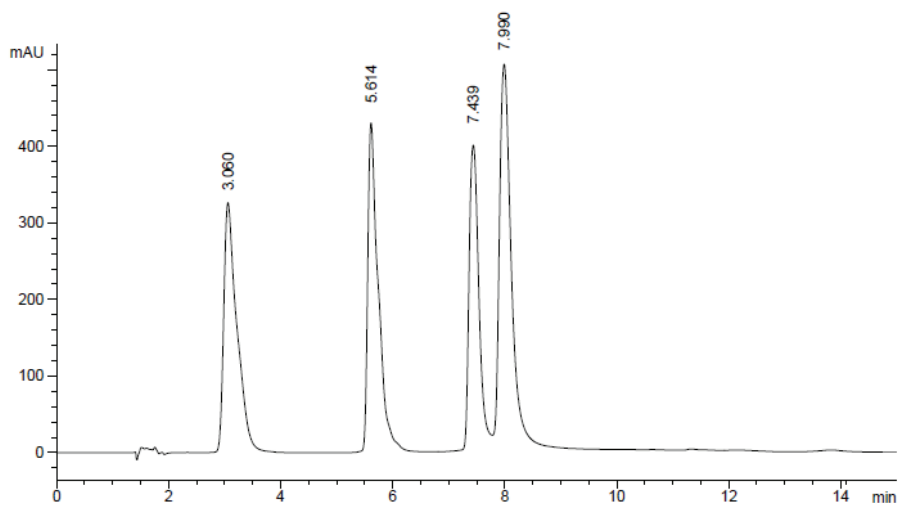
^{13}C NMR (D_2O , 125 MHz).spectrum of UDP-1C-glc **2.15**.



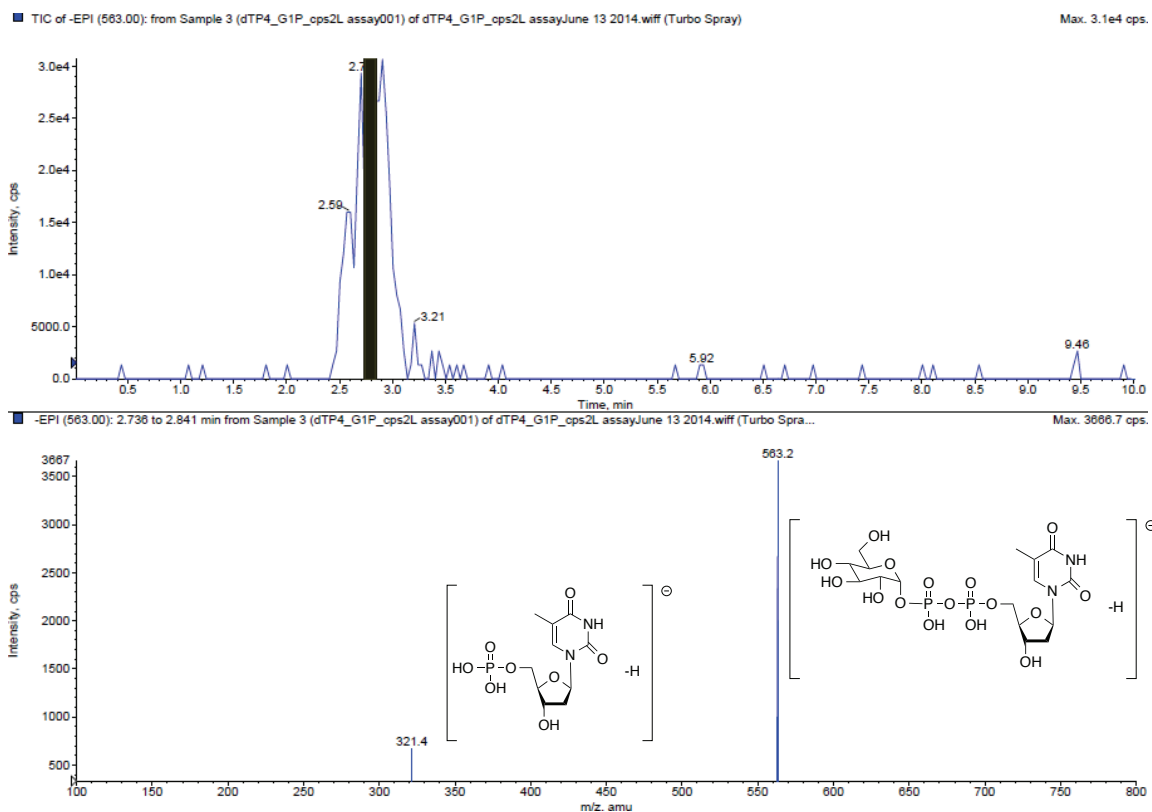
$^{31}\text{P}\{^1\text{H}\}$ NMR (D_2O , 202 MHz) spectrum of UDP-1C-glc **2.15**.



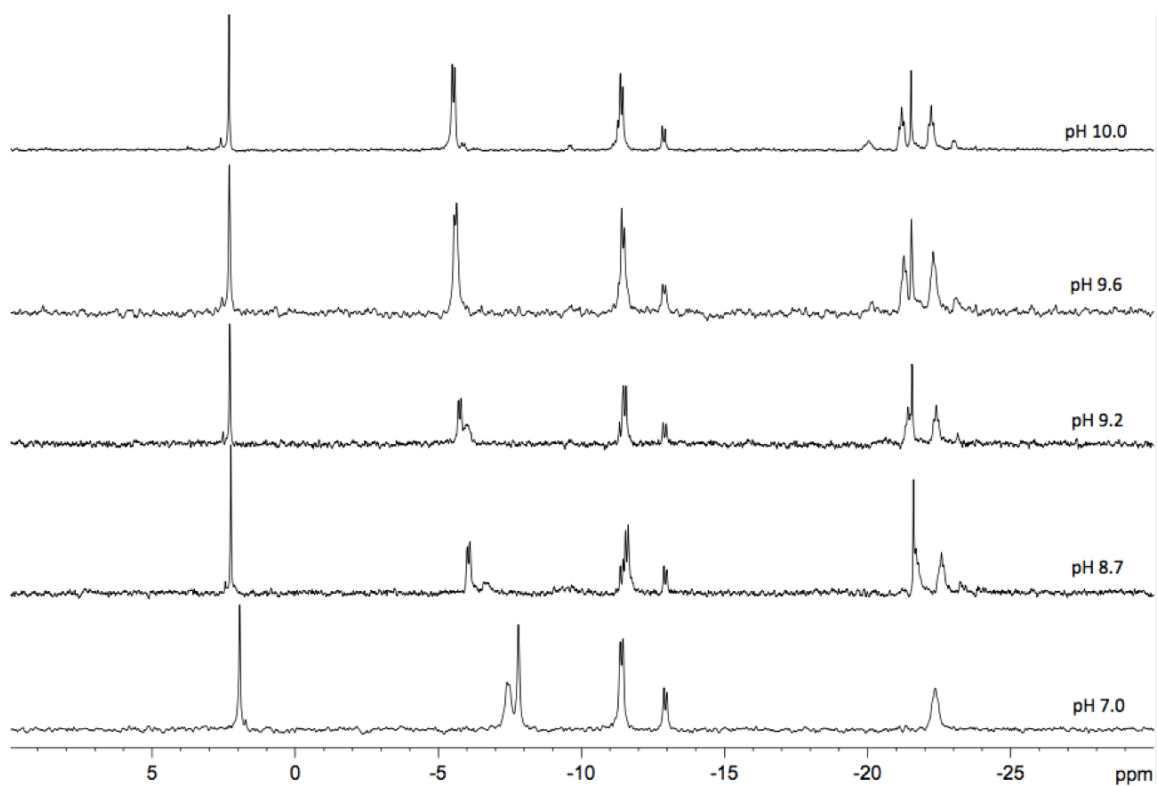
Appendix B: Supplementary materials for Chapter 2.3.



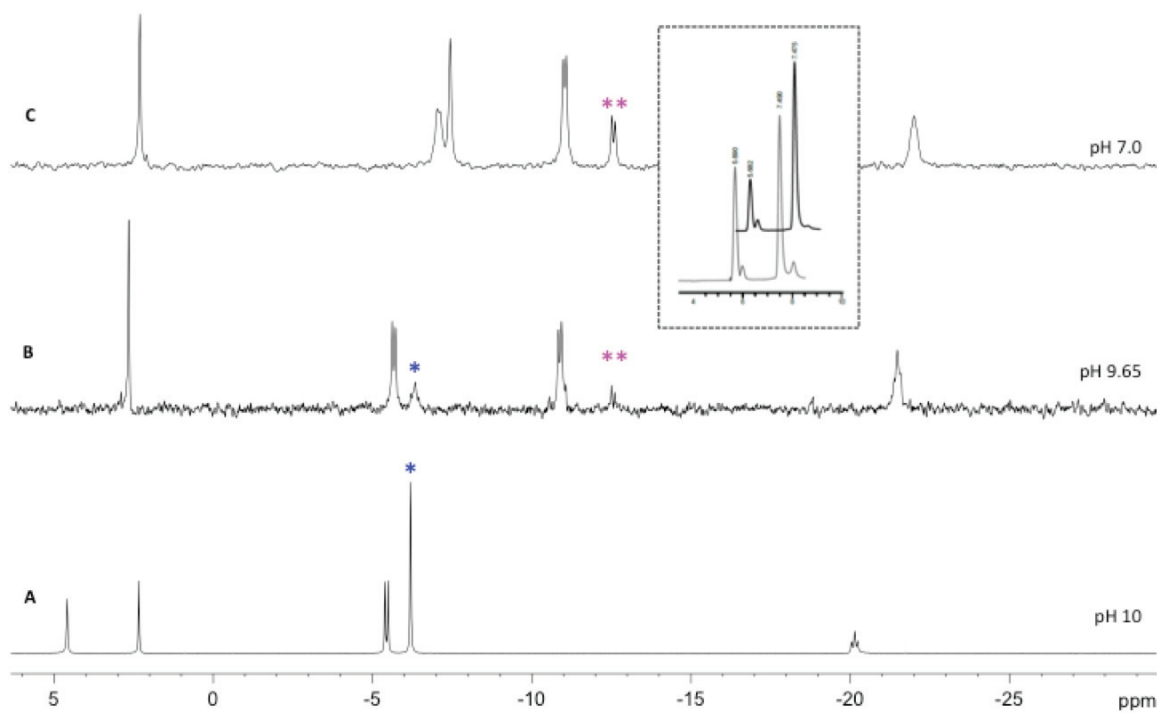
HPLC trace of a reference sample containing dTMP (R_T 3.0 min), dTDP-Glc (R_T 5.6 min), dTTP (R_T 7.4 min), and P₄dT (R_T 8.0 min).



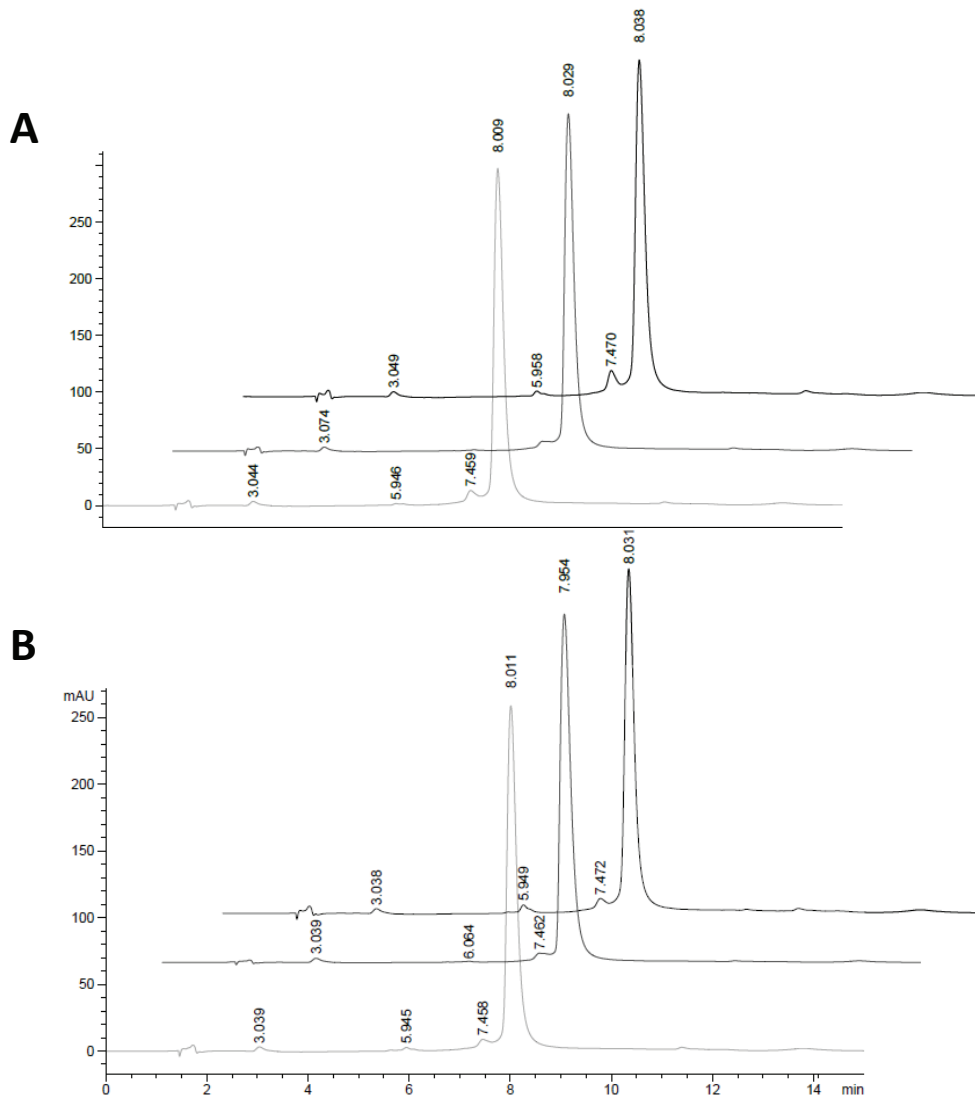
LC-MS EPI experiment scanning the product dTDP-Glc (m/z [M-H] 563) produced from the reaction of p_4dT and Glc 1-P.



Effect of pH on chemical shifts in the $^{31}\text{P}\{^1\text{H}\}$ NMR spectra (202 MHz) for the Cps2L catalysed reaction of p₄dT.

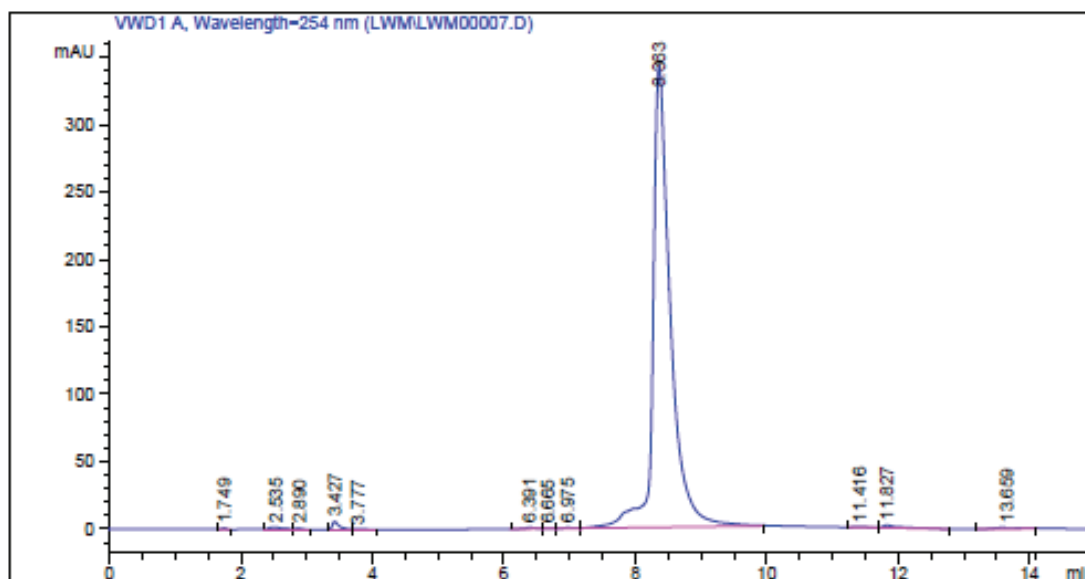
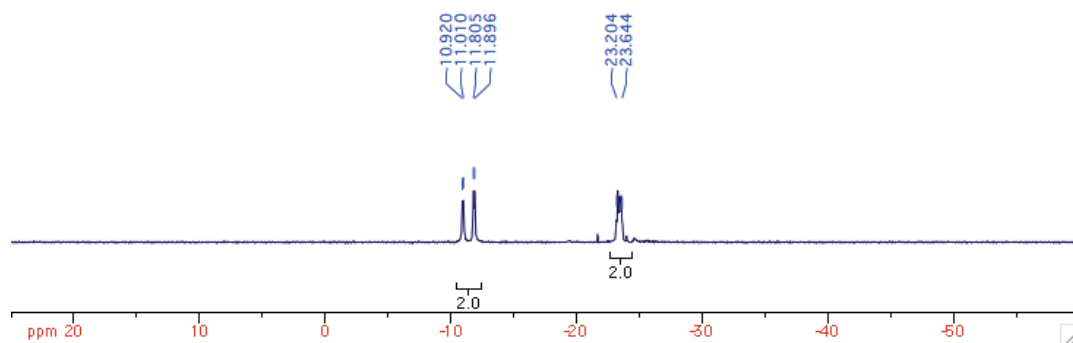


Production of PP_i (*) in the physiological reaction observed by $^{31}\text{P}\{^1\text{H}\}$ NMR spectroscopy (202 MHz); (A) A reference spectrum containing P_i , PP_i , P_3 , and Glc 1-P; (B) Cps2L-catalysed reaction of dTTP to dTDP-Glc (**) after 1 hour with pH adjusted to 9.6; (C) Cps2L-catalysed reaction of dTTP to dTDP-Glc (**) after 1 hour at pH 7. Inset: HPLC traces showing the shift in equilibrium from sugar nucleotide product back to dTTP upon adjustment to pH 9.65 (dTDP-Glc:dTTP ~1:3.4) from pH 7 (dTDP-Glc:dTTP ~1:1.5).

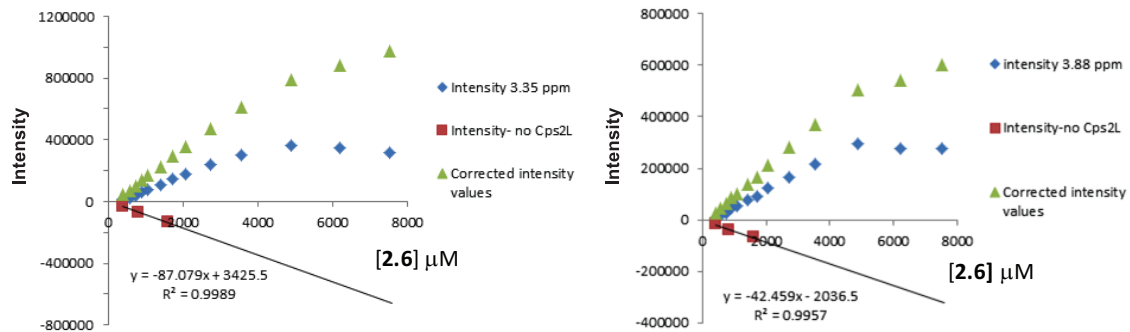


P₄dT degradation study (A) p₄dT (2 mM), Mg²⁺ (1.1 mM), TRIS-HCl (20 mM, pH 7.5) monitored at 1 min, 7 h, and 24 h; 3% break-down to dTTP observed after 24 h; (B) p₄dT (2 mM), Mg²⁺ (1.1 mM), Cps2L (96 μM), TRIS-HCl (20 mM, pH 7.5) monitored at 1 min, 7 h, and 24 h; 6% break-down to dTTP observed after 24 h.

$^{31}\text{P}\{^1\text{H}\}$ NMR (D_2O , 202.4 MHz) spectrum of p4dT.



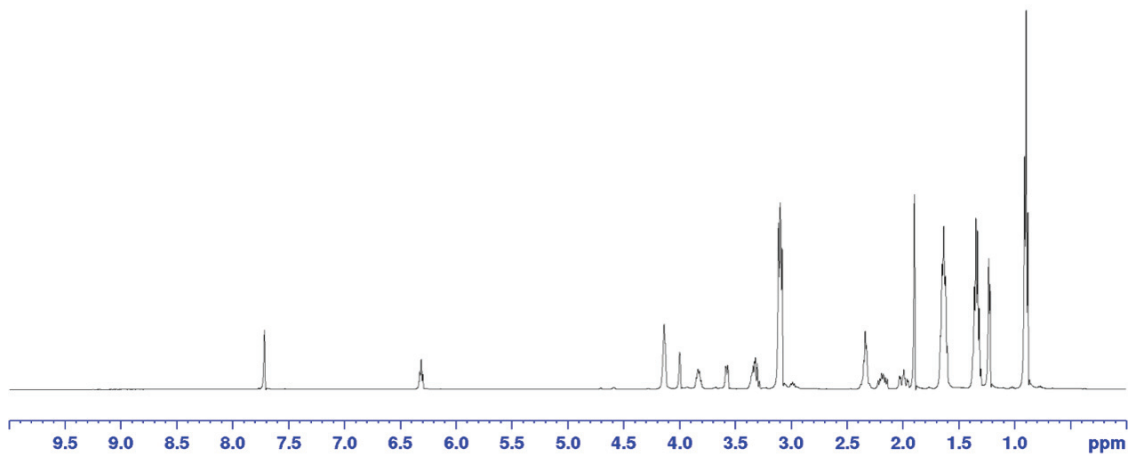
HPLC trace for purified p4dT (Rt 8.0 min, 97 % purity)



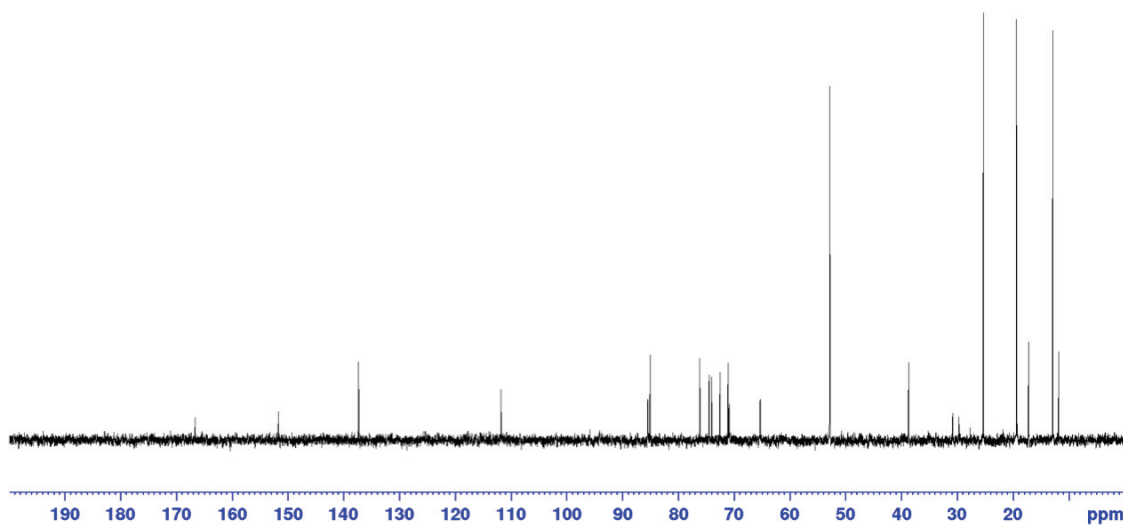
Determination of K_d for **2.6** binding to Cps2L in the presence of dTTP. Plot of signal intensity with (♦) and without (■) Cps2L and corrected signal intensity (▲) vs concentration of **2.6** for peaks at 3.35 ppm (left) and 3.88 ppm (right). Corrected data points were used as (L) in the dose-response equation.

Appendix C: Supplementary materials for Chapter 2.4

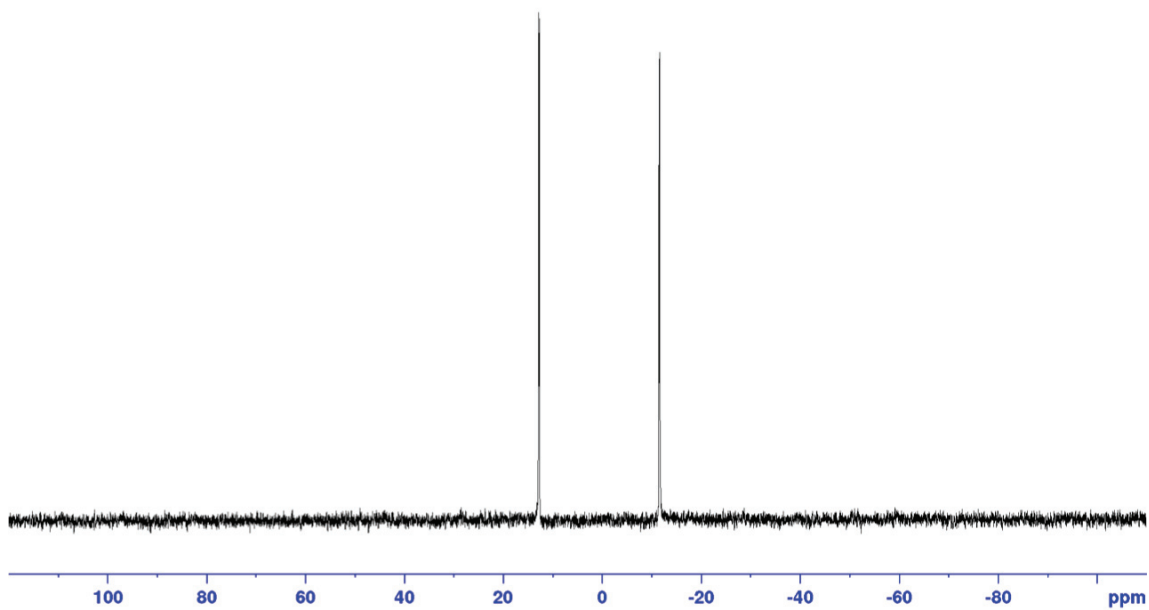
^1H NMR (D_2O , 500 MHz) spectrum of dTDP-1C-Rha.

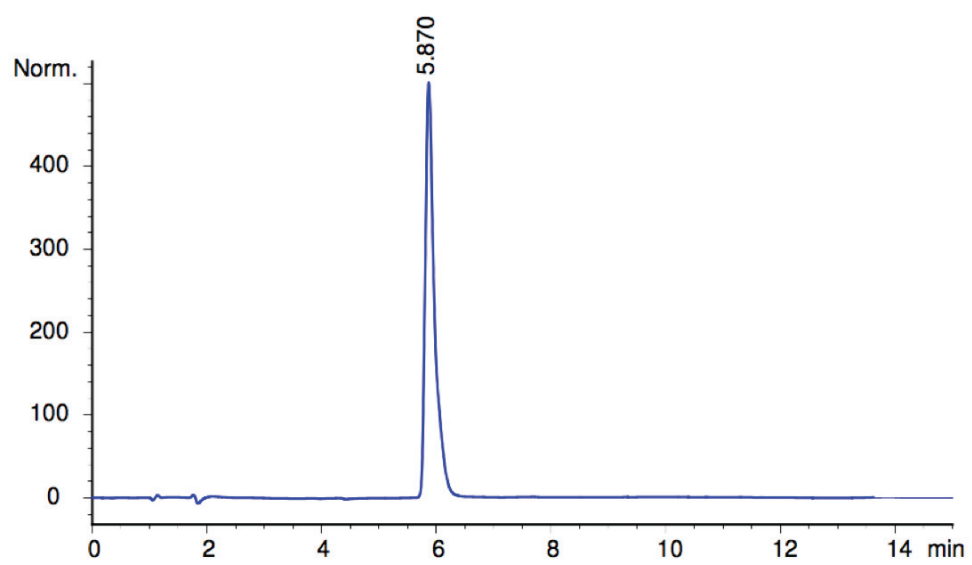


^{13}C NMR (D_2O , 125 MHz) spectrum of dTDP-1C-Rha.



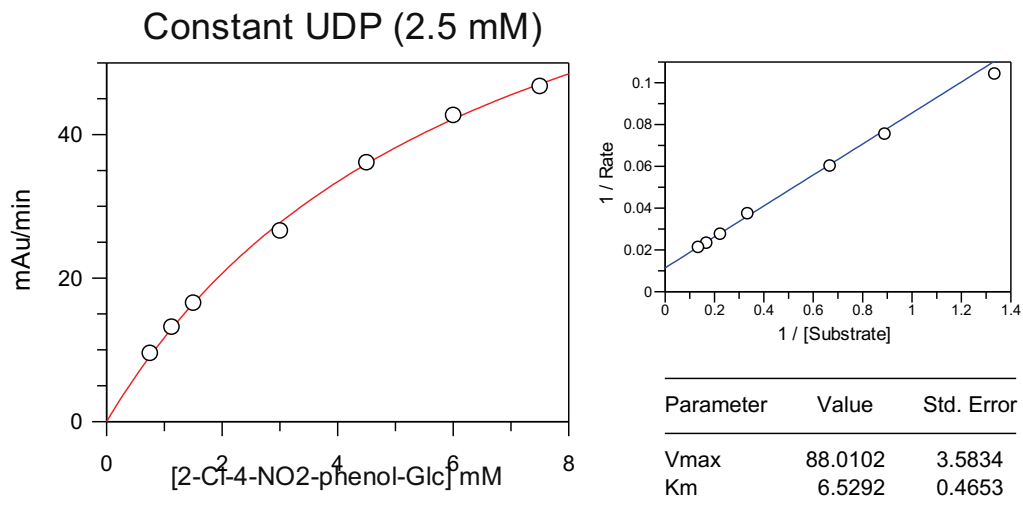
$^{31}\text{P}\{^1\text{H}\}$ NMR (D_2O , 202 MHz) spectrum of dTDP-1C-Rha.



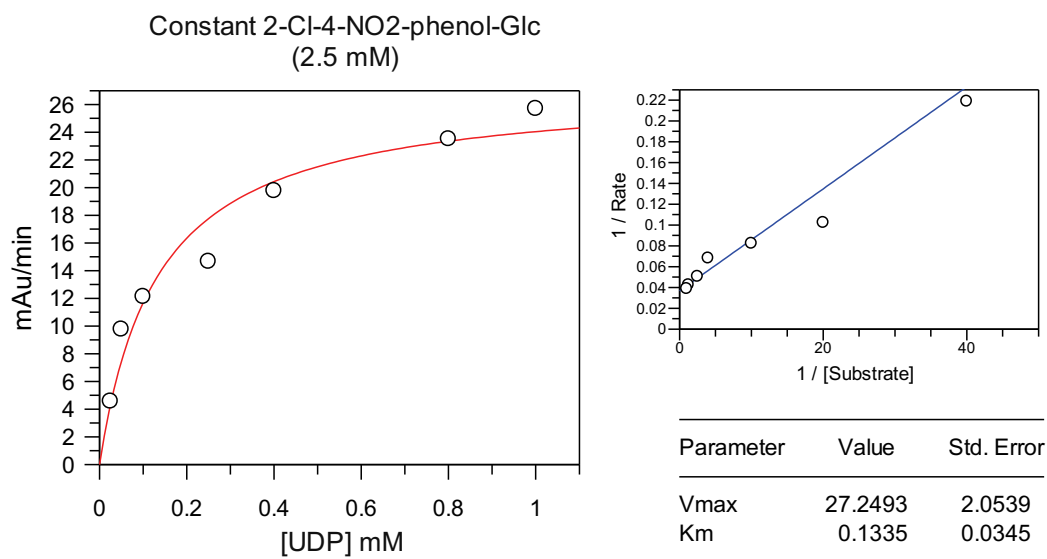


HPLC trace of dTDP-1C-Rha.

Appendix D: Supplementary materials for Chapter 2.5



Michaelis-Menten and Lineweaver-Burk plots for Sv0189 with constant UDP and variable 2-chloro-4-nitro-phenol- β -D-glucopyranoside



Michaelis-Menten and Lineweaver-Burk plots for Sv0189 with constant 2-chloro-4-nitro-phenol- β -D-glucopyranoside and variable UDP.

Antismash V 4.0 result summary for *S. venezuelae* (NCBI NC_018750.1)

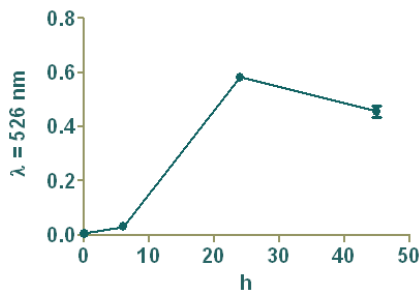
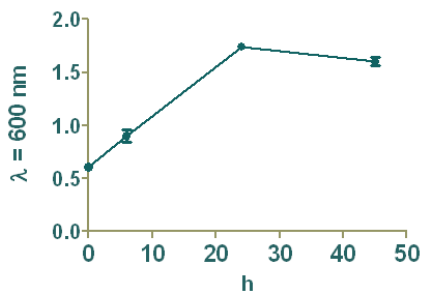
Cluster	Gene cluster type	Product
1	cf_putative	
2	cf_putative	
3	cf_putative	
4	ectoine	
5	terpene	
6	cf_putative	
7	cf_saccharide	
8	t3pks-t1pks-nrps	venezuelin (product a), isopyochelin (product b)
9	lantipeptide-terpene	(+)-isodauc-8-en-11-ol
10	lantipeptide	venezuelin
11	indole	
12	cf_putative	
13	cf_putative	
14	other	chloramphenicol
15	cf_saccharide	
16	cf_putative	
17	cf_putative	
18	cf_putative	
19	cf_putative	
20	cf_putative	
21	cf_putative	
22	cf_putative	
23	other	
24	cf_putative	
25	cf_putative	
26	cf_putative	
27	cf_fatty_acid	
28	cf_putative	

Cluster	Gene cluster type	Product
1	cf_putative	
29	cf_putative	
30	cf_saccharide	
31	siderophore	
32	cf_putative	
33	cf_saccharide	
34	cf_putative	
35	cf_putative	
36	cf_putative	
37	lassopeptide	
38	cf_putative	
39	cf_putative	
40	cf_putative	
41	cf_fatty_acid	
42	cf_putative	
43	cf_putative	
44	cf_putative	
45	other	
46	butyrolactone	gaburedin
47	cf_putative	
48	cf_putative	
49	cf_putative	
50	cf_putative	
51	cf_putative	
52	cf_putative	
53	melanin-cf_saccharide	
54	cf_saccharide	
55	cf_putative	
56	cf_putative	
57	butyrolactone	

Cluster	Gene cluster type	Product
1	cf_putative	
58	thiopeptide	
59	t3pks	
60	siderophore	
61	siderophore	
62	cf_putative	
63	cf_putative	
64	bacteriocin	
65	cf_putative	
66	cf_putative	
67	t2pks-butyrolactone	jadomycin
68	other	
69	ladderane-cf_fatty_acid - nrps	
70	cf_putative	
71	cf_fatty_acid	
72	cf_putative	
73	terpene	
74	bacteriocin	
75	t2pks	
76	melanin	
77	cf_putative	
78	cf_putative	
79	cf_putative	
80	nrps	foroxymithine
81	terpene	
82	cf_saccharide	
83	t3pks	
84	terpene-nrps	

Appendix E: Supplementary materials for Chapter 3.2

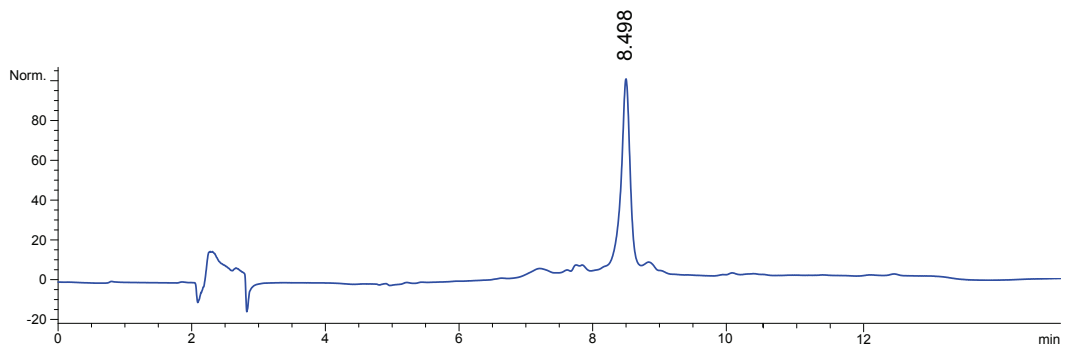
Growth curves (OD₆₀₀ and A₅₂₆) for *S. venezuelae* VS1099 jadomycin productions with TFAL



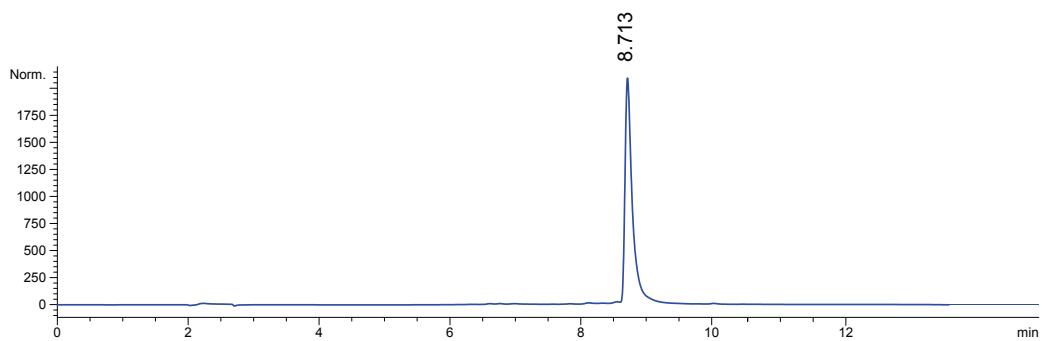
Low resolution MS² (ESI) data.

Compound	[M+H] ⁺ parent ion	ESI ⁺ fragmentation	[M-H] ⁻ parent ion	ESI ⁻ fragmentation
3.1	661	531, 306		
3.2			675	631, 527
JdK	565	521, 436, 356, 306		
JdK	566 (isotope peak)	522, 437, 357 and 356 ^a , 307 and 306 ^a		
Jdε¹⁵NK	566	522, 436, 357, 306		
Jdα¹⁵NK	566	522, 437, 357, 307		

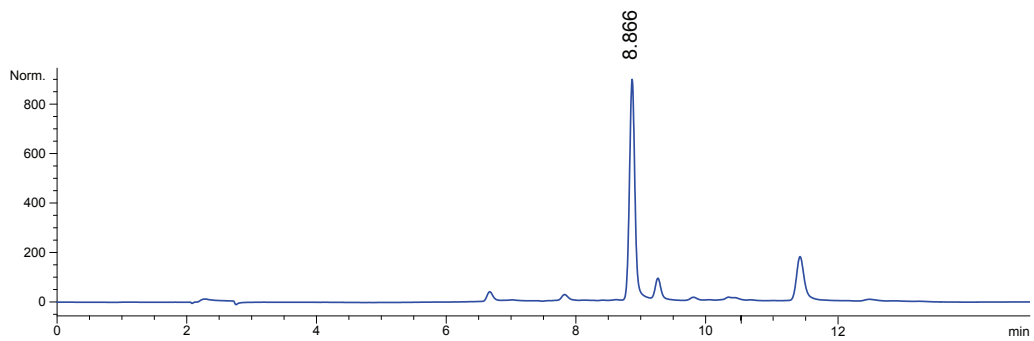
^a Indicated ions were approximately of equal intensity.



HPLC trace of **3.1**.

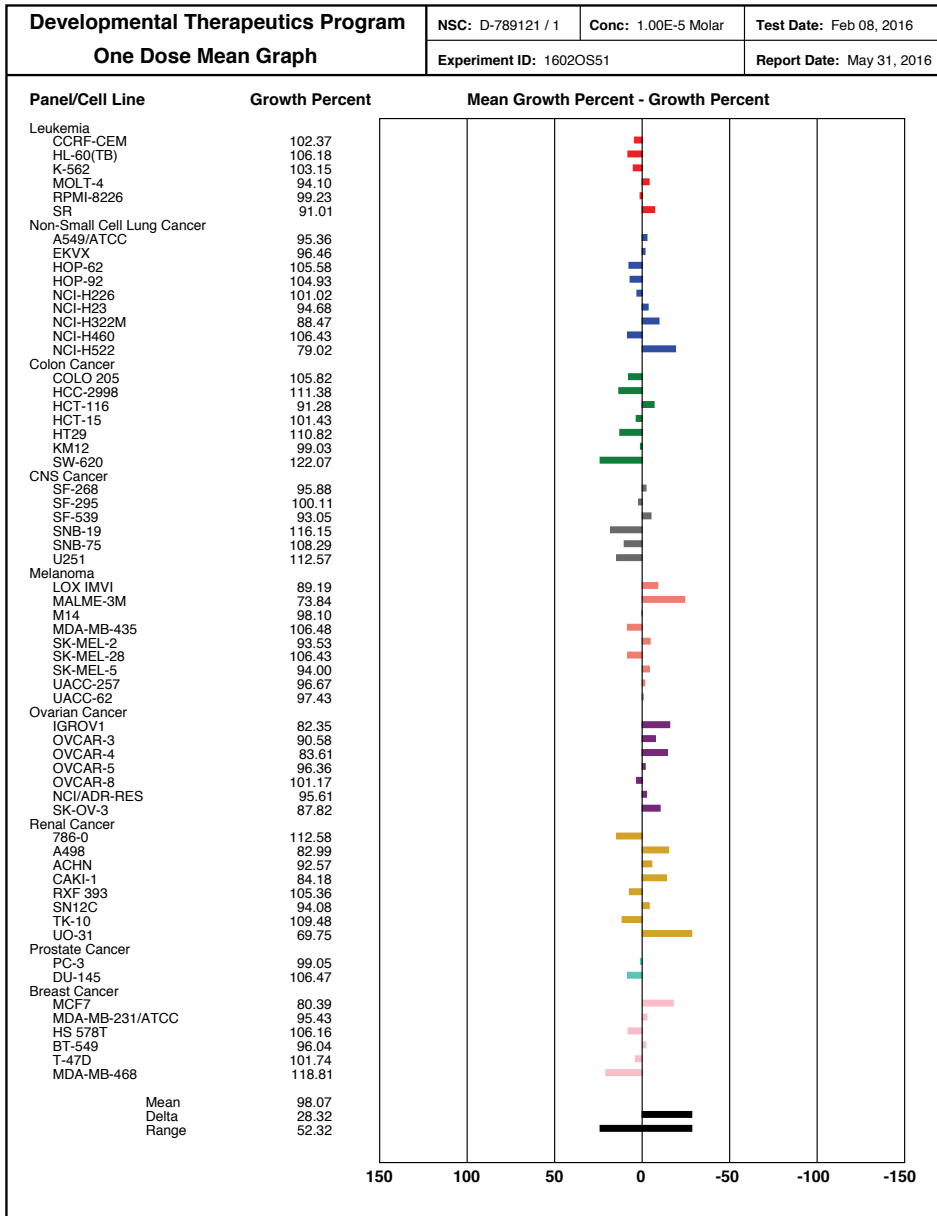


HPLC trace of **3.2**.

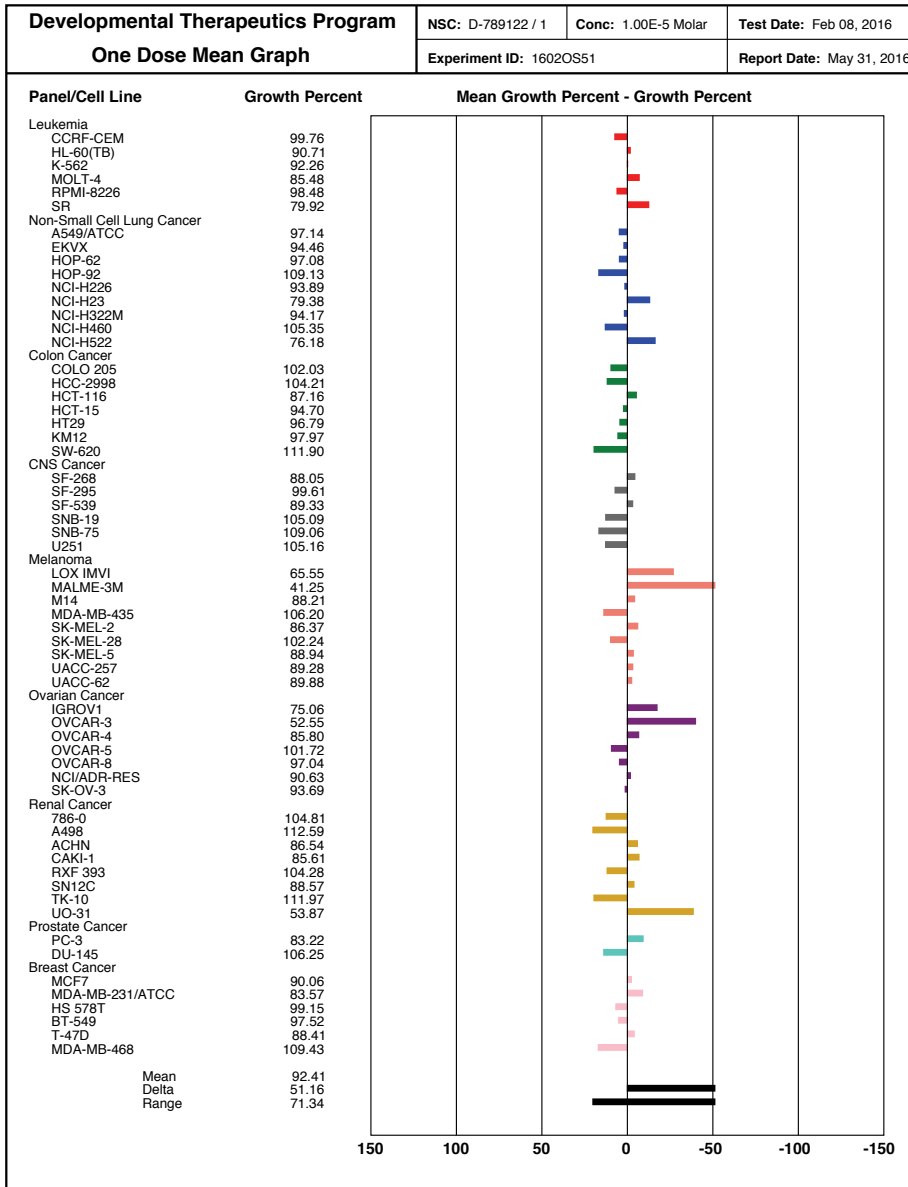


HPLC trace of mixture of **3.3** and **3.4**.

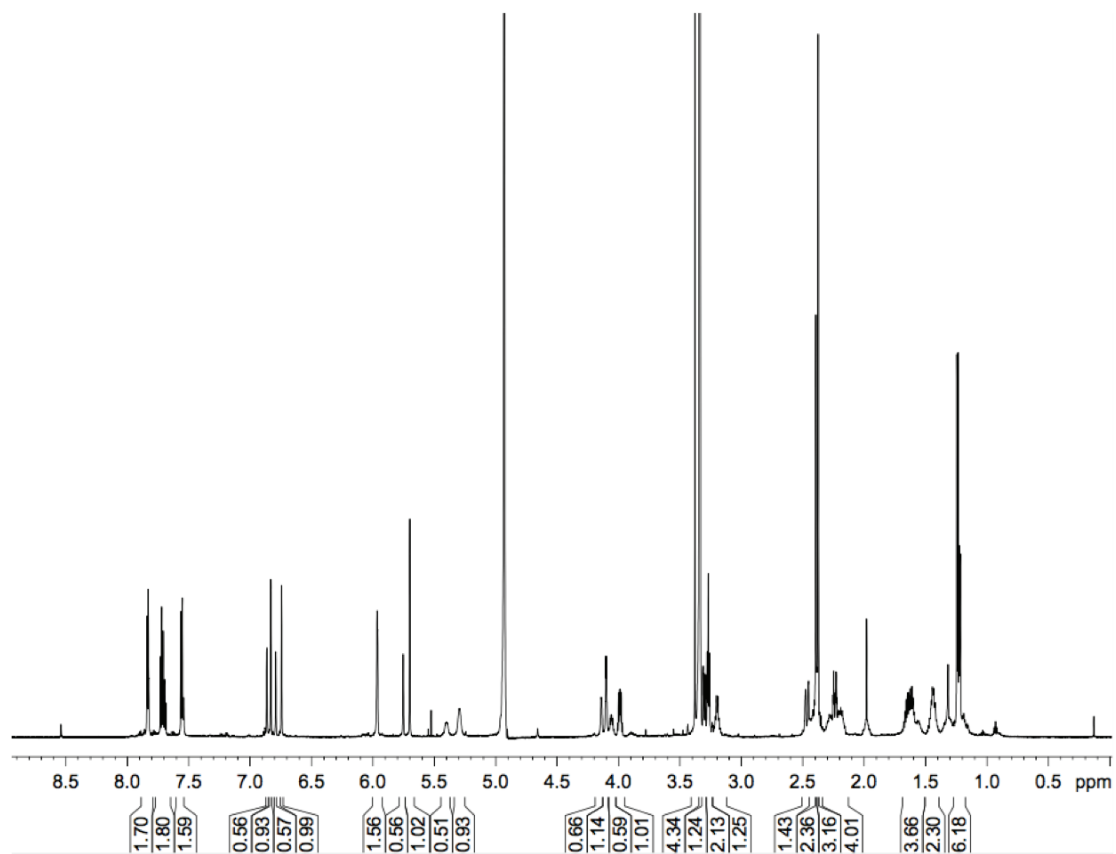
One-dose screening results for 3.2 (data collected by the NCI)



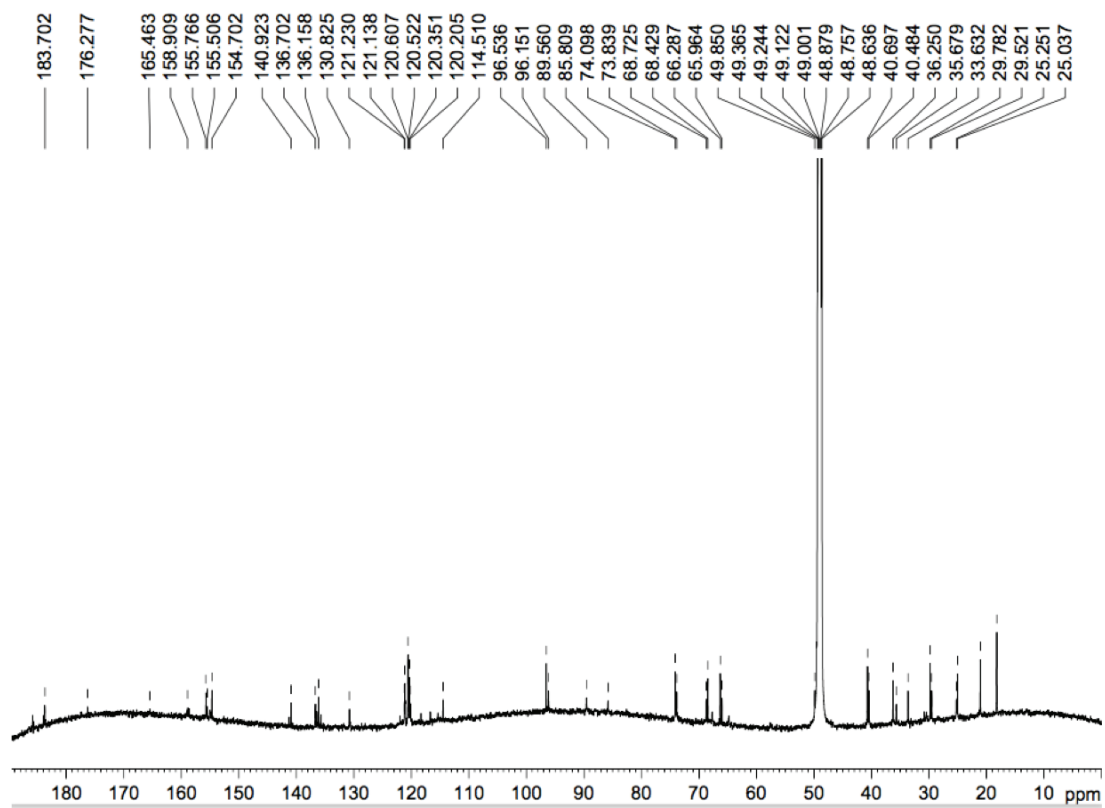
One-dose screening results for 3.3 and 3.4 (data collected by the NCI)



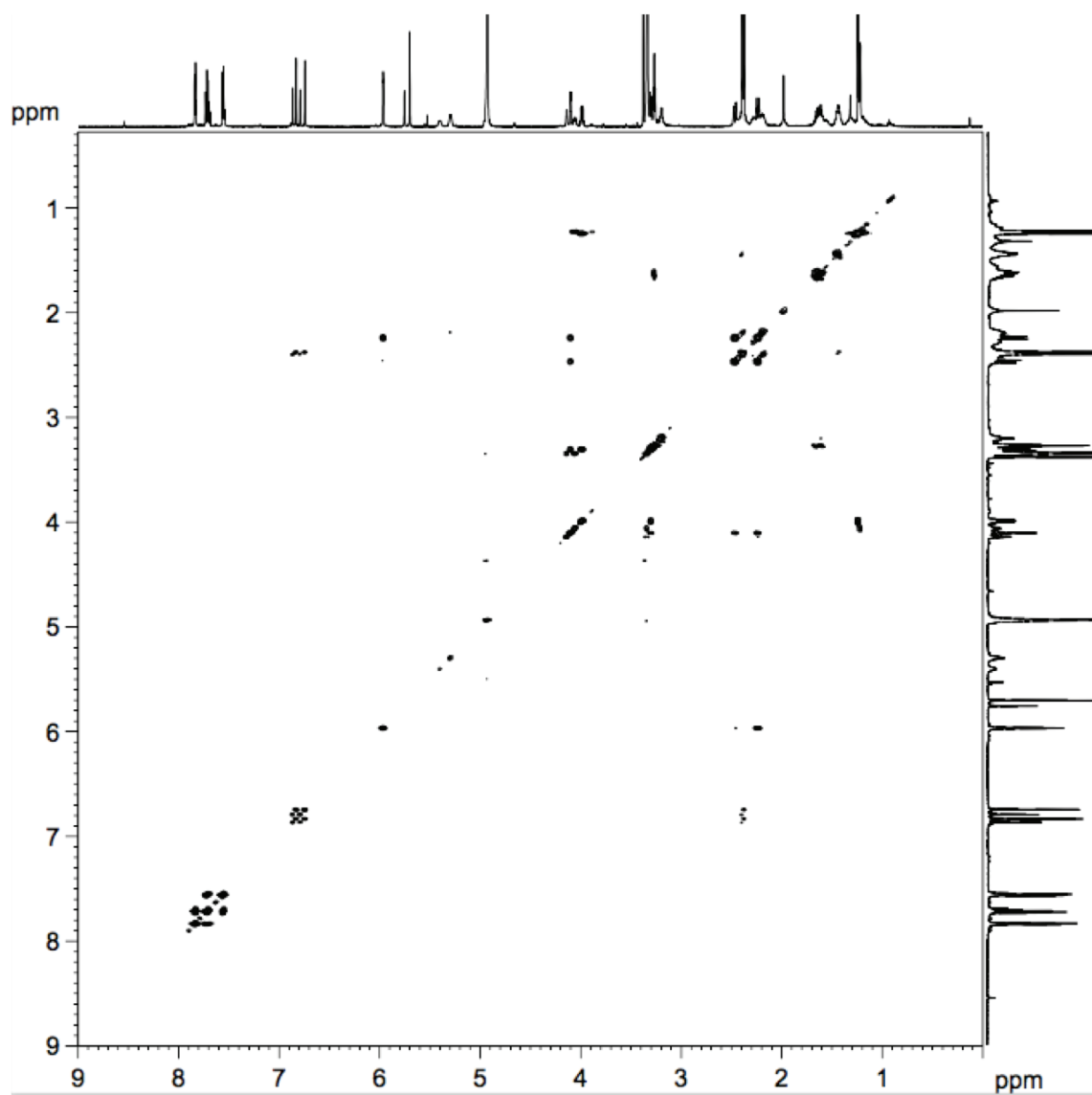
^1H NMR (700 MHz, methanol- d_4) spectrum of **3.1**.



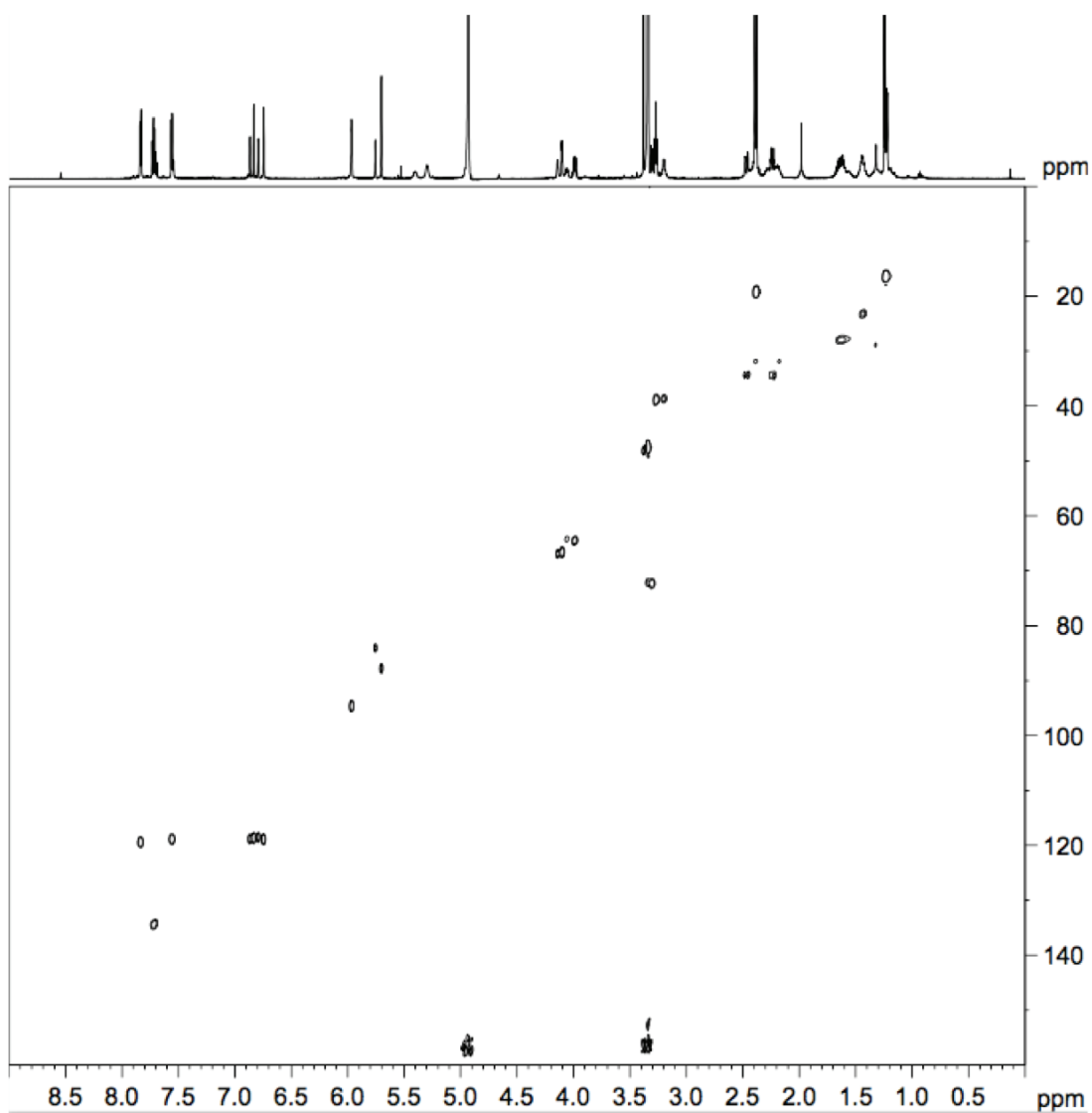
$^{13}\text{C}\{^1\text{H}\}$ NMR (176 MHz, methanol- d_4) spectrum of **3.1**.



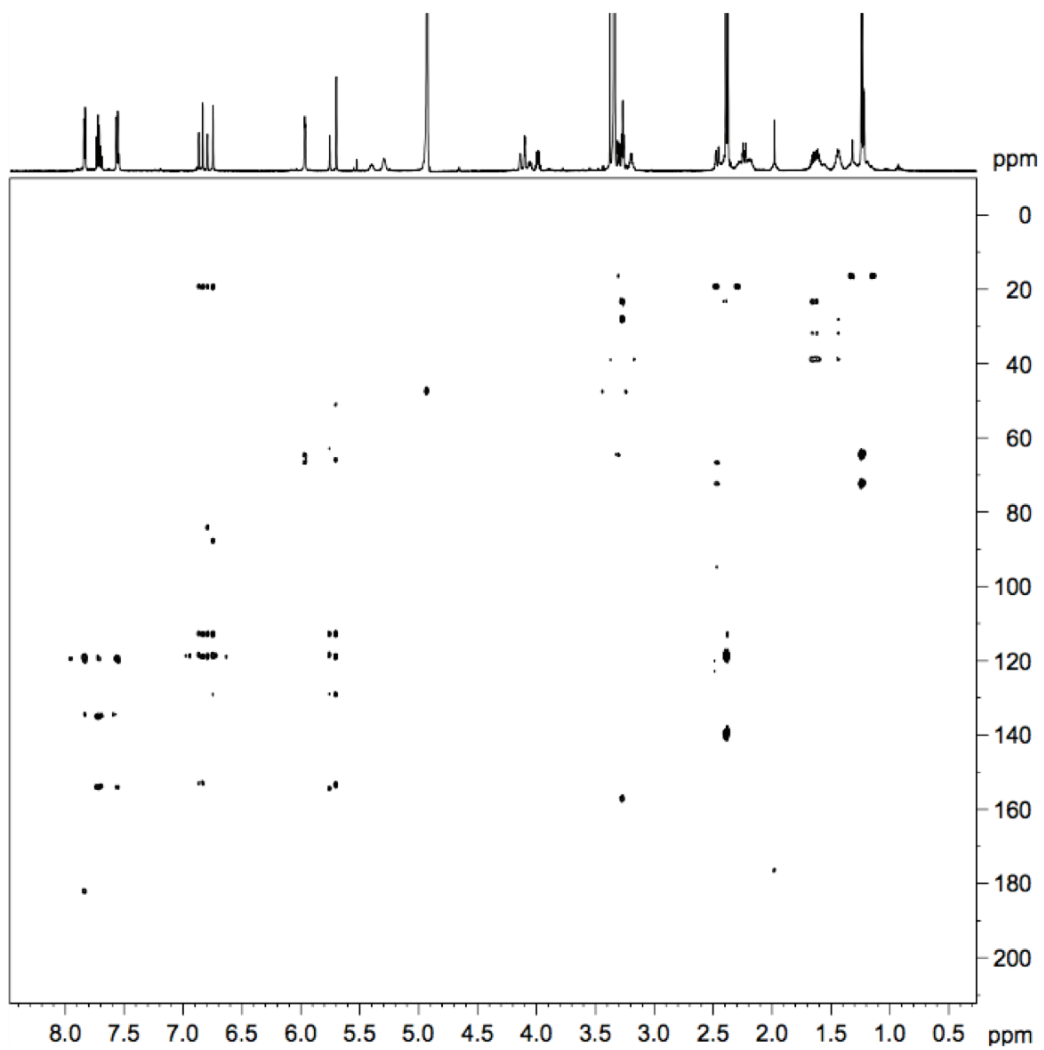
COSY NMR (700 MHz, methanol-*d*₄) spectrum of **3.1**.



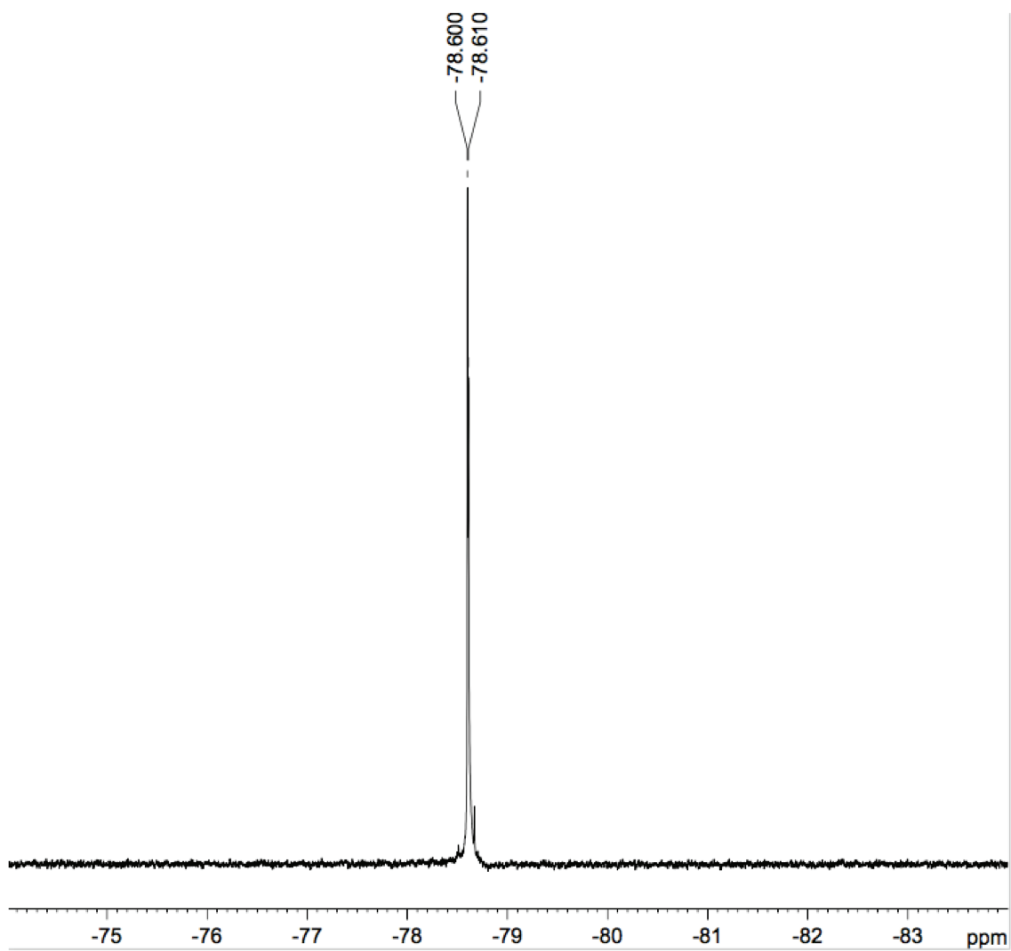
HSQC NMR (700 MHz, methanol-*d*₄) spectrum of **3.1**.



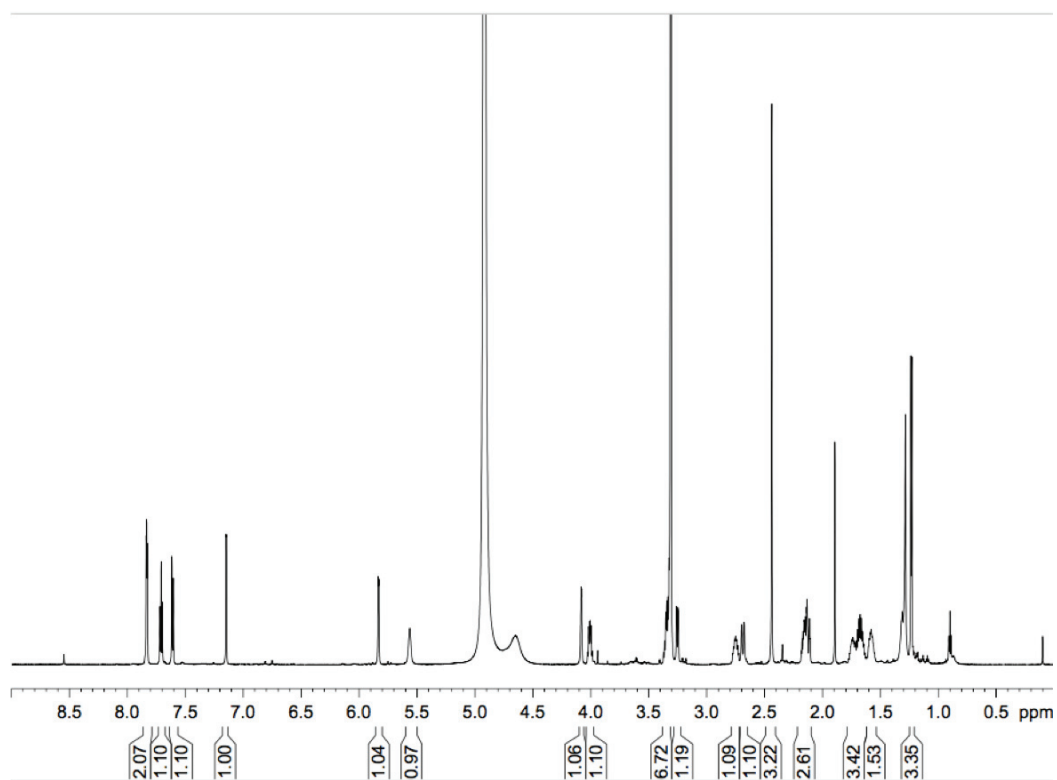
HMBC NMR (700 MHz, methanol-*d*₄) spectrum of **3.1**.



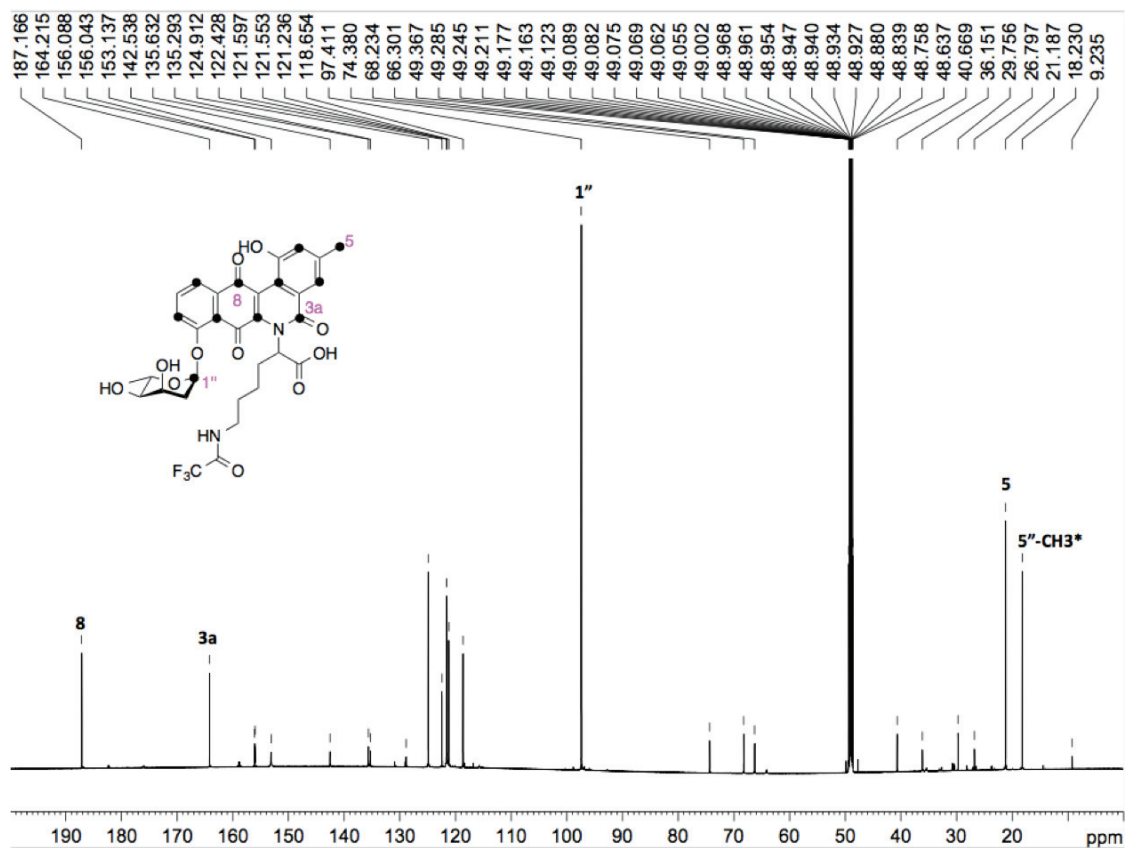
$^{19}\text{F}\{^1\text{H}\}$ NMR (470 MHz, methanol-*d*₄) spectrum of **3.1**.



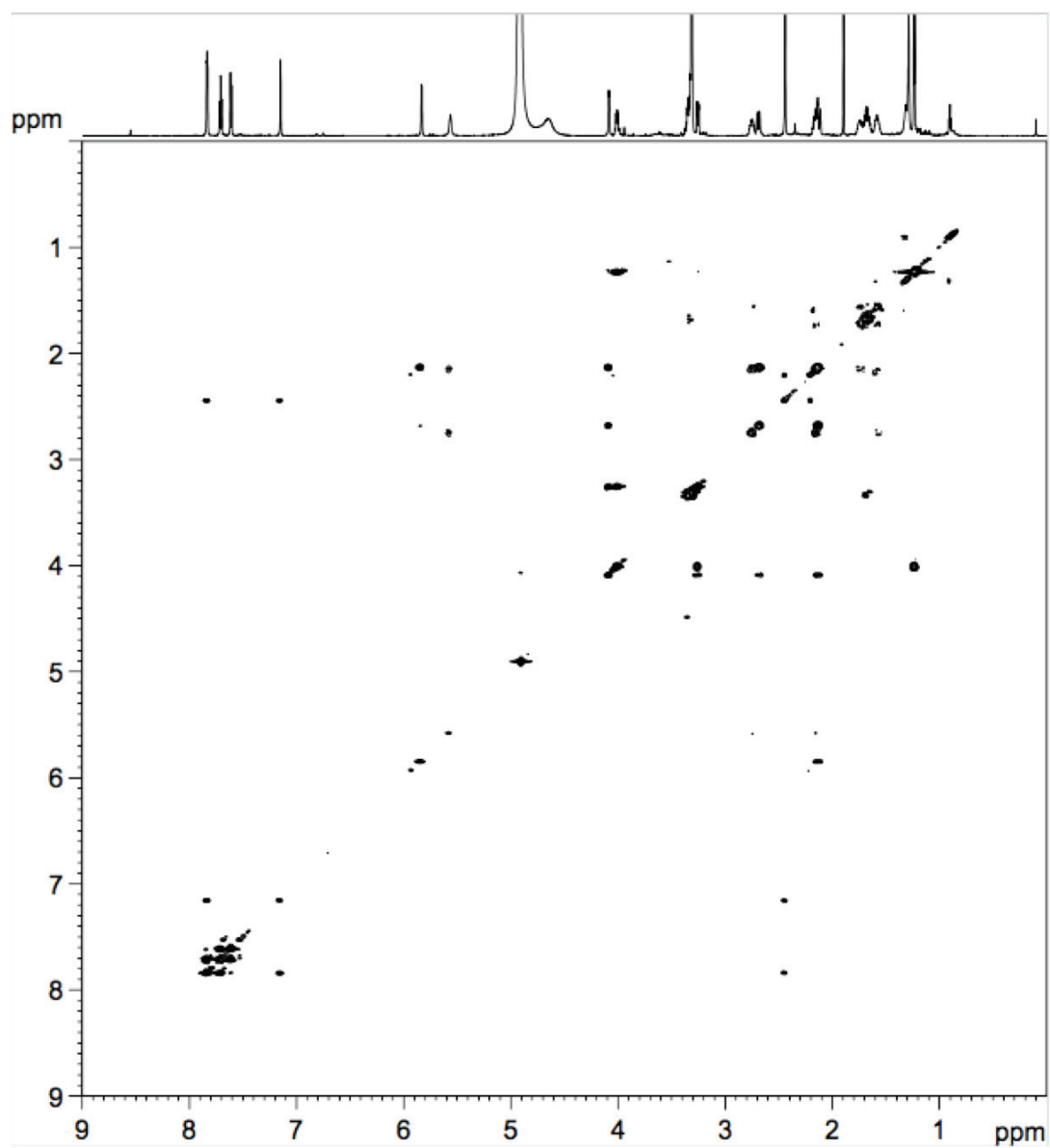
^1H NMR (700 MHz, methanol- d_4) spectrum of **3.2**.



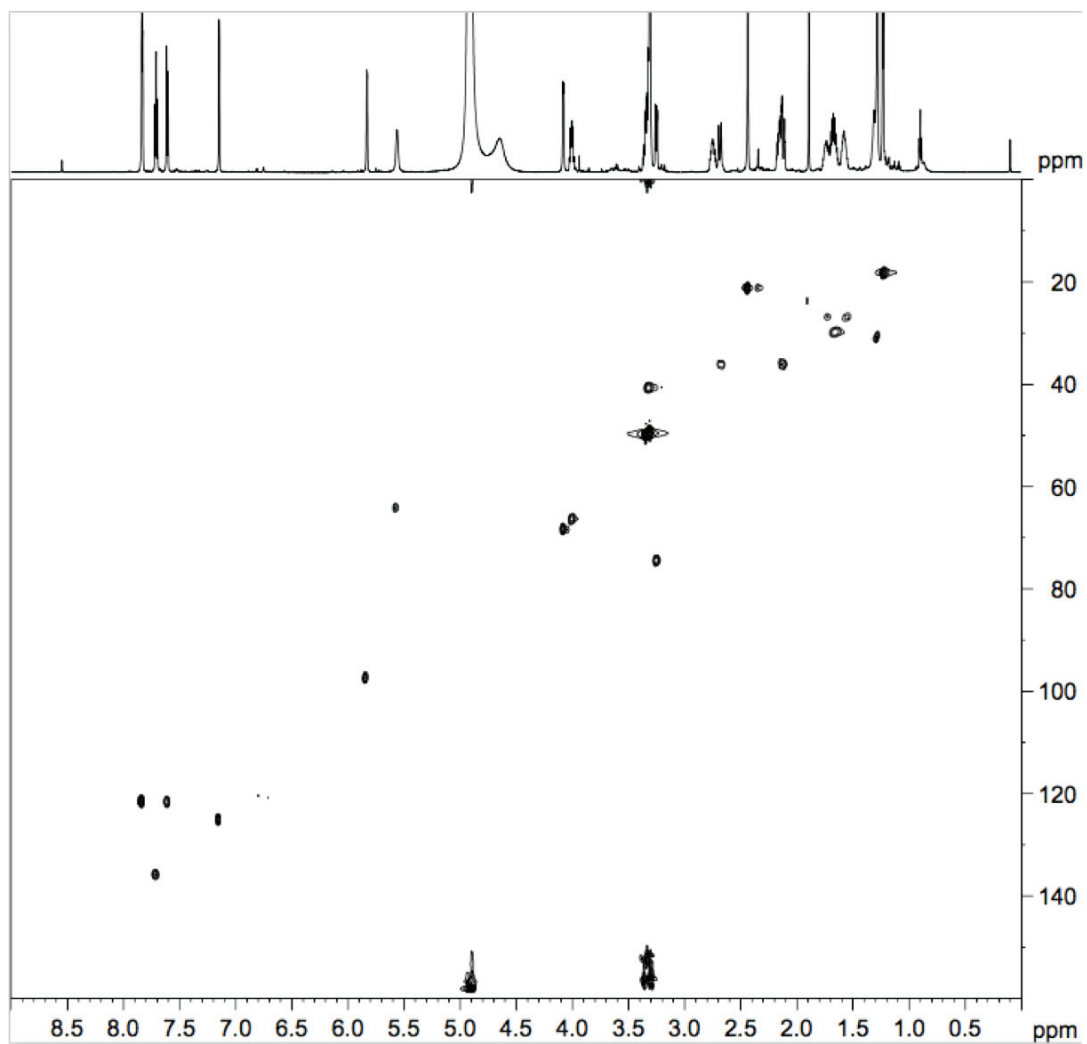
$^{13}\text{C}\{^1\text{H}\}$ NMR spectrum of **3.2** supplemented with ^{13}C -1 glucose production (125 MHz, methanol-*d*₄). Key assignments are indicated. *Due to the reversibility of glycolysis some labeling of C5''-CH₃ is evident.



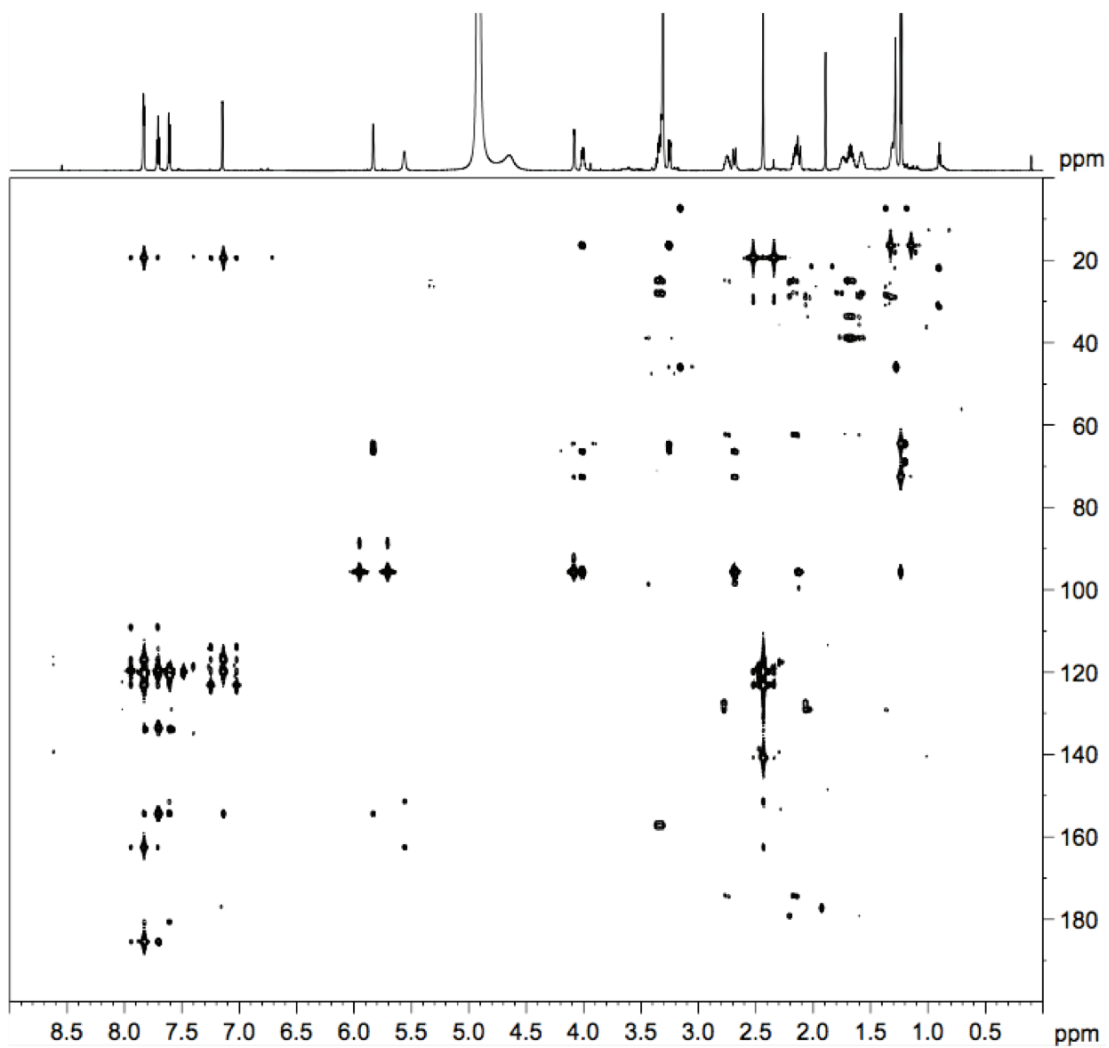
COSY (700 MHz, methanol-*d*₄) spectrum of **3.2**.



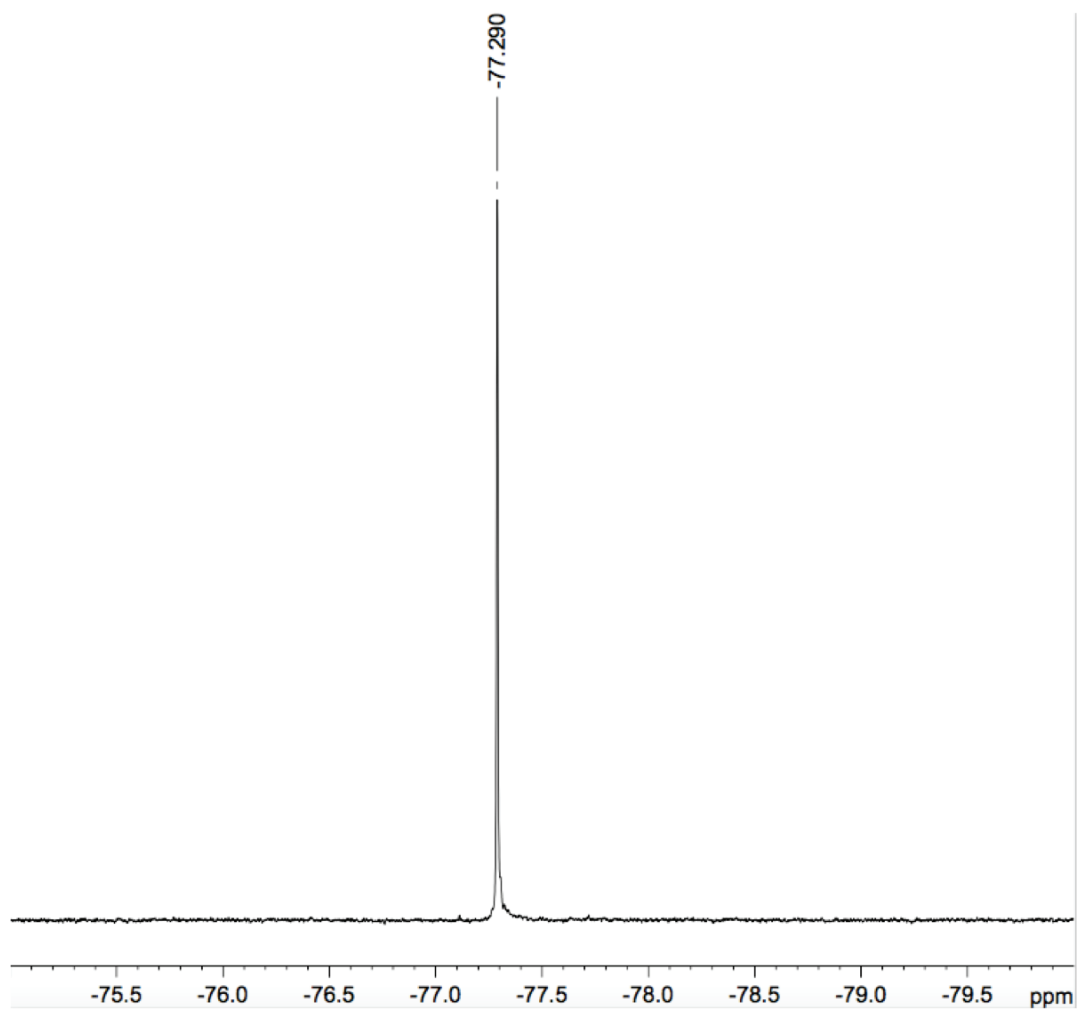
HSQC (700 MHz, methanol-*d*₄) spectrum of **3.2**.



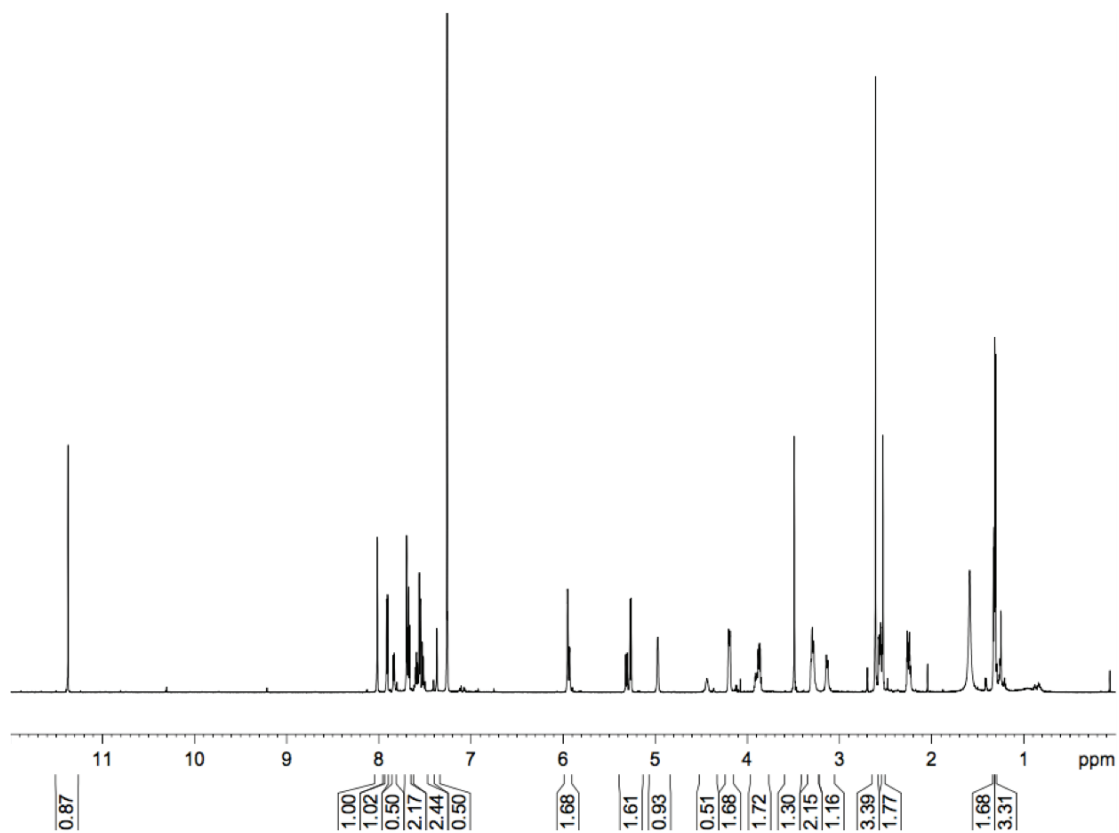
HMBC (700 MHz, methanol-*d*₄) spectrum of ¹³C-1 supplemented **3.2**.



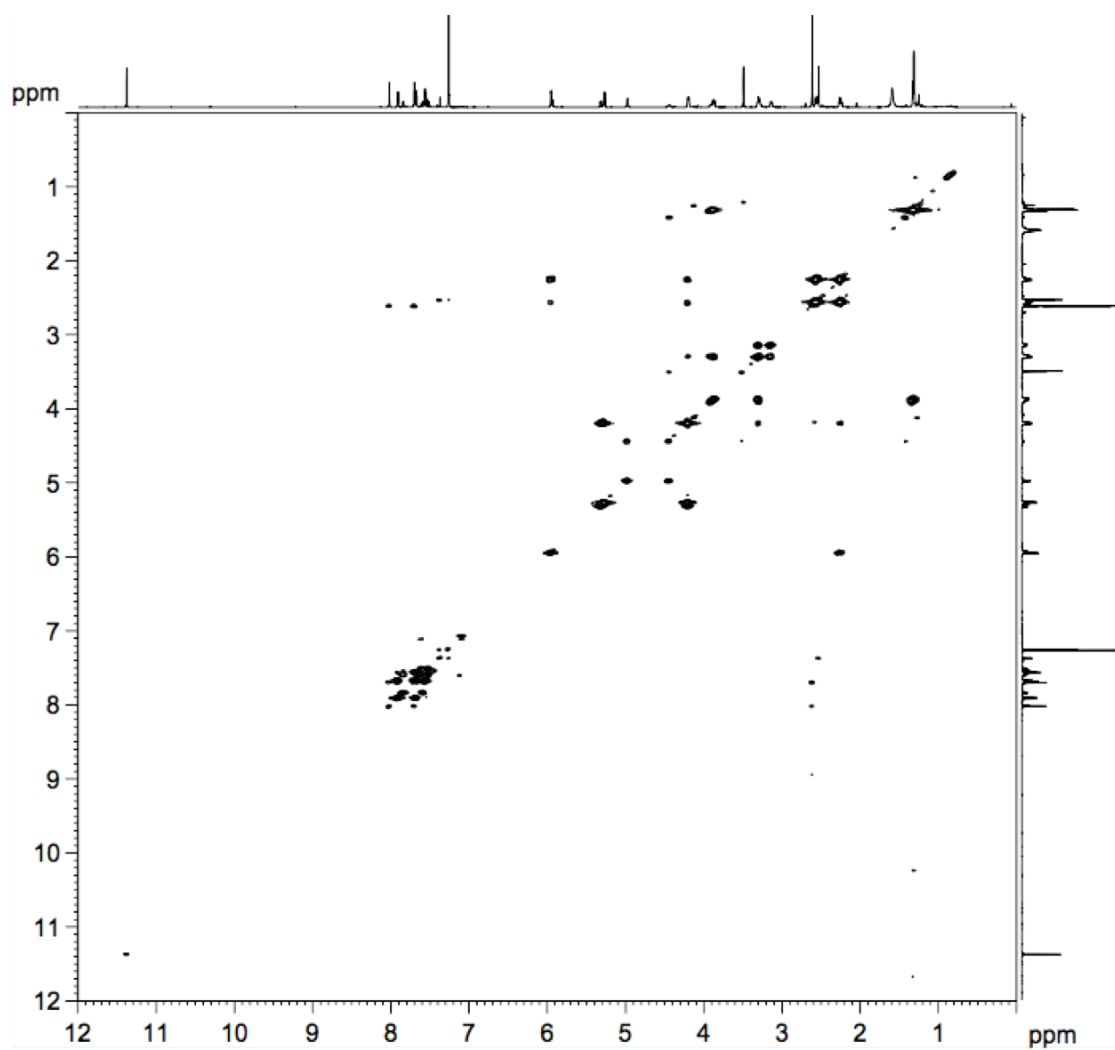
$^{19}\text{F}\{^1\text{H}\}$ (470 MHz, methanol-*d*4) spectrum of ^{13}C -1 supplemented **3.2** .



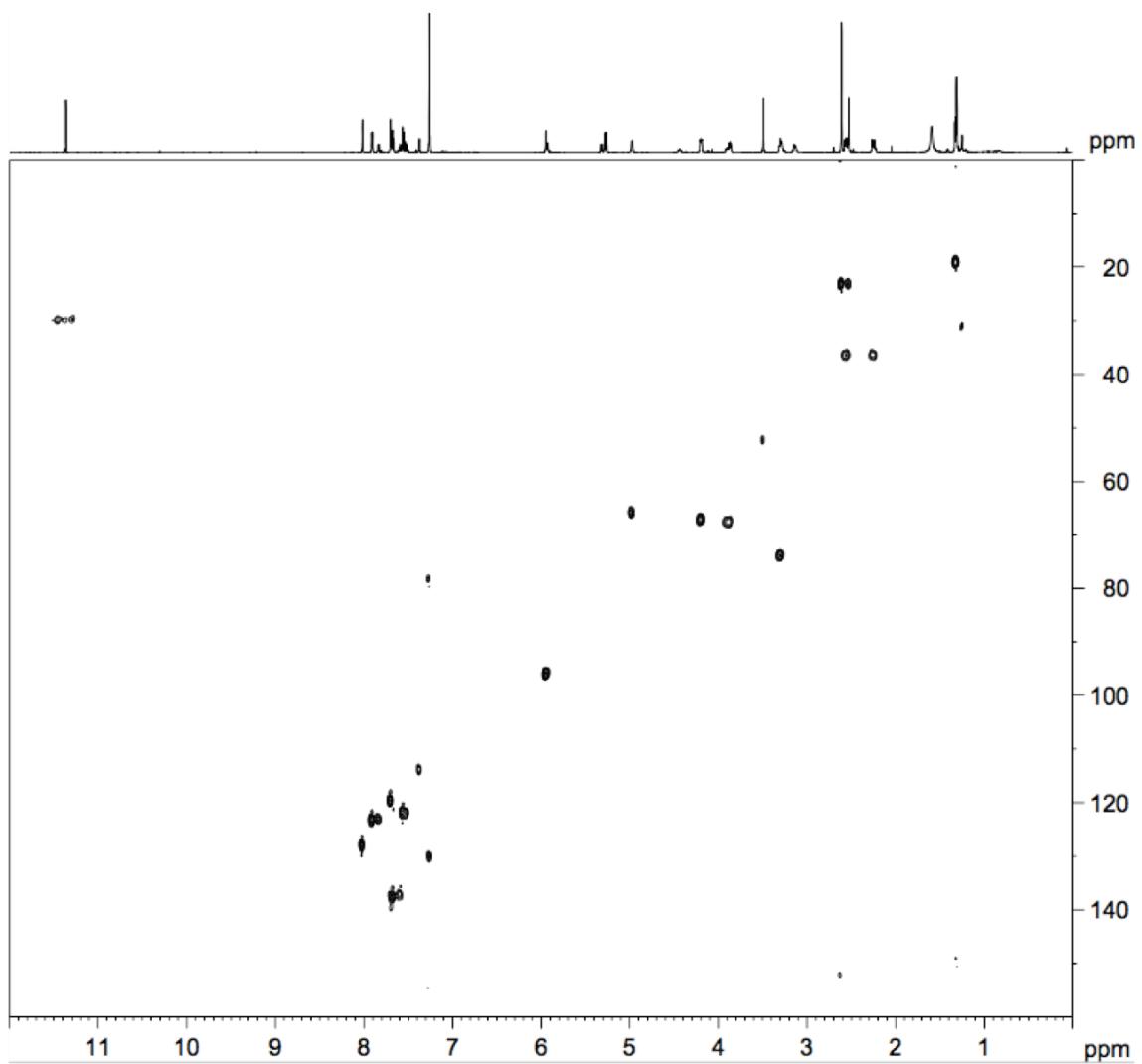
^1H NMR (700 MHz, CDCl_3) spectrum of **3.3** and **3.4**.



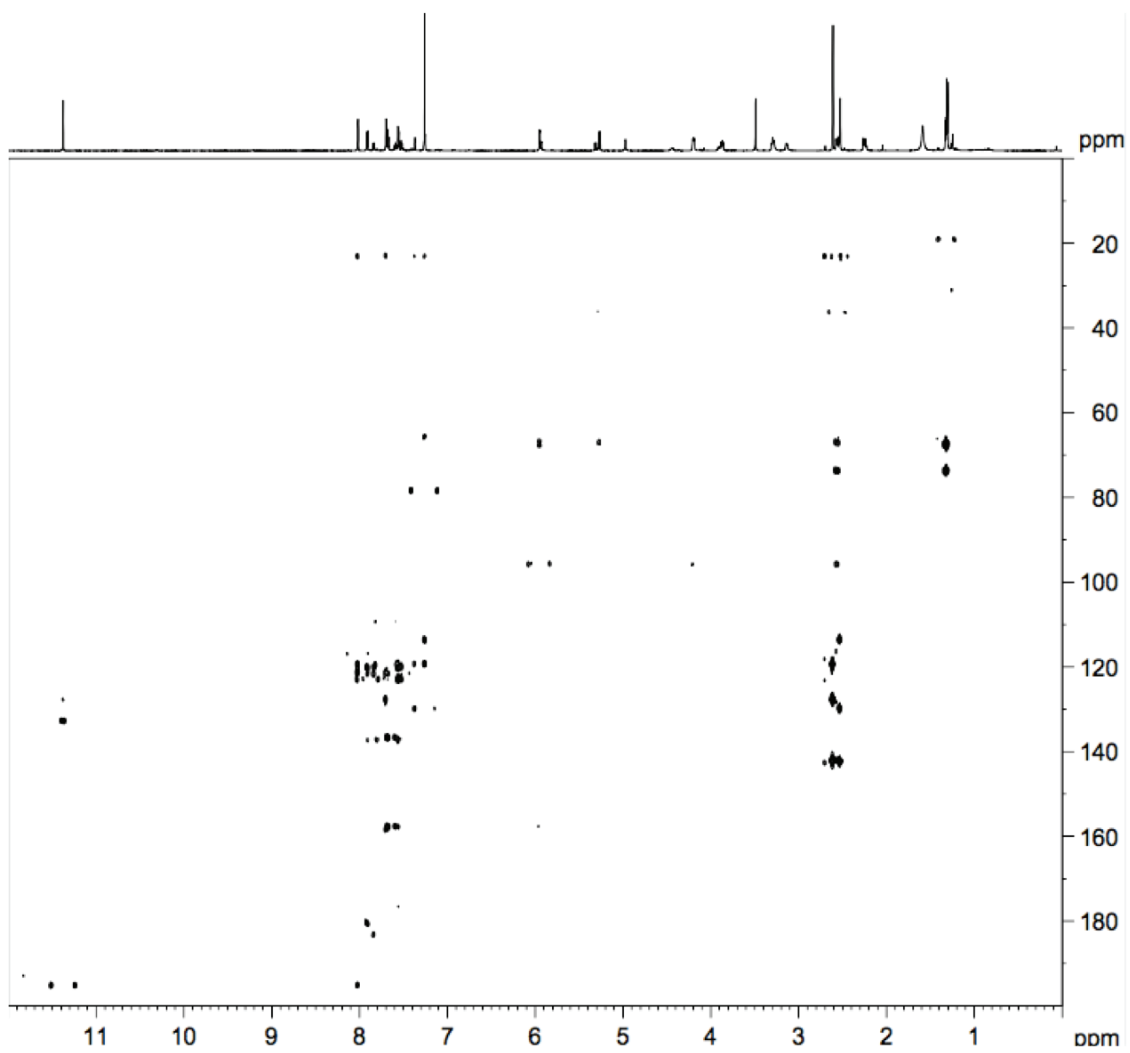
COSY (700 MHz, CDCl₃) NMR spectrum of **3.3** and **3.4**.



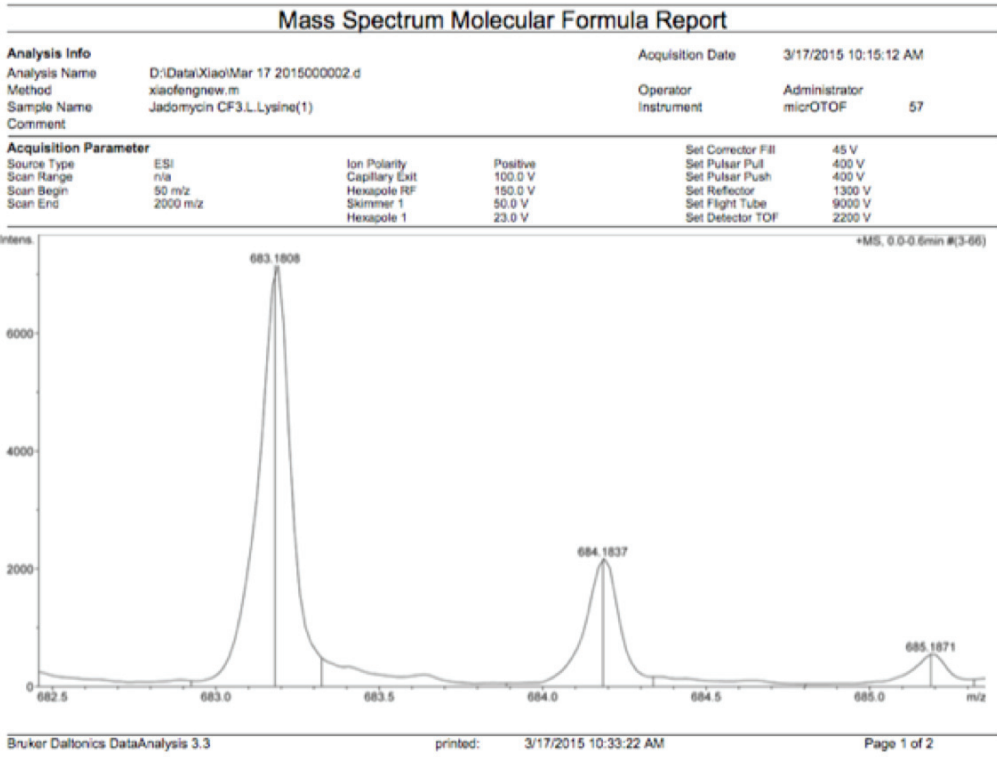
HSQC (700 MHz, CDCl₃) spectrum of **3.3** and **3.4**.



HMBC (700 MHz, CDCl₃) spectrum of **3.3** and **3.4**.



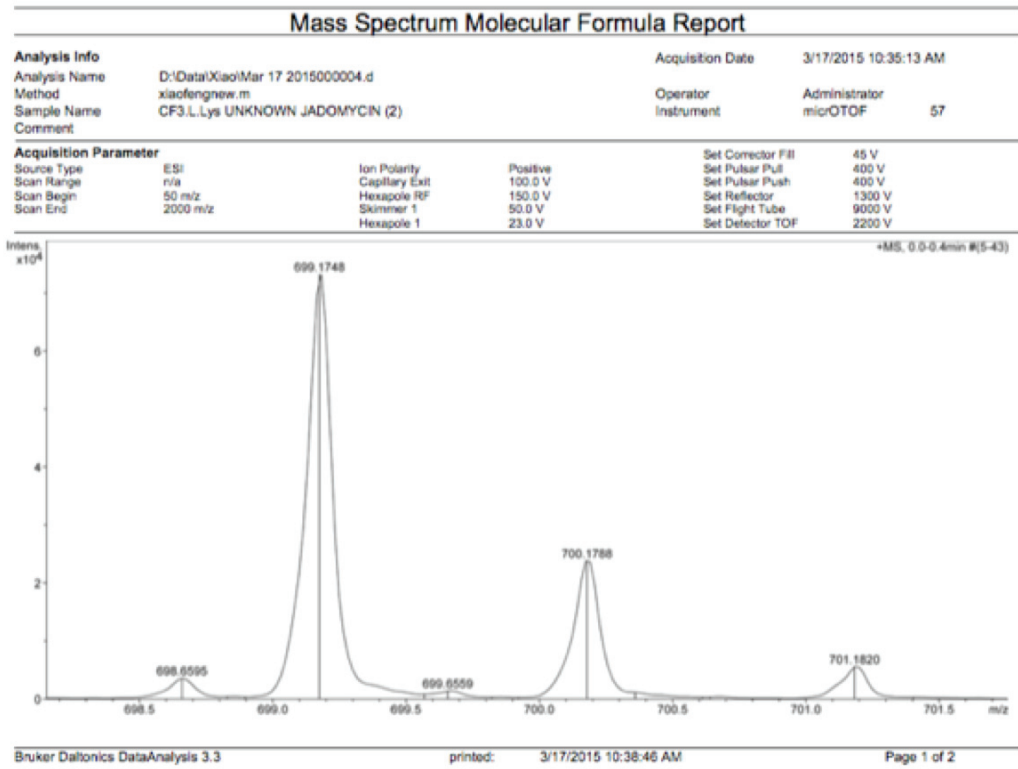
HRMS data for jadomycin TFAL 3.1.



Mass Spectrum Molecular Formula Report

Sum Formula	Sigma	m/z	Err [ppm]	Mean Err [ppm]	rdB	N Rule	e ⁻
C ₃₂ H ₃₁ F ₃ N ₂ NaO ₁₀	0.03	683.1823	2.13	2.18	16.50	ok	even

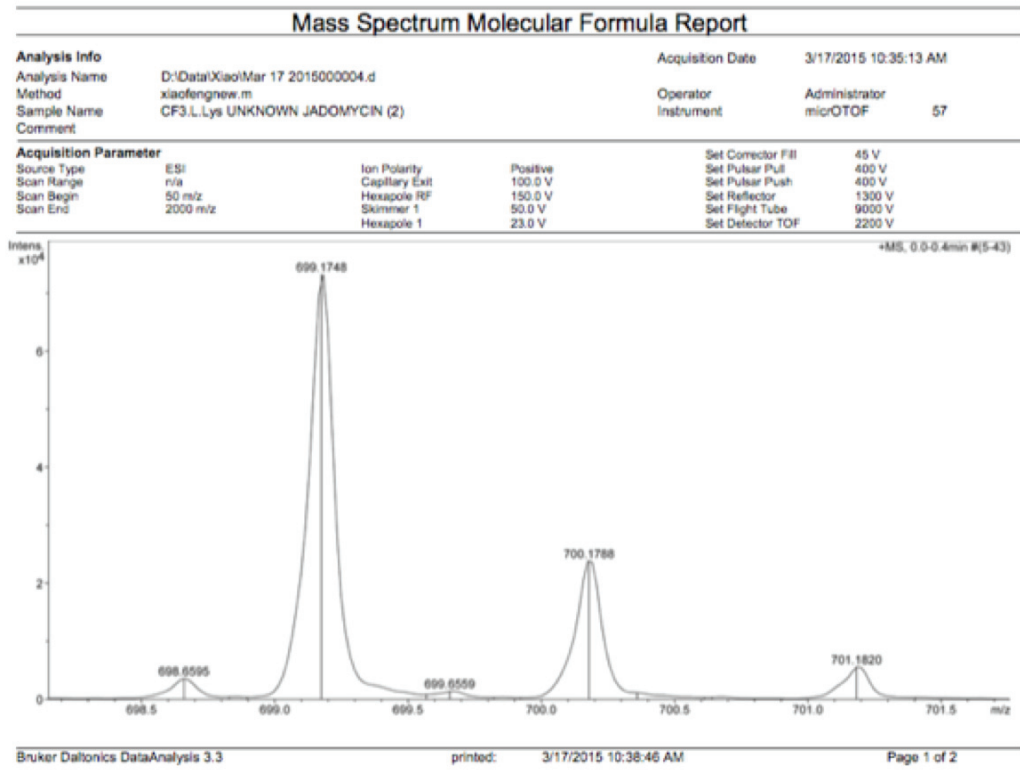
HRMS data jadomycin TFAL lactam 3.2.



Mass Spectrum Molecular Formula Report

Sum Formula	Sigma	m/z	Err [ppm]	Mean Err [ppm]	rdb	N Rule	e ⁻
C 32 H 31 F 3 N 2 Na 1 O 10	0.03	683.1823	2.13	2.18	16.50	ok	even

HRMS data jadomycin TFAL lactam 3.2.



Mass Spectrum Molecular Formula Report

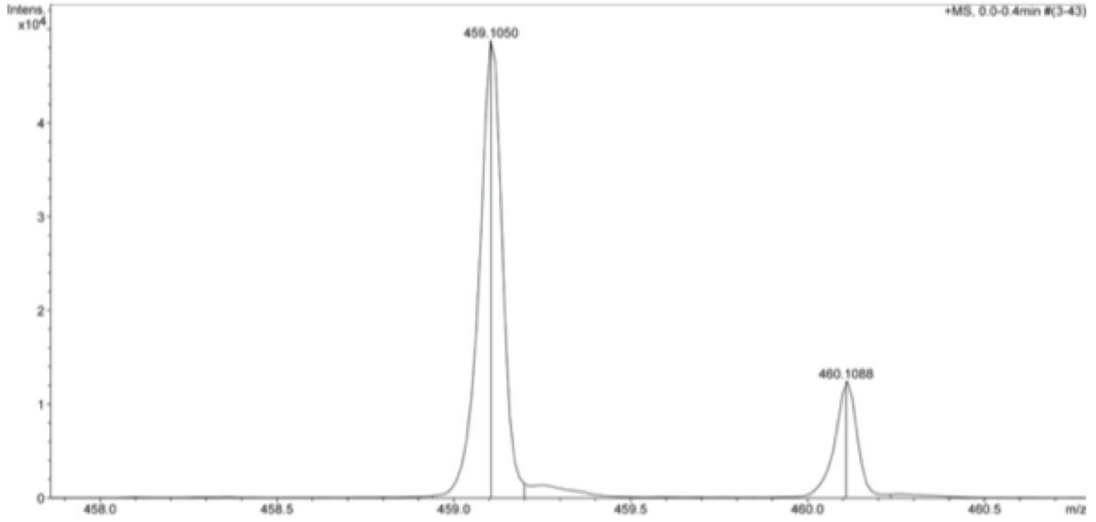
Sum Formula	Sigma	m/z	Err [ppm]	Mean Err [ppm]	rdB	N Rule	e ⁻
C 32 H 31 F 3 N 2 Na 1 O 11	0.02	699.1772	3.40	3.31	16.50	ok	even

HRMS data for jadomycin furan 3.3.

Mass Spectrum Molecular Formula Report

Analysis Info		Acquisition Date	4/10/2015 3:09:45 PM
Analysis Name	D:\Data\Xiao\April 10 2015\000002.d	Operator	Administrator
Method	xiaofengnew.m	Instrument	micrOTOF 57
Sample Name	Unknow-L-digi-jadom-yellow		
Comment			

Acquisition Parameter			
Source Type	ESI	Ion Polarity	Positive
Scan Range	n/a	Capillary Exit	100.0 V
Scan Begin	50 m/z	Hexapole RF	150.0 V
Scan End	2000 m/z	Skimmer 1	50.0 V
		Hexapole 1	23.0 V
		Set Corrector Fill	45 V
		Set Pulsar Pul	400 V
		Set Pulsar Push	400 V
		Set Reflector	1300 V
		Set Flight Tube	9000 V
		Set Detector TOF	2200 V

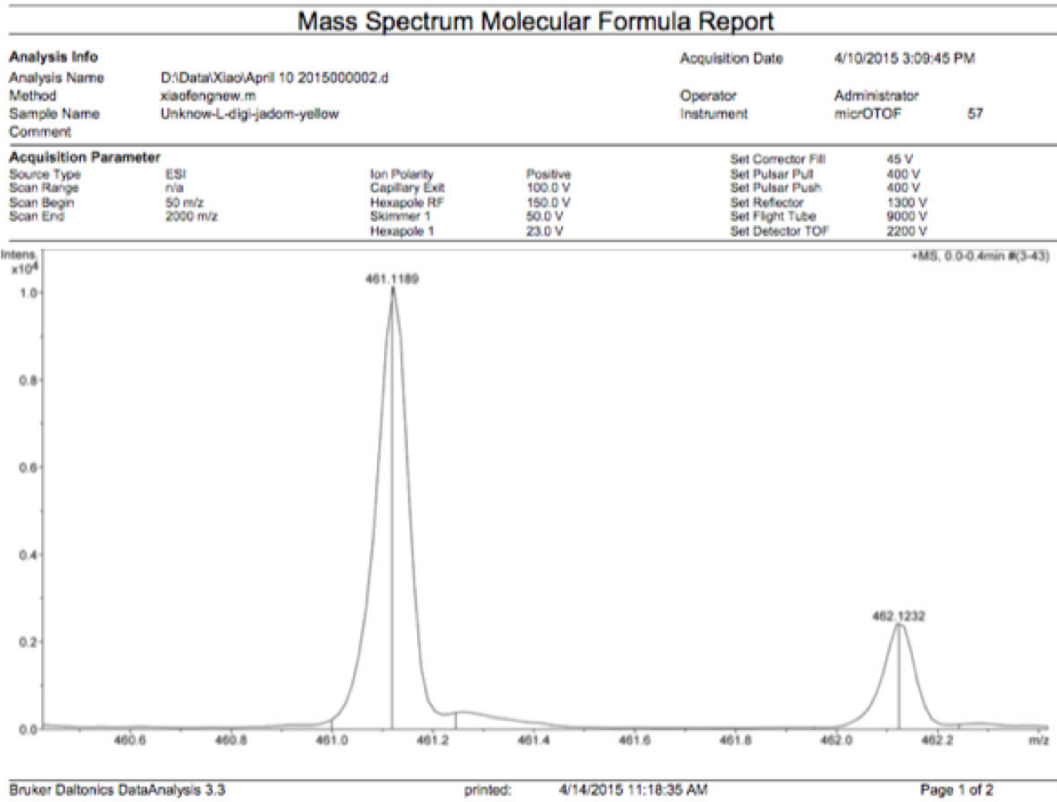


Brucker Daltonics DataAnalysis 3.3 printed: 4/10/2015 3:14:49 PM Page 1 of 2

Mass Spectrum Molecular Formula Report

Sum Formula	Sigma	m/z	Err [ppm]	Mean Err [ppm]	rdB	N Rule	e ⁻
C ₂₄ H ₂₀ Na ₁ O ₈	0.09	459.1050	0.14	-1.58	14.50	ok	even

HRMS data for jadomycin furan 3.4.



Mass Spectrum Molecular Formula Report

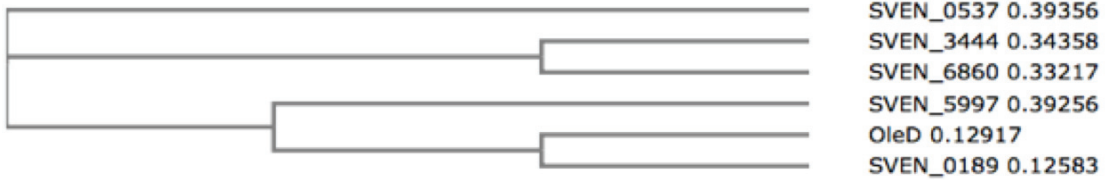
Sum Formula	Sigma	m/z	Err [ppm]	Mean Err [ppm]	rdB	N Rule	e ⁻
C ₂₄ H ₂₂ Na ₁ O ₈	0.02	461.1207	3.92	3.93	13.50	ok	even

Appendix F: Supplementary materials for Chapter 3.3

Identity matrix and phylogenetic tree generated by ClustalOmega (1.2.1) analysis:

Percent Identity Matrix - created by Clustal2.1

1: SVEN_0537	100.00	20.81	26.24	17.56	21.78	23.21
2: SVEN_3444	20.81	100.00	32.43	24.70	20.47	21.21
3: SVEN_6860	26.24	32.43	100.00	20.98	23.03	22.07
4: SVEN_5997	17.56	24.70	20.98	100.00	23.32	23.45
5: OleD	21.78	20.47	23.03	23.32	100.00	74.50
6: SVEN_0189	23.21	21.21	22.07	23.45	74.50	100.00



Clustal Omega (1.2.1) alignment glycosyltransferase family 1 enzymes from *S. venezuelae* (ATCC 10712) and OleD. OleD and SVEN_0189 are 74% identical, whereas JadS is 21% identical with them both.

```

SVEN_0537 -----MNILLCPLSDGGYLYPAIAAGRELRR
SVEN_3444 -----MVGLAVRLRE
SVEN_6860 MRTGRTPRQPTPRLRITSSPMLGRRAPVGQTGGVRIVMMTAGSRGDVAPYTGLSAGLVR
SVEN_5997 -----MRYLFTTIPGTSHTLPLVPLAHAALA
OleD -----MTTQTPAHIAMFSIAAHGHVNPSEVIRELVA
SVEN_0189 -----MVVMTTASRAHIAMFSIAAHGHVNPSEVIRELVA

SVEN_0537 RGHVSVLA--RSSAAPVVAESGLPCLP-----AED---FGGRRAFSATWGGTTGAAQ
SVEN_3444 LGAEVRVCAPPDEEFTELLYIGVPPVPVVGAPVRPLVTTVVP-----STEGLA-
SVEN_6860 AGHEVTLA--AHGVFEPLVTGSGVRFRA--LPVDPRAE LHS PRGRLHD---ARTGAGK
SVEN_5997 AGHEVAFAA--SGPALRAANAAGLQTIAA-----AGD--EAAEPYE-ELIAK
OleD RGH RVTYAI--PPVFADKVAATGARPVLYHSTL-----PGPD--ADPEAWGSTLLDN
SVEN_0189 RGH RVSYAV--PASFAEKVAATGATPVVYTSTL-----PT-D--DDPDAWGTE LIDN
      * . *                *

SVEN_0537 YRAV-----VRAARETRAELLVTSVLCNGALLAAEALDLPVVVVGLSV
SVEN_3444 -----KRVSDLIAAQFGAVAAAEGCDALVAT---GPLPVTAGA--RSVAEKLGRY
SVEN_6860 LVRLASMARSAADEMTAAL--VEVARE--GDVLLVGGALGPLGYAIAD--GLSVPAMGLHL
SVEN_5997 VTSDLAQEFPGPKILPYV--SGIFGEV GARLV-----EGVAEAARTWRADAVVFPNH
OleD VEPF-LN---DAIQALPQL--ADAYADDIPDLVLDITSYPARVLARRWGVPVAVSLPNL
SVEN_0189 LEPF-LR---DAEQALPQL--AEAFDRDRPDLVLDITSYPAPVLAHSWGVPVAVSLWPNL
                                * : . . .

SVEN_0537 HLWDYRAGGDGEPHLGRTR--ESRTLCRGILAA TREEVGLAGRA--SRWDDPLL----
SVEN_3444 VHASHTPVSLSPHQ--PPPGRGRPLPP-EV-SDNRELWDIDARNANEMFGEVLN----
SVEN_6860 Q-PLHPTGEFPAPVLGTRSLGAVGNRLS GRAVMTTVELLFADAVRSLRRRYGLVTT----
SVEN_5997 VAGLLAARMTG LPAVLHGI-----GTPRPVFAP-----ALAYLEPVAARLGVDLP
OleD VAWKGYEE EVAEPMWREPR-----QTER-----GRAYYARFEA-----
SVEN_0189 VPWEGYEE EVAEPM LAELK-----ASPR-----GKAYYTRFAD-----
                                *

SVEN_0537 --GDALLLRGDPAL---EYPGGELPERVRFVGPMDWEPA-----
SVEN_3444 --AHRAGIGLPPVDNVRDYAF TDS PWLATDPVLS PWRPTDL-----GVV
SVEN_6860 --GPRRGRRARPVL--HGYSR-----LVVPRPRD WSP-----ELE

```

```

SVEN_5997      APVADVEIDLNP-----ASLTAPS----LGGPGGGGPAAAHRLPMRYTSYNGGA---EI
OleD          -WLKENGITEHP-----DTFASHPPRSLVLIPKALQPH-ADRVDEDVYTFVGACQGDRA
SVEN_0189     -WLAEHGIDTDP-----DRFVARPRRAIVLIPKALQPQ-ADRVDES VYTFVGACQGERA
                *                               *

SVEN_0537     -----PGRGESEAVADHLARTGKPVVYVHLGRF--FGGRSLW--PRLNEAFT-GGPF
SVEN_3444     QTGAWLRPDERPLPELV-AFLDAGTAPVYVGF GSM--PLGDAKGIARA AVG AIR-AQGR
SVEN_6860     VAGYWPHETGRLSQELE-DFLAAGPPPVFVGLGSA--TVPDPERVSREIVTALR-TANV
SVEN_5997     PPGLLGR-----GERPRVAVTLGSLAALYEGE-TMLREIVDGS A-DLGI
OleD          EGGWQRPA-----GAEKVVLVSLGSA--FTKQP-AFYRECVRAFGNLPGW
SVEN_0189     EQGTWQRPA-----DAEKVVLVSLGSA--FTKLP-GFYRDCVEAFAGLPGW
                * * ; *

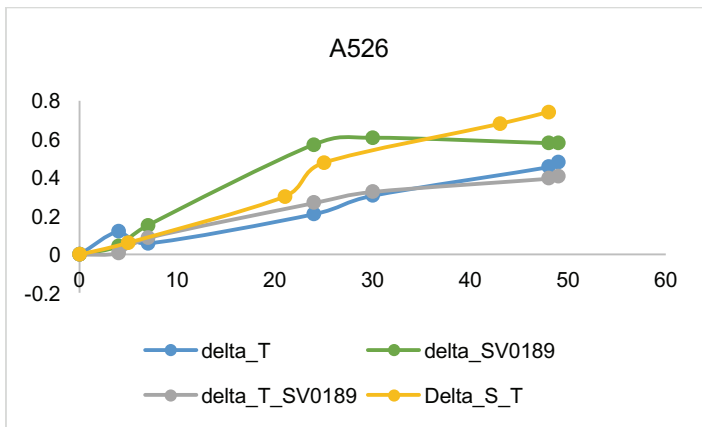
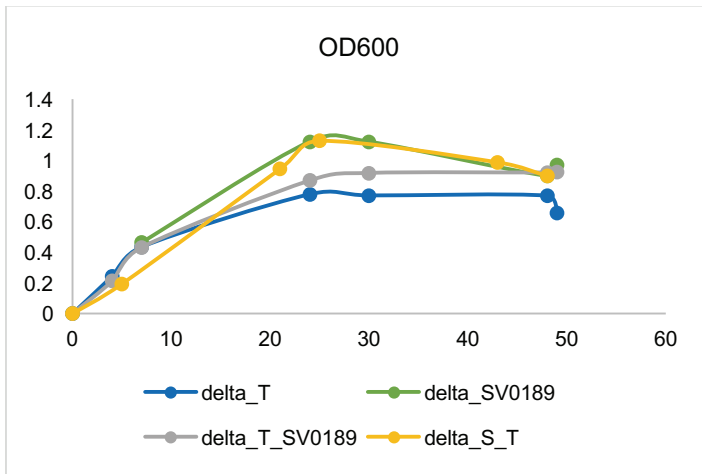
SVEN_0537     QAVVEQGRSTEPQGP--DADILLVRKPMWGPLVDLAGLVVANGTSAPVLAALLRGRPLA
SVEN_3444     RVVLSRGWAELGPIDD--RDDCFAVGEVNQQALFAEVA AVVHHGSAGTTTAA RAGAPQV
SVEN_6860     RGIVQRGWAGLDA--R--SDDILTVDEVP HSLFPRTAAVVHHAGAGTTGAVLRAGVPSV
SVEN_5997     ELVITTTGAE LPA LTGSLPHVTCVDWVPLR TLLASCD AIVHHGGMGSTFTAFDAGVPQL
OleD          HLVLQIGRKVTPAELGELPDNVEVHDWVPQLAILRQADLFVTHAGAGGSQEGLATATPMI
SVEN_0189     HVVLQIGKFVDP AELGTVPSNVEVRSWVPQLAILRQADGFVTHAGAGGSQEGLATGTPMV
                . : * . : . * . . *

SVEN_0537     LSPNGSEQPLL TGACV---RAGVAV---RDPKTPSADLSALLESAWHDEGLRTRARALGD
SVEN_3444     VVPQGADQSYWADRVD---DLGIGA AHAGPVA-TTASLSAALQVALAPG-TRARATAVAG
SVEN_6860     PVPVQFDAAF WASRLT---ALGTAPGAVPLRRLTSGALSEALVGATADGRHRTRARALAD
SVEN_5997     AIPLTGPE SVSNGRVAADRGTGIVLDPPLSVPLTAA TVKSSLHELLSNPAHR TAAAEVAA
OleD          AVPQAVDQF-GNADM--LQGLGVARKLATE-EATADLLRETALALVDDPEVARRLRRIQA
SVEN_0189     AVPQAVDQF-GNADM--LQSLGVARHLPM D-EVTPERLRTAMLALLGDPEVARRAREIQE
                *                               *                               :                               :

SVEN_0537     RLAAAGGAARAADIVERVAVASAI PKEDHEYAISRPR--
SVEN_3444     TVRADGAVVA-ARMLLEATPTRAEGAAT-----R----
SVEN_6860     RLAAEDGVAPVLAALARLAP-----
SVEN_5997     EMREMPAPAA TLVQLNALLGGTA-----
OleD          EMAQEGGTRRAADLIEAELPARHERQEPV---GDRPNGG
SVEN_0189     SMAREGGTLRAADLIEAELAGS-----
                : . :

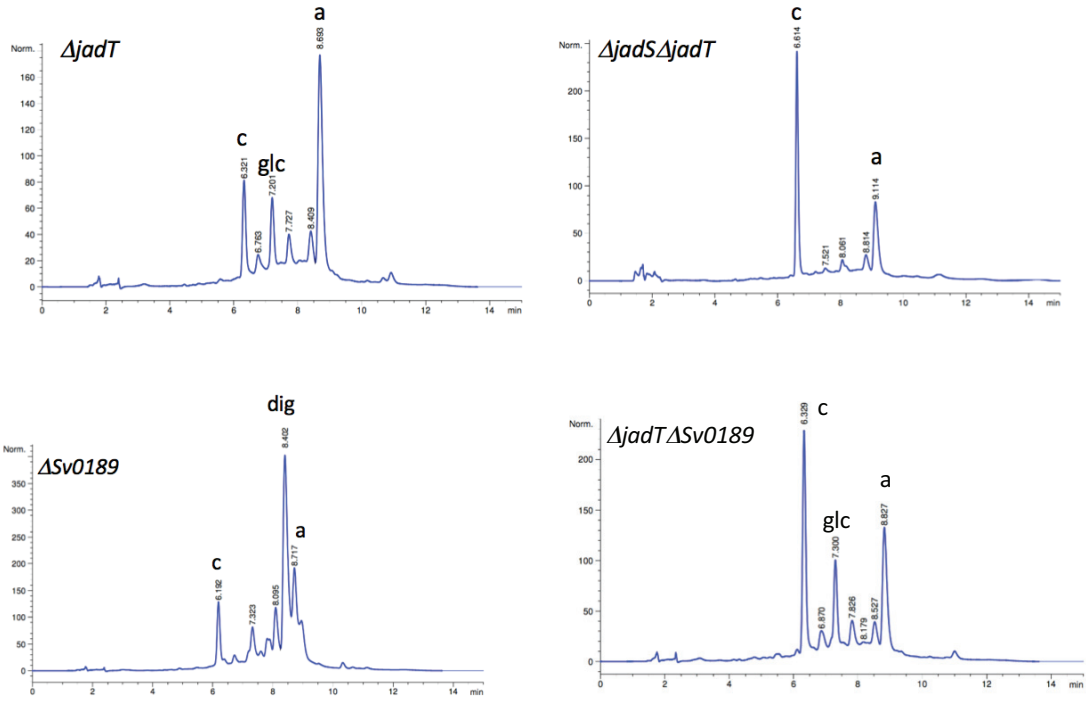
```

S. venezuelae Δ jadT mutant (blue), *S. venezuelae* Δ Sv0189 (green), *S. venezuelae* Δ jadT Δ Sv0189 (purple), and *S. venezuelae* Δ jadS Δ jadT mutant (yellow), growth curves measured at 600 nm (OD₆₀₀) and measured at 526 nm (Abs₅₂₆) estimating production of colored compounds. Y axis is absorbance, X axis is time (hours).

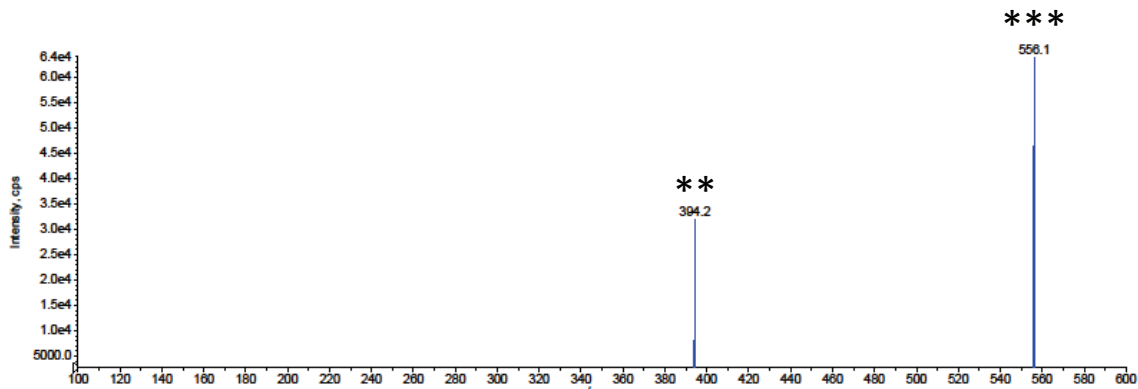


HPLC traces of the methanol extract from the phenyl column for indicated strains.

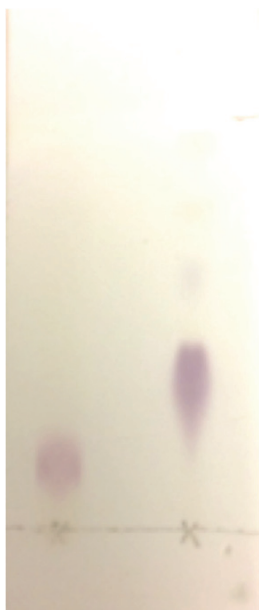
c, chloramphenicol; **a**, jadomycin aglycon; **dig**, JdDS; **glc**, glc-JdDS.



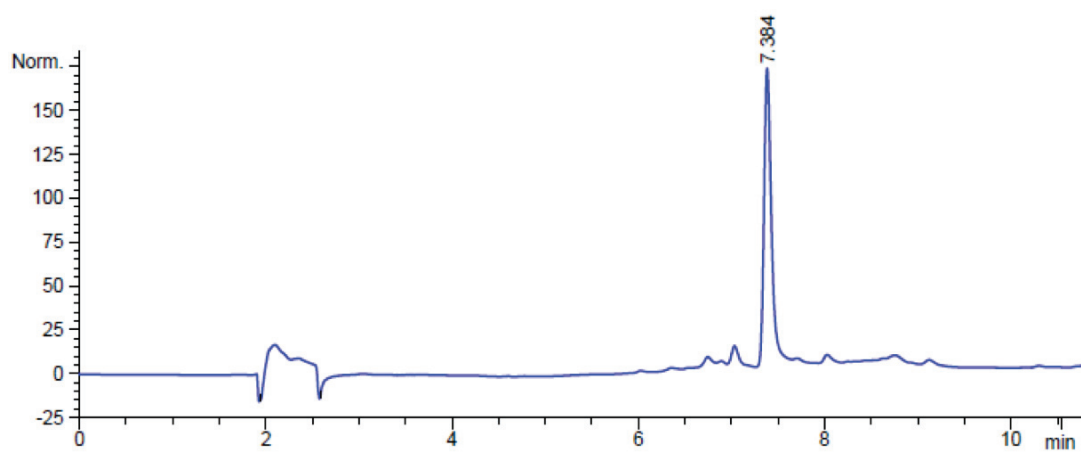
LC-MS/MS fragmentation of **3.9** (parent ion $[M+H]^+$ 556, showing $[M+H]^+$ (***) and cleavage of the sugar $[M+H-C_6H_{10}O_5]^+$ (**).



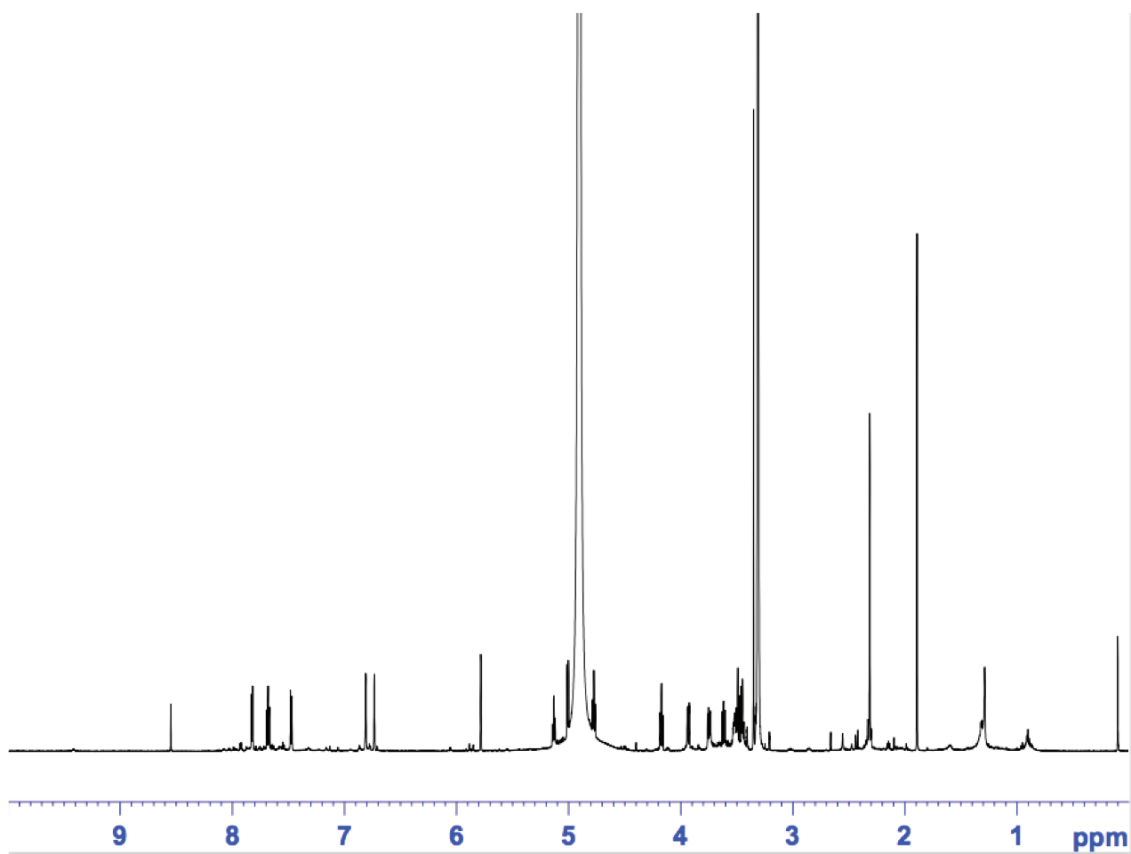
TLC of **3.9** (left) and **JdDS** (right), running solvent 8:2 dichloromethane:methanol



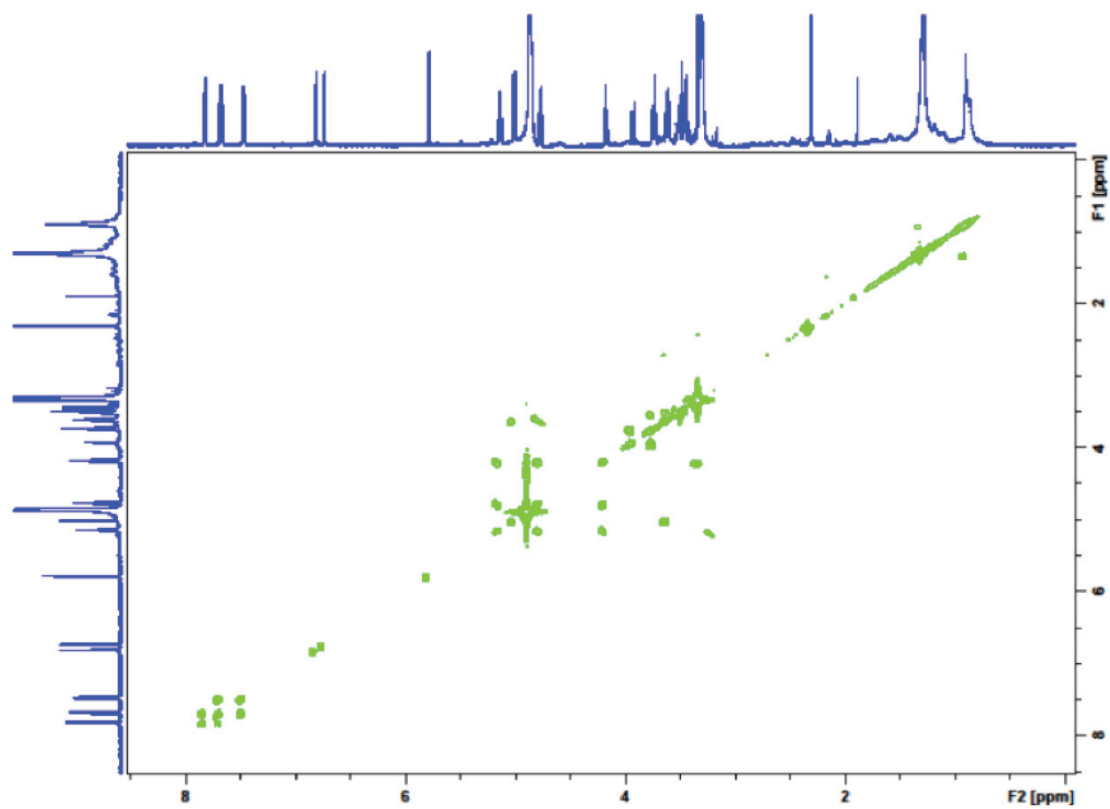
HPLC trace of purified **3.9**.



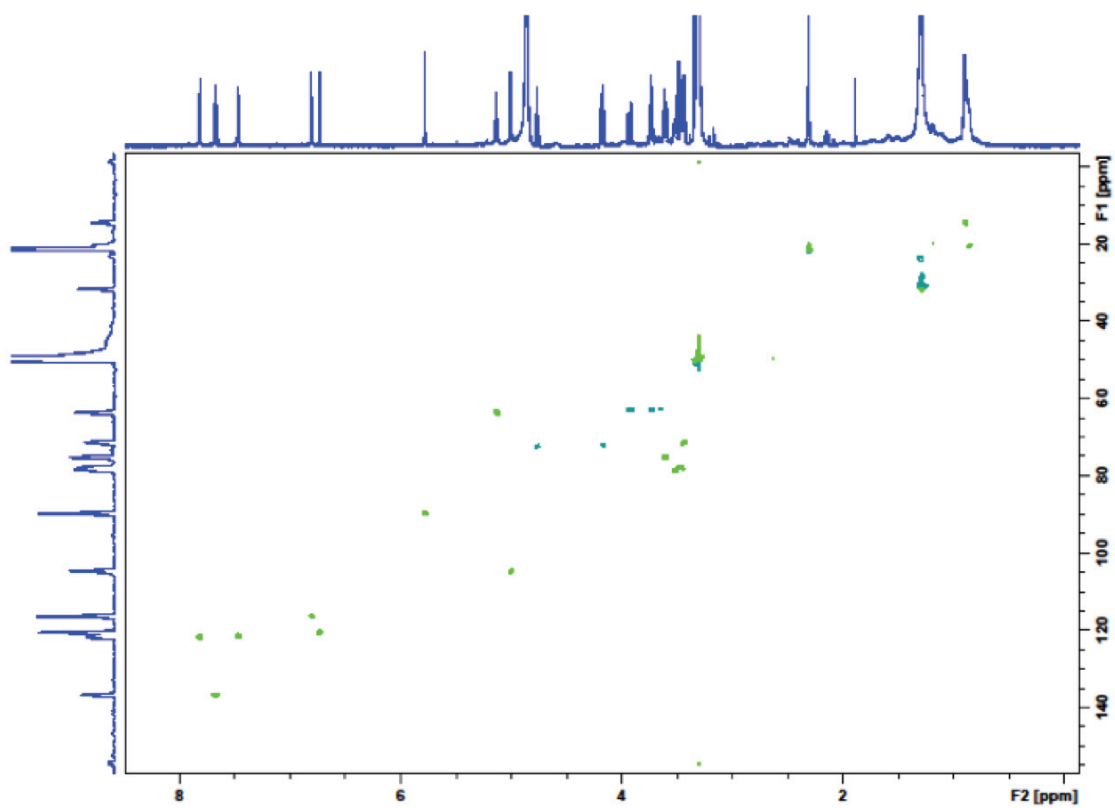
^1H NMR (700 MHz, methanol- d_4) spectrum of **3.9**.



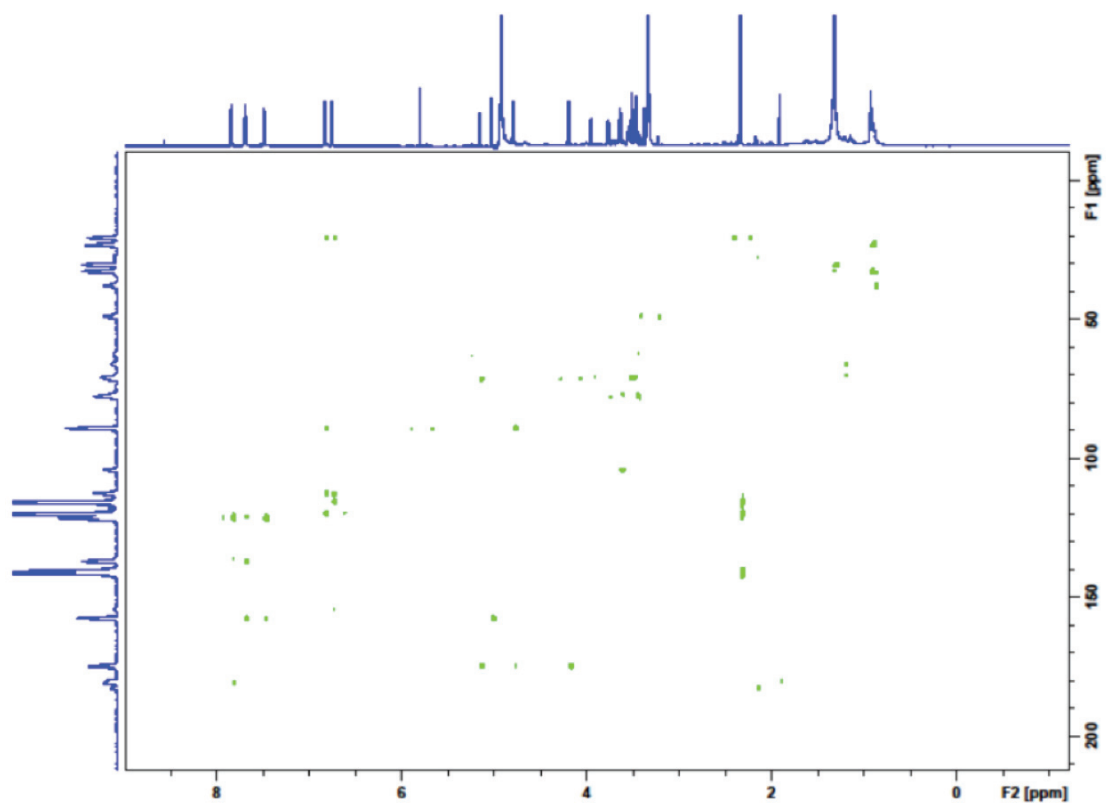
COSY (700 MHz, methanol- d_4) NMR spectrum of **3.9**.



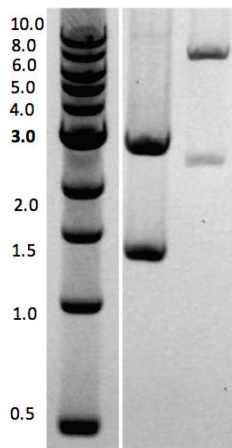
Edited-HSQC (700 MHz in methanol- d_4) NMR spectrum of **3.9**.



HMBC (700 MHz in methanol- d_4) NMR spectrum of **3.9**.

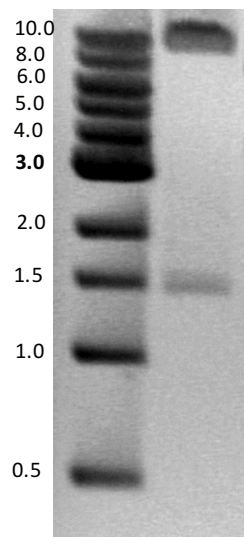


Appendix G: Supplementary materials for Chapter 3.4

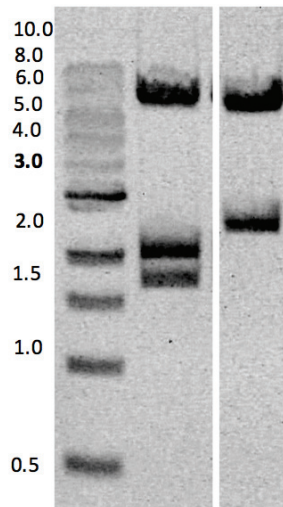


Left: pUC57::*kijC3* XbaI/StuI restriction digest (1.3 kb, 2.5 kb)

Right: pKC1139::*jadUV* HindIII/EcoRI restriction digest (6.5, 2.2 kb)

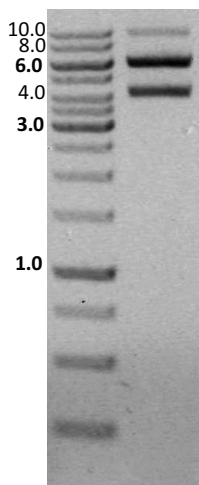


pKC1139::*kijC3* restriction digest EcoRI/ NcoI (1.4, 8.6 kb)

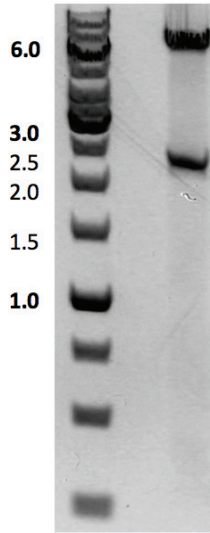


(Left) pKC1139::*kijC4kijC3* FspI restriction digest (7.5, 2.1, 1.7 kb)

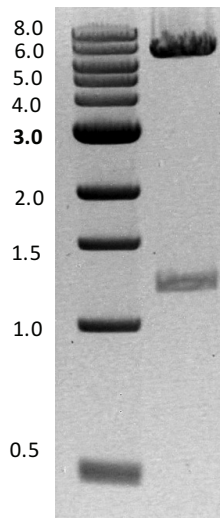
(Right) pKC1139::*kijC4* FspI restriction digest (7.5, 2.6 kb)



pKC1139::*kijC4(XhoI)* XhoI restriction digest (5.4 and 4.0 kb)



pKC1139 Δ *jadV* EcoRI/HindIII restriction digest (2.4, 6.5 kb)



pSE34::*kijC4* XbaI/HindIII restriction digest (1.2, 7.5 kb)